Long-term genetic modification of the ocular outflow tract and the retinal pigment epithelium with feline immunodeficiency viral vectors

Thesis

UNRESTRICTED

Long-Term Genetic Modification of the Ocular Outflow Tract and the Retinal Pigment Epithelium with Feline Immunodeficiency Viral Vectors

Nils Loewen, MD

A thesis submitted in partial fulfillment of the requirements of the Open University for the degree of Doctor of Philosophy.

April 30, 2008

Sponsoring Establishment:

Mayo Graduate School

200 First Street SW
Rochester, MN 55905, USA

Director of Studies:

Dr. Eric M. Poeschla

Molecular Medicine Program

Guggenheim 1811A

Phone: 001-507-284-3178

Email: Poeschla.eric@mayo.edu

DATE OF SUBMISSION: 22 APRIL 2004
DATE OF AWARD: 25 MAY 2008.

Abstract

The central goal to engineer feline immunodeficiency viral (FIV) vectors into a more modular platform for long-term ocular gene therapy was accomplished collaboratively by separating envelope, packaging and transfer function, the latter of which I optimized. FIV mediated gene transfer to the aqueous humor outflow tract and to the retina was established and long-term vector function and biocompatibility were confirmed. Transduction of the outflow tract was highly efficient and resulted in genetic modification of nearly the entire trabecular meshwork. For this purpose, I developed methods for administration and sensitive monitoring of FIV vectors in the anterior chamber and a novel subretinal injection technique.

Bicistronic FIV vectors generated high levels of two different transgenes eGFP and β-galactosidase, which allowed live in vivo tracking and sensitive yet specific cell labeling in tissue specimen, respectively. An integrase mutant control vector that differed in only one amino acid resulted in no significant transduction while preserving all other biochemical properties.

I developed a novel protocol for scaled-up production FIV vectors using cell factories and large-volume concentration that proved useful in the animal studies of this thesis. Especially the results achieved in the larger animal model, the domestic cat, validated the protocol for large-scale production. Transient transfection of 10 times less DNA into 293T cells within high surface area cell factories and high volume, fixed-angle ultracentrifugation resulted in high titer vectors.

Table of Contents

1. HYPOTHESIS ..... - 8 -

1.1. SPECIFIC AIMS ..... - 8 -

1.1.1. Refinement of an FIV vector system for ocular gene therapy. ..... - 8 -

1.1.2. Development of scaled-up lentiviral vector production and concentration. ..... - 8 -

1.1.3. Establishment of in vitro and in vivo FIV-mediated gene transfer to the aqueous humor outflow tract with long-term assessment of vector function. ..... - 8 -

1.1.4. Establishment of in vivo FIV-mediated gene transfer to the retinal pigment epithelium with long-term assessment of vector function. ..... - 9 -

2. TABLE OF FIGURES ..... - 10 -

3. TABLES ..... - 17 -

4. PUBLICATIONS ..... - 18 -

4.1. PAPERS ..... - 18 -

4.2. CHAPTERS ..... - 19 -

4.3. PATENTS ..... - 19 -

4.4. ABSTRACTS ..... - 20 -

5. ACKNOWLEDGEMENTS ..... - 25 -

6. INTRODUCTION ..... - 27 -

6.1. EYE STRUCTURE AND FUNCTION ..... - 27 -

6.1.1. Overview of the Mammalian Eye Anatomy ..... - 28 -

6.1.1.1. Tunicas of the Eye ..... - 28 -

6.1.1.2. Anterior and Posterior Segment ..... - 28 -

6.1.2. Aqueous Humor Production and Outflow ..... - 29 -

6.1.3. Central Fundus and Optic Nerve Head in Glaucoma ..... - 32 -

6.1.4. Anatomy, Cell Biology and Function of the Retina ..... - 34 -

6.1.4.1. Layers and cell types of the Neuro-Retina ..... - 36 -

6.2. HUMAN OCULAR DISEASES ..... - 42 -

6.2.1. Glaucoma ..... - 42 -

6.2.1.1. Overview ..... - 42 -

6.2.1.2. Aqueous Humor Outflow ..... - 44 -

6.2.1.3. Clinical Perspective ..... - 46 -

6.2.1.4. Current Status of Glaucoma Therapy ..... - 49 -
6.2.1.5. Rational for Developing Gene Transfer to the Trabecular Meshwork ..... - 51 -
6.2.2. Retinal and Choroidal Diseases ..... - 54 -
6.2.2.1. Vasoproliferative Retinal and Choroidal Diseases ..... - 55 -
6.2.2.2. Degenerative Retinal and Choroidal Diseases ..... - 58 -
6.2.2.3. Rational for Gene Therapy for Retinal and Choroidal Diseases ..... - 61 -
6.2.3. Mediators of Ocular Angiogenesis ..... - 62 -
6.2.4. Models of Retinal and Choroidal Neovascularization ..... - 64 -
6.3. GENE THERAPY ..... - 65 -
6.3.1. Definition ..... - 65 -
6.3.2. History ..... - 67 -
6.3.3. Types of Gene Transfer Vectors ..... - 68 -
6.3.3.1. Adenoviral Vectors ..... - 68 -
6.3.3.2. Retroviral Vectors ..... - 72 -
6.3.3.3. Lentiviral Vectors ..... - 76 -
6.3.3.4. Non-Viral Gene Transfer ..... - 85 -
6.3.3.5. Adeno-associated virus ..... - 87 -
6.3.3.6. Herpes simplex virus ..... - 91 -
6.3.4. Current Gene Therapy Trials ..... - 94 -
6.3.5. Ocular Gene Transfer ..... - 104 -
6.3.5.1. Anterior Segment ..... - 105 -
6.3.5.2. Posterior Segment ..... - 120 -
6.3.5.3. Ocular Malignancies ..... - 126 -
7. MATERIALS AND METHODS ..... - 129 -
7.1. MATERIALS ..... - 129 -
7.1.1. Amplification of Plasmid DNA in Bacteria ..... - 129 -
7.1.2. DNA Analysis ..... - 129 -
7.1.3. Cloning using Plasmid Vectors ..... - 129 -
7.1.4. Polymerase Chain Reaction ..... - 129 -
7.1.5. DNA Sequencing ..... - 129 -
7.1.6. Cloning of Viral Vectors ..... - 129 -

7.1.6.1. Feline Immunodeficiency Virus (FIV) vectors ..... - 130 -
7.1.6.2. Murine Leukemia Virus (MLV) beta-galactosidase expressing vector LZRNL[462] ..... - 130 -
7.1.6.3. Human Immunodeficiency Virus (HIV) vectors[240, 250] ..... - 130 -
7.1.6.4. Adenoviral Vector ..... - 131 -
7.1.7. Cell Cultures ..... - 131 -
7.1.7.1. Cell Cultures ..... - 131 -
7.1.7.2. Cell Cultures for Retroviral Vector Production ..... - 131 -
7.1.7.3. Cell Cultures for Production in Cell Factories ..... - 131 -
7.1.7.4. Cell Cultures for Production in T75 Flasks ..... - 132 -
7.1.7.5. Human Ocular Anterior Segment Cultures ..... - 132 -
7.1.8. Transfections ..... - 132 -
7.1.8.1. Cell Factories ..... - 133 -
7.1.8.2. T75 Flasks ..... - 133 -
7.1.9. Vector Harvest ..... - 133 -
7.1.9.1. Cell Factories ..... - 133 -
7.1.9.2. T75 Flasks ..... - 133 -
7.1.10. Vector Concentration ..... - 133 -
7.1.10.1. Cell Factories ..... - 133 -
7.1.10.2. T75 Flasks ..... - 134 -
7.1.11. In Vivo Applications ..... - 134 -
7.1.11.1. Animals ..... - 134 -
7.1.11.2. Imaging ..... - 134 -
7.1.11.3. Pressure recording ..... - 135 -
7.1.11.4. Subretinal Injection in Rats ..... - 135 -
7.2. METHODS ..... - 135 -
7.2.1. Manipulation of Vector Components ..... - 135 -
7.2.1.1. Cloning using Plasmid Vectors ..... - 135 -
7.2.1.2. Amplification of Plasmid DNA in Bacteria ..... - 137 -
7.2.1.3. DNA Analysis ..... - 140 -
7.2.1.4. Polymerase Chain Reaction ..... - 141 -
7.2.1.5. DNA Sequencing ..... - 142 -
7.2.1.6. FIV Vector Components ..... - 142 -

7.2.2. Cell Cultures ..... *- 154 -*

7.2.2.2. Trypsinizing Cells ..... - 157 -

7.2.2.3. Counting Cells ..... - 158 -

7.2.2.4. Seeding and Growing Cells ..... - 159 -

7.2.3. Generation of Vectors ..... *- 160 -*

7.2.3.1. Feline Immunodeficiency Virus Vectors ..... - 160 -

7.2.3.2. Feline Immunodeficinecy Virus Mock Vectors ..... - 161 -

7.2.3.3. Adenovirus Vectors ..... - 162 -

7.2.3.4. Murine Leukemia Virus Vectors ..... - 162 -

7.2.3.5. Human Immunodeficiency Virus Vectors ..... - 163 -

7.2.4. Scaled-up Lentiviral Vector Production ..... *- 163 -*

7.2.4.1. Production of High-Titer FIV Vector Stocks by Transient Transfection of 293T Cells ..... - 164 -

7.2.4.2. Concentration by Large Volume Ultracentrifugation ..... - 165 -

7.2.5. Titration of Transducing Units ..... *- 166 -*

7.2.5.1. Enhanced (eGFP) and Renilla (rGFP) Green Fluorescent Protein Transducing Units ..... - 166 -

7.2.5.2. Beta-Galactosidase Transducing Units ..... - 167 -

7.2.6. In Vitro and Ex Vivo Methods ..... *- 167 -*

7.2.6.1. In Vitro Human Trabecular Meshwork Cells ..... - 167 -

7.2.6.2. Ex Vivo Human Donor Eyes ..... - 168 -

7.2.7. Tissue Processing and Marker Detection ..... *- 170 -*

7.2.7.1. Beta-Galactosidase Detection with the X-Gal Assay ..... - 170 -

7.2.7.2. Beta-Galactosidase Detection by Anti-Body Labeling ..... - 171 -

7.2.7.3. Antibody Labeling of Enhanced Green Fluorescent Protein (EGFP) ..... - 172 -

7.2.8. Animal Handling and Vector Application ..... *- 174 -*

7.2.8.1. Animals ..... - 174 -

7.2.8.2. Anesthesia ..... - 176 -

7.2.8.3. Intraocular Application of Vectors ..... - 177 -

7.2.9. Ex Vivo and In vivo Imaging of Transduced Cells Expressing Fluorescent Proteins ..... *- 180 -*

7.2.9.1. Ex Vivo Imaging ..... - 180 -

7.2.9.2. Non-Invasive In Vivo Monitoring of Enhanced (eGFP) and Renilla (rGFP) Green Fluorescent Protein Expression in the Cat Eye ..... - 181 -

7.2.10. Quantification and Statistics ..... *- 182 -*

8. RESULTS ..... - 184 -

8.1. TRANSGENESIS OF THE OCULAR OUTFLOW TRACT WITH LENTIVIRAL VECTORS AS A BASIS FOR GENE THERAPY OF GLAUCOMA ..... - 184 -

8.1.1. FIV transfer vectors and Production Procedures ..... - 184 -

8.1.1.1. Transfer Vector Modification ..... - 184 -

8.1.1.2. Production Procedures ..... - 184 -

8.1.2. Transduction of Primary Human Trabecular Meshwork Cells with FIV LacZ Transfer Vector CT25 ..... - 185 -

8.1.1. Transduction of Primary Human Trabecular Meshwork Cells with FIV eGFP Transfer Vector GINWF ..... - 186 -

8.1.2. Transduction of Human TM ..... - 188 -

8.1.2.1. Transduction of Cultured Human Eyes: Extent and Time Course of Transgene Expression in the Trabecular Meshwork ..... - 188 -

8.1.2.2. Dose Response ..... - 191 -

8.1.2.3. Pairwise Comparison of Trabecular Meshwork Transduction by Oncoretroviral and Lentiviral Vectors ..... - 192 -

8.1.2.4. Expression of eGFP and β-Galactosidase in Human TM ..... - 192 -

8.1.3. Effects on Outflow Facility ..... - 195 -

8.1.4. Transgene Expression In Vivo ..... - 195 -

8.2. TRANSGENESIS OF THE RETINAL PIGMENT EPITHELIUM WITH FIV VECTORS AS A BASIS FOR GENE THERAPY OF RETINAL AND CHOROIDAL DISEASES ..... - 205 -

8.2.1. Comparison of Wild-Type and Class I Integrase Mutant-FIV Vectors in the Retina Demonstrates Sustained Expression of Integrated Transgenes in Retinal Pigment Epithelium ... - 205 -

8.2.1.1. Results ..... - 205 -

8.2.2. Long-Term Retinal Transgene Expression with FIV versus Adenoviral Vectors ..... - 210 -

8.2.2.1. Results ..... - 210 -

9. DISCUSSION ..... - 215 -

9.1. TRANSGENESIS OF THE OCULAR OUTFLOW TRACT WITH LENTIVIRAL VECTORS AS A BASIS FOR GENE THERAPY OF GLAUCOMA ..... - 215 -

9.1.1. Genetic Modification of Human Trabecular Meshwork with Lentiviral and Adenoviral Vectors versus Type-C Retroviral Vectors ..... - 215 -

9.1.2. Preservation of Aqueous Outflow Facility after FIV-Mediated Transduction of Anterior Segments of Human Eyes ..... - 216 -

9.1.3. Long-Term Genetic Modification of the Outflow Tract Coupled with Non-Invasive Imaging of Gene Expression In Vivo ..... - 218 -

9.1.4. Conclusions from Studies of Genetic Modification of the Outflow Tract and Future Directions ..... - 221 -

9.2. TRANSGENESIS OF THE RETINAL PIGMENT EPITHELIUM WITH FIV VECTORS AS A BASIS FOR GENE THERAPY OF RETINAL AND CHOROIDAL DISEASES ..... - 225 -

9.2.1. Comparison of Wild-Type and Class I Integrase Mutant-FIV Vectors in the Retina Demonstrates Sustained Expression of Integrated Transgenes in Retinal Pigment Epithelium ... - 225 -

9.2.2. Long-Term Retinal Transgene Expression with FIV versus Adenoviral Vectors ..... - 228 -

10. CONCLUSION ..... - 230 -

11. REFERENCES ..... - 232 -

12. CURRICULUM VITAE ..... - 273 -

1. Hypothesis

Feline immunodeficiency viral vectors can be engineered into a modular platform that allows long-term ocular gene transfer to the ocular outflow tract and the retinal pigment epithelium and monitoring of function with standard ophthalmology techniques.

1.1. Specific Aims

1.1.1. Refinement of an FIV vector system for ocular gene therapy.

An FIV vector system will be engineered that has versatile, exchangeable components of envelope, packaging, and transfer, fulfills safety requirements, and allows simultaneous delivery of several transgenes.

1.1.2. Development of scaled-up lentiviral vector production and concentration.

Higher titers and larger volumes of vectors are needed for in vivo or ex vivo organ culture than for in vitro applications. A method will be developed that allows scaled-up and efficient generation of several liters of vector and subsequent large volume concentration.

1.1.3. Establishment of in vitro and in vivo FIV-mediated gene transfer to the aqueous humor outflow tract with long-term assessment of vector function.

Gene delivery to ocular tissue will be established stepwise in vitro, in ex vivo organ cultures of perfused anterior human eye segments and in the domestic cat. Efficiency of gene delivery and toxicity will be assessed. Vector long-term function will then be studied in the outflow tract and retina that constitute the target tissue for gene therapy of glaucoma and retinal neovascularization, respectively. New techniques will be developed for the microsurgical delivery of vectors to the anterior chamber and the subretinal space and for monitoring of transgene expression.

1.1.4. Establishment of in vivo FIV-mediated gene transfer to the retinal pigment epithelium with long-term assessment of vector function.

Gene delivery to ocular tissue will be established stepwise in vitro, in ex vivo organ cultures and in animal models. Initial studies will adjust efficiency of gene delivery and assess toxicity. Vector long-term function will then be studied in the outflow tract and retina that constitute the target tissue for gene therapy of glaucoma and retinal neovascularization, respectively. New techniques will be developed for the microsurgical delivery of vectors to the anterior chamber and the subretinal space and for monitoring of transgene expression.

2. Table of Figures

Figure 1: Impaired outflow of aqueous humor may result in increased intraocular pressure (left) and glaucomatous optic neuropathy (right) (National Eye Institute, National Institutes of Health).....- 42 -

Figure 2: Gradual deterioration of the visual field from the periphery (A) and figurative representation of the effect on the visual field in a late stage of glaucoma (B) (National Eye Institute, National Institutes of Health).....- 51 -

Figure 3: Simulation of normal visual field (A) and with diabetic retinopathy (B). Neovascularization, exudates and preretinal bleeding can be found in the proliferative state of diabetic retinopathy (C). The treatment consists of panretinal laser therapy and ablates healthy retina in the periphery (D) (National Eye Institute, National Institutes of Health).....- 55 -

Figure 4: Normal central fundus (A) and Amsler grid (C) and in wet age-related macular degeneration (B and D). Central vision is missing entirely or appears distorted (D) (National Eye Institute, National Institutes of Health).....- 58 -

Figure 5: Quantification of retinal neovascularization in a model of oxygen induced retinopathy. Flat mounted, stained retina is divided into clock hours and pathological vessel buds (arrows) are counted.[393].....- 64 -

Figure 6: Gene types transferred in clinical gene therapy trials (data from the online database provided by The Journal of Gene Therapy).....- 66 -

Figure 7: Reverse transcription (after ref.[497], p. 1052).....- 79 -

Figure 8: Lentiviral life cycle with highlighting of several genome processing/trafficking events: encapsidation, dimerization and central DNA flap formation. Both spliced (subgenomic) and unspliced (genomic) viral mRNAs exist in an infected cell, and these in turn represent only a small fraction of the total cellular RNA. Proper virion assembly requires a highly discriminating mechanism for preferential encapsidation of the full-length genome. The pre-integration complex (PIC) is shown with a central DNA flap; proteins know to be associated, e.g., integrase, Vpr, MA in HIV-1, are not shown. Drawn by Dyana Saenz, reproduced with permission.[498].....- 80 -

Figure 9: Gene therapy trials by phases. ..... - 96 -

Figure 10: Vector types used in gene therapy clinical trials (data from free online database provided by The Journal of Gene Therapy). ..... - 97 -

Figure 11: Disease types addressed by gene therapy clinical trials (data from free online database provided by The Journal of Gene Therapy). ..... - 98 -

Figure 12: Genomic structure of FIV and derivative packaging constructs. Top: Genome of FIV34TF10. LTR is long terminal repeat; U3, 3'-unique region of LTR; U5, 5'-unique region of LTR; R, repeat element of LTR; SD, major splice donor; Gag, group antigen (encodes structural components of virion core particle); Pol encodes a polyprotein that is cleaved by the viral protease into the five enzymatic activities: reverse transcriptase, integrase, RNAse H, protease, and dUTPase; Vif, virion infectivity factor; SU, surface envelope glycoprotein; TM, transmembrane portion of the envelope glycoprotein; RRE, rev response element. Orf2 is open reading frame 2. The Orf2 gene product may have LTR transactivating activity similar to HIV-1 Tat. However, ORF2 is not expressed by FIV 34TF10 because of the illustrated premature stop codon, and in any case, the vector system dispenses with the promoter activity of the FIV U3 element entirely by using a CMV promoter substitution and fusion at the TATA box (explained below). Middle: First generation packaging construct pCF1 *env*. Bottom: Second generation packaging construct pFP93. Note deletions of *vif*, *Orf2*, additional *env* sequences, and removal of all viral sequences upstream of *gag*. Deletions of *vif* and *orf 2* are attenuating to FIV in vivo. ..... - 145 -

Figure 13: Class I FIV integrase mutations. The three universally conserved amino acids (D64, D116, and E152) that are required for function of the integrase catalytic center are illustrated. The aspartic acid (D) at position 64 was mutated to valine (V) by site-directed mutagenesis. Subsequently, addition of a second mutation (D116A) has been shown to preserve class I properties. ..... - 146 -

Figure 14: Second-generation bicistronic transfer vector. The central DNA flap[492] and WPRE[733] have been inserted, and *gag* has been reduced to 311 nt. ..... - 150 -

Figure 15: HIV vector with self-inactivating (SIN) LTR modification (after ref. [736]). - 151 -

Figure 16: Hematocytometer counting chamber. Rulings cover 9 square millimeters. Boundary lines of the Neubauer ruling are the center lines of the groups of three. (These are indicated in the illustration below.) The central square millimeter is ruled

into 25 groups of 16 small squares, each group separated by triple lines, the middle one of which is the boundary. The ruled surface is 0.10mm below the cover glass, so that the volume over each of the 16 small squares is .00025 cubic mm..... - 158 -

Figure 17: Anterior chamber perfusion model.[750] Left: Schematic side view. Media enteres hemidisected eye centrally and exits following the natural route through the TM and episcleral veins collecting in the well surrounding the eye. A pressure transducer to measure IOP is also connected to the anterior chamber and enters from underneath (not shown). Right: Top view of open culture chamber. ..... - 168 -

Figure 18: Vector production, concentration, and injection. Supernatants of transfected 293T cells are collected, filtered, and concentrated by ultracentrifugation. For a subretinal injection, the needle is inserted through a sclera tunnel with the bevel of the needle facing the center of the eye (middle). An intravitreal injection requires a steeper angle and the bevel is rotated outwards (right). Injury of the large rodent lens must be avoided to prevent cataract formation. ..... - 178 -

Figure 19: Subretinal injection technique. (A) Size of a 7 day old rat in comparison to the tip of a pen. (B) When full anesthesia is reached, lids are spread open with forceps and the lateral palpebral fissure is extended by 1 mm. (C) A latex membrane with a central cut of 2 mm is placed on top of the eye and the eye prolapsed with curved forceps in a backward motion while the slit is stretched open. (D) Creation of a sclera tunnel using a 30ga hypodermic needle. (E) Tangential insertion of a 33ga needle mounted on a custom made Hamilton syringe through the sclera tunnel. (F) A forming retinal detachment can be seen as a translucent crescent in animals without dark pigmentation. ..... - 179 -

Figure 20: Top view of anesthetized cat on restrainer (A) and side view of restrainer under modified microscope (B). The trabecular meshwork can be seen as a black ring in the mirror of the gonioscope that is placed on the cornea (C). ..... - 181 -

Figure 21: Grading system for β-galactosidase expression. Grades were defined prospectively on a scale with a range from 0 to 5. Grade 5 = confluent transduction of entire retinal surface area, grade 4 = large confluent areas of at least half of retinal surface area, grade 3 = confluent areas with less than half the retinal surface area, grade 2 = large areas of non-confluent transduced cells, grade 1 = isolated, discrete transduced cells, grade 0 = no detectable β-galactosidase activity. ..... - 183 -

Figure 22: Primary trabecular meshwork cell transduction and effect of growth arrest. Cells isolated from human trabecular meshwork and plated in 24-well plates were transduced with 300 *m*l of unconcentrated supernatant containing a 2.5 x 10^6-TU/ml concentration of MuLV vector (*top*) or FIV *lacZ* vector (*bottom*). Growth arrest with aphidicolin (15 *m*g/ml, right-hand side) blocked MuLV but not FIV transduction. Percent transduction is shown at the bottom..... - 186 -

Figure 23: Vector dose escalation experiments. (a) Dose-escalation experiment with GINWF in primary cultured human TM cells. Shown are contact-inhibited TM cells at 1 month post transduction. The vector encodes enhanced (codon-humanized) green fluorescent protein (GFP) under the transcriptional control of the human CMV promoter. No toxicity was observed at any dose. ..... - 187 -

Figure 24: Transduction of human trabecular meshwork. *Left*: Representative TM biopsies obtained on day 3 after transduction. *Middle* and *right*: Representative chamber angles and histological sections, respectively, from eyes evaluated for reporter gene expression 16 days after transduction. TM, Trabecular meshwork; SC, Schlemm's canal. ..... - 189 -

Figure 25: Fluorophore-labeled anti-β-galactosidase antibody labeling of the trabecular meshwork 16 days after injection of 10^8 TU of FIV vector (a), 10^8 TU of HIV-1 vector (b), or 10^8 TU of MuLV vector (c) or mock FIV vector (d). SC, Schlemm's canal. ..... - 190 -

Figure 26: Dose response and trabecular meshwork preservation. Percent transduction (a) and total trabecular cells (b) in four eye pairs perfused with the indicated doses of vector. A section from each quadrant of an eye was counted and the mean was compared with the simultaneously perfused and untransduced fellow eye. Bars represent the SD. (c and d) TMs from a pair of fellow eyes perfused with medium alone (c) or 10^8 TU of FIV vector (d). ..... - 191 -

Figure 27: (a) Confocal microscopy view with frontal and sagittal view of TM 5 days after transduction with GiNWF and the TM in the fellow control eye. Imaging depth of 20 μm with wide pinhole. (b) Conventional fluorescence microscopic view. 400x magnification. ..... - 193 -

Figure 28: Chamber angles 5 days after injection of CT26 (a), and CT26.mock vector (b). Sections are stained with X-Gal to detect expression of β-galactosidase. SC, Schlemm's canal. ..... - 194 -

Figure 29: Intraocular pressure. (a) Recording of eye injected with CT26 and CT26.mock vector control. (b) Ratio of outflow facility (1/R) before transduction (C_0) and at recorded minimum (Cmin) and C0 and 72 hours after transduction (C72h). Outflow facility ratio of transduced eyes was significantly different from the control at the recorded minimum (*$P = 0.02$), but returned to stable baseline at 72 hours. ...- 195 -

Figure 30: Gonioscopic in vivo expression grades. GFP fluorescence in the TM of living cats was serially photographed and graded by direct gonioscopy (a cornea-shaped lens with a mirror is used to enable visualization of the anterior chamber angle). There was a high linear correlation ($R^2 = 0.9$) between expression grade and histologic transduction efficiency (grade 1, 2% ± 0.3%; grade 2, 21% ± 1%; grade , 39% ± 3%; and grade 4, 94% ± 5%). ..... - 196 -

Figure 31: View of trabecular meshwork in living animal in standard (top and bottom) and corresponding UV light gonioscopic views (center). All four quadrants from an eye with grade 4 expression after transduction with 10^8 TU are shown (SN = superionasal, IN = inferionasal, IT = inferiotemporal, ST = superiotemporal). Transduction was virtually complete and was confined to the TM. ..... - 197 -

Figure 32: Representative examples of reporter gene expression in animals in group 1 and 2. (a) Renilla GFP (right eye) and GFP (left eye) expression in group 1. (b) Paired comparison of GFP (right eye) and ß-galactosidase expression (left eye) in group 2. Shown are photos of TM as seen via UV light gonioscopy (the 13 day ß-galactosidase eye was fixed and stained with X-gal after sacrifice). Detectable Renilla GFP expression was always shorter-lived than that of GFP, while ß-galactosidase expression persisted longer than GFP only at the highest dose, when over-expression toxicity of GFP was observed. ..... - 199 -

Figure 33: Antibody labeling for GFP confirms gonioscopic extent of transduction. GFP expression was limited to the TM and collector channels. Comparison DAPI staining of transduced TM (left) and control TM (right) demonstrates preserved cellularity in GFP-expressing TM. AC = anterior chamber, P = plexus. ..... - 200 -

Figure 34: Rate of initial GFP accumulation determines whether successful long-term GFP expression is established. (a) Expression slowly reached peak levels in two cats from group 1 transduced with 10^8 TU GFP vector (right eye) and Renilla GFP vector (left eye), resulting in stable fluorescence of GFP, but not Renilla GFP. (b) Rapid GFP over-expression in animals of group 3 that were also transduced with 10^8 TU GFP vector triggered an iritis that eliminated transduced cells. Dotted red line illustrates onset of expression. Inserted photos show actual gonioscopic view of TM as indicated..... - 202 -

Figure 35: Antibody staining for T-cells (anti-CD3: a, b and c), macrophages (anti-myelomoncyte: d, e and f) and DAPI staining (g, h and i). Shown are sections from a TM transduced with eGFP (a, d and g) after loss of expression and the β-galactosidase transduced partner eye (b, e, h). Only the eGFP transduced TM is infiltrated by T-cells (a), but not macrophages (d), while there is no infiltrate in the other eye. Control c is an isotype control section from the same eGFP eye (c). Control f the corneo-conjunctival junction where macrophages are expected (f and i)..... - 203 -

Figure 36: Proportion of eyes transduced 2 and 7 days after either subretinal or intravitreal injection..... - 206 -

Figure 37: Representative eyes injected *subretinally* with (a) CT25 vector and (b) subretinal injection control, or injected *intravitreally* with (c) CT25 vector and (d) intravitreal injection control. Note the larger area of transduced retina with subretinal injection (a versus c, arrow). Endogenous β-galactosidase activity in the ciliary body was occasionally observed, and was equivalent in both uninjected and injected eyes, as seen in panels (b)–(d) (blue ring). ..... - 207 -

Figure 38: Examples of representative cross-sectional histology confirming transduction of the RPE. Paraffin sections (a and b) counterstained with neutral red showing β-galactosidase activity as blue stain within the RPE at both low power (a, 65x) and high power (b, 1100x). Antibody labeling for β-galactosidase confirmed limitation of marker gene expression to the RPE (400x; INL = inner nuclear layer, ONL = outer nuclear layer, RPE = retinal pigment epithelium). CT25 injected eye with (c) anti-β-galactosidase antibody staining and (d) DAPI counterstain. (e, f) Non-injected control eye..... - 208 -

Figure 39: Cross-sectional histology (a and d) and whole eye cups (b, c and e, f) of representative eyes 3 (a–c) and 7 months (d–f) after subretinal injection with CT25 vector (b and e), and CT25.D66V (c and f). Vector particles, which differ in only one amino acid, were normalized to equal RT units. ..... - 209 -

Figure 40: Time course of β-galactosidase expression. FIV is shown in panel A, and Ad vectors are shown in panel B. Circle sizes represent the number of animals at each grade. FIV expression reached a maximum extent at 3 months and then decreased, while expression from Ad vectors reached its maximum extent at 1 week. ..... - 211 -

Figure 41: Representative eye cups and histological sections through the transduced retina of eye pairs from the same animal. Right eyes were injected with FIV, left eyes with Ad vector. When a retinal detachment was present in the section, images of neurosensory retina and RPE are shown in their normal spatial relationship. Insert: large, macrophage-like cells with abundant cytoplasm appeared to contain phagocytosed β-galactosidase positive material (arrows). Macrophage infiltrates were often seen in Ad transduced eyes after 3 months. Abbreviations (for control eye section): GCL = retinal ganglion cell layer, INL = inner nuclear cell layer, ONL = outer nuclear layer, PR = photoreceptor outer segments, RPE = retinal pigment epithelium. ..... - 214 -

3. Tables

Table 1: Specific diseases addressed in current gene therapy trials. .....- 100 -

Table 2: Lentiviral vector trials.....- 102 -

Table 3: Paired comparison of retroviral vectors – percent transduction after injection of 10^8 TU per eye. a) Percent transduction values for the individual eyes represent means 6 SD of counts from four TM sections, one from each eye quadrant. b) Aggregate mean 6 SEM was derived for each three-eye set. .....- 192 -

Table 4: Characteristics of transgene expression imaged serially in vivo. .....- 200 -

Table 5: Differences of eGFP expression. SIN modification of the FIV-LTR slightly improves eGFP expression levels from internal CMV.eGFP.IRES.neo cassette. Cpm/ml = counts per minute per ml in RT assay, eGFP TU/ml = eGFP transducing units per ml determined with flow cytometry, GINWF = internal CMV.eGFP.IRES.neo cassette, FGINSIN = internal CMV.eGFP.IRES.neo cassette.- 204 -

4. Publications

4.1. Papers

Khare P., **Loewen N.**, Teo W., Barraza R., Saenz D.T., Johnson D.H., Poeschla E.M. Durable, Safe, Multi-gene Lentiviral Vector Expression for Over Two Years in Feline Trabecular Meshwork. Molecular Medicine.

Loewen N., Chen J., Dudley V.J., Sarthy V.P., Mathura J.R., Jr. Angiogenic Network in Hypoxic Müller Cells Involves the Very Low Density Lipoprotein Receptor. Submitted.

Fautsch MP, Bahler CK, Vrabel AM, Howell KG, Loewen N, Teo WL, Poeschla EM, Johnson DH. Perfusion of HIS-tagged eukaryotic myocilin increases outflow resistance in human anterior segments in the presence of aqueous humor. Invest Ophthalmol Vis Sci. 2006 Jan;47(1):213-21.

Loewen N., Poeschla E.M. Lentiviral Vectors. Adv Biochem Eng Biotechnol. 2005;99:169-91.

Loewen N., Fautsch M.P., Teo W., Bahler C.K., Johnson D.H., Poeschla E.M. Long-term, targeted genetic modification of the aqueous humor outflow tract coupled with non-invasive imaging of gene expression in vivo. Invest Ophthalmol Vis Sci. 2004 Sep;45(9):3091-98.

Loewen N., Leske D.A., Cameron J.D., Chen Y., Teo W., Fautsch M.P, Poeschla E.M., Holmes J.M. Long-term retinal transgene expression with FIV versus adenoviral vectors. Mol Vis. 2004 Apr 13;10:272-80.

Saenz D.T., **Loewen N.**, Peretz M., Whitwam T., Howell K.G., Holmes J.M., Good M., Poeschla E.M. Unintegrated lentiviral DNA persistence and accessibility to expression in nondividing cells: analysis with class I integrase mutants. J. Virol. 2004 Mar;78(6):2906-20.

Loewen N., Leske D.A., Chen Y., Teo W., Saenz D.T., Peretz M., Holmes J.M., Poeschla E.M. Comparison of wild type and class I integrase mutant-FIV vectors in retina demonstrates sustained expression of integrated transgenes in retinal pigment epithelium. J Gene Med. 2003 Dec;5(12):1009-17.

Loewen N., Bahler C., Teo W., Whitwam T., Peretz M., Xu R., Fautsch M., Johnson D.J., Poeschla E.M. Preservation of aqueous outflow facility after second-generation FIV vector-mediated expression of marker genes in anterior segments of human eyes. Invest Ophthalmol Vis Sci. 2002 Dec;43(12):3686-90.

Loewen N., Fautsch M.P., Peretz M., Bahler C.K., Cameron J.D., Johnson D.H., Poeschla E.M. Genetic modification of human trabecular meshwork with lentiviral vectors. Hum Gene Ther. 2001 Nov 20; 12(17): 2109-19.

Barry J.C., **Loewen N.** The use of cycloplegic agents. Results of a 1999 survey of German-speaking centers for pediatric ophthalmology and strabology. Klin Monatsbl Augenheilkd 2001 Jan; 218(1): 26-30.

Loewen N., Barry J.C. The use of cycloplegic agents. Results of a 1999 survey of German-speaking centers for pediatric ophthalmology and strabology. Strabismus 2000 Jun; 8(2):91-9.

4.2. Chapters

Saenz D.T., Barraza R., **Loewen N.,** Teo W., Poeschla E.M. Production and Use of Feline Immunodeficiency Virus (FIV)-Based Lentiviral Vectors. Cold Spring Harbor Press. In Press.

Loewen N., Barraza R., Whitwam T., Saenz, D.T., Kemler I., Poeschla E.M. FIV Vectors. In M. Federico: Lentiviral gene engineering protocols. Humana Press, USA, 2002: 251-273.

4.3. Patents

A highly engineered FIV vector system useful for delivering genes to cells (co-inventor, patent application 9/2004, Mayo Medical Venture # MMV-04-133).

An Auto-Regulated, Doxycycline-Inducible FIV-Based Lentiviral Vector (co-inventor, patent application 6/2002, Mayo Medical Venture # MMV-02-098).

4.4. Abstracts

Loewen N., Chen J., Dudley V.J., Sarthy V.J., Mathura J.R. Jr Angiogenic Network in Hypoxic Müller Cells Involves the Very Low Density Lipoprotein Receptor. Association for Research and Vision in Ophthalmology 2007. Fort Lauderdale, Florida, USA. Poster.

Loewen N., Mehta M.P., Dudley V.J., Mathura J.R. Jr. VLDLR and TRIB3 is Expressed in Rat Mueller Cells and Upregulated in Hypoxia. Association for Research and Vision in Ophthalmology 2006. Fort Lauderdale, Florida, USA. Poster.

Khare P.D., **Loewen N.**, Barraza R., Fautsch M., Johnson D.H., Poeschla E.M. A Glaucoma Gene Therapy Model: Eighteen Cat Study Revealing Long-Term Targeted Genetic Modification of the Anterior Chamber by Lentiviral Vectors. American Society for Gene Therapy 2006, Baltimore, MD, USA. Talk.

Khare P.D., **Loewen N.**, Poeschla E.M. Suppression of Human Pancreatic Cancer Growth by Lentiviral Vector-Mediated Gene Transfer of Pigment Epithelium Derived Factor (PEDF). American Society for Gene Therapy 2006, Baltimore, MD, USA.

Poeschla E.M., **Loewen N.**, Rasmussen C., Teo W., Khare P., Kaufman P.L. Transduction of Nonhuman Primate Trabecular Meshwork With Lentiviral Vectors. Association for Research and Vision in Ophthalmology 2006. Fort Lauderdale, Florida, USA. *Talk.*

Khare P, Teo W, **Loewen N.**, Barraza R., Fautsch MP, Johnson D.H., Poeschla E.M. Long-Term Genetic Modification of Trabecular Meshwork by Lentiviral Vectors: An 18 Cat Study. Association for Research and Vision in Ophthalmology 2006. Fort Lauderdale, Florida, USA. *Talk.*

Fautsch M.P., Bahler C.K., Vrabel A.M., Howell K.G., **Loewen N.**, Poeschla E.M., Johnson D.H. Recombinant Myocilin Purified From Human Trabecular Meshwork Cells Increases Outflow Resistance in Human Anterior Segments but Only in the Presence of Aqueous Humor. Association for Research and Vision in Ophthalmology 2005. Fort Lauderdale, Florida, USA. *Talk.*

Loewen N., Fautsch M.P., Teo W., Bahler C.K., Johnson D.H., Poeschla E.M. Long-Term. Genetic Modification of the Ocular Outflow Tract Coupled with Non-Invasive

Real-Time Imaging of Gene Expression. American Society of Gene Therapy 2004, Minneapolis, Minnesota. *Talk.*

Saenz D., **Loewen N.**, Leske D., Good M., Howell K., Holmes J.M., Poeschla E.M. Cell Cycle-Dependent Transcription from Unintegrated Lentiviral Vector DNA Internal Promoters: Analyses with Class I Integrase Mutants. American Society of Gene Therapy 2004, Minneapolis, Minnesota. *Talk.*

Saenz D., **Loewen N.**, Leske D., Good M., Holmes J.M., Poeschla E.M. Class I lentiviral integrase mutants reveal cell-cycle dependent expression from persistent unintegrated proviral DNA: implications for HIV-1. International Workshop on HIV Persistence during Therapy 2004. Saint Martin, French West Indies. *Talk.*

Poeschla E.M., Fautsch M.P., **Loewen N.**, Teo W., Johnson D.H. Wild-type and mutant myocilin co-expression causes heterodimer formation and intracellular retention of wild-type protein without impairing proteasome function. Association for Research and Vision in Ophthalmology 2003. Fort Lauderdale, Florida, USA. Poster.

Loewen N., Teo W., Fautsch M.P., Bahler C.K., Johnson D.H., Poeschla E.M. Dose-dependent, transgene specific in vivo toxicity in FIV transduced feline TM. Association for Research and Vision in Ophthalmology 2003. Fort Lauderdale, Florida, USA. Poster.

Saenz D., **Loewen N.**, Barraza R., Teo W., Whitwam T., Peretz M., Poeschla E. Markedly cell cycle-dependent expression phenotypes of class-I-integrase mutants of 2 lentiviruses (FIV, HIV): wild-type level expression from unintegrated lentiviral DNA. 10^{th} Conference on Retroviruses and Opportunistic Infections 2002, Boston, USA. Poster.

Loewen N., Bahler CK., Teo W., Whitwam T., Barraza R., Fautsch MF., Peretz M., Johnson DH., Poeschla EM. Second-Generation FIV vectors: Expression of eGFP in TM of Domestic Cats and Effects on Aqueous Outflow Facility in Human Anterior Segments. International Congress of Eye Research 2002, Geneva, Switzerland. *Talk.*

Holmes JM., **Loewen N.**, Leske DA., Teo W., Saenz T., Peretz M., Chen Y., Poeschla EM. Genomic integration and sustained transgene expression using an FIV-based lentiviral vector in retinal gene therapy. International Congress of Eye Research 2002, Geneva, Switzerland. Poster.

Loewen N., Chen Y., Leske DA., Poeschla EM., Holmes JM. Increase of Neovascularization by Subretinal Injection in a Rat Model for Gene Therapy of Retinal Neovascularization (NV). American Society of Gene Therapy 2002, Boston, Massachusetts. Poster.

Saenz D., **Loewen N.**, Poeschla E. An auto-regulated, doxycycline-inducible FIV-based lentiviral vector. American Society of Gene Therapy 2002, Boston, Massachusetts. Poster.

Loewen N., Leske DA., Chen Y., Saenz DT., Teo W., Fautsch MP., Holmes JM., Poeschla EM. Retinal gene expression after transduction with FIV and control FIV (class I integrase mutant) vectors: comparison to adenovirus vectors and validation of an important control for FIV vectors. American Society of Gene Therapy 2002, Boston, Massachusetts. Poster.

Saenz D., **Loewen N.**, Poeschla E. A class I FIV integrase mutant reveals short-term gene expression from unintegrated lentiviral vector DNA in non-dividing cells. American Society of Gene Therapy 2002, Boston, Massachusetts. *Talk.*

Loewen N., Bahler CK., Teo W., Whitwam T., Barraza R., Fautsch MF., Peretz M., Johnson DH., Poeschla EM. Transduction of Human and Feline Eye Trabecular Meshwork with a Second Generation FIV Vector System: Effects on Aqueous Outflow and Monitoring of Expression in Live Animals. American Society of Gene Therapy 2002, Boston, Massachusetts. Poster.

Holmes JM., Chen Y., **Loewen N.**, Leske DA., Poeschla EM. Subretinal Injection Increases Neovascularization in Oxygen-Induced Retinopathy in the Neonatal Rat. Association for Research and Vision in Ophthalmology 2002. Fort Lauderdale, Florida, USA. Poster.

Leske DA., **Loewen N.**, Chen Y., Fautsch MP., Poeschla EM., Holmes JM.. Comparison of FIV and Adenovirus Mediated Long Term Transgene Expression in the Neonatal Rat Retina. Association for Research and Vision in Ophthalmology 2002. Fort Lauderdale, Florida, USA. Poster.

Loewen N., Fautsch MP., Bahler CK., Johnson DH., Poeschla EM. Effects of FIV-Based Lentiviral Vector Transduction of Trabecular Meshwork on Aqueous Outflow Facility and In Vivo Monitoring of Expression in Cats. Association for Research and Vision in Ophthalmology 2002. Fort Lauderdale, Florida, USA. *Talk.*

Loewen N., Saenz DT., Poeschla EM. A tetracycline inducible FIV-based lentiviral vector with full autoregulation of all components. Building Bridges Research Forum 2001, Mayo Foundation, Rochester, Minnesota. Poster.

Whitwam T.A, Peretz M., **Loewen N.**, Poeschla EM. Identification and Characterization of a Central DNA Flap in Feline Immunodeficiency Virus. Keystone Meeting 2001, Colorado. Poster.

Whitwam T.A, Peretz M., **Loewen N.**, Poeschla EM. Identification and Characterization of a Central DNA Flap in Feline Immunodeficiency Virus. American Society of Gene Therapy 2001, Seattle, Washington. *Talk.*

Loewen N., Fautsch M., Xu R., Johnson DH., Poeschla EM. Transduction of Human Trabecular Meshwork with Lentiviral Vectors. American Society of Gene Therapy 2001, Seattle, Washington. *Talk.*

Loewen N., Good M.S., Krebsbach V., Poeschla E.M., Johnson D.H. Transduction of retinal ganglion cells in culture using feline immunodeficiency virus. American Society of Gene Therapy 2001, Seattle, Washington. *Talk.*

Loewen N., Leske D.A., Chen Y., Poeschla E.M., Holmes J.M. Gene transfer into neonatal rat retina using a lentiviral FIV vector. American Society of Gene Therapy 2001, Seattle, Washington. Poster.

Leske D.A., **Loewen N.**, Chen Y., Poeschla E.M., Holmes J.M. Gene transfer into neonatal rat retina using a lentiviral FIV vector. Association for Research and Vision in Ophthalmology 2001. Fort Lauderdale, Florida, USA. *Talk.*

Good M.S., Krebsbach V., **Loewen N.**, Poeschla E.M., Johnson D.H. Transduction of retinal ganglion cells in culture using feline immunodeficiency virus. American Glaucoma Association, California, USA, 2001. *Talk.*

Loewen N., Fautsch M., Xu R., Johnson DH., Poeschla EM. Comparison of lentiviral, type C retroviral, and adenoviral vectors for transduction of human trabecular meshwork. Association for Research and Vision in Ophthalmology 2001. Fort Lauderdale, Florida, USA. *Talk.*

Loewen N., Cameron JD., Fautsch M., Johnson DH., Poeschla EM. Highly Efficient Transduction of the Human Trabecular Meshwork with a New Minimal Lentiviral FIV Vector: Preclinical Investigations of Gene Therapy for Glaucoma and Rating of

Different Vectors in a Human Eye Explant Model. From Molecule to Mankind 2000. Rochester, Minnesota, USA. Poster.

Loewen N., Cameron JD., Fautsch M., Johnson DH., Poeschla EM. Minimal FIV Vector for the Transduction of the Trabecular Meshwork in a Human Eye Explant Model: Preclinical Investigations of Gene Therapy for Glaucoma. Stockholm, Sweden. 8th Meeting of the European Society of Gene Therapy, J Gene Med. 2000;2(5 Suppl):39. Poster.

Loewen N., Fauser S. Ocular Gene Therapy with FIV. Bonn, Conference of the Federal Department of Research and Education, 1999. Poster.

Loewen N., Dietrich TJ., Seelig B., Schiefer U. Fundus-oriented perimetry (FOP) for early detection of visual field defects in glaucoma. Berlin, Germany. 97th Conference of the German Society of Ophthalmology, 1999. *Talk.*

Loewen N., Barry JC. The use of cycloplegic agents. Results Of a 1999 survey of German-speaking centers for pediatric ophthalmology and strabology. Cologne, Germany. 7th Conference of the Bielschowsky-Society, 1999. *Talk.*

Loewen N., Weirich J. Heterogeneity of the electric activity within the ventricular wall: regionally different proarrhythmic effects of a potassium channel blockage of the fast component of the delayed rectifier. Vienna, Austria. 21st Conference of the Austrian Society of Cardiology, 1997. Poster.

Loewen N., Weirich J. Electrophysiological properties of slices from the deep myocardium of the ventricular wall: regionally different effects of potassium channel blockage with the class-III antiarrhythmic MK499. Mannheim, Germany. 63rd Conference of the German Society of Cardiology, 1995. *Talk.*

5. Acknowledgements

I am deeply indebted to my mentor, Dr. Eric Poeschla, for allowing me to join his laboratory to participate in the dawn of non-human primate lentiviral gene therapy. His continued guidance and advice throughout my research with him was crucial in refining early vectors and applying them to models of chronic ocular disease.

Dr. Poeschla is a role model of a clinician scientist who is able to translate ideas from the laboratory to the bedside. My time with him has increased my enthusiasm for basic science and confirmed my intention to pursue an academic career. I would like to thank all members in Dr. Poeschla's laboratory, in particular Dr. Todd Whitwam for collaborating on transfer vector development and allowing me to incorporate the central polypurine tract modification into vectors used in my thesis, Dr. Iris Kemler, for making a minimal packaging sequence available that I used in my transfer vectors, Dr. Dyana T. Saenz for her collaboration on exploring properties of the D66V integrase mutant that I created, Roman Barraza for his modification of the packaging vector used here, Wu-Lin Teo for his assistance with vector production and animal husbandry and Mary Peretz for her help with plasmid purification. Individual contributions will be pointed out in this thesis where they occurred.

I would like to further acknowledge Dr. Douglas Johnson for his mentorship and guidance of my dual interest in glaucoma and lentiviral gene therapy. He helped to apply lentiviral vector methodology to an area that has been insufficiently addressed in the past. He allowed me to use his models and techniques to explore our ideas and generously provided his own laboratory's personnel and equipment for this purpose. A clinician scientist himself, Dr. Johnson has corroborated my direction towards an career as a glaucoma specialist. I would like to thank the scientists in Dr. Johnson's laboratory, in particular Dr. Michael Fautsch, for all his help and advice and Cindy Bahler for her help in culturing human anterior segments.

I am grateful to Dr. Jonathan Holmes for his guidance in exploring lentiviral gene transfer in models of ocular neovascularization. My thanks extent to him and his laboratory, in particular to David Leske, for having provided resources, knowledge and help for this endeavor. Dr. Holmes has also provided me with invaluable advice to shape my clinical career.

Finally, I would like to thank my wife and my family for their patience, understanding and support during this time.

6. Introduction

At the center of this thesis was the realization that the current treatment modalities for several chronic eye diseases still resulted in progressive visual loss. These include glaucoma in particular and various degenerative but also vasoproliferative disorders of the retina and choroid in general. The knowledge of the genetic defects and resulting molecular pathology of these diseases had dramatically increased in the preceding years. At the same time new tools had become available to manipulate cellular pathology on its most basic level in the form of viral vectors. When in 1998 Dr. Eric M. Poeschla developed the first non-primate lentiviral vector that promised to combine both the power of permanent genetic modification and safety of being non-pathogenic in humans,[1] I decided to pursue my idea of lentiviral gene therapy for these diseases and moved from Germany to start my studies in Dr. Poeschla's laboratory.

The following will introduce the reader to the structure of the eye, to glaucoma and choroidal and retinal diseases and to ocular gene therapy.

6.1. Eye Structure and Function

I will review the eye structure and function that is relevant to this thesis as well as diseases affecting them in the following. The ocular outflow tract for which I developed genetic long-term modification is situated in the *anterior segment* of the eye. In contrast, the retinal pigment epithelium is situated in the *posterior segment* underlying the neuroretina. The most applicable diseases that affect these structures are glaucoma, a progressive optic neuropathy caused by intraocular pressure that is relatively too high for the affected eye, and degenerative as well as vasoproliferative diseases of the retina that originate in the retinal pigment epithelium.

Glaucoma is typically caused by a decreased outflow facility in the anterior segment but causes degeneration of retinal ganglion cell axons in the posterior segment. Degenerative and vasoproliferative eye diseases are for the most part limited to the posterior segment but may progress to engulf the anterior segment at advanced stages.

6.1.1. Overview of the Mammalian Eye Anatomy

6.1.1.1. Tunicas of the Eye

The mammalian eye consists of three separate layers that serve different functions: the *fibrous tunic*, the *vascular tunic*, and the *nervous tunic*.

The *fibrous tunic* is the most outer layer of the globe and consists of cornea and sclera giving the eye its rigidity and spherical shape. It is composed of dense connective tissue that contains collagen as its main component.

The *vascular tunic* is the middle layer of the eye and includes the iris, the ciliary body and the choroid. The iris regulates the amount of light that enters the eye but is also coupled to accommodation to increase depth of field and image quality. As discussed in more detail below, the ciliary body produces the aqueous humor and serves accommodation by allowing the lens to change shape and. The choroid holds a dense vascular network that provides high blood flow to supply the retina with oxygen and metabolites but also to maintain a consistent temperature. The choroid has a high concentration of melanocytes to minimize light scatter.

The *nervous tunic* consists of the neuroretina that captures the light with the first neuron of the visual pathway, the photoreceptor, processes it as described below and further conducts these signals via the second neuron, the bipolar cell and the third neuron, the retinal ganglion cell, the axons of which form the optic nerve.

6.1.1.2. Anterior and Posterior Segment

Division of the eye into *anterior* and *posterior segment* is somewhat arbitrary but provides useful categories in ophthalmology. The anterior segment can be thought of as the active part responsible for focusing light and maintaining that function, while the posterior segment has a more passive function consisting of receiving and processing light.

The anterior third of the eye is called the *anterior segment* and includes the cornea, the anterior chamber, the trabecular meshwork, Schlemm's canal, the iris, the lens and the posterior chamber, a space between the iris and the anterior vitreous face. The air-cornea interface is the main refractive part of the eye, while the lens adds to this and allows change of focal length by accommodation. The ciliary body and the outflow system are discussed in detail below.

The *posterior segment* comprises the posterior two-thirds of the eye from the anterior hyaloid membrane onward and includes the vitreous, retina, choroid, sclera and optic nerve.

6.1.2. Aqueous Humor Production and Outflow

Intraocular pressure is dependent on aqueous humor production and its outflow. Aqueous humor is produced by the ciliary body.[2] The trabecular meshwork is the principal, pressure-dependent path for aqueous egress and represents the structure by whose resistance intraocular pressure is maintained. Flow is affected by the interaction of the ciliary body and its tendinous connections to the trabecular meshwork.

Besides production of aqueous humor other functions of the ciliary body are accommodation by interaction with the crystalline lens via zonular fibers and alteration of aqueous outflow through the trabecular meshwork.

Anatomically, the ciliary body can be subdivided into the pars plicata and pars plana. The pars plicata contains between 70 and 80 major and minor ridges on its inner surface that extend into the posterior chamber of the eye by about 1 mm. The pars plana has a flat inner surface and the ciliary body is much thinner and less vascularized than the pars plicata. Zonulae that hold the crystalline lens originate as a continuous layer on the surface of the pars plana and run into the valleys between the ciliary processes from where they are directed towards the lens equator where they insert directly at, anterior and posterior to it.

The ciliary body possesses ciliary processes with a fibrovascular core that is continuous with the ciliary body stroma and covered by a bi-layered epithelium. As a result of the invagination of the optic cup during embryogenesis, the ciliary epithelia consist of a double layer that is joined apically while the basement membrane of the inner, non-pigmented epithelium is facing the posterior chamber. The vasculature is connected to the major circle of the iris,[3] and served by a set of anterior and posterior arterioles[4] which supply the large diameter capillaries (near the crest of the processes) and the smaller caliber capillaries deep within each process, respectively. Blood flows toward the network of choroidal veins to leave the eye via the vortex veins. A

sphincter-like system regulates blood flow that allows adjustment of filtration pressure and consequentially, aqueous humor production.[4-6]

As other capillaries from the posterior arterioles, the capillaries of the ciliary muscle are non-fenestrated and impermeable to plasma proteins. However, the capillaries from the anterior arteriole in the stromal core of the ciliary processes lack tight junctions and are instead lined by fenestrated endothelial cells, allowing passage of macromolecules, ions and water. The ciliary non-pigmented epithelium serves as a selective barrier. It forms the blood-aqueous barrier in the ciliary body[7] with zonulae occludentes, adherentes and desmosomes.[8, 9] Primarily the epithelium at the tip of the ciliary processes contains carbonic anhydrase, a pharmacological target in glaucoma[10-12] and Na-K-ATPase to produce aqueous humor. Aqueous humor is a clear, water like fluid to provide good optical properties but it still has to provide nutrients to the avascular tissues of the eye. Although the total protein content of aqueous humor is less than 1% of that in plasma to prevent light scatter, the free amino acid levels are almost equivalent.[13] Disruption of the junctional complexes that form the blood-aqueous barrier in intraocular inflammation results in leaking of macro-proteins and flare that can be observed at the slit lamp.[14]
Despite the increased leakiness during inflammation, intraocular pressure is usually lower, not higher because gap junctions that serve intercellular metabolic and electronic coupling of ciliary epithelial cells disappear,[15, 16] resulting in reduced aqueous humor net production and decreased intraocular pressure.[14]

Aqueous humor leaves the eye via two routes, the uveoscleral and the conventional outflow tract. It is estimated that under normal conditions about 10% of total aqueous outflow occurs via the uveoscleral pathway by absorption into uveal tissues[17, 18] which may increase to as much as 60% during intraocular inflammation or pharmacologically by analogous substances such as prostaglandins and prostamides. Ninety percent pass the trabecular meshwork into the circumferential Schlemm's canal and subsequently via circuitous channels toward the surface of the sclera where they join the circulation of the episcleral vasculature. Flow through the uveoscleral pathway is essentially pressure independent.[17-19] Flow occurs from the posterior chamber through the pupil and anterior chamber directly into the ciliary muscle to follow connective tissue fascicles that collect toward the supraciliary space which is contiguous with the suprachoroidal space. From here, the aqueous exits the

eye either by diffusing through the sclera or through the scleral emissaria of the vortex veins. Prostaglandin analogues in the medical treatment of glaucoma increase the uveoscleral outflow through up-regulation of matrix metalloproteinases that break down extracellular matrix material facilitating fluid movement through the interstitial space of the ciliary muscle.[20, 21]

In conventional outflow, aqueous drains through the trabecular meshwork of the iridocorneal angle. Because the flow occurs down a pressure gradient, any obstruction at the level of the trabecular meshwork such as blood or lens proteins or further downstream obstacles such as 360 degree encircling buckles used for retinal detachment repair, intentional episcleral vein cauterization for creation of glaucoma models or carotid-cavernous sinus fistulas can lead to increased intraocular pressure and glaucoma.

The trabecular meshwork is a wedge-shaped tissue band that bridges the anterior chamber angle connecting the peripheral edge of Descemet's membrane of the cornea (Schwalbe's line) anteriorly and the scleral spur, ciliary body and iris stroma posteriorly. Iris processes are often seen that attach to the beams of the trabecular meshwork. The innermost trabecular meshwork is termed uveoscleral trabecular meshwork as its beams project into the stroma of the ciliary body and iris which are both part of the uvea. Trabecular meshwork posterior to an imaginative line between Schwalbe's line and the scleral spur is called corneoscleral meshwork. Contraction of longitudinal meshwork bundles of the ciliary muscle will pull the scleral spur posterior and consecutively stretch the uveoscleral and corneoscleral meshwork, a mechanism by which miotics can increase conventional outflow.

Cord-like beams of collagen and elastin that branch and connect to each other form the backbone of the uveoscleral meshwork and are coated by endothelial cells capable of phacocytosis.[22] Similar to the corneal endothelium, these cells are nondividing and subject to age related attrition.[23] It is not clear whether this contributes to the development of glaucoma.[24, 25] The larger spaces of the most inner trabecular meshwork become smaller towards Schlemm's canal.[26] The juxtacanalicular trabecular meshwork directly overlying Schlemm's canal is fundamentally different consisting of an open connective tissue matrix with fibroblast-like cells rather than endothelial cells. Despite this difference, tendons from the longitudinal bundle of the ciliary muscle extend also into the juxtacanalicular trabecular meshwork and system

of elastic fibers that insert into the inner wall of Schlemm's canal termed the cribiform plexus.[27] The juxtacanalicular meshwork is the main source of outflow resistance.[28] Past suggestions that increase in outflow resistance in primary open angle glaucoma derive from accumulation of extracellular matrix material in the open spaces of the uveal and corneoscleral trabecular meshwork have recently been shown to be problematic as the hyaluronans decrease with age and POAG.[29-31] Aqueous humor passes through the juxtacanalicular trabecular meshwork and the inner wall of Schlemm's canal through micropores in unique giant vacuoles that form pressure-dependent[32, 33] and energy independent.

Around 30 external collector channels drain from the outer wall of Schlemm's canal towards the scleral surface into a deep scleral plexus that leads to the deep scleral veins and eventually to the episcleral veins. Despite this small caliber vascular network and its ability to regulate flow[34] the vast majority of the conventional outflow resistance is the trabecular meshwork.[35] Several unique vessels termed the aqueous veins of Ascher bypass the deep scleral plexus directly into the episcleral veins that can easily identified during slit lamp exam by their dual string of blood and aqueous humor that yet has to mix.

6.1.3. Central Fundus and Optic Nerve Head in Glaucoma

The approximately 1 to 1.5 million axons that form the optic nerve from the retinal ganglion cells run towards the optic disc in a characteristic pattern. Axons that originate nasal from the fovea take a direct course toward the disc, while ones that originate more temporal to the fovea arc around the macula and enter the upper and lower pole of the optic nerve. The macula axons run directly to the temporal quadrant of the disc in the papillomacular bundle. Retinal ganglion cell axons are organized in a retinotopic pattern throughout the visual pathway.[36-39] Axons are grouped together by sheets of Muller cells[40-45] which gives the retina a striated pattern[46] during funduscopic examination. This striation is most prominent near the nerve fiber layer is thickest. This is the most common site of the typical notching when retinal ganglion cell loss occurs in glaucoma. The polarizing properties of this striated fiber layer and its loss is utilized in nerve fiber analyzer strategies (retinal scanning laser polarimetry).[47, 48] It can most commonly be observed at the inferior and superior

arcuate bundles.[49-54] The reflective properties is determined by the cylindrical nature and size of axonal microtubules producing a directional, spectral and polarization (retardation).[47, 55-57]

Localized damage to retinal never fiber bundles or in the optic disc cause well circumscribed scotomas, while more diffuse pressure on the posterior optic nerve e.g. by a mass lesion or demyelinating disease produces a central scotoma and diffuse visual dysfunction of the macula such as impaired color vision and decreased visual acuity. Axons exit the eye through a chorioscleral canal that passes through the outer retina, the pigment epithelium, Bruch's membrane, the choriocapillaris, the outer choroid and the sclera. It is variable in size resulting in a cup-disc ration that is used clinically to quantify likeliness of axonal loss. A typical optic disc has a vertical size between 1.5 to 2 mm and a cup to disc ration that does not exceed 0.5 but varies depending on the relation of size of the chorioscleral canal and space required for axons, supporting glial cells and vessels.[58, 59] To accommodate the greater number of axons entering the superior and inferior pole the chorioscleral canal usually is taller than wide giving it an oval shape.[60] The neuroretinal rim is usually the greatest inferior, superior, nasal and temporal rim which has been termed the "ISNT" rule.[61]

Increased intraocular pressure can result in increase of the physiological cupping or take on more focal changes at the neuroretinal rim in glaucoma. Conversely, lowering intraocular pressure can halt axonal loss[62, 63] although apoptosis may contribute to continuing fiber loss even if the initial trigger is removed.[64] There is considerable individual variation between actual height of intraocular pressure and anatomic and functional changes typical of glaucoma: while about half of eyes with an IOP greater than 35 mm Hg will develop glaucoma, others can suffer degeneration of the optic nerve with IOP in the statistically normal range ("normal tension glaucoma").[65] Known risk factors for glaucomatous optic nerve damage include reduced central corneal thickness[66], family history of glaucoma and impaired microcirculation.[67-70] In typical glaucoma, damage occurs over a prolonged period of time. Progression can be associated with splinter hemorrhages that appear at the optic disc.[71, 72] Typical axonal loss occurs in the upper and lower quadrants resulting in a vertical increase of the cup[60] with corresponding arcuate loss of retinal ganglion cells. However, when

axonal loss is diffuse, the cup expands concentrically,[73] resulting in a generalized visual field depression.

In addition to change of visual threshold as measured in standard visual field testing, contrast sensitivity, acuity and color sense are among the functions lost.[74] Detection is more challenging with diffuse axonal loss unless a baseline has been established in that person with prior visual fields. Comparison to the opposite eye must take into account that this eye, too, may be affected by glaucoma. In contrast a circumscribed axonal loss with a well defined arcuate scotoma may be detected much earlier. The combination of visual field testing and funduscopic examination is usually able to detect glaucoma at a relatively early stage by corresponding visual field loss and cupping, asymmetry of age-adjusted field depression in upper and lower fields, asymmetry of cupping and field loss between the two eyes consistent with asymmetric intraocular pressure or simply by a change from baseline photography or threshold perimetry. Any interpretation must take other causes of visual depression into account such as amblyopia and different media clarity (e.g. cataracts), anisometropia.

6.1.4. Anatomy, Cell Biology and Function of the Retina

The following describes the anatomy, cell biology and function of the retina relevant to the use of lentiviral vectors for transduction of the retinal pigment epithelium and retina. This chapter includes the description of the human macula because of its relevance in leading causes of blindness as it is the object of intense focus of novel therapies including gene therapy. However, the murine eye that is used in this thesis as a model does not have a macula. The retinal histology is otherwise very similar.

The retina is derived from the optic vesicle that develops from the diencephalon in humans around 25 days of fetal development. The optic vesicle then invaginates in the fourth week to form a cup resulting in an inner and outer wall. The inner wall further differentiates into the multi-layered neurosensory retina, while the outer wall becomes the retinal pigment epithelium. The two walls can later separate again creating a retinal detachment from various causes such as vitreoretinal traction, subretinal exudation or a retinal hole that allows fluid to access this potential space. Surgically,

this space can be used to subretinally inject vectors,[75, 76] insert implants,[77-79] remove neovascular membranes[80] and to facilitate retinal translocation.[81, 82]

The retinal pigment epithelium (RPE) is a monolayer of hexagonal cells that extends from the margin of the optic disc to the ora serrata, where it is continuous with the pigmented epithelium of the pars plana of the ciliary body. The RPE cells are cuboidal in cross section and joined near their apical margins by junctional complexes that include maculae and zonulae adherentes (intermediate spot and belt junctions, respectively), as well as zonulae occludentes (tight junctions). The zonulae occludentes between RPE cells form the outer blood-retinal barrier that is impermeable to water, ions and proteins. RPE cells are polarized cells that phagocytose shed outer segments with their long microvilli and provide the matrix surrounding the photoreceptor inner and outer segments. They also participate in the vitamin A metabolism and absorb light.[83] RPE cells are smaller and contain more melanin in the macula and are flatter and about 4 times wider with less pigment in the periphery. There is a relatively constant ratio of 45 photoreceptors per RPE cell throughout the retina.[84]

RPE cells may accumulate lipofuscin granules over times which represent residual outer segment lipids that are incompletely digested. The highest density of those can be found in the macula. Because of this association, it has been suggested to contribute to macular degeneration.[85] Ion pumps and passive ion channels cause water movement across the RPE towards the choroid, promoting adhesion of the neurosensory retina and RPE.[84]

The potential space into which FIV vectors were injected in this thesis is delineated by the zonulae occludentes (tight junctions) of RPE cells and by the external limiting membrane formed by the intermediate junctions (zonulae adherentes) between photoreceptor inner segments and Muller cell apical processes.[86] This space is filled with various proteins, glycoproteins, enzymes, glycosaminoglycans and proteoglycans that surround the rod and cone inner and outer segments and are called the interphotoreceptor matrix. Vitamin a transport between photoreceptors and RPE is enabled by the interphotoreceptor-retinoid binding protein of the interphotoreceptor matrix. Matrix sheaths surround the individual photoreceptor outer segments to maintain outer segment orientation and to isolate individual photoreceptor segments but also contribute to the attachment of photoreceptors to RPE cells.[87]

Rods and cones are the two types of photoreceptors found in vertebrate retinas. Rods are used in low light (scotopic) and cones in bright light (photopic) vision and allow to discern colors as they contain different opsins (red (564 nm; L cones), green (533 nm; M cones), or blue (437 nm; S cones)).[88] The minority of cones are blue-sensitive. Photoreceptors, external limiting membrane, outer nuclear layer and layer of photoreceptor axons and synapses constitute the outer retina. Rods have a long, thin outer segment that contains rhodopsin with an absorption maximum at 500 nm. Overall, there are 4.6 million cones with a peak foveal cone density of 199,00 cones/mm2 and 92 million rods that have the highest rod density of 150,000 rods/mm^2 in a ring around the fovea with an eccentricity of the optic disc.[89] Blue-sensitive cones are most numerous (2000 cells/mm^2) in a ring at 0.1 to 0.3 mm from the foveal center but absent in the fovea itself. They constitute only 7% of cones in the periphery.[90]

Rod and cone outer segments consist of stacked membranes with rhodopsin or cone opsin. The inner segments of photoreceptors contain mitochondria, ribosomes, endoplasmatic reticulum and Golgi apparatus. Rhodopsin is continuously added into newly forming discs that pinch off from the outer membrane at the base of the rod outer segment. The turnover of the entire outer segment that involves RPE phagocytosis and lysosomal degradation of shed discs is approximately 2 weeks. In contrast, rod outer segment membranes are continuous with the surface membrane. Shedding of cone outer segments occurs stepwise when large parts are deposed off at night while regrowth happens during the day.[91] Outer and inner segments are connected by the cilium that functions as a conduit for transport of newly made proteins and originates in the centriole of the inner segment. It accommodates nine microtubule doublets arranged in a ring that can be found in sensory cilia. However, the central pair of microtubules that is characteristic of motile cilia is absent.

6.1.4.1. Layers and cell types of the Neuro-Retina

Several layers of the neuroretina can be distinguished histologically and will be discussed in the following:

1. the outer photoreceptor layer,
2. External limiting membrane,
3. the outer nuclear layer (nuclei of photoreceptors),

4. Middle limiting membrane,
5. the outer plexiform layer,
6. the inner nuclear layer (nuclei of horizontal, bipolar and amacrine cells),
7. the inner plexiform layer,
8. the ganglion cell layer.

6.1.4.1.1. Outer Photoreceptor Layer

The *external limiting membrane* at the level of the photoreceptor inner segments consists of intermediate junctions (zonulae adherentes) between rod and cone inner segments and the apical processes of Muller cells. These junctions form the inner border of the subretinal space are form a diffusion barrier to large molecules[86] that may include viral vectors. This layer contains rods and cones, the number of which is equal in the macula while the overall ratio is 1:20 rods to cones (120 million rods to 6 million cones). When dark adapted, rods are 1000 times more sensitive than cones when dark adapted. They are in a ring 20 to 40 degrees around the fovea. Fifty percent of cones are located in the macula and have the highest density in the fovea.

6.1.4.1.2. External limiting membrane

The external limiting membrane is situated external to photoreceptor nuclei and consists of fenestrated intercellular bridges. It interconnects photoreceptor cells to Muller cells and photoreceptors.

6.1.4.1.3. Outer Nuclear Layer

The *outer nuclear layer* consists of cells bodies and nuclei of photoreceptors. It contains 8 to 10 rows of nuclei that belong mainly to cones in the par fovea and 5 rows of nuclei (single row of cone nuclei and 4 rows of rod nuclei internal to them).[92]

6.1.4.1.4. Middle limiting membrane

The middle limiting membrane consists of synapses and is located between the outer nuclear layer and the outer nuclear layer. It forms the approximate border of the vascular inner portion and avascular outer portion of the retina whereas the central retinal artery supplies the retina from the internal limiting membrane to the middle

limiting membrane and the choriocapillaris the external retina from middle limiting membrane to the retinal pigment epithelium. It has been described as diffusion barrier to fluids such as exudates and hemorrhages.[93]

6.1.4.1.5. Outer Plexiform Layer

Synapses of rod and cone photoreceptors and dendrites of horizontal and bipolar cells are located in the *outer plexiform layer*. The outer plexiform layer is thickest in the macula where it forms the *fiber layer of Henle* with its characteristic radially radiating axons. Rod and cone terminals are arranged as invaginating synapses and encompass two lateral processes from horizontal cells, and a single central process from a bipolar cell. Cone pedicles have further small flat synapses on their surfaces that originate from "off" cone bipolar cells. Small lateral gap junctions also exist between rod and cone terminals but do not contain synaptic vesicles.

6.1.4.1.6. Inner Nuclear Layer

Bipolar cells, horizontal cells, Muller cells, interplexiform cells and amacrine cells are the five cell types can be found in the *inner nuclear layer.*

Dendrites of horizontal cells innervate the photoreceptor axon terminals in the outermost row in the inner nuclear layer. The two different horizontal cell types (H1, H2, H3)[94] form widespread syncytia. Horizontal cells generate receptive fields and color opponent properties of bipolar and ganglion cells.[95] H1 cells have a large cell body and receive input from M and L cones but have no input from S cones. Each H1 cell has a long axon with a terminal arbor connected to rod spherules[96] H2 cells have smaller cell bodies and receive input from all three cone types. Their axons contact mainly S cones. They receive input from L and M cones and have a large and often asymmetric field. H3 are similar to H1 cells but are only known in human retina.[94] They receive input from L and M cones and have a large and often asymmetric field.

Bipolar cells receive direct input from photoreceptors (15 to 20 in the central retina, 40 to 50 in the periphery) and connect to amacrine and ganglion in the *inner plexiform layer* with their axon.[97] There are only "on" rod bipolar cells but "on" as well as "off" cone bipolar cells, the later ones terminating in the outer strata of the inner plexiform layer.[98] Cone bipolars connect to several or single cones (midget bipolar cells). L- and

M-cone input occur to six diffuse cone bipolar types and each foveal cone synapses onto one "on" and one "off" midget bipolar cell. In contrast, the "on" blue cone bipolar cell receives input exclusively from S cones.[95,99]

The cell bodies of the interplexiform cells lie among amacrine cells and synapse with bipolar and amacrine cells in the inner nuclear layer. They gather input from several bipolar cells. Different from all other retinal cells, interplexiform cells are arranged centrifugally in that they send processes into the outer plexiform layer where they form synapses with cone pedicles and dendrites of rod and cone bipolar cells.[100] Their function is to regulate receptive fields of horizontal cells.

The *amacrine cells* form the inner row of cells of the inner nuclear layer. There are 40 types of amacrine cells that can be distinguished by morphology and neurotransmitter.[98, Dacey, 2000 #7576, Vaney, 1990 #7577] The density of amacrine cells is similar in the central and peripheral retina. Amacrine cells receive lateral input from bipolar and other amacrine cells in the inner plexiform layer and synapse to those cells as well as to ganglion cells.

6.1.4.1.7. Inner Plexiform Layer

The *inner plexiform layer* consists of the synapses from inner nuclear layer cells, the outer part of which contains layers S1 and S2 and the inner layer contains S3, S4 and S5. "on" center ganglion cells that respond when light is turned on have dendrites in the inner layer and "off" center ganglion cells in the outer layer.

While many rods converge onto a single rod bipolar cell in the outer plexiform layer, fewer cones converge onto a cone bipolar cell or may synapse onto various cone bipolar cell types. The rod and cone circuits are separate. Rod bipolar axons terminate in sublamina b of the inner plexiform layer onto dendrites of amacrine cells. Amacrine type II cells from chemical synapses with "on" ganglion cells whose dendrites branch in sublamina b. AII amacrines further form gap junction (electrical) synapses in sublamina b with dendrites of "on" diffuse cone bipolar cells, whose axons connect to both "on" and "off" ganglion cells. As a result, rod signals reach both "on" and "off" center ganglion cells.

In sublamina A some cone bipolars synapse with "off" ganglion cells, while others synapse in sublamina B with "on" ganglion cells. Overall, much fewer cones converge

to one cone bipolar cell than the many rods that create an input to a rod bipolar and fewer cone bipolar cells converge onto a ganglion cell. In the fovea a single M or L cone synapses onto one "on" and one "off" midget bipolar cell that synapses onto two midget ganglion cells ("on" and "off") to provide the highest resolution in the visual pathway. Amacrine cells modify the ganglion cell receptive fields and center response also for the cone system.

6.1.4.1.8. Ganglion Cell Layer

The ganglion cells that form the *ganglion cell layer* are the projection neurons of the retina that constitute the third neuron of the visual pathway. The total count of ganglion cells can vary between 0.7 to 1.5 million per retina.[101] Outside the central retina the ganglion cell layer has one single row of cells and up to 10 rows within the macula and the highest concentration in the parafovea.[101] More than 20 different classes of ganglion cells have been described based on different staining, molecular markers, electrophysiological behavior or central projections.[102] The different ganglion cells have a characteristic receptive field, receiving input from the inner plexiform layer and one single projecting axon.

The inner surface of the retina is covered by a basal lamina that is derived from the Müller glial cells. This 2 µm *internal limiting membrane* is closely associated with the Müller end feet and merges with collagen fibrils of the vitreous. Müller cells are radial glia that extend from the vitreal surface of the retina to the subretinal space, while their body and nuclei are in the inner nuclear layer. Their apical cell processes extends to the external limiting membrane forming microvilli that project into the subretinal space around the photoreceptor inner and outer segments. Müller apical processes and photoreceptor inner segments are connected by band of intermediate junctions of the external limiting membrane. Müller cells have fine cytoplasmic processes that reach into the retinal parenchyma surrounding all neurons and their processes. Because of this, retinal neurons only contact each other at the synapses but are otherwise completely engulfed. Muller cells also surround bundles of ganglion cell axons and terminate against the basal laminae of blood vessels in the inner retina. Besides structural and metabolic support of retinal neurons, Muller cells regulate potassium levels, neurotransmitters, CO_2, pH levels in the retina and are involved in angiogenesis, differentiation and gliosis (Loewen et al., submitted).[103]

Astrocytic glia are located mainly in the nerve fiber layer and a few in the ganglion cell layer. Their wide foot processes surround the walls of retinal vessels. These stellate cells with oval nuclei are abundant in the prelaminar portion of the optic disc. Microglia are derived from the bone marrow and function as tissue macrophages. In the retina these cells form regular mosaics between the nerve fiber and ganglion cell layers as well as the inner nuclear and outer plexiform layers.[104] As they are closely associated with the retinal vasculature they are absent in the foveal avascular zone. Microglia become activated during repair in traumatized or degenerating retina. They scavenge debris and present antigens to T lymphocytes.[105]

RPE, photoreceptors and the outer retina receive supply from the choriocapillaris, whose endothelial cells are fenestrated and allow diffusion of variously sized molecules along the lateral walls of RPE cells. About 65 to 85% of ocular blood flow occurs through the choriocapillaris while the remainder enters the inner retinal circulation. Tight junction between RPE cells block diffusion of larger serum components into the subretinal space constituting the outer blood-retina barrier. In contrast, the inner blood-retinal barrier is formed by endothelial cells of the central retinal circulation that lack fenestrations entirely and have zonulae occludentes. The central retinal artery has four branches to supply all quadrants. Its main branches lie in the nerve fiber layer and send capillaries to all levels of the inner retina. The arterial branches have smooth muscle walls and an endothelium but lack an internal elastic lamina. The branches of the central retinal vein have thin walls of smooth muscle and an endothelium, and the walls of the venules and capillaries contain mural cells (pericytes) enclosed within a basal lamina continuous with that of the endothelial cells. Capillaries are absent in the fovea in an area 0.25 to 0.6 mm in diameter because the foveal pit contains only photoreceptors and RPE cells.[23, 106]

6.2. Human Ocular Diseases

6.2.1. Glaucoma

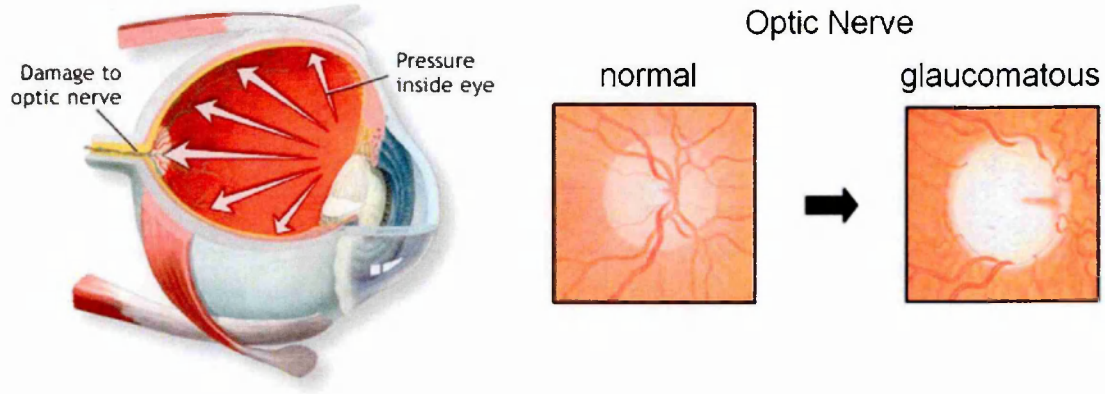

Figure 1: Impaired outflow of aqueous humor may result in increased intraocular pressure (left) and glaucomatous optic neuropathy (right) (National Eye Institute, National Institutes of Health).

6.2.1.1. Overview

Glaucoma is a descriptive term that identifies a group of clinical conditions with different etiology and the final common outcome of degenerative optic neuropathy (**Figure 1**).[107] Categories are based upon whether increase of intraocular pressure (IOP) by aqueous humor outflow obstruction occurs in the presence of an open chamber angle (primary open-angle glaucoma, POAG) or a closed chamber angle (primary angle-closure glaucoma, PACG) and can further be subdivided into primary or secondary causes. The new American Academy of Ophthalmology (AAO) definition of primary open-angle glaucoma (POAG) states that the disease is multifactorial in origin but that it primarily affects the optic nerve. IOP is the most important cause of optic nerve damage, but not the only one. Characteristic findings include progressive thinning of the neurosensory retinal rim, notching, asymmetry, or nerve fiber layer defects. Because early glaucoma typically has no associated visual field loss (**Figure 2**),[108, 109] visual field function screening (perimetry) has the goal to detect already moderate to advanced states of glaucoma.[107]

Glaucoma afflicts 67 million people and is the leading cause of irreversible blindness worldwide.[110] Risk of blindness remains high despite the availability of several

treatments.[111] For patients treated and monitored for open angle glaucoma, Kaplan–Meier cumulative probabilities of monocular and binocular blindness at 20 years are 27 and 9%, respectively.[112] These risks are increased when damage to the optic disc is present at the time of diagnosis.

It is estimated that 15 million Americans would be classified as having glaucoma based on optic nerve head criteria.[113] In 1992 direct and indirect costs exceeded $2.4 billion in the US.[114] About 50% of people affected by glaucoma are unaware of their disease.[107] Age is a strong risk factor to develop glaucoma (30-fold increase)[115, 116] and so is race (10-fold).[117] Mathematical models indicate that at IOPs of over 28 to 30 mm Hg chances of optic nerve damage exceeds 50%.[118-122] Conversely, lowering IOP by 30% from baseline was associated with a 50% reduction in visual field loss over.[123, 124]

Even with treatment, long-term outcome of POAG is poor and may result in progression of visual field loss in up to 8% of patients annually.[125-128] These risks are increased when damage to the optic disc is present at the time of diagnosis. Glaucoma is the cause of blindness (best visual acuity of less than 20/200 or best visual field less than 20°) in 80,000 adult Americans.[107] Impaired vision is associated with measurably decreased quality of life[129-131] and increased risk of falls, hip fractures, and decreased physical mobility.[132] Decreased vision is also directly related to difficulties in vision-related tasks.[133-135]

The major causal risk factor in most forms of glaucoma is intraocular hypertension, which is caused by impaired outflow of aqueous humor from the anterior chamber,[136, 137]but low tension glaucoma with average or below average intraocular pressure also exists.[138] Maintaining intraocular pressure in a narrow range (10–21 mmHg) is essential for viability of the neuroretina. In the most common form of glaucoma, primary open angle glaucoma, as well as angle closure glaucoma, sustained higher pressures directly damage optic nerve axons and also may impair vascular supply, resulting in irreversible loss of retinal ganglion cells. There is experimental support that advanced axonal loss can lead to increased shear forces and disadvantageous biomechanical properties at the lamina cribrosa.[139-141] In addition, instead of a percentage attrition resulting in an asymptotic decay curve, the rate of retinal ganglion cell loss in glaucoma accelerates with progressive disease at least in animal models.[142]

Aqueous humor is produced by the ciliary body and exits the eye primarily through Schlemm's canal and its downstream tributaries, the collector channels and episcleral veins. To enter Schlemm's canal, fluid must first traverse the trabecular meshwork (TM), a wedge-shaped reticulum of metabolically active, yet mitotically quiescent endothelial- like cells located in the angle of the anterior chamber (a and b). Although it is known that the TM generates most of the resistance to aqueous humor outflow,[136, 137] the responsible cellular mechanisms are poorly understood. Nevertheless, progress has been made in identifying human genes that are involved in the pathogenesis of some forms of glaucoma.[143-150] A glaucoma-specific gene expression profile has been identified in human TM.[150] Stable transcriptional reprogramming is suggested by the consistency of this abnormal profile in diverse forms and stages of the disease, and by its persistence in TM cells after primary subculture removes them from glaucomatous conditions in the eye.[150]

6.2.1.2. Aqueous Humor Outflow

Aqueous humor outflow occurs through several structures. Pores can be seen between Schlemm's canal cells as well as within cells themselves.[33, 151, 152] Eyes with higher outflow facility have a higher number of such pores.[152] Giant vacuoles also contribute to outflow. These structures are pressure-dependent, energy-independent protrusions of canal cells that may sense pressure by stretching.[153]

Through interactions with integrins and cell adhesion molecules that is produced by trabecular meshwork cells, the extracellular matrix contributes to regulation of the so called *conventional outflow* through the trabecular meshwork.[154] Proteoglycans, laminin, fibronectin, collagen, matricellular proteins and glycosaminoglycans (GAGs) make up this extracellular matrix. Cell-matrix interactions are modulated by matricellular proteins such as thrombospondins, tenascin and secreted protein acidic and rich cysteine (SPAC), that are nonstructural adaptors proteins.[155] Although matricellular proteins are generally seen during development and tissue repair, these proteins are found in abundance in the trabecular meshwork.[156, 157] At this point it is unknown how these proteins regulate outflow. The negatively charged GAGs are primarily found in the extracellular matrix and on the cell surface. Because of their size these molecules can increase the viscosity of fluids and play a role in retaining

and releasing water e.g. in cartrilage.[158] In eyes with primary open angle glaucoma more chondroitin sulfate and less hyaluronic acid is seen compared to healthy eyes.[31]

A hydraulic-like system has been described that may influence the actin cytoskeleton. Ciliary muscle tendons and elastin fibers extend to the endothelium of Schlemm's canal and transmit any tension resulting in a change of shape of the trabecular meshwork.[137] It is thought that while cellular contraction can change the outflow acutely, the extracellular matrix is more likely to modulate resistance in the long-term.[159, 160]

A second route of aqueous humor outflow exists through the supraciliary space as well as across the anterior and posterior sclera through emissarial canals around vortex veins or into choroidal vessels. This outflow route is termed *uveoscleral outflow* and accounts for up to 60% in non-human primates[161] but this can vary considerably from e.g. 8% in rabbits to 80% in mice.[162] In humans, uveoscleral outflow decreases with age[163] and the conventional pathway becomes more important. A range from 4% to 60% has been reported in different studies.[18, 164]

Although many differences have been identified between normal and glaucomatous eyes and changes during the course of the disease, the pathogenesis of primary open angle glaucoma is not understood. It is known that normal trabecular meshwork cells become more sparse and altered behavior: proteomic studies identified a total of 368 proteins expressed in TM and differential expression of 52 proteins that were only seen in glaucomatous and 177 only in normal trabecular meshwork.[165] Vascular endothelial growth factor (VEGF),[166] tumor growth factor beta 2 (TGFβ2),[167] endothelin,[168] plasminogen activator inhibitor (PAI)[169] and soluble CD44[170] are elevated in aqueous humor of glaucomatous eyes and may change the phenotype. TGF-ß2 has attracted interest because it induces secretion of additional extracellular matrix molecules which increases the outflow resistance.[171]

Other factors might play a role in glaucoma pathogenesis but their role is less certain. Oxidative stress for instance has been identified in other eye diseases such as cataract formation and macular degeneration. Oxidative DNA damage can be demonstrated in the trabecular meshwork of glaucoma patients.[172] More evidence suggests that NF-κB release after oxidative stress causes up-regulation of ELAM-1 which has been suggested as a marker for glaucoma in the past.[150] Welge-Lussen et al. found that

tissue transglutaminase is expressed in the HTM and can be induced by TGF-ß1 or -ß2 in cultured HTM cells.[173] Tissue transglutaminase can polymerize fibronectin causing an increase of irreversibly cross-linked ECM proteins. This mechanism might play a role for the increased outflow resistance seen in glaucomatous eyes.

In 1997 involvement of myocilin in glaucoma pathogenesis was recognized.[143, 174, 175] Stone et al. identified point mutations in the olfactomedin domain, which is highly conserved among species, that are associated with and believed to be causative in primary open-angle glaucoma (POAG), including juvenile and adult forms of open-angle glaucoma.[143] Research was further accelerated when the gene coding for myocilin, MYOC, was published.[175] Since then, a number of mutations associated with glaucoma have been confirmed in the third exon of MYOC[176-182] although the process leading to the development of glaucoma remains unclear. The idea of physiologic as well as pathologic effects of changes in myocilin production, degradation, or binding is supported by findings that normal myocilin can contribute to outflow obstruction in the anterior segment perfusion model[183] and can interact with other myocilin molecules to form complexes.[184]

Myocilin is a secreted 55–57 kDa glycoprotein with a myosin-like domain, a leucine zipper region and an olfactomedin domain.[175] It is highly expressed in the trabecular meshwork (TM), within the cytoplasm and in association with fibrillar extracellular matrix components.[144, 185-190] Secreted myocilin can be found in the aqueous humor[191] and is expressed in sclera,[187, 192] ciliary body,[187, 192, 193] and iris,[187, 192, 193] and at lower amounts in the retina[187] and optic nerve head.[187, 192, 194-196] The expression in TM cells is induced upon treatment with dexamethasone,[144, 197] transforming growth factor-β[144] and mechanical stretch.[144]

6.2.1.3. Clinical Perspective

6.2.1.3.1. Intraocular Pressure is Causatively Linked to Glaucoma: A Brief History

Intraocular pressure (IOP) has been causatively linked to glaucoma development, progression and treatment. From its very first description to contemporary approaches IOP plays the most noteable role in glaucoma. However, this was not always the case and its significance was passionately disputed as late as in the 1980s in the dawn of evidence-based medicine.[198]

The first time of glaucoma was described as a blinding disease associated with high IOP was by the Persian physician Ali ibn Rabban at-Tabari (810-861) in the writings Firdaws al hikma (Paradise of Wisdom).[199] This association was later pointed out by Richard Banister of England in 1622: "A treatise of one hundred and thirteen diseases of eye": "if one feele the Eye by rubbing upon the Eie-lids, that the Eye be growne more solid and hard than naturally it should be."[200] The Dutch ophthalmologist Franciscus C. Donders (1818-1889) coined the expression "simple glaucoma" for increased IOP occurring without any inflammatory symptoms. In 1973 Drance provided for the first time the definition of glaucoma as an optic neuropathy caused by increased IOP and other associated risk factors.[201]

An association of IOP and open angle glaucoma was eventually confirmed in studies in the 1990s but still not in the form of a cause-result relationship: in the Baltimore Eye Survey[118] and the Barbados Eye Study[202] IOP was found to be an important factor in glaucoma that correlated with increased prevalence and incidence.[203] It was not until the large randomized trials of the late 1990s that demonstrated beyond correlation that a true causal relationship existed by showing that lowering IOP can slow or prevent POAG progression. The two most noteworthy trials in that regards are the Ocular Hypertension Treatment Study (OHTS)[204] and the Early Manifest Glaucoma Trial (EMGT).[205] These studies have direct practical implications for daily ophthalmic care today and are summarized in the following. While there are other risk factors for glaucoma, IOP remains the single most important modifiable variable used to prevent or delay progression. Other strategies, such as vascular[206,207], neuroprotective[207-210] or metabolic management[211] appeared promising in animal experimentation and were recognized as risk factors (reviewed in[206,212]) but influence on the course of manifest glaucoma could not yet be established in randomized clinical trials.

6.2.1.3.2. Elements of Intraocular Pressure

Intraocular pressure can be calculated using the Goldmann equation[213] which consists of four elements:

$IOP = F / C + Pv - U$

whereas F is the aqueous humor formation rate in microliters per minute, C is the facility of outflow in microliters per minute per millimeter of mercury, Pv is the episcleral venous pressure in millimeters of mercury and U is the rate of outflow of aqueous humor via all channels that are intraocular pressure independent.

F, C and U are most commonly manipulated to alter IOP, while increased epivenous pressure might have to be addressed surgically.

Under physiological conditions, between 70% to 95% of outflow occurs through the trabecular meshwork and is pressure dependent[163, 214-216] but the pressure independent uveoscleral outflow can significantly increase during inflammation or second to prostaglandin analogues and very effectively lower IOP under those circumstances.

6.2.1.3.3. Important Randomized Clinical Trials

6.2.1.3.3.1. Ocular Hypertension Treatment Study OHTS

The purpose of the Ocular Hypertension Treatment Study (OHTS)[204] was to determine whether the medical reduction of elevated IOP can prevent glaucoma and to define risk factors for glaucoma development. Topical ocular hypotensive medication was effective in delaying or preventing onset of POAG in individuals with elevated IOP by about 50%. Results to date have shown an approximate 50% reduction in conversion from OHT to POAG with a 20% reduction in intraocular pressure (IOP).[63] OHTS demonstrated that medical treatment of people with intraocular pressure (IOP) of > or =24 mm Hg reduces the risk of the development of primary open-angle glaucoma (POAG) by 60%.[217]

6.2.1.3.3.2. Early Manifest Glaucoma Trial (EMGT)

The Early Manifest Glaucoma Trial (EMGT)[205] compared how glaucoma progression was affected by immediate medical (betaxolol) or laser therapy for newly diagnosed POAG with normal or moderately elevated IOP versus late or no treatment. Treatment caused an average reduction of IOP of about 5 mm Hg (25%) which reduced glaucoma progression to 45% compared to 62% in the control group and occurred later.

6.2.1.3.3.3. Collaborative Normal Tension Glaucoma (CNTG) trial

Before the Collaborative Normal Tension Glaucoma (CNTG) trial[218] it was not known whether IOP that was in the normal statistical range was at all involved in glaucomatous optic nerve damage and visual field loss. During the study it became apparent that - similar to simple POAG - participating patients had a slower glaucoma progression (no progression in 5 years) when IOP was lowered by 30%.

6.2.1.3.3.4. Conclusion from Randomized Trials

These randomized clinical trials proved that lower intraocular pressure delays or prevents progression of POAG as evidenced by delay or complete prevention of development of glaucomatous optic neuropathy from ocular hypertension, visual field defects from pre-existing optic nerve changes and reduced progression of existing visual field defects. However, another conclusion was that despite good IOP control in many actively treated patients, POAG can still progress and can result in blindness in an unacceptable large number of patients.[112, 219]

6.2.1.4. Current Status of Glaucoma Therapy

The site of the highest resistance to outflow of aqueous humor is the juxtacanalicular trabecular meshwork.[28, 136] This structure is the principal site of pathology in primary open angle glaucoma (POAG).[137, 220, 221] Current interventional approaches for moderate to advanced POAG circumvent this resistance,[222] induce remodeling[223] or permanently disrupt the trabecular meshwork (TM).[224] Pharmacotherapy either decreases aqueous humor production or increases uveoscleral outflow as the main mechanisms.[225]

Traditional therapies for advanced glaucoma attempt to lower intraocular pressure surgically by circumventing the outflow resistance of the TM by shunting aqueous humor to the subtenon space (e.g. *trabeculectomy, glaucoma drainage device*).[222] These filtering procedures have a high rate of complication and failure[226] despite the introduction of antimetabolites and improvement of drainage device design, respectively.

Trabeculoplasty has been employed to lower intraocular pressure by inducing remodeling of the TM and extracellular matrix.[223] However, the extent of pressure reduction is much smaller than in filtering procedures and can only be used in early stages of the disease.

Complete disruption of the TM and wall of Schlemm's canal has recently been achieved with the *trabectome*,[224] but this disruption is irreversible creating a permanently open connection to the downstream drainage system.

Pharmacotherapy has primarily been successful in reducing intraocular pressure by decreasing aqueous humor production (e.g. β-blockers, alpha adrenergic receptor agonist, carbonic anhydrase inhibitor) and improving uveoscleral outflow (e.g. prostaglandin analogues, alpha adrenergic receptor agonist).[225] The only medication that addresses the primary pathology of reduced conventional outflow, pilocarpine,[227] has been abandoned because of its side effects and reduction of non-conventional outflow.[17]

Little is known about the actual pathophysiology on a molecular level and the cause of failing TM regeneration.[146, 228] Both normal and POAG TM cells are non-dividing in situ but can be cultured and expanded *in vitro*.[229-231] A few studies have examined TM regeneration responses but these were limited to focal destruction with laser.[232-235] It would be desirable to ablate the entire tissue that creates outflow resistance yet to do so selectively in order to study cell turn over and regeneration.

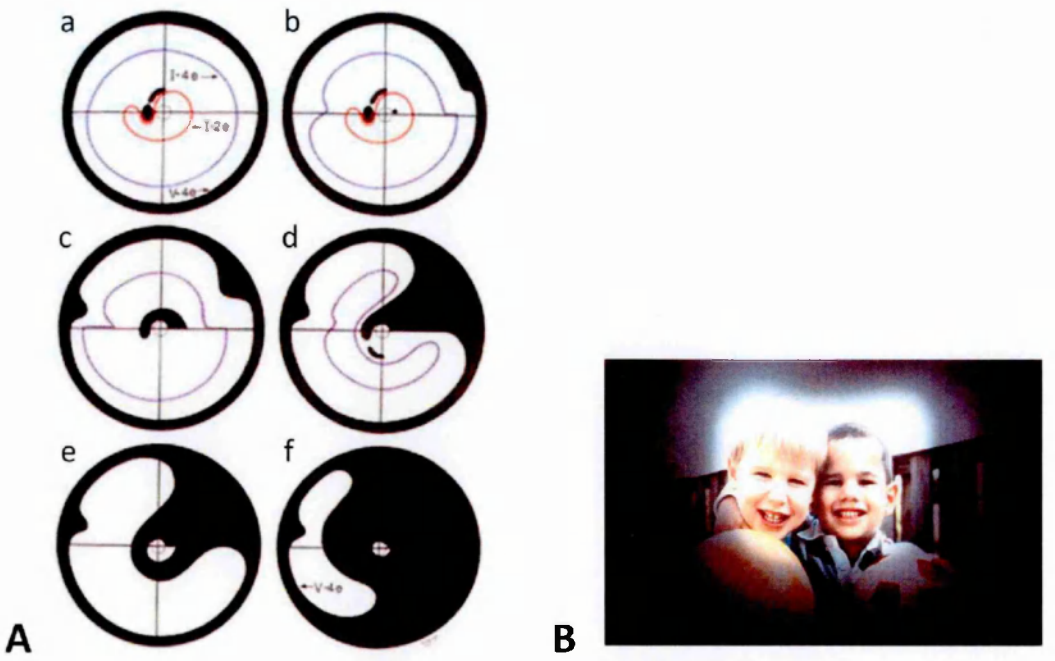

Figure 2: Gradual deterioration of the visual field from the periphery (A) and figurative representation of the effect on the visual field in a late stage of glaucoma (B) (National Eye Institute, National Institutes of Health).

6.2.1.5. Rational for Developing Gene Transfer to the Trabecular Meshwork

In the presence of poor long-term outcome of vision in glaucoma patients with current strategies gene therapy may offer solutions to permanently correct aqueous humor outflow. Lentiviral vectors have evolved as the only vector type that allows stable and targeted genetic modification of the trabecular meshwork providing new tools for development of glaucoma therapy and animal models through tissue specific transgenesis. Permanent genetic reprogramming of anterior chamber outflow tract physiology by gene therapy has attracted attention as an ideal solution in theory because of the disease's life-long chronicity and the emerging understanding of its genetic basis.[143, 236-238] The trabecular meshwork (TM), is a key intraocular structure to target since it controls IOP by controlling outflow of aqueous humor.[136, 137]

Strategies for gene therapy for glaucoma must not only consider the chronic nature of the disease but also the generally nondividing nature of the target cells. Two general approaches have emerged. One focuses on the intraocular pressure problem, and the other on blocking its sequelae, retinal ganglion cell death.[236, 239] The accessibility of the anterior chamber and the restricted anatomic target are favorable for gene therapy

directed at the TM. Gene therapy with retroviral vectors has appeal, because these vectors undergo reverse transcription of their single-stranded RNA genomes, generating a linear double-stranded DNA intermediate that that is subsequently integrated into the host genome in a reaction catalyzed by the retroviral integrase. Therefore, these vectors result in permanent transgenes and have potential to address the chronicity of glaucoma pathophysiology. However, an important consideration is that TM cells do not normally divide. Unlike conventional retroviral vectors based on, for example, murine leukemia viruses (MLVs), lentiviral vectors, such as those derived from HIV and FIV, integrate into the genomes of both dividing and nondividing cells.[1, 240]

Glaucoma is a particularly appropriate disease to investigate for corrective gene therapy because of its chronicity and anatomically restricted pathology. However, this approach would require stable expression of candidate genes in the aqueous outflow tract. Correcting the primary aqueous outflow pathophysiology, and the complementary aim of expressing antiapoptosis genes in retinal ganglion cells,[239, 241] are both likely to require not only gene transfer to nondividing cells, but also transgene stability commensurate to the chronicity of the disease. Trabecular meshwork cells are highly metabolically active and display pronounced phagocytic and secretory function, but appear to undergo limited cell division in vivo; less than 0.5% have been estimated to be mitotically active at any one time.[235, 242, 243] Although adenoviral and herpes simplex vectors transduce nondividing cells and can mediate gene transfer to the TM,[244, 245] these vectors are best suited to short-term gene expression because they do not generate integrated transgenes. In addition, these vectors can trigger marked inflammatory responses. Oncoretroviral vectors, such as those derived from murine leukemia viruses (MuLVs), do achieve stable integration, but only in target cells that are proliferating at the time of transduction.[246, 247] The latter requirement could hinder effective gene transfer to the trabecular meshwork, although this question has not been investigated.

In contrast to these vectors, lentiviral vectors integrate permanently into the genomes of both dividing and nondividing cells. This property, which enables the universal lentiviral strategy of propagating through tissue macrophages, has been attributed to multiple determinants in virion proteins[248] and within the reversed transcribed DNA[249] that facilitate nuclear import of lentiviral preintegration complexes. Envelope

glycoprotein-pseudotyped lentiviral vectors have been derived from primate lentiviruses[240, 250-256] and from nonprimate animal lentiviruses.[1, 257-260] Feline immunodeficiency virus (FIV) vectors exploit compartimentalized blocks to productive cross-species infection, because they complete the postentry stages of the infection cycle in nondividing human cells despite blocks to viral transcription and other life cycle mechanisms that prevent productive replication.[1, 258, 260, 261] Human immunodeficiency virus type 1 (HIV-1) vector systems have so far received more extensive validation and molecular engineering for vector optimization.[254]

Additional features make glaucoma an intriguing potential proof-of-concept disease for gene therapy. The small amount of tissue that would require targeting, and its accessibility, could enhance the feasibility of adequate levels of corrective gene transfer. In the absence of a selective growth advantage for gene-altered cells, and/or a tissue that supports proliferation in vivo after ex vivo gene transfer,[262] achieving permanent transduction of most of a relevant tissue has remained a major hurdle in most gene therapy situations. Specific tissue targeting is problematic if the target cells cannot be isolated ex vivo (e.g., ref.[262]). The anterior chamber can also be visualized through clinically feasible imaging methods, suggesting a means to monitor the in vivo expression of an integrated transgene over time during gene therapy developmental studies.

Long-term, stable, high-grade, and properly targeted transgene expression in the trabecular meshwork has not been achieved. Liposomes,[263] adenovirus,[244, 264] adeno-associated virus,[265] and herpes simplex virus vectors[245] have been limited by short duration, inflammation, or lack of sufficient, targeted transduction. In contrast to DNA virus- or plasmid-based vectors, lenti-retroviral vectors integrate permanently into the genomes of transduced cells as an obligate part of the life cycle.[254] The advantage over conventional onco-retroviral vectors is their ability to integrate in nondividing cells.

Not only could long-term transgene expression in the trabecular meshwork be utilized to study therapeutic transgenes, it would also enable transgenesis that is selective to the outflow tract and technically more simple than the generation of entire transgenic animals. Prior to either therapeutic or experimental gene transfer, proof-of-principle has to be established with marker genes, the most common ones of which are beta-galactosidase that allows intensely blue staining of galactose breakdown products and

fluorescent proteins such as the humanized, enhanced green fluorescent protein (eGFP), or a renilla reniformis green fluorescent protein (rGFP). The construction of these vectors is described below in detail. LacZ as a marker gene has the advantage that it can be detected with the beta-galactosidase assay after short fixation and the blue product of the assay is compatible with other conventional tissue staining techniques e.g. of paraffin sections. It can be detected even at low multiplies of infection (m.o.i.) or low enzyme activity. It can also be stained with immunohistochemistry staining techniques as numerous antibodies are commercially available. A disadvantage is that it cannot be visualized in vivo easily. In contrast, eGFP and rGFP can be visualized in vivo with a variety of techniques as long as the correct exciting wavelength is applied. E.g. standard cobalt blue light and observation with a slitlamp,[264] gonioscopic visualization with a histopathology microscope as described in the techniques section of this thesis or excitation and capture with a scanning laser ophthalmoscope[266] are possible.

6.2.2. Retinal and Choroidal Diseases

A spectrum of chronic retinal diseases is suitable for gene therapy: vasoproliferative retinal and choroidal diseases that include retinopathy of prematurity, proliferative diabetic retinopathy and exudative age-related macular degeneration as well as degenerative retinal and choroidal diseases that include retinitis pigmentosa, Best disease, choroideremia and Favre Goldmann syndrome. All of these diseases fulfill criteria such as chronicity, identified genetic defect and limited or no available treatment options. These diseases are introduced in the following and the rational for gene therapy for retinal and choroidal diseases is discussed further below.

6.2.2.1. Vasoproliferative Retinal and Choroidal Diseases

6.2.2.1.1. Retinal Neovascularization

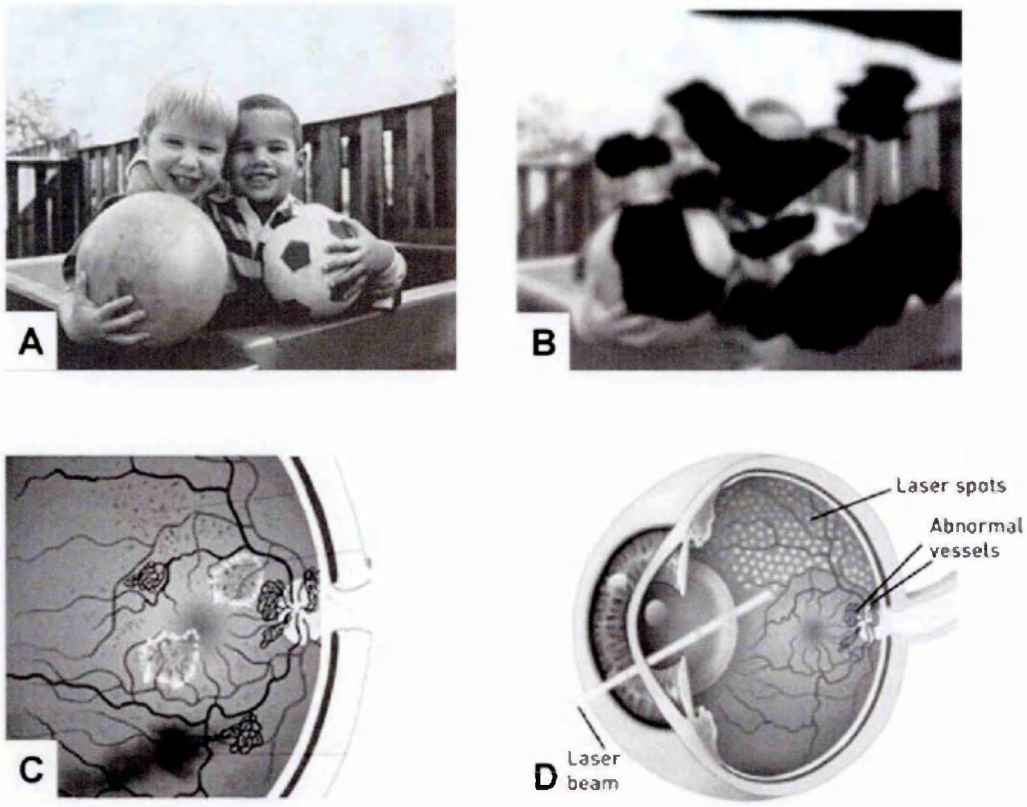

Figure 3: Simulation of normal visual field (A) and with diabetic retinopathy (B). Neovascularization, exudates and preretinal bleeding can be found in the proliferative state of diabetic retinopathy (C). The treatment consists of panretinal laser therapy and ablates healthy retina in the periphery (D) (National Eye Institute, National Institutes of Health).

Retinal neovascularization (e.g. in diabetic retinopathy, exudative macular degeneration and retinopathy of prematurity, **Figure 3**) is currently treated by ablating healthy retina to prevent release of growth factors that cause neovascularization. As in glaucoma, integrating vectors could provide a permanent cure because they allow expression of therapeutic genes for the whole life of a cell.

Ocular neovascularization is a central feature of retinopathy of prematurity, diabetic retinopathy and age-related macular degeneration. These conditions constitute a leading cause of blindness in infants, individuals of working age and the elderly, respectively.[267-272] Neovascularization is the final common pathway of these and several other disorders that are multifactorial in etiology and involve an imbalance between pro- and anti-angiogenic factors.[273, 274] Visual loss is a result of increased

vascular permeability that causes retinal edema, hemorrhage from vascular fragility and fibrovascular proliferation with tractional retinal detachment.[275]

Present therapies are of limited efficacy and adapt destructive measures with significant adverse effects in order to reduce production of angiogenic factors.[276, 277] As the pathophysiology is better understood, a number of new angiogenic and angiostatic molecules has been identified. While systemic angiostatic therapy would be problematic, local application in proximity to the affected tissue is promising. While effects of intraocular injection of angiostatic substances would be short-lived, gene transfer through vectors allows local and long-term delivery of therapeutic molecules.

Lentiviral vectors are attractive vectors for therapy of retinal and choroidal neovascularization (e.g. diabetic retinopathy, age related macular degeneration, retinopathy of prematurity) as well as of degenerative RPE diseases that do not involve neovascularization (dry age-related macular degeneration, Leber's amaurosis, choroideremia, atrophia gyrata, Best's disease, Stargardt's disease), because achieving long-term expression is a vital goal for these chronic conditions. Since transduction from subretinally injected lentiviral vectors is mostly limited to the RPE,[75, 76, 278, 279] except when injected immediately after birth,[280, 281] these vectors would be similarly useful to AAV vectors for degenerative RPE diseases.[282]

6.2.2.1.2. Retinopathy of Prematurity

Retinopathy of prematurity (ROP) is an ischemia-induced proliferative retinopathy, which affects premature infants with low birth weight. Retinal neovascularization in ROP may lead to traction, retinal detachment, and blindness. Infants born at the gestational age of 31 weeks or less are at risk for ROP. Of these, 66% of infants weighing less than 1251 g at birth, and about 82% less than 1000 g develop this disease.[283] Current treatments for ROP, using laser or cryotherapy, are only somewhat successful in preventing blinding sequelae.[284] It is generally accepted that the pathogenesis of ROP is multifactorial. Documented risk factors include oxygen exposure, prematurity, and acidosis during the early neonatal period. One hypothesis implicates relative hypoxia of the peripheral retina.[285] As with other instances of

retinal neovascularization, vascular endothelial growth factor (VEGF), which can be counteracted by PEDF,[286] plays a central role.[287-289]

ROP is a two-phase process that occurs during the timeframe of early vessel development and maturation. In the first phase, developing retinal capillaries obliterate when exposed to hyperbaric oxygen concentrations, while under physiological conditions, there would be a balance between developing and degenerating capillary buds. When excess oxygen is removed, the acute ischemia leads to vascular proliferation. Newly formed vessels induced by VEGF break through the internal limiting membrane and grow into the subvitreal space. In the later healing phase glial-fibrocellular scar tissue develops that can cause significant visual loss, ectopia of the macula, as well as serous and tractional detachments of the retina. Although cryosurgery and laser retinal ablation of avascular retina improve chances of a favorable outcome, vision impairment still occurs in up to 44% of patients.[290]

6.2.2.1.3. Proliferative Diabetic Retinopathy

Hyperglycemia in diabetic retinopathy **Figure 3** is thought to cause ischemia through microvascular occlusion. Up-regulation of angiogenic growth factors results in vessel growth from the inner retinal surface into the vitreous.[291] Present treatment for proliferative diabetic retinopathy is retinal laser photocoagulation, a destructive procedure that can affect visual function adversely.[292] 60% of diabetics develop retinopathy within 15 years of diagnosis.[283] As in ROP, the blindness results from retinal detachment associated with pre-retinal neovascularization. It is hypothesized that hypoxia of the neural retina contributes to the pathogenesis. PEDF levels are low in diabetic retinopathy.[293, 294]

6.2.2.1.4. Exudative Age-Related Macular Degeneration (AMD)

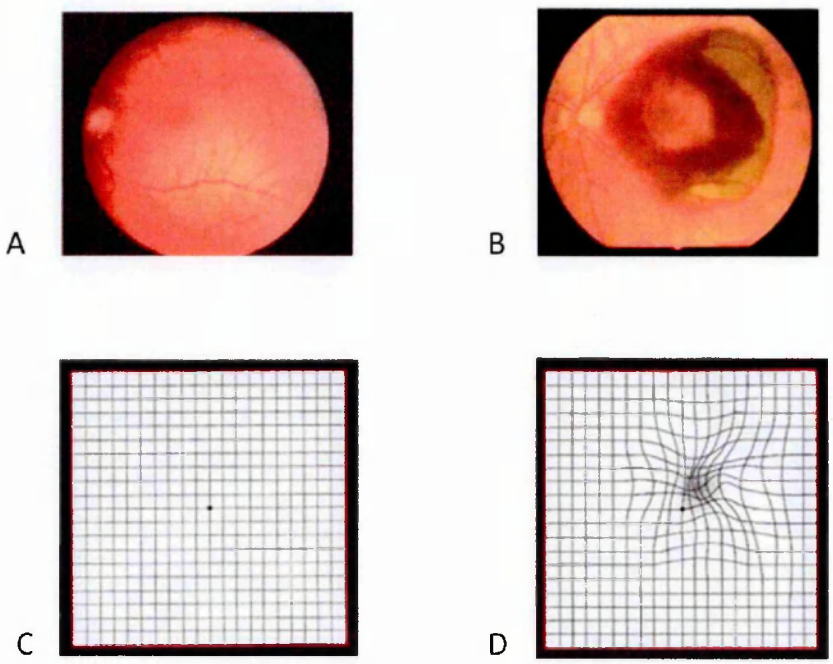

Figure 4: Normal central fundus (A) and Amsler grid (C) and in wet age-related macular degeneration (B and D). Central vision is missing entirely or appears distorted (D) (National Eye Institute, National Institutes of Health).

Choroidal neovascularization in AMD **Figure 4** is the result of retinal pigment epithelium hypoxia from thickening of Bruch's membrane or changes in choroidal perfusion,[295-298] which leads to production of angiogenic growth factors.[299, 300] Visual loss is a consequence of hemorrhage from neovascular vessels extending from the choroidal vasculature through breaks in Bruch's membrane.[301, 302] Treatment options include laser photocoagulation and photodynamic therapy, offering some short-term benefits to certain subgroups of patients.[303-308] Exudative age-related macular degeneration (ARMD) typically occurs in individuals 60 years of age and older, and is responsible for blindness in 16,000 people in the US per year.[283]

6.2.2.2. Degenerative Retinal and Choroidal Diseases

The list of potential therapeutic target diseases for gene therapy is comprehensive but as with any therapeutic, development has to be guided not only by feasibility but also by socioeconomic relevance. As devastating as many hereditary fundus dystrophies are as challenging it would be to proceed through all steps from the drawing board to

animal models, clinical trials and approval. It might be more applicable to focus on a common cause such as neovascularization in vasoproliferative disorders or on neuroprotective or anti-apoptotic strategies in degenerative disorders. In addition, an animal model is needed as a crucial step.

6.2.2.2.1. Retinitis Pigmentosa

Although the term retinitis implies inflammation it is a group retinal degeneration without inflammatory features. Retinitis pigmentosa is a term broadly applied to disorders in which nyctalopia and progressive peripheral vision loss occurs followed by late central vision loss. More than 100 genes have been identified that have a similar appearance on clinical exam but may affect primarily either the retina or the retinal pigment epithelium. Approximately 50% cases are sporadic while about 25% are autosomal dominant, 20% are autosomal recessive, 10% are X linked. In 30% of patients hearing loss can be observed as a systemic association known as Usher syndrome. Rods of the mid-periphery are primarily affected followed by cones. The frequency is about 1 in 3000 while the carrier state is about 1 in 100 in the USA with a worldwide estimated prevalence of 1 in 5000. On a genetic level, about 30% of autosomal dominant cases are caused by rhodopsin mutations and approximately 15% of those are single point mutations. RetNet, steadily growing online database is a collaborative effort to catalogue these (http://www.sph.uth.tmc.edu/Retnet/): the autosomal dominant form of RP can be caused by mutations in 12 different genes while more than 60 genes are identified for the autosomal recessive form and only 2 for X-linked RP (75% of those in the RPGR gene (retinitis pigmentosa GTPase regulator)). Retinitis pigmentosa that is the result of a retinal pigment epithelium defect (RPE65, RBP, RDH5) can be seen as a bystander phenomenon where photoreceptor death is the consequence. An exception is the ABCA4 gene that can cause both retinitis pigmentosa and Stargardt's disease by primarily affecting the RPE. The mutation affects a flippase of the photoreceptor outer segments that moves photo-transduction molecules through the membrane that build up when defective and are phagocytosed by the RPE. Other noteworthy major genes are the RDS/peripherin gene and the beta-phosphodiesterase of the photo-transduction cascade.

In the following hereditary fundus dystrophies are described that are rare but cause profound visual loss. Because the genetic defect is identified and animal models exist, these are amenable to a gene therapy approach in theory.

6.2.2.2.2. Best Disease

Juvenile Best disease has an AD inheritance. Vision is usually acceptable until the fifth decade after which there is a sharp decline due to macular scarring, choroidal neovascularization, geographic atrophy or hole formation. The course of the disease can be staged according to the fundus exam: stage 0 (pre-vitelliform) is characterized by a subnormal electrooculogram and normal fundus, stage 1 shows pigmentary macular mottling, stage 2 (vitelliform) presents in the first to second decades. Stage 3 is characterized by a pseudohypopyon due to partial absorption of lipofuscin while stage 4 has the vitelliruptive ("scrambled egg") lesion with diminished vision. [5904376, 10737974] The most common mutation is found in VMD2 that encodes bestrophin, a multispan transmembrane protein preferentially expressed in the RPE that is localized at the basolateral plasma membrane and functions as an oligomeric chloride channel. VMD2 is highly and preferentially expressed in the RPE [9662395 9700209]. Although accumulation of lipofuscin-like material within and beneath the RPE is also seen in age-related macular degeneration of patients with age-related macular degeneration show that VMD2 does not play a major role in this common disorder [10854112 10453731]. Guziewicz et al. suggested that canine multifocal retinopathy, an autosomal recessive disorder of multiple dog breeds that shares a number of clinical and pathologic similarities with Best macular dystrophy may be used as an animal model for Best disease.[17460247] In this study two disease-specific sequence alterations were identified in the canine VMD2 gene: a C(73)T stop mutation in cmr1 and a G(482)A missense mutation in cmr2.

The adult-onset vitelliform macular dystrophy is a rare autosomal dominant disorder with incomplete penetrance and highly variable expression that only causes mild metamorphopsias in the fourth to sixth decades. It is considered a subtype of patterned dystrophy of the retinal pigment epithelium (RPE).

6.2.2.2.3. Choroideremia

Choroideremia is an x-linked recessive diseases in which female carriers have mild patchy peripheral RPE changes however in males nyctalopia already presents in the first decade.[309] Progressive, diffuse atrophy of the choroid and RPE occurs with consecutive photoreceptor death. The scotopic electroretinogram is non-recordable and the photopic is severely subnormal as is the electrooculogram. Second to the RPE atrophy on fluorescein angiography prominent filling of retinal and large choroidal vessels can be seen with central blockage at the fovea surrounded by hyperfluorescence. Most patients retain some useful vision up to the sixth decade after which very sever visual loss occurs.

The choroideremia gene encodes for a protein, the Rab escort protein-1 (REP1), which is involved in membrane trafficking and several point mutations have been described[310] that introduce a premature termination codon. Tomachova et al.[311] created a knockout mouse model of the CHM gene in which heterozygous-null females display the features of choroideremia.

6.2.2.2.4. Favre Goldmann Syndrome

Favre-Goldmann syndrome is an autosomal recessive disease that causes nyctalopia already in childhood. Signs on exam are vitreous degeneration, congenital retinoschisis, pigmentary retinopathy and white, dendritiform, arborescent peripheral retinal vessels. The electroretinogram is reduced and the prognosis is poor. The genetic defect is located in the NR2E3 gene (nuclear receptor subfamily 2, group E, member 3 PNR, which encodes a retinal nuclear receptor that is a ligand-dependent transcription factor that regulates embryonic development and is required for regular maintenance in the adult. In early human NR2E3 disease demonstrates an S-cone hyperfunction in a thickened retina. Akhmedov et al. showed that in the rd7 mouse a deletion in a photoreceptor-specific nuclear receptor is responsible for the retinal degeneration ob served.

6.2.2.3. Rational for Gene Therapy for Retinal and Choroidal Diseases

Ocular gene therapy offers a novel approach to treating eye diseases characterized by retinal neovascularization (e.g. diabetic retinopathy, age related macular degeneration,

retinopathy of prematurity),[278, 312-314] or chronic retinal degeneration.[281, 282, 315-320] Several different viral vector systems have been proposed, including lentiviral and adenoviral (Ad) vectors as used in this thesis. These vectors have markedly different biologic properties; lentiviral vectors, such as those based on the feline immunodeficiency virus (FIV),[1, 279, 321] require integration into the host genome as an obligate part of the life cycle and have shown little direct immunogenicity or toxicity,[322-324] which may facilitate long-term expression.[76, 240, 254] In contrast, Ad vectors remain episomal, persist variably, undergo dilutional attrition with cell division and are often immunogenic, which may result in shorter-term expression.[325-328]

Parameters for lentiviral transduction efficiency were examined in the neonatal rat in particular because these animals have been used to study retinopathy of prematurity, and they are useful to investigate anti-angiogenic factors *in vivo*.[329-333] Retinal and subretinal neovascularization is common to a number of ocular diseases, many of which are leading causes of blindness, e.g. diabetic retinopathy, exudative age-related macular degeneration, and retinopathy of prematurity. These diseases are good candidates for RPE-targeted gene therapy since specific growth factors that modulate neovascularization are secreted by the RPE or neighboring cell types.[285, 286] However, the tropism of lentiviral vectors within the rodent retina appears to depend on the route of injection, transgene promoter, age, and species.[266, 278, 280, 281, 334-339] In particular, age (injecting within the first five days post-natal) has been a critical factor favoring lentiviral transduction of photoreceptors.[280]

6.2.3. Mediators of Ocular Angiogenesis

The development of ocular neovascularization depends on the balance of angiogenic and angiostatic elements,[340] both of which can be exploited in gene therapy. Relevant growth factors and inhibitors include vascular endothelial growth factor (VEGF), insulin-like growth factor-1 (IGF-1),[341, 342] pigment epithelium-derived factor (PEDF),[312, 314, 343-349] matrix metalloproteinases (MMPs),[350-354] tissue inhibitors of MMPs (TIMPs),[314] angiostatin,[313, 355, 356] endostatin,[314, 349, 357, 358] and others.

VEGF is a potent endothelial-cell-specific mitogen[359, 360] expressed by pigment epithelial cells, pericytes, vascular endothelial cells, neuroglia and ganglion cells.[300,

[359, 361, 362] It plays a crucial role during retinal development.[363] Expression of VEGF is up-regulated by hypoxia[362, 364] through the hypoxia-inducible factor-1 (HIF-1) transcriptional element.[365] VEGF acts through high affinity receptor tyrosine kinases specific receptors, fms-like tyrosine kinase (Flt)-1 and fetal liver kinase-1 (Flk-1)/kinase insert domain-containing receptor (KDR) phospholipating Cγ and other proteins to form diacylglycerol (DAG) activate protein kinase C (PKC) ultimately leading to endothelial cell proliferation, migration, and increased vascular permeability.

Patients with proliferative diabetic retinopathy, retinopathy of prematurity, vascular occlusion and choroidal neovascularization have increased levels of VEGF[366-368] that can be simulated in experimental models of retinal ischemia.[361, 369] Many novel therapies target VEGF as a central molecule of angiogenesis: neutralizing VEGF antibodies,[288, 370, 371] soluble VEGF-like receptors,[372] oligonucleotides,[373-375] VEGF receptor sFlt-1 (sequestrates VEGF),[376, 377] inhibition of VEGF-specific protein kinase.[360]

Insulin-like growth factor 1 (IGF-1) mediates effects of growth hormone,[342] but can also induce angiogenesis directly.[378] Inhibition of IGF-1 by a receptor antagonist was able to suppress retinal neovascularization in mice.[379]

Pigment epithelium derived factor (PEDF) is a new member of anti-angiogenic molecules successfully used in animals to inhibit neovascularization. A non-inhibitory member of the serine protease inhibitor (serpin) superfamily of proteins,[380] PEDF was first described as a neurotrophic factor.[381-384] The potent anti-angiogenic properties of PEDF, possibly promoted though endothelial cell apoptosis,[348] were only discovered much later.[286] Imbalance between PEDF and VEGF have been proposed as a mechanism of action in retinal neovascularization.[273, 286, 385-388] Pigment epithelium-derived factor (PEDF) was recently identified as an inhibitor of angiogenesis and is among the most potent in comparative studies.[286] PEDF has specific inhibitory activity against VEGF, a substance thought to be responsible for OIR.[287-289] The physiologic source of PEDF in the eye is the RPE, from which it diffuses into other retinal layers. Normal roles of PEDF appear to be stopping retinal vascularization at appropriate points in development and inhibition of neovascularization in adult life.[286] PEDF levels may be decreased in eyes with pathological neovascularization, e.g. diabetic retinopathy[294, 385, 386] and age-related macular degeneration.[273]

Angiostatin and endostatin, in particular, have yielded promising results in experimental models,[313, 314, 349, 355, 357, 358] although these inhibitors have yet to be evaluated in clinical trials for ocular neovascular disorders.[389]

Subretinally expression of VEGF inhibitor sFlt-1,[390] PEDF[312] and angiostatin[313] was also able to reduce neovascularization in models of choroidal neovascularization.

Finally, tissue inhibitors of matrix metalloproteinase[314] and a soluble form of the Ang2 receptor[391, 392] have been proposed as therapeutic molecules for gene therapy of retinal neovascularization.

6.2.4. Models of Retinal and Choroidal Neovascularization

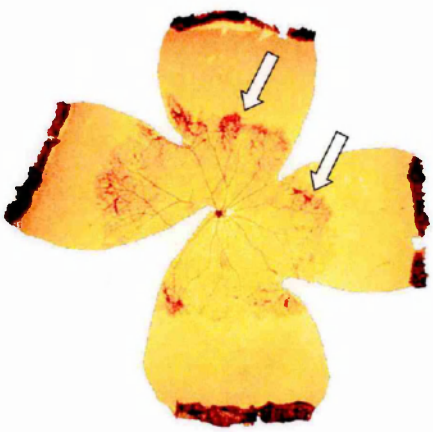

Figure 5: Quantification of retinal neovascularization in a model of oxygen induced retinopathy. Flat mounted, stained retina is divided into clock hours and pathological vessel buds (arrows) are counted.[393]

The most common animal models for retinal neovascularization are models of oxygen-induced retinopathy in the mouse[394] or rat[333, 395, 396] that allow reliable induction of neovascularization and its quantification[393] (Figure 5). In these models, newborn mice or rats that are exposed to cycling oxygen levels develop retinal neovascularization during the relative hypoxia on return to room air. In addition, newborn rats may be kept in expanded litters of n = 25 to mimic the low birth weight of premature human neonatals. I used this litter design in the experiments described below already to develop marker gene delivery as a basis for future gene therapy.[75, 76]

Other models of neovascularization include choroidal neovascularization induced by rupture of Bruch's basement membrane with laser[397, 398] or the local application of VEGF[399, 400] and basic fibroblast growth factor.[401]

The neonatal rat model has the advantage that it is more established than these models, is widely used in various models of retinal neovascularization, particularly for retinopathy of prematurity and diabetic retinopathy.[329-333, 393, 402]

6.3. Gene Therapy

6.3.1. Definition

In gene therapy, diseases are treated by manipulating the genetic material in a targeted cell population to change its expression pattern. Genetic reprogramming requires detailed knowledge of the genetic basis of a disease. The most common and ethically accepted form of gene therapy is somatic gene therapy, which seeks to correct gene expression without propagation of this correction to the next generation. Treatment goals have a wide range from specific repair of genetic defects to less specific amendment of or interference with nongenetic disease processes. Classically, the genetic material is delivered to a cell in the form of DNA or RNA for the expression of therapeutic proteins (

Figure **6**), but recently discovered features of RNA (small interfering RNA,[403-406] reviewed in[407] and ribozymes,[408-410] reviewed in[411, 412]) have increased the options.

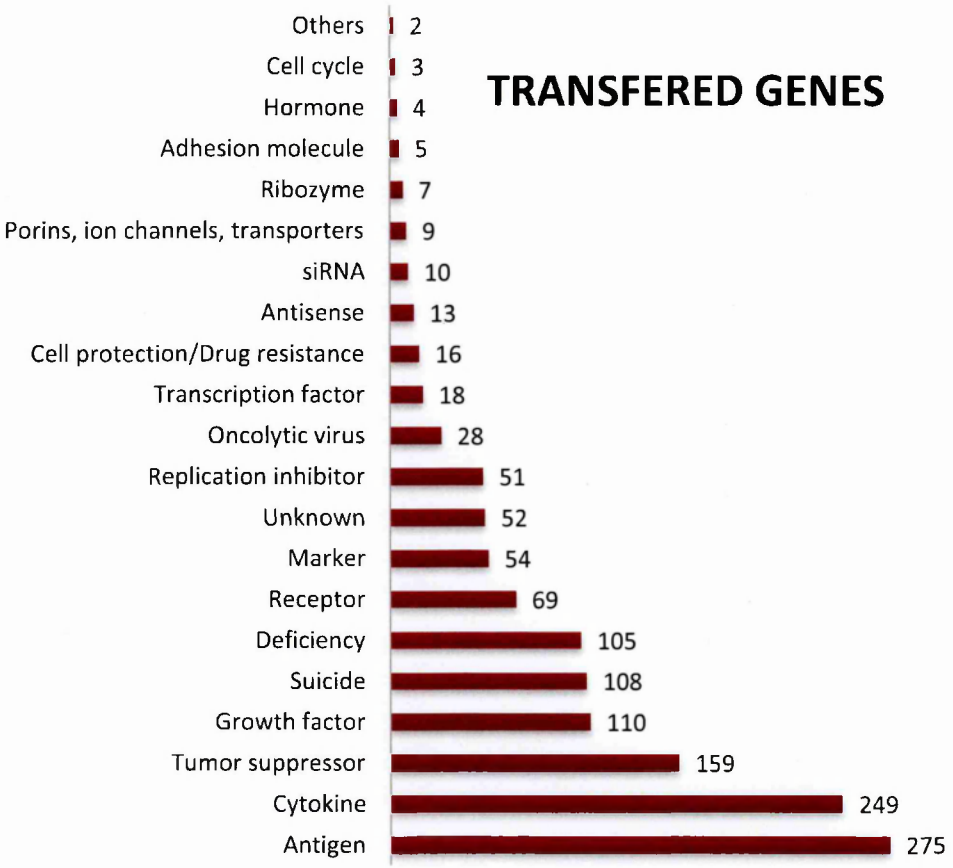

Figure 6: Gene types transferred in clinical gene therapy trials (data from the online database provided by The Journal of Gene Therapy).

Fundamental goals in gene therapy are the *specificity*, *efficiency,* and *safety* of gene delivery. Vehicles that encapsulate therapeutic genes for delivery are called "vectors". For chronic diseases, expression from these vectors should ideally persist for the whole life of the cell and lead to a permanent cure, while short-term function is sufficient for acute diseases.

Most vectors currently in use are based on attenuated or modified versions of viruses and exploit the highly efficient targeting and gene delivery that have evolved from the adjustment of a pathogen to its host, by abandoning their pathogenicity and effectively turning them into a Trojan horse. Commonly used viral vectors are derived from adeno-associated virus, type-C retroviruses, lentiviruses, adenovirus, herpes simplex virus, but other viruses such as measles, alphaviruses, and paramyxoviruses

have also been engineered into vectors. A variety of non-viral gene delivery systems is available that are based on cationic, cholesterol-containing liposomes, peptide-lipid vectors, activated dendrimers (branched DNA-binding carbohydrates), bacteria, artificial chromosomes or artificial viruses (liposomes with viral components).

6.3.2. History

Ideas for the genetic reprogramming of cells appeared already in 1967, when Nobel laureate Marshall Nirenberg reflected on reprogramming cells with synthetic messages in an editorial in Science entitled "Will Society Be Prepared?"[413] that addressed the concerns raised by molecular geneticists. Nirenberg contended that the impulse to exploit molecular genetics could only be kept in check by sobriety and caution: "When man becomes capable of instructing his own cells, he must refrain from doing so until he has sufficient wisdom to use this knowledge for the benefit of mankind. [...] decisions concerning the application of this knowledge must ultimately be made by society, and only an informed society can make such decisions wisely." In a draft of his Nobel acceptance speech[414] Nirenberg stressed that knowledge of the genetic code made it likely that "man eventually will ... influence his own biological evolution. One can predict that a new area of research will emerge during the next twenty-five years, that of molecular evolution, in which the effects of synthetic genes upon the economy of the cell will be explored in a systematic fashion."

This prediction rapidly materialized, when Stanfield Rogers attempted to treat two patients suffering from hyperargininemia with the Shope papilloma virus (SPV) in the early 1970s.[415] Four years later first regulations of recombinant DNA research became available when the National Institutes of Health (NIH) created the Recombinant DNA Advisory Committee (RAC). The acceptance of gene therapy experienced a setback when in 1980 Martin Cline performed recombinant DNA transfer into bone marrow cells of two patients with hereditary blood disorders, but tried to avoid review by this body and conducted these studies abroad under questionable circumstances.[416-425] In 1984 the RAC created a new group, called the Human Gene Therapy Working Group (later called the Human Gene Therapy Subcommittee (HGTS)) to specifically review gene therapy protocols[426], the first two of which it received in 1990. One protocol by Michael Blaese and French Anderson proposed treatment of SCID,[427] a fatal and

incurable childhood disorder that has become one of the greatest successes of gene therapy.[262]

6.3.3. Types of Gene Transfer Vectors

As obligate intracellular parasites, viruses are optimized gene transfer vehicles by design that have evolved mechanisms to enter and take reprogram the infected host with great specificity and efficiency. These mechanisms can be exploited by replacing non-essential genes with genes of interest that can be transferred for a therapeutic or experimental purpose. Non-essential genes that are still needed during vector production can be provided in trans from other plasmids the genetic information of which will not become part of the physical vector particle. Because of the intricate host-virus interaction of their parent virus vectors may elicit a similar immune response.

In the following the most commonly used vector types are briefly reviewed to help put lentiviral feline immunodeficiency viral vectors used in this thesis into context. The order of discussion follows the percentage of usage in clinical trials as listed above.

6.3.3.1. Adenoviral Vectors

Despite early short comings, adenoviral vectors are used in 25% (337 trials) of all clinical gene therapy trials. Adenoviruses have a large genome of 35 kb 30 kb of which can be replaced with foreign DNA allowing for an exceptionally large cargo among current gene therapy vectors. They are non-enveloped viruses that contain a linear double stranded DNA genome. Most of the 40 serotypes cause benign respiratory tract infections in humans. Subgroup C serotypes 2 and 5 are commonly used as vectors. Adenoviruses do not integrate into the host genome but replicate as episomes. As a result potential disadvantages are that patients often are pre-immunized due to prior exposure, that permanent expression is difficult to achieve and that vectors can aerosolize during production.

Four early transcriptional elements (E1 through 4) have regulatory functions while a late transcript codes for structural proteins. In early adenoviral vectors either E1 or E3 were inactivated and supplied during the production process in trans as can be done

with HEK293 cells.[428] Second generation vectors utilize an E2a temperature sensitive mutant[429] or an E4 deletion.[430] More recent so called gutless vectors contain only the inverted terminal repeats and packaging sequence around the transgene while all other needed viral genes are provided in trans by a helper virus.[431]

A major advantage is the broad tropism and the relative ease compared to other vectors with which very high titers of adenoviral vectors can be achieved enabling injection of small volumes in restricted spaces or small species. However, expression is generally short lived, especially in earlier generation vectors with E1 deletion. After intravenous administration up to 90 percent are already removed and broken down in the liver.[432] Transduced cells are often eliminated by cytotoxic T cells (CTLs) within a short time and promoter shut down may follow in those that are not ablated by CTLs.[430] Immune suppression[433, 434] or oral induction of tolerance[435] or administration of CTLA4Ig, which is known to block co-stimulatory signals between T cells and antigen presenting cells,[436] can prolong transgene expression or permit repeat application. Occasionally, adenoviral vectors can induce an unpredictable toxicity the resulting inflammation of which has even resulted in a fatal outcome in one case in one patient.[437] Adenovirus type 3, 4 and 11 more often results in toxicity compared to others[438] (adenovirus type 5 was used in Jesse Gelsinger) but the mechanism is still poorly understood.

Later generation vectors contain fewer adenoviral genes or no adenovirally expressed genes ("gutless vector"[439]). However, even such gutless vectors may trigger an immune response to the viral proteins that engulf the transferred DNA. Clinical application is nevertheless limited because a large proportion of the population has already been exposed to adenovirus.[440]

Adenovirus update occurs in a two stage process that involves interaction of the fiber coat protein with MHC class I molecules[441] and the Coxsackie virus-adenovirus receptor.[442] The penton base protein then binds to integrins[443] and is internalized via receptor mediated endocytosis. Most cells express primary receptors for the adenovirus fiber coat protein but the process of internalization is more selective.[444] Uptake into target cells can be improved by stimulating expression of appropriate integrins,[445] antibody targeting by conjugating vectors with antibodies[446, 447] or by incorporating receptor binding motifs into the fiber coat protein.[448]

Rosenfeld et al. were the first ones to transduce rat respiratory epithelium with human alpha 1AT, the gene for alpha 1-antitrypsin deficiency resulting in functional secretion from analyzed lung tissue. The major shortcoming of adenoviral vectors, short-term expression and immunogenicity was noticed as expression could only be followed for one week.[449]

Other historically important studies include Akli et al.'s transfer of beta-galactosidase into rat brain using an adenoviral vector with E1 and partial E3 deletion.[450] For the first time the authors described adenoviral gene transfer to post-mitotic, neuronal tissue. A formidable target for gene transfer as type C retroviral vectors cannot be used for this purpose. The authors find that 3 x 10^5 TU delivered in 10 microliters did not result in any tissue toxicity but note that this could be seen at 10^7 TU per 10 microliter. This highlights the relative ease with which high titers of vectors can be generated. Similar results were quickly replicated elsewhere.[451] Adenoviral vectors experienced a surge of popularity

The first functional mammalian odorant receptor could be expressed in sensory neurons in the rat olfactory epithelium using adenoviral vectors.[452] Zhao took an elegant approach to demonstrate receptor function and specificity by using recombinant adenovirus expressing a hybrid mRNA encoding the I7 odorant receptor and green fluorescent protein and introducing them into the nasal cavity of rats. Imaging of the GFP in the olfactory neuroepithelium revealed that up to 10% of the cells expressed GFP and that the virus selectively infected the neuronal cell population. The authors assessed the electrophysiological response of wild-type and infected epithelium to individual odorant application by a measurement of transient, induced electrical potential, the electroolfactogram. The use of real olfactory neurons to direct the expression of introduced G protein-coupled receptors circumvents the previous difficulties in protein translocation and receptor function. Those receptor receptors were difficult to study because no particular mammalian receptor had been definitely paired with a ligand.

An interesting idea of ameliorating telomere loss was accomplished by adenoviral vector mediated essential telomerase RNA (mTR) gene in telomerase-deficient mice. In these mice, telomere dysfunction is associated with defects in liver regeneration and accelerated development of liver cirrhosis in response to chronic liver injury. Adenoviral delivery of mTR into the livers of mTR(-/-) mice with short dysfunctional

telomeres restored telomerase activity and telomere function, alleviated cirrhotic pathology, and improved liver function.

Recombinant, replication-incompetent adenovirus serotype 5 (rAd5) vector-based vaccines for human immunodeficiency virus type 1 and other pathogens have proved highly immunogenic in preclinical studies but are limited by the high prevalence of pre-existing anti-Ad5 immunity in human populations. Roberts et al. showed that recombinant adenoviral vectors serotype 5 can be engineered to circumvent anti-Ad5 immunity.[453] The authors constructed novel chimaeric Ad5 vectors in which the seven short hypervariable regions (HVRs) on the surface of the Ad5 hexon protein were replaced with the corresponding HVRs from the rare adenovirus serotype Ad48. These HVR-chimaeric rAd5 vectors were produced at high titers and were stable through serial passages in vitro. HVR-chimaeric rAd5 vectors expressing simian immunodeficiency virus Gag proved comparably immunogenic to parental rAd5 vectors in naive mice and rhesus monkeys. In the presence of high levels of pre-existing anti-Ad5 immunity, the immunogenicity of HVR-chimaeric rAd5 vectors was not detectably suppressed, whereas the immunogenicity of parental rAd5 vectors was abrogated. These data demonstrated that functionally relevant Ad5-specific neutralizing antibodies are focused on epitopes located within the hexon HVRs. Moreover, these studies showed that recombinant viral vectors can be engineered to circumvent pre-existing anti-vector immunity by removing key neutralizing epitopes on the surface of viral capsid proteins.

The opposite approach, taking advantage of the immunogenicity of adenovirus is to use vectors to develop vaccines. Shiver et al. used a replication incompetent adenovirus type 5 vector expressing the SIV gag protein to illicit a protective immune response to infection with a pathogenic HIV-SIV hybrid virus.[454] Ad5 vectors immunized animals exhibited the most pronounced attenuation compared to plasmid DNA or modified vaccinia Ankara (MVA) virus. A similar strategy was applied by Letvin et al[455] who immunized monkeys with E1 deleted, E3-defective adenoviral vectors encoding SIV gag, pol and env. Although tested monkeys demonstrated a reduction in viremia only in the early phase of SIV challenge, this was associated with prolonged survival and preserved central memory CD4+ T lymphocytes.

6.3.3.2. Retroviral Vectors

Retroviral vectors have been used for many years in clinical trials contributing to 22.6 percent of clinical trials because they can easily be pseudotyped allowing for a broad host range, high titers can be achieved by ultracentrifugation and vector production cell lines can be made[456] as these vectors integrate. In contrast to adenovirus, prior exposure to retroviruses in treated subjects is highly unlikely and pre-existing immunity is not expected.[457] As described in the section reviewing AAV vectors, pre-existing immunity has recently been found to be an unexpectedly grave problem with AAV vectors that can cause destruction of transduced cells although no AAV capsid proteins are synthesized de novo.[458]

In the following discussion "retroviruses" refers to both type C retroviruses and lentiviruses unless mentioned otherwise. Retroviruses are enveloped, single stranded RNA viruses of 7 to 11 kb and 80 to 100 nm size although pseudotyped particles may be slightly larger. After cell entry the RNA is reverse transcribed into a double stranded DNA that is eventually integrated into the host genome. Gag (group specific antigen, core protein), pol (polymerase, coding for reverse transcriptase and env (envelope) are the three genes that can be found in any retrovirus. These are usually replaced with transgenes with exception of the packaging signal that is contained in gag. Removal of non-essential genes and separation of packaging, envelope and transfer function to different plasmids has made vector production a lot safer. There are long terminal repeats (LTRs) at each end of the genome that contain promoter and enhancers for the integration. Several splice sites are responsible for the generation of the different RNAs during the viral life cycle and can complicate vector design.

Some retroviruses contain proto-oncogenes that must be removed in vector design. Retroviral genomic integration, a required step in the viral life cycle, is mutagenic by definition. Retroviral integration is usually well tolerated but may be oncogenic itself if it occurs near a cellular proto-oncogene or by disrupting a tumor suppressor gene or alteration of transcription start sites which are favored integration sites for the Moloney murine leukemia virus (MLV).[459] Most retroviral vectors are based on the Moloney murine leukemia virus, an amphotrophic virus that is capable of entering both mouse and human cells which allows production in mouse cells and transduction of human target cells. The packaging capacity is limited to about 7.5 kb which requires use of cDNA. Because transduced cells are permanently altered, retroviral

vectors can be used to generate cell lines. This is usually accomplished by co-transfer of a non-cap dependent, internal ribosomal entry site-mediated marker[460] that can be selected for by resistance or visualized and sorted for instance by fluorescence-activated cell sorting (FACS). The tropism of the retroviral envelope is a key determinant determining the target cell range. Attempts have been made to retarget retroviral vectors (reviewed in[461]) but often this interferes with efficiency of vector uptake.[444]

Pseudotyping is an easier approach to target transduction yet potentially less specific than direct modification of retroviral envelope proteins. Retroviruses can use a surprisingly wide range of envelope proteins from other viruses that are not at all related to the family of retroviruses. The most commonly used pseudotype, vesicular stomatitis G protein, allows for a broad target range and provides high stability for concentration by ultracentrifugation.[462] A well known example of altering the tropism by pseudotyping is use of the rabies glycoprotein in retroviral vector envelop which facilitates transduction of neurons.[463] Others are the Jaagsiekte sheep retrovirus,[464] maedi-visna virus,[465] gibbon ape leukemia virus,[466] equine infectious anemia virus,[467] avian leucosis-sarcoma virus,[468] baculovirus,[469] Lassa virus,[470] rabies virus,[471] Mokola virus,[471] filovirus,[472-474] influenza,[266] lymphocytic choriomeningitis virus,[266] Ross river virus.[475]

Type C retroviral vectors, but not lentiviral vectors, require the target cell be dividing to access to the genome.[247] As a result, gene therapy with type C retroviral vector may require removal of a patients resting cells (e.g. hematopoietic stem cells) and induction of cell division.[476] Despite genomic integration, long-term expression can be difficult to achieve because of promoter interference of interferons, specifically IFNα and IFN-γ, with viral LTRs[477] and methylation of the integrated retroviral genome and flanking host DNA sequences.[478]

Because of the need for cell division and for high multiplicities of infection per target cells, retroviral gene therapy typically requires extraction of the target tissue (e.g. harvesting of hematopoietic stem cells) and transduction ex vivo prior to re-implantation. This adds the additional safety benefit of being able to select for desired characteristics of transduced cells before patient exposure to genetically modified material.

Several breakthrough therapies have been developed using retroviral vectors to treat previously incurable diseases. Hacein-Bey-Abina et al. achieved a functionally adaptive immune system in patients with X-linked severe combined immunodeficiency (SCID).[479] In this disease, a mutation in the gene encoding the common gamma chain is lethal unless an allogenic stem-cell transplantation is performed. The study authors infused autologous hematopoietic stem cells that had been transduced in vitro with the gamma gene using an MLV vector. Transduced T cells and natural killer cells appeared in the blood of four of the five patients within four months. The numbers and phenotypes of T cells, the repertoire of T-cell receptors, and the in vitro proliferative responses of T cells to several antigens after immunization were nearly normal up to two years after treatment. Patients developed a normal sized thymus gland. Although the frequency of transduced B cells was low, serum immunoglobulin levels and antibody production after immunization were sufficient to avoid the need for intravenous immunoglobulin. Correction of the immunodeficiency eradicated established infections in some patients and allowed them to live a normal life. However, almost 3 years after gene therapy, uncontrolled exponential clonal proliferation of mature T cells occurred in two patients.[480] Both patients' clones showed retrovirus vector integration in proximity to the LMO2 proto-oncogene promoter, leading to aberrant transcription and expression of LMO2. Retroviral vector insertion triggered deregulated premalignant cell proliferation. The analysis showed that this was most likely driven by retrovirus enhancer activity on the LMO2 gene promoter.

Aiuti et al. used hematopoietic stem cell gene therapy for adenosine deaminase (ADA) deficient SCID.[481] The authors used an MLV vector to replace the defective ADA and achieved sustained engraftment of engineered HSCs with differentiation into multiple lineages resulted in increased lymphocyte counts, improved immune functions (including antigen-specific responses), and lower toxic metabolites. Both patients are currently at home and clinically well, with normal growth and development. These results indicate the safety and efficacy of HSC gene therapy combined with nonmyeloablative conditioning for the treatment of SCID.

Morgan et al. demonstrated that regression of metastatic melanoma can be achieved using genetically engineered lymphocytes.[482] In this study autologous lymphocytes

were harvested from peripheral blood and transduced with a retroviral vector encoding the alpha and beta chains of the anti–MART-1 T-cell receptor. These genes were cloned from a tumor infiltrating lymphocyte clone obtained from a cancer patient who demonstrated a near complete regression of metastatic melanoma after adoptive cell transfer. Adoptive transfer of the transduced cells resulted in durable engraftment for at least 2 months after infusion and objective regression of metastatic melanoma lesions. Although this outcome could only be achieved in 2 out of 15 patients it demonstrates the therapeutic potential of genetically engineered cells for the biologic therapy of cancer.

Different from the above trials that involved correcting a lymphoid immunodeficiency, Ott et al. successfully corrected and clinically improved subjects suffering from X-linked chronic granulomatous disease (X-CGD),[483] a primary immunodeficiency caused by a defect in the oxidative antimicrobial activity of phagocytes resulting from mutations in gp91(phox). Substantial gene transfer could be noted in the two participating children's neutrophils that lead to a large number of functionally corrected phagocytes. A large-scale retroviral integration site-distribution analysis showed activating insertions in MDS1-EVI1, PRDM16 or SETBP1 that had influenced regulation of long-term hematopoiesis by expanding gene-corrected myelopoiesis three- to four-fold in both individuals. The risks associated with the use of retroviral vectors for X-CGD was estimated to be low because $gp91^{phox}$ is not known to provide a survival or growth advantage to transduced cells, and abnormal hematopoiesis or leukemogenesis have not been observed in animal models of X-CGD transplanted with $gp91^{phox}$-expressing cells.

Alzheimer disease is characterized by loss of cholinergic neurons as one of its cardinal features. Nerve growth factor (NGF) stimulates cholinergic function, is able to prevent cholinergic degeneration in animal models and improve memory. Tuszynski et al. transduced autologous skin fibroblasts with an NGF MLV vector in subjects with early probable Alzheimer.[484] This trial is remarkable for several reasons: it involved subjects with a relatively early stage of the disease and addressed an ailment that is – in contrast to the previously mentioned studies – not lethal. In the contrary, several medical treatment options exist. After transduction, NGF production was measured, and cells were stereotactically injected into the cholinergic basal forebrain over a region of 1 cm in length in awake but sedated subjects. NGF induced

cholinergic axon sprouting into the site of NGF delivery. At mean follow-up of 22 months no long-term adverse effects of NGF occurred. Evaluation of the Mini-Mental Status Examination and Alzheimer Disease Assessment Scale-Cognitive subcomponent suggested improvement in the rate of cognitive decline. Serial PET scans showed significant ($P < 0.05$) increases in cortical 18-fluorodeoxyglucose after treatment. Brain autopsy from one subject suggested robust growth responses to NGF.

Junctional epidermolysis bullosa (JEB) is a devastating and often fatal skin adhesion skin disorder. In an Italian study,[485] a single individual with nonlethal JEB was treated with a retroviral vector expressing LAMB3 CDNA encoding LAM5-beta3, the basement membrane component that is defective in this disease. The patient was a double-heterozygous carrier of a null allele and a single point mutation (E210K) in the *LAMB3* gene who had suffered from blistering skin occurring spontaneously or after minimal injury. Epidermal stem cells were transduced, expression of LAM5 was conformed and nine graft were transplanted onto surgically prepared regions. This skin remained stable at the 1 year follow up without blisters, infections or rejection.

6.3.3.3. Lentiviral Vectors

A subfamily of retroviruses, lentiviruses (lenti = Latin for slow) typically cause slowly progressing diseases with incubation times that can amount several years. As lentiviruses, lentiviral vectors permanently integrate in both dividing and nondividing cells as Naldini et al. showed in their elegant study.[240] Others have confirmed these results or applied those vectors to other hard to transduce cell types.[280, 486]

Lentiviruses are considerably more complicated than type C retroviruses and – in the case of HIV - contain the additional six genes tat, rev, vpr, vpu, nef and vif in addition to gag, env and pol. As for type C retroviral vectors, packaging cell lines can be generated[487] and the other afore mentioned advantages of retroviral vectors apply. A recent study by Yanez-Munoz et al. demonstrated that lentiviral integration is not always a requirement in order to obtain expression levels high enough to achieve therapeutic transgene levels when subretinal delivery of an integration-deficient HIVvector carrying a functional human *RPE65* transgene led to expression of *RPE65* in transduced RPE with functional rescue as assessed by electroretinography for at least 8 weeks.[488] FIV vectors can express transgenes in non-dividing cells in the

absence of a functional integrase but that expression is lost when growth-arrested cells are allowed to divide again.[279] Transduction is negligible in dividing cells. The retinal pigment epithelium that Yanez-Munoz studied is non-dividing in vivo.

Replication-defective lentiviral vectors were originally derived entirely from the human lentivirus human immunodeficiency virus type 1 (HIV-1).[489, 490] Application of pseudotyping with broadly tropic, physically stable envelope glycoproteins[462] permitted efficient transduction of nonlymphocytes by HIV-1 vectors in vitro and in vivo.[240, 491] The first nonprimate lentivirus-based vector was derived from feline immunodeficiency virus (FIV).[1] Subsequently, substantial improvements have been made in the design and capabilities of FIV vectors, and recently identified FIV elements (central polypurine tract, central termination sequence, and packaging signal) have been incorporated.[492, 493]

6.3.3.3.1. Important Lentiviral Properties

Retroviral reverse transcription (**Figure 7**) yields a linear double-stranded DNA intermediate that is integrated into the target cell genome (Figure 8) in a reaction catalyzed by the viral integrase. Therefore, retroviral vectors generate permanent transgenes, a process that makes the former appealing for therapy of chronic diseases. This capability was first demonstrated for vectors derived from simple oncoretroviruses, e.g., murine leukemia viruses. Oncoretroviral vectors have now been incrementally optimized to the point that clinical utility has been demonstrated for diseases that are recognized to be the targets most accessible to gene therapy. For example, children with common gamma chain deficiency, in which gene-altered cells have a marked survival advantage, have sustained clinical improvement.[262, 494] However, it became apparent early on that oncoretroviral vectors achieve integration only in target cells that are proliferating at the time of transduction.[246, 247] This limitation, which precludes targeting many clinically relevant cell types, is a consequence of the fact that the reverse-transcribed linear DNAs (preintegration complexes) of these simple retroviruses cannot traverse the intact nuclear envelopes of interphase cells. Completion of the replication cycle instead depends on breakdown of the envelope during mitosis.[246, 247] In contrast, the lentiviral preintegration complex is imported through the nuclear pore, permitting integration in nondividing cells.[240, 250, 251, 254] The capacity to infect nondividing cells is fundamental to the universal

lentiviral strategy of propagating through terminally differentiated macrophages and has been the principal motivation for engineering viral vectors from these highly pathogenic viruses. The mechanism of nuclear import remains controversial, but it has been attributed to multiple determinants in virion proteins[248] and to a plus strand discontinuity, the central DNA flap, which results from lentiviral initiation of plus strand synthesis at two locations.[249, 492]

While genomic integration is mutagenic by definition there are significant differences between type C retroviruses and lentiviruses. Montini et al. studied hematopoietic stem cell transduction of a tumor prone mouse model (Cdkn2a-/- mice).[495] In a comparison of integration site selection and tumor development in transplanted mice retroviral vectors retroviral vectors caused dose-dependent acceleration of tumor onset dependent on long terminal repeat activity. Insertions at oncogenes and cell-cycle genes were enriched in early-onset tumors suggesting cooperation in tumorigenesis. Surprisingly, tumorigenesis was unaffected by lentiviral vectors and did not enrich for specific integrants, despite a higher integration load and robust expression of lentiviral vectors in all hematopoietic lineages. Unlike the gamma-retrovirus MLV, EIAV and HIV-1 vectors do not integrate preferentially into the promoter region or the 5' end of the transcription unit.[496]

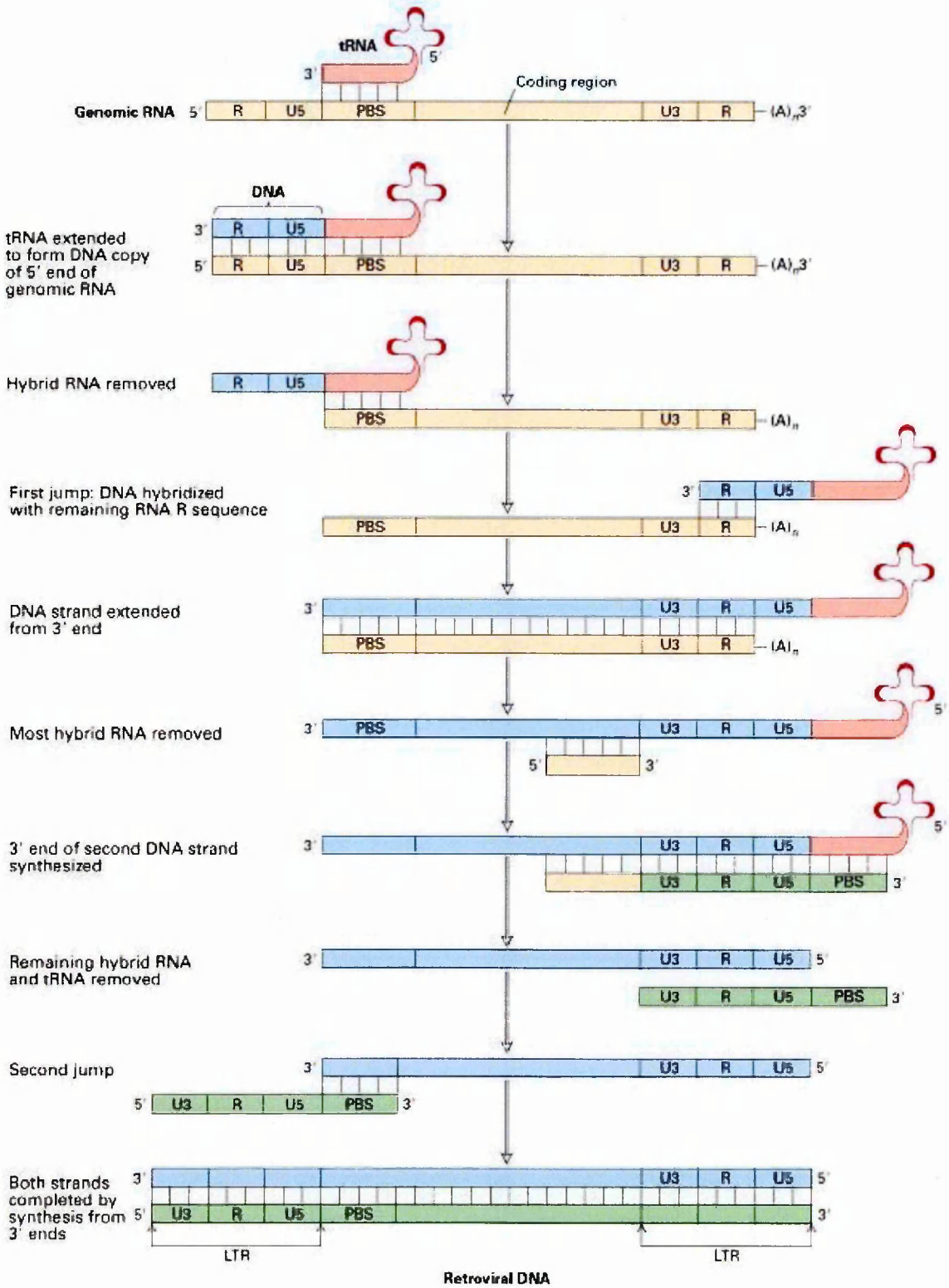

Figure 7: Reverse transcription (after ref.[497], p. 1052).

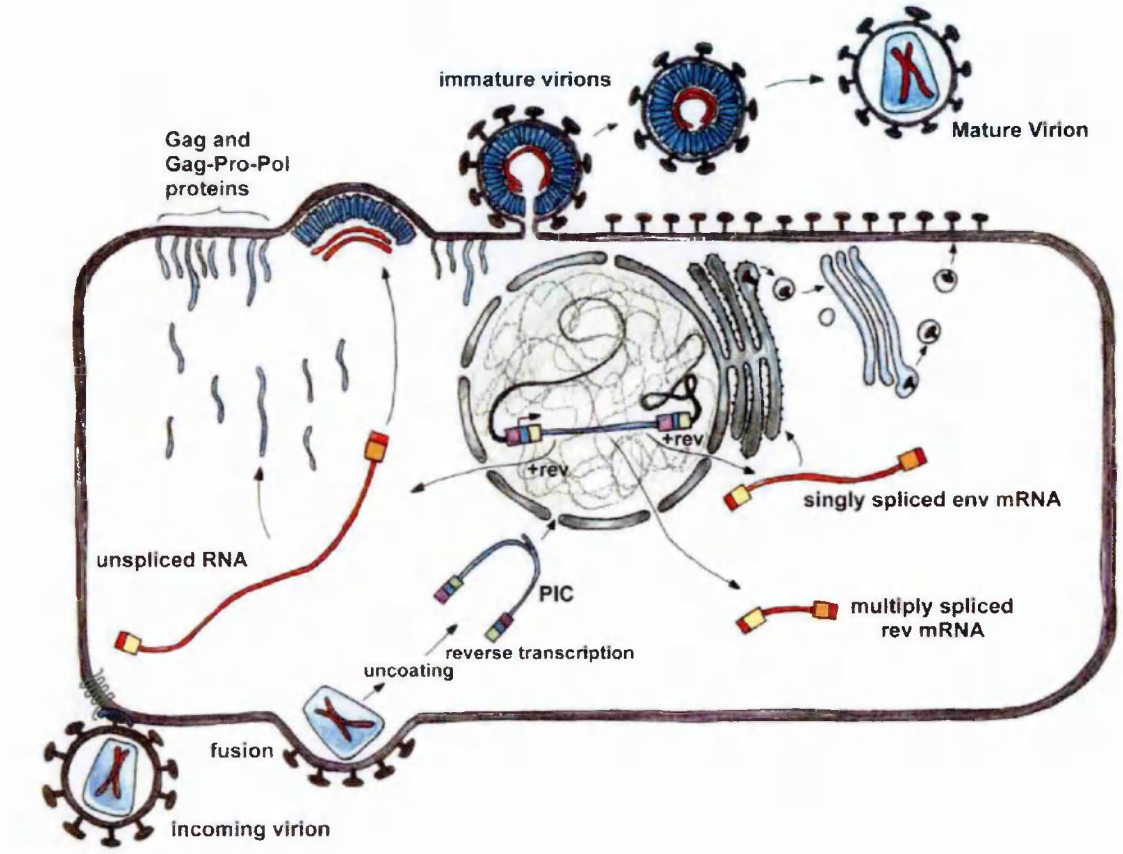

Figure 8: Lentiviral life cycle with highlighting of several genome processing/trafficking events: encapsidation, dimerization and central DNA flap formation. Both spliced (subgenomic) and unspliced (genomic) viral mRNAs exist in an infected cell, and these in turn represent only a small fraction of the total cellular RNA. Proper virion assembly requires a highly discriminating mechanism for preferential encapsidation of the full-length genome. The pre-integration complex (PIC) is shown with a central DNA flap; proteins know to be associated, e.g., integrase, Vpr, MA in HIV-1, are not shown. Drawn by Dyana Saenz, reproduced with permission.[498]

6.3.3.3.2. FIV and FIV Vectors

Three groups of lentiviruses infect primates, ungulates, and felines respectively. Feline immunodeficiency virus infects 10–20% of domestic cat populations worldwide, as well as many free-roaming, nondomestic Felidae, but is pathogenic only for the domestic cat. **Figure 12** (Top) illustrates the genomic structure of FIV 34TF10,[499] the clone used as the substrate for replication-defective FIV vector work to date. FIV has typical lentiviral morphology and genetic structure, although only three nonstructural genes (vif, rev, and orf2) are encoded in comparison to the six encoded by the primate lentiviruses.[500, 501] Other peculiarities are a Rev response

element (RRE) that overlaps the 3' end of env rather than the SU-TM junction and a pol-encoded dUTPase, which may facilitate reverse transcription under conditions of low nucleotide tension.[502]

6.3.3.3.3. Primate versus Nonprimate

No lentiviral vector system will proceed to clinical use without documentation of effective mechanisms to prevent and to screen for the most recognized threat: generation of replication-competent retroviruses. Other, theoretical considerations can be marshaled for and against use of lentiviral vectors, but empirical data are lacking. Nevertheless, there are some reasons to hypothesize that FIV vectors could eventually have higher acceptability for a broad range of applications. A practical consideration for vector workers and for potential gene therapy recipients is that FIV lacks any capacity to generate immunological cross-reactivity with HIV, for example in diagnostic HIV antibody enzyme-linked immunosorbent assays (ELISAs).[499, 501, 503] In addition, there is an extensive record of a lack of human infection or disease despite widespread human exposure to wild-type FIV via its principal and very efficient natural mode of interfeline transmission, biting (which frequently transmits other pathogens to humans), and despite the ability of the wild-type virus to use a human chemokine receptor for entry.[1, 261, 501] This epidemiological record of prevalent, direct, and efficient human inoculation without sequelae is unique among the lentiviruses. Another consideration is that FIV vectors can be tested in an animal model that is susceptible to disease causation by the parental virus.

FIV vectors efficiently complete the postentry stages of the infection cycle in nondividing human cells despite a severe block to transcription from the FIV long terminal repeat (LTR) and to other life cycle mechanisms that prevent productive replication.[1, 261, 324, 504] The replication-defective FIV vector[1]derived from the infectious clone FIV34TF10[499] was the first demonstration of the feasibility of using a nonprimate lentivirus as a substrate for vectors. The negligible FIV expression observed in human cells[261] was an initial obstacle to transfer vector production. This was overcome by substitution of the 5' FIV U3 (but not the 3' U3) with a heterologous promoter by a fusion at the TATA box just upstream of the R repeat.[261] The change enabled expression of high levels of FIV proteins and FIV vectors in human cells,[1, 261] revealing that previously suggested blocks to other productive phase functions, e.g.,

Rev,[505] do not exist, at least in the relevant human cell lines. Use of a human cell line for clinical vector production (such as 293 cells, which have been approved for adenoviral vector production by the Food and Drug Administration, FDA) is important since feline vector producer cells would be unacceptable for human clinical application because of the risk of known and unknown adventitious agents. For example, feline cells harbor multiple copies of an inducible, xenotropic, replication-competent type C endogenous retrovirus (RD114) that can replicate in human cells, resists inactivation by human serum complement, and is related at the nucleotide sequence level to a primate retrovirus (baboon endogenous virus).[506-509]

The transcriptional silence of the FIV U3 in most human cell types provides a first level self-inactivating or SIN feature, as it is copied to both LTRs in the human target cell. A standard U3 deletion can also be made to produce a conventional SIN vector as described below. In the initial studies, FIV vectors incorporating the hybrid 5' promoter were shown to transduce dividing, growth-arrested, and postmitotic human targets.[1] These results have been reproduced by others,[258, 260] and envelope glycoprotein-pseudotyped lentiviral vectors have now been derived from all three subgroups of primate lentiviruses, HIV-1, HIV type 2 (HIV-2), and simian immunodeficiency virus (SIV),[240, 250-256, 491, 510] and from the ungulate group of lentiviruses.[257, 259, 511] HIV-1 vector systems have so far received more extensive validation and molecular engineering for vector optimization,[254] but there is growing interest in exploring the potential of nonprimate lentiviral systems. It should be emphasized that no direct, methodologically rigorous comparisons of transducing efficiencies per particle in vivo are available for different lentiviral vector systems, or for that matter in human tissues, although equivalent efficacy per transducing units of FIV and HIV vectors has been demonstrated in one human organ.[504]

The following landmark studies elegantly demonstrate the most important feature of lentiviral vectors: permanent transduction of post-mitotic or terminally differentiated cells. Pawliuk et al. showed that sickle cell disease can be corrected in a transgenic mouse model using lentiviral gene therapy.[512] Sickle cell disease is caused by a single point mutation in the human betaA globin gene that results in the formation of the abnormal hemoglobin HbS (alpha2betaS2). In homozygotes, the abnormal hemoglobin polymerizes in long fibers upon deoxygenation within red blood cells, which become deformed, rigid and adhesive resulting microinfarction, anemia and

organ damage. Using a betaA globin gene variant that prevents HbS polymerization, a third generation HIV vector achieved expression for 10 months at the study endpoint and presence of the anti-sickling protein in up to 52% of total hemoglobin or 99% of circulating red blood cells. Red blood cell sickling could be successfully prevented in two mouse models and hematological parameters, splenomegaly and urine concentration defects could be prevented.

In a study involving a nonhuman primate model of Parkinson's disease, HIV vectors were engineered to express the glial cell line-derived neurotophic factor.[457] Nonlesioned aged rhesus monkeys and young adult monkeys treated with MPTP received injections into the striatum and substantia nigra. Dopaminergic function was augmented in aged monkeys while in lesioned monkeys functional deficits of hand-reach tasks hand-reach task, in which the time to pick up food treats out of recessed wells was measured, were reversed and nigrostriatal degeneration completely prevented. These functional improvements were also found using a modified parkinsonian clinical rating scale. Fluorodopa PET scans displayed solid uptake in the GDNF-treated animals. Expression was followed for 8 months in control animals. Sections from all monkeys were stained for CD45, CD3, and CD8 markers to assess the immune response after lentiviral vector injection which are markers for activated microglia, T cells, and leukocytes including lymphocytes, monocytes, granulocytes, eosinophils, and thymocytes. Staining for these immune markers was weak, or absent. Mild staining for CD45 and CD8 was seen in two animals and some CD45-immunoreactive cells displayed a microglial morphology. Most monkeys displayed virtually no immunoreactivity.

Lentiviral equine infectious anemia viral (EIAV) vectors expressing RNAi were designed to specifically target the human SOD1 gene, the dominant mutation of which (SOD1(G93A)) is responsible for a fatal neurodegenerative disease, amyotrophic lateral sclerosis.[513] RNAi is a post-transcriptional mechanism of gene silencing that is mediated by small interfering RNA molecules (siRNAs), 19- to 23-nucleotide double-stranded RNA duplexes that promote the cleavage of specific mRNAs. Long-lasting RNAi-mediated gene knockdown can be achieved using lentiviral vectors that express the siRNAs. SOD1 encodes superoxide dismutase, an enzyme that neutralizes superoxide radicals, which can damage cells if their levels are not controlled. Superoxide radicals are byproducts of normal cell processes,

particularly energy-producing reactions that occur in mitochondria. Motor neurons are particularly sensitive to SOD dysfunction when mitochondria cannot meet the high energy demands, additionally apoptosis may be induced and misfolded superoxide dismutase is toxic. In Ralph et al.'s study vectors were injected into various muscle groups in a SOD1 mouse model that is overexpressing SOD1(G93A). SOD1 levels were efficiently reduced resulting in prolonged survival of vulnerable motor neurons in the brainstem and spinal cord. This led to measurable motor performance in these animals and a considerable delay in the onset of ALS symptoms as well as extension of survival time by almost 80%. This study demonstrated how lentiviral vectors can be used efficiently to deliver RNAi to treat a presently incurable disease. Early concerns that retroviral viral vectors that require packaging of vector RNA containing RNAi target sequences would be destroyed by production of interfering RNA in the same cell could not be confirmed.

Another lethal disease, metachromatic leukodystorphy, was successfully addressed by HIV lentiviral gene therapy in a study by Consiglio et al. involving a mouse model.[514] Metachromatic leukodystrophy (MLD) is an inborn lipidosis caused by lysosomal enzyme arylsulfatase A (ARSA). ARSA is required to catalyze the first step in the degradation pathway of galactosyl-3-sulfate ceramide (sulfatide), a major sphingolipid of myelin. MLD is characterized by myelin degeneration in both the central and peripheral nervous system, associated with the accumulation of sulfatide in glia cells and neurons. Children affected by the severe form of MLD display progressive neurologic symptoms, including ataxia, seizures, quadriplegia, and die decerebrated early in infancy. Currently there is no effective treatment for MLD or other storage diseases affecting the CNS (central nervous system). HIV vectors delivered the functional human ARSA gene into the brain of adult mice with germ-line inactivation of the mouse gene encoding ARSA, As2. Purified, concentrated vector stocks were slowly injected under stereotactic guidance into the right fimbria. Expression of the active enzyme was sustained throughout a large portion of the brain, with long-term protection from development of neuropathology and hippocampal-related learning impairments.

In another well publicized study, Dupre et al. compared HIV vectors to MLV vectors to restore function in T cells for Wiskott-Aldrich syndrome (WAS) patients,[515] an X-linked primary immunodeficiency with a median survival below the age of 20 due to

infections, hemorrhage and lymphomas. While transplantation of hematopoietic stem cells from HLA-identical siblings can be a definite treatment, it is only available for a minority of patients. Lentiviral vectors transduced T cells form WAS patients at higher rates compared to MLV vectors and efficiently transduced both activated and naïve WAS T cells. A selective growth advantage of HIV transduced T cells was found.

6.3.3.4. Non-Viral Gene Transfer

Although lentiviral and the adenovirus associated viral vectors are less immunogenic than for instance adenoviral and herpes viral vectors, those foreign proteins may still elicit some immune response and their capacity is limited. In addition large scale production is relatively difficult to achieve. Non-viral methods in contrast require only a small number of proteins, the capacity is much larger, there is little risk of infectious agents and industrial production much more easily achievable. This explains the popularity and use of naked DNA in approximately 18 percent and lipofection in 8 percent of clinical gene therapy trials.

As a major disadvantage of non-viral gene transfer methods, transgene expression tends to be transient with notable exception of complex strategies that mimic entire chromosomes.[516] Methods of non-viral DNA transfer include use of *naked DNA*, *liposomes* or *molecular conjugates*. Currently, approximately 8 percent of clinical trials use non-viral DNA transfer the majority of which (7.6 percent) are liposomes.

Naked plasmid DNA can be directly injected into the target cell[517] or administered intravenously[518] although this is not very effective. Alternatively, particles can be coated with DNA and literally shot into the target tissue with a gene gun.[519] This has been used to vaccinate with DNA, an elegant way of circumventing pre-existing immunity that is also inexpensive, allows delivery of several antigens on one single plasmid and co-expression of immunogenic cytokines where needed.[520]

Liposomes are a lipid belayed that entraps aqueous fluid. DNA typically associates to the external surface of cationic liposomes which interact with the cell membrane.[521] Liposome transfection is effective in vitro but very cell type dependent and often disappointing when used on non-dividing cells or in vivo. In an attempt to target and facilitate uptake into cells as endosomes various proteins have been included, e.g.

anti-MHC antibody,[522] Senday virus F protein[523] or transferring.[524] Use of Senday virus allows the plasmid DNA to avoid degradation in the endosome.[523]

Molecular conjugates are protein or other synthetic ligands to which a DNA binding agent has been attached. Similar strategies as with liposomes have been exercised including transferrin[525], polymeric IgA[526] and complexes of nonmodified human adenovirus particles and a protein conjugate consisting of N-acetyl-glucosamine-modified bovine serum albumin.[527]

Kusano et al. showed that direct injection of plasmid DNA into myocardium can result in effective gene transfer with rather dramatic results.[528] In an attempt to improve recovery from acute and chronic myocardial ischemia after ligation of the proximal left anterior descending artery branch of the left coronary artery, a plasmid encoding human sonic hedgehog (Shh) was injected subepicardially with a curved 27-gauge needle into 5 sites along the anterior and posterior left ventricular wall in rats in 600μg/0.1ml and 100μg/0.02ml in mice. In pigs the ischemic area was mapped by nonfluoroscopic electroanatomical mapping to guide injections of 800 μg/3 ml into 6 sites with an injection catheter. Shh is a crucial regulator of organ development during embryogenesis. Gene transfer resulted in tissue preservation and repair by initiating a repertoire of signaling pathways in the local tissue and by recruiting circulating progenitor cells to engage in the repair process. Left ventricular function was preserved in both acute and chronic myocardial ischemia.

An example of highly engineered nanoparticles is the study of Hood et al. who used cationic nanoparticles coupled to an integrin alphavbeta3-targeting ligand to deliver genes selectively to angiogenic blood vessels in tumor-bearing mice.[529] As a proof of principle nanoparticles were conjugated to a mutant Raf gene, ATPmu-Raf, which blocks endothelial signaling and angiogenesis in response to a variety of growth factors. During vascular remodeling and angiogenesis, endothelial cells show increased expression of several cell surface molecules that potentiate cell invasion and proliferation, integrin alphavbeta3 being one of them. This molecule plays a key role in endothelial cell survival during angiogenesis in vivo and potentiates the internalization of various viruses. The authors found pronounced M21-L cell tumor regressions in athymic WEHI mice.

Oritz-Urda et al. reported an innovative non-viral method to achieve stable genetic correction for an inherited human skin disease by transfecting a construct that sues the phi C31 bacteriophage integrase to deliver COL7A1 cDNA into genomes of primary epidermal progenitor cells.[530] Phi C31 bacteriophage integrase stably integrates large DNA sequences containing a specific 285-base-pair attB sequence into genomic pseudo-attP sites. In this study epidermal progenitor cells were obtained from unrelated patients with a blistering skin disorder called recessive dystrophic epidermolysis bullosa (RDEB) that is caused by mutations in the COL&A1 gene. Skin regenerated on SCID mice including type VII collagen protein expression, anchoring fibril formation and dermal-epidermal cohesion. The authors argue that viral vectors, in particular type C retroviral and lentiviral vectors, suffer from biosafety concerns that currently prevent them from being used more broadly. They fail to acknowledge that any form of integration is mutagenic by definition and that predictions that lentiviral vectors will be similarly oncogenic as retroviral vector do not hold true in practice as discussed above.[495] It will remain to be seen whether use of a prokaryotic integration system will be advantageous for eukaryotic DNA especially in the presence of a mature immune system.

6.3.3.5. Adeno-associated virus

Adeno-associated viral (AAV) vectors are currently used in only 4% of clinical gene therapy trials but enjoy increasing popularity for several reasons: AAV is not associated with human disease and there is little immunogenicity. Long-term expression can be achieved in dividing and non-dividing cells even without genomic integration (formation of intracellular concatomers). Disadvantages are that many patients had prior exposure and likely have some immunity against AAV, only relatively small transgenes can be used and that cloning can be difficult due to the sequence of the flanking terminal repeats. Achieving high titers and large volumes is still technically challenging. Although the AAV wild-type integrates preferentially into AAVS1 in chromosome 19q.[531] AAV vectors favored integration in active genes[532] and in that regards are reason for the same concerns that exist with lentiviral vectors.

Adeno-associated viruses (AAV) are small, non-enveloped viruses that belong to the parvovirus family, genus dependovirus. As such, AAV requires a helper virus, for

instance adenovirus or herpes simplex virus, in order to replicate. In the absence of such helper virus, AAV can establish a latent infection within the cell by either site-specific integration or as an episome. The AAV capsid contains a linear single-stranded DNA genome of 4.7 kb and is only 22 nm in diameter. The genome has either plus or minus polarity.[533, 534] Inverted terminal repeats (ITRs) at the termini consist of 145 nucleotides that form a hairpin structure due to the multipalindromic nature of its 125 bases. This structure is needed to initiate replication and packaging and flanks the two large open reading frames (ORF) of the viral genome.[535] AAV does not encode its own polymerase. The replication ORF (Rep) encodes for four replication proteins through the use of alternative splicing. The right capsid ORF (Cap) encodes for three viral structural proteins. Rep and cap are replaced by the transgene in AAV vectors but have to be provided in trans along with helper gene products. In contrast to wild-type AAV, in the absence of rep vectors will integrate as a single provirus preferentially in active genes or at random sites.[532] Rather than integration, the most common state are head to tail concatomers one the terminal repeats have slightly degraded.[536, 537]

AAV2 vectors rapidly gained popularity following the pioneering work of Laughlin et al[538] and Hermonat et al,[539] because of their long-term persistence without detrimental effects to the host and a wide range of infectivity that include both dividing and non-dividing cells. AAV is relatively resistant to heat, solvents and change of pH.[540] Other serotypes with different tissue tropism have recently been found that facilitate targeted transduction.

Disadvantages of AAV are the size limitation, slow onset of gene expression and a possible association between AAV2 vector gene transfer and tumorigenesis as described in an animal model of mucopolysaccharidosis.[541] Similar to lentiviral vectors, AAV preferentially integrates into active chromatin[532] although the frequency of true integration is low and in contrast to retroviral and lentiviral vectors not a required part of the life cycle.

AAV2 vectors have entered preclinical studies for hemophilia, cystic fibrosis, α1-anti-trypsin deficiency, Duchenne muscular dystrophy and rheumatoid arthritis. Genetic disease are the leading group of indications (32%), but also tumor (19%), and at about equal percentage ocular, cardiovascular and neurological diseases. Present AAV-based gene therapy trials are mainly focused on monogenic diseases (53%), followed

by cancer (23%).[542] The first clinical trial was concerned with cystic fibrosis,[543] which is still the leading indication.[542] Other trials are focused on infantile neuronal ceroid lipofuscinosis,[544] Canavan disease,[545] α1-anti-trypsin deficiency[546] and Parkinson's disease[547] (all phase I) and cystic fibrosis[548, 549] (phase II).

The completed studies and trials demonstrated that while AAV2 based gene therapy is generally safe, there are significant shortcoming in transduction efficiency and more organ-specific transduction. Attempts have been made to improve efficiency by manipulating the AAV2 capsid (reviewed in[550]) through site-directed mutagenesis, chemical conjugation and peptide display libraries. Other strategies employed packaging of AAV genomes with two different ITR serotypes, use of capsid serotype mosaics, pseudopackaging rAAV genomes and self-complementary AAV2 vectors[551] to circumvent the rate-limiting second-strand DNA synthesis.[550, 552]

I will review important studies with AAV vectors in the following. AAV vectors haven been used extensively for ocular gene therapy. These will be reviewed in a separate chapter about ocular gene therapy.

Manno et al. transduced the liver of seven patients with severe hemophilia B using an AAV vector expressing human factor IX by infusing vector through the hepatic artery in a dose escalation study.[458] The authors find that vector infusion up to 2×10^{12} vector genomes per kg was not associated with acute or long-lasting toxicity and that therapeutic levels were achieved at the highest dose tested. However, different from highly successful pre-clinical studies with dogs[553] and mice,[554] therapeutic levels could only be achieved for about 8 weeks when a gradual decline of factor IX was observed that was accompanied by asymptomatic elevation of liver transaminases that eventually resolved. Destruction of hepatocytes was caused by cell-mediated immunity targeting antigens of the AAV capsid. This is a remarkable finding because unlike factor IX, AAV capsid antigens, are not synthesized in transduced cells. MHC class I presentation pathways favor peptides derived from de novo produced proteins; nevertheless, alternative pathways exist that allow for appropriate presentation of proteins passively taken up by cells. These sufficed for recognition of AAV-transduced hepatocytes by CD8+ effector T cells. Unlike experimental animals, humans are naturally infected by AAV-2 during childhood. Because AAV is naturally replication defective, this initial infection invariably takes place together with a helper virus infection such as adenovirus. Although AAV-2 on its own may not induce

inflammatory reactions needed for stimulation of a maximal adaptive immune response, in combination with the helper virus, which causes activation of the innate immune system, it is likely that CD8+ T cells directed to the antigens of the helper virus and of AAV are formed. Upon controlling the infection, the frequency of AAV-specific CD8+ T cells would be expected to decline, leaving behind a small pool of memory T cells, which through homeostatic proliferation are maintained throughout the life of an individual. On re-exposure to AAV capsid, these memory CD8+ T cells are activated and eliminate the AAV capsid–harboring cells.

Chamberlain et al[555] showed that AAV vectors can be used to rescue dystrophic muscle through U7 snRNA-mediated exon skipping. The majority of the clinically severe Duchenne muscle dystrophy is caused by a frame shift or stop in the mRNA. The authors were able to achieve persistent exon skipping (exon skipping occurs at low frequency and sometimes eliminates the mutation). The mutated exon on the dystrophin mRNA of the mdx mouse was rescued by a single administration of AAV vector expressing antisense sequences linked to a modified U7 small nuclear RNA. This resulted in the sustained production of functional dystrophin at physiological levels in entire groups of muscles and the correction of the dystrophy in those.

Strong neuroprotection of nigral dopamine neurons and rescue of the parkinsonian behavioral phenotype could be achieved in study by Luo et al[556] who used AAV vectors to deliver glutamic acid decarboxylase, the enzyme that catalyzes synthesis of the neurotransmitter GABA in excitatory glutamatergic neurons of the subthalamic nucleus in rats. The abnormalities of Parkinson's disease are caused by alterations in basal ganglia network activity that includes the disinhibition of the subthalamic nucleus and excessive activity of the major output nuclei. After transduction, neurons were responding appropriately to electrical stimulation with GABA release.

Another study with AAV vectors is remarkable in that it demonstrated successful targeting and correction of a genetic defect in stem cells ex vivo. Chamberlain et al. used a strategy of homologous sequence targeting to disrupt the dominant-negative mutant COL1A1 collagen gene to osteogenesis imperfecta.[555] Similar to retroviral vectors described in this review chapter, the study authors harvested and transduced mesenchymal stem cells ex vivo. These cells can differentiate into a variety of tissues including bone, fat, cartilage and muscle. Transduced cells could be specifically re-transfused into bone most severely affected. One shortcoming is that the gene

targeting strategy is not mutation specific. However, phenotypical correction is still possible because individual cells may synthesize entire collagen fibrils without mixing of peptide chains from different cells, genetic mosaics for lethal forms of osteogenesis imperfect have a mild clinical course and the cells expressing wild-type collagen may have a growth advantage.

An example of relatively non-specific gene therapy that is able to modify a complex dysfunction is the study by Haberman et al. who successfully treated a model of focal seizure genesis in the rat inferior collicular cortex. In this model, electrical stimulation of a specific region in the inferior collicular cortex causes brief poststimulus wild-running seizure activity, in which the seizure behaviors exactly coincide with localized after discharge. In addition, in the absence of any perturbation, the electrical stimulation threshold for seizure genesis remains stable for long periods of time. The authors targeted the N-methyl-D-aspartic acid (NMDA) excitatory amino acid receptor with an AAV-delivered antisense oligonucleotide.

6.3.3.6. Herpes simplex virus

The size of complete genomic loci precludes their use in most viral systems with exception of herpes simplex virus type I (HSV-1) amplicon vectors. HSV-1 is an enveloped DNA virus that belongs to the herpesviridae family, subfamily alphaherpesvirinae. The virion is 120 to 200 nm in diameter and contains a double-stranded DNA genome of 152 kb. The transgene capacity is sufficient to accommodate approximately 95 percent of human genomic loci. Due to their neurotropism HSV vectors are attractive vehicles for gene therapy of neurological diseases and make for approximately 3 percent of all clinical gene therapy trials.

Disadvantages are similar to adenoviral vectors and include common immunity to HSV in the population and remarkable toxicity. Depending on whether amplicons or recombinant viruses are used the production can be technically demanding.

Two unique regions, termed UL and US for unique long and unique short, are linked by long and short internal repeat sequences (IRL and IRS) in both directions and are flanked at the non-linker end by terminal repeats (TRL and TRS). Depending on the strain, the HSV-1 genome consists up to 81 genes of which approximately 50 percent are not necessary for growth in cell culture.[557] Up to 50 kb of transfer DNA can be

accommodated after deletion of these genes. HSV genes are grouped into immediate-early (IE or alpha) genes, early (E or beta) and late (L or gamma) genes. During lytic infection, VMW65, a tegument structural protein, activates the immediate early genes IP0, ICP4, ICP22, ICP27 and ICP477 which transactivate production of early genes. Early genes in return are responsible for nucleotide metabolism and DNA replication. Late genes are activated by early genes and code for structural proteins. This entire cycle that end with the death of the infected cell takes approximately 10 hours to complete.

Because herpes simplex virus is a human neurotropic virus use of derived vectors has mainly focused on transfer to the nervous system. A key feature of HSV is the ability to either proceed into a lytic life cycle or to persist as an intranuclear episome during latency. Because of the prevalence of HSV in the population, antibodies exist in most individuals.

The latency associated transcripts (LAT) located in the IRL region drive gene expression during latency and are involved in establishing of and reactivation from latency.[558]

HSV-1 vectors can be produced using either amplicons or recombinant HSV-1 viruses. Amplicons contain the E1 ori of E. coli, OriS, the HSV-1 origin of replication, HSV-1 packaging sequence and the transgene under control of an immediate-early promoter and selectable marker.[559] The amplicon is transfected into a cell line that contains a helper virus which provides the missing structural and regulatory genes in trans. More recent amplicons utilize an Epstein-Barr virus derived sequence for episomal maintenance.[560] Replication deficient recombinant virus can be constructed by deleting one of the immediate-early genes and providing it in trans (often ICP4). While these attenuated viruses can direct transgene expression to neuronal tissue, they are still toxic to neurons in culture.[557] Deletion of several immediate-early genes reduces cytotoxicity further and use of promoters that would be silenced otherwise in the wild type virus when latent. Such promoters are under investigation for long-term expression. Another option is use of replication-conditional mutants that can only replicate in certain cell lines that supply missing factors or enzyme e.g. the neurovirulence factor g34.5,[561] UTPase, ribonuclease reductase[562] or thymidine kinase.[563]

The main concern remains the strong inflammatory response to HSV-1 vectors at the application site as well as sites supplied by neurons originating from the area of injection.[564] In some studies fatality rates as high as 20 percent were observed among experimental animals.[565] York et al. found that removal of ICP47 can attenuate vector toxicity.[565] Because HSV is neurotrophic by nature, gene therapy strategies have focused on neurological diseases. Potential uses of herpes simplex virus (HSV) vectors for gene therapy of neurodegenerative disorders and CNS malignancies.

HSV vectors had fallen in disfavor after initial optimism about exploiting its neurotropism and ability of episomal survival. Early studies received great attention: During et all showed that it is possible to maintain efficient behavioral and biochemical recovery for 1 year after gene transfer of human tyrosine hydroxylase in a Parkinson rat model with partially denervated striatum from 6-hydroxydopamine. Persistence of tyrosinase could be detected by RNA and immunoreactivity.[563] One problem is the immunogenicity of HSV thymidine kinase that is utilized now in suicide gene therapy when high levels of toxic acyclovir conversion products allow reliable ablation of expressing cell. However, HSV-tk may otherwise cause prolonged inflammation that is not desirable.[566]

HSV vectors have regained interest recently as their biology has become better understood. Exploiting neurotropism, the ability of the virus to spread through the nervous system and to form latent infections in neurons that last for the lifetime of the infected individual is the main topic in experimental applications. Replication-deficient HSV-1 vectors encoding human prepro-enkephalin were efficacious in reducing nociceptive behaviors and this reduction of nociceptive behaviors was abrogated by pretreatment using intrathecal opiate antagonist naloxone. Lu et al. demonstrated now that treatment of inflamed pancreas with enkephalin encoding HSV-1 recombinant vector reduces inflammatory damage and behavioral sequelae.[567] A fascinating finding is the seemingly paradox use of a potentially highly inflammatory virus to achieve both pain control and suppressed inflammation that provides better understanding of how close these two are. The study assessed the efficacy of pancreatic surface delivered enkephalin (ENK)-encoding herpes simplex virus type 1 (HSV-1) on spontaneous behaviors and spinal cord and pancreatic enkephalin expression in an experimental pancreatitis model. Replication-defective HSV-1 with proenkephalin complementary DNA was applied to the pancreatic

surface of rats with dibutyltin dichloride (DBTC)-induced pancreatitis. On day 6, the treated rats had significantly improved spontaneous exploratory activities, increased met-ENK staining in the pancreas and spinal cord, and normalized c-Fos staining in the dorsal horn.

In an attempt to take advantage of HSV neurotropism and the HSV latency-associated promoter (LAP2) to attenuate damage to peripheral nerves, Chattopadhyay et al. transduced rat dorsal root ganglia.[568] Interestingly, this could be achieved by subcutaneous rather than direct inoculation of replication-incompetent HSV-based vectors containing nerve growth factor (NGF) or neurotropin-3 (NT-3). When a pure sensory neuropathy was induced by overdose of pyridoxine and animals assessed 6 months later the nerve damage was diminished in animals treated with the LAP2-NGF vector. Sensory amplitude, H-wave amplitude and behavioral measures of proprioceptive function were 30% to 85% of normal rats. Neurotrophin-3 treated animals had an even greater effect in preserving the largest myelinated fibers from degeneration.

A nonreplicating HSV vector expressing erythropoietin that was inoculated into the striatum of a MPTP mouse model of Parkinson disease was able to preserve behavioral function and tyrosine hydroxylase levels in the substantia nigra and dopamine transporter-immunoreactive terminal sin the striatum.[569] Intranasal administration of the growth-compromised HSV-2 vector DeltaRR was able to prevent kainate-induced seizures and neuronal loss in rats and mice.[570] The anti-apoptotic HSV gene ICP10PK was able to halt for at least 42 days kainic acid-induced seizures, neuronal loss, and inflammation, in both rats and mice.

6.3.4. Current Gene Therapy Trials

At the time of this writing a total of 1347 clinical gene therapy trials are under way or are awaiting approval (Figure 9) which are the result of intense basic science research and preclinical studies.

Clinical trials involving new drugs are commonly classified into four phases, each phase of which is treated as a separate clinical trial. The drug-development process will normally proceed through all four phases over many years. If the drug successfully passes through Phases I, II, and III, it will usually be approved by the

national regulatory authority for use in the general population. Phase IV are post-approval studies. Extensive pre-clinical studies are conducted before clinical trials are started. It is difficult to count those in gene therapy but an estimate can be made with a Medline search for "gene therapy" as the Medical Subject Heading (MeSH is the U.S. National Library of Medicine's controlled vocabulary used for indexing articles for MEDLINE/PubMed that provides a consistent way to retrieve information that may use different terminology for the same concepts): an astonishing 17803 papers are concerned with this topic, 5580 of which are reviews.

Phase I trials are the first stage of testing in human subjects for which a small group of healthy volunteers of 20-80 is selected. This phase includes trials designed to assess the safety, tolerability, pharmacokinetics, and pharmacodynamics of a drug. In March 2008, 820 gene therapy trials were underway (**Figure 9**).

Once the initial safety of the study drug has been confirmed in Phase I trials, Phase II trials are performed on larger groups (20-300) and are designed to assess how well the drug works, as well as to continue Phase I safety assessments in a larger group of volunteers and patients. In March 2008, 262 gene therapy trials were pending Phase II approval while 216 were already ongoing. When the development process for a new drug fails, this usually occurs during Phase II trials when the drug is discovered not to work as planned, or to have toxic effects. While some Phase II trials are designed as case series, other Phase II trials are designed as randomized clinical trials, where some patients receive the drug/device and others receive placebo/standard treatment.

Phase III studies are randomized controlled multicenter trials on large patient groups (300–3,000 or more depending upon the disease/medical condition studied) and are aimed at being the definitive assessment of how effective the drug is, in comparison with current gold standard treatment. Because of their size and comparatively long duration, Phase III trials are the most expensive, time-consuming and difficult trials to design and run, especially in therapies for chronic medical conditions. Thirteen gene therapy trials were pending Phase III approval and a total of 36 were already in progress.

Phase IV trial is also known as Post Marketing Surveillance Trial. Phase IV trials involve the safety surveillance and ongoing technical support of a drug after it receives permission to be sold. The safety surveillance is designed to detect any rare

or long-term adverse effects over a much larger patient population and longer time period than was possible during the Phase I-III clinical trials. Because of the newness of gene therapy, no gene therapy trial has reached this phase yet.

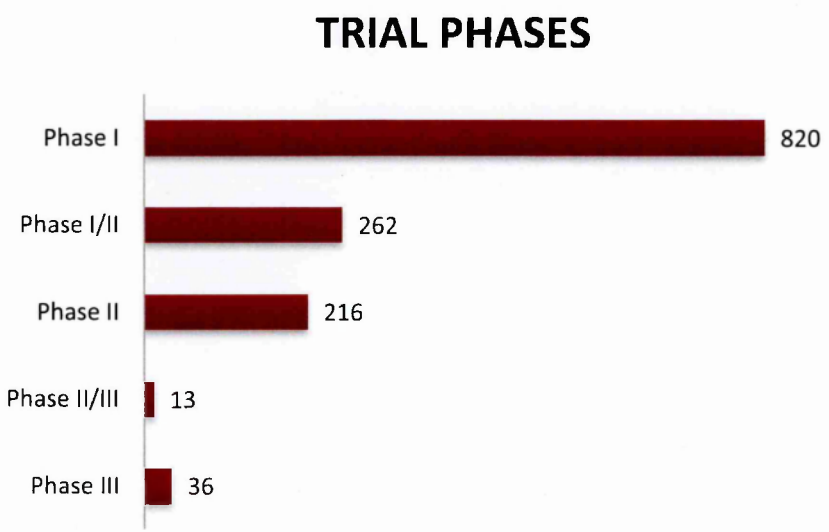

Figure 9: Gene therapy trials by phases.

Adenoviral and retroviral vectors account for 25% and 23% of vectors used or 337 and 304 trials, respectively (**Figure 10**). Naked DNA follows closely with surprising 18% (n= 244) of trials and lipofection (8%, n=102). In contrast, adeno-associated (AAV) and lentiviral vectors, the two most promising vector types for long-term therapy of noncycling cells, contribute to only 4% (n = 54) and 0.8% (n = 11) of trials, respectively. Indications of the AAV studies range from cystic fibrosis to bleeding disorders and Parkinson disease, while most lentiviral vector studies are concerned with treatment of already HIV positive subjects. The asymmetry of only a few studies with AAV and lentiviral vectors in contrast to numerous retro- and adenoviral studies reflects how much less preclinical experience with these vectors exists as well as how challenging large-scale production and safety concerns are.

Given that with 1 lethality per 1,000,000 vaccinia virus – a poxvirus - is potentially more dangerous than AAV it is equally surprising that it is used more often (4.9%, n=66) than AAV (**Figure 10**). Poxvirus itself is used in 61 or 4.5% of gene therapy trials, respectively. Herpes virus has become more popular in recent years and there are currently 43 trials (3%).

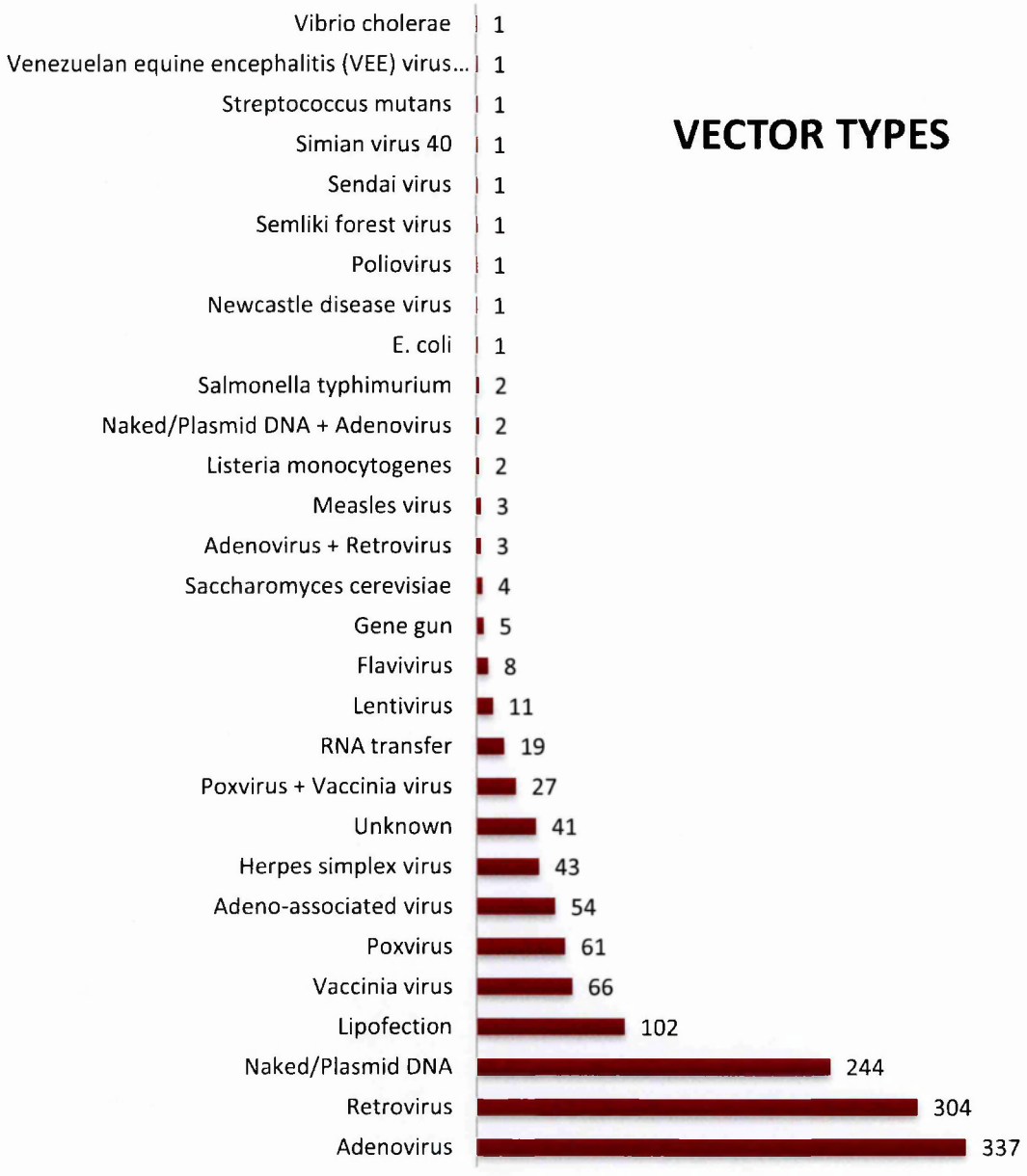

Figure 10: Vector types used in gene therapy clinical trials (data from free online database provided by The Journal of Gene Therapy).

By far the most common indication for short-term gene therapy is cancer (n=896), often fatal and with few therapy options, followed by 121 cardiovascular disease trials, 110 monogeneic and 89 infections disease gene therapy trials (Figure 11). A closer look at specific diseases reveals that most monogenic disorders are severe, often lethal disorders for which no good treatment options exist in most cases. Table 1 provides a list of specific disease in the above categories.

Figure 11: Disease types addressed by gene therapy clinical trials (data from free online database provided by The Journal of Gene Therapy).

Although the vast majority of all studies are Phase 1 studies to assess the safety, first therapeutic successes have been reported. The treatment of a fatal form of severe combined immunodeficiency-X1 (SCID-X1), an X-linked hereditary disorder characterized by an early block in the development of T and natural killer (NK) cells due to mutations in the γc cytokine receptor subunit, is the most prominent one. Stimulated hematopoietic stem cells were transduced ex vivo with a murine leukemia viral vector expressing the receptor subunit and re-infused.[262] T and NK cells counts and function was restored to comparable levels of age-matched controls in 9 of 10 children. This protocol profited from the selection advantage that γc-expressing lymphocyte progenitor cells had over the present cell population affected by the mutation. No exogenous selection strategy had to be applied.

Monogenic disorders	**Cancer**
Cystic fibrosis	**Gynecological**
Severe combined immunodeficiency (SCID)	breast, ovary, cervix
Alpha-1 antitrypsin deficiency	**Nervous system**
Hemophilia A and B	glioblastoma, leptomeningeal carcinomatosis, glioma, astrocytoma, neuroblastoma
Hurler syndrome	**Gastrointestinal**
Hunter syndrome	colon, colorectal, liver metastases, post-hepatitis liver cancer, pancreas
Huntington's chorea	**Genitourinary**
Duchenne muscular dystrophy	prostate, renal
Becker muscular dystrophy	**Skin**
Canavan disease	melanoma
Chronic granulomatous disease (CGD)	**Head and neck**
Familial hypercholesterolemia	nasopharyngeal carcinoma
Gaucher disease	**Lung**
Fanconi's anemia	adenocarcinoma, small cell, non small cell
Purine nucleoside phosphorylase deficiency	**Mesothelioma**
Ornithine transcarbamylase deficiency	**Hematological**
Leukocyte adherence deficiency	leukemia, lymphoma, multiple myeloma
Gyrate atrophy	**Sarcoma**
Fabry disease	**Germ cell**
Familial amyotrophic lateral sclerosis	
Junctional epidermolysis bullosa	**Neurological diseases**
Wiskott-Aldrich syndrome	Alzheimer's disease
Lipoprotein lipase deficiency	Carpal tunnel syndrome
Late infantile neuronal ceroid	Cubital tunnel syndrome

lipofuscinosis	
RPE65 mutation (retinal disease)	Diabetic neuropathy
Mucopolysaccharidosis	Epilepsy
	Multiple sclerosis
Cardiovascular disease	Myasthenia gravis
Peripheral vascular disease	Parkinson's disease
Intermittent claudication	Peripheral neuropathy
Critical limb ischemia	
Myocardial ischemia	**Ocular diseases**
Coronary artery stenosis	Age-related macular degeneration
Stable and unstable angina	Diabetic macular edema
Venous ulcers	Glaucoma
Vascular complications of diabetes	Retinitis pigmentosa
Pulmonary hypertension	Superficial corneal opacity
Heart failure	
	Other diseases
Infectious disease	Inflammatory bowel disease
HIV/AIDS	Rheumatoid arthritis
Tetanus	Chronic renal disease
Epstein-Barr virus	Fractures
Cytomegalovirus infection	Erectile dysfunction
Adenovirus infection	Anemia of end stage renal disease
Japanese encephalitis	Parotid salivary hypofunction
Hepatitis C	Type I diabetes
Hepatitis B	Detrusor overactivity
Influenza	Graft versus host disease

Table 1: Specific diseases addressed in current gene therapy trials.

The long-term outcome of this promising trial experienced a setback when two patients developed T cell leukemia. While the mechanism is still under investigation, it is thought that a combination of several factors led to this outcome in 2 of 8 patients.[571] The clones of both patients showed retrovirus vector integration in proximity to the LMO2 proto-oncogene promoter, leading to aberrant transcription and expression of LMO2, a transcription factor considered a central regulator of hematopoiesis. It is possible that insertion of onco-retroviral vectors can trigger deregulated premalignant cell proliferation by retrovirus enhancer activity on the LMO2 gene promoter at a much higher rate than previously thought.[572] Additional factors might have been a varicella–zoster virus infection five months before clinically detectable lymphoproliferation that increased the immune reactivity of the T-cell clone and the selective growth advantage of the transduced cells. As the sister and a first-degree relative of one proband developed medulloblastomas there might have been an additional genetic predisposition for childhood cancer.

Only low levels of transduced progenitor cells were observed in an earlier treatment of adenosine deaminase (ADA) deficiency in another study, where patients received ADA preparations in addition to the transduced cells. This probably prevented selective outgrowth of the transduced cells,[573-577] as supported by the observation that the number of peripheral blood mononuclear cells expressing the transgene increased after external application of ADA was stopped. B and NK cells counts decreased in these patients, but the number of T cells and function remained within normal limits.

Use of MLV vectors, based on type C retroviruses, requires extensive manipulation of stem cells and stimulation with cytokines to induce cell cycling to achieve transduction.[246, 247] This is undesirable because it may result in differentiation. The development of lentiviral vectors, which are able to transduce non-dividing cells at high efficiencies, will facilitate the long-term genetic manipulation of such tissues.

Trial ID	Title
US-488	A Phase I Open-Label Clinical Trial of the Safety and Tolerability of Single Escalating Doses of Autologous CD4 T Cells Transduced with VRX496 in HIV Positive Subject
US-646	A Phase I/II, Open-Label, Multicenter Study to Evaluate the Safety, Tolerability, and Therapeutic Effect of Repeated Doses of Autologous T Cells Transduced with VRX496 in Antiretroviral Experienced HIV-Positive Patients
US-667	A Phase I/II, Open-Label, Single Center Study to Evaluate the Tolerability, Trafficking and Therapeutic Effects of Repeated Doses of Autologous T Cells Transduced with VRX496 in HIV-Infected Subjects
US-725	A Phase I Pilot Study of Safety and Feasibility of Stem Cell Therapy for AIDS Lymphoma using Stem Cells Treated with a Lentivirus Vector Encoding Multiple Anti-HIV RNAs
US-737	A Pilot Study of Safety and Feasibility of T Cell Immunotherapy Using Lentivirus Vector-Expressed RNAi in Autologous T Cells of HIV-1 Infected Patients Who have Failed Anti-Retroviral Therapy
US-758	Lentiviral-Mediated, Hematopoietic-Directed Gene Therapy for MPS VII
US-791	Treatment and Biological Imaging of Patients with Locally Advanced or Metastatic Melanoma with Lentiviral Vector MART-1 TCR/HSV1-sr39k (FUW-M1-TCR/sr39k) Engineered Lymphocytes, MART-1 26.35-Pulsed Dendritic Cells, and Interleukin-2 after a Nonmyeloablative Conditioning Regimen
US-793	Pilot Study of Redirected Autologous T Cells Engineered to Contain Anti-CD19 Attached to TCRz and 4-1 BB Signaling Domains in Patients with Chemotherapy Resistant or Refractory CD19+ Leukemia and Lymphoma
US-852	A Phase I Open-Label Clinical Trial for the Treatment of Beta-Thalassemia Major with Autologous CD34+ Hematopoietic Progenitor Cells Transduced with Thalagen, a Lentiviral Vector Encoding the Normal Human Beta-Globin Gene
US-871	A Phase I/II, Open-Label Study to Evaluate the Safety and Antiviral Activity of Autologous T-Cells Transduced with VRX496 in Treatment of Naive Subjects with Earl Stage HIV-1 Infection
US-875	A Rollover Study to Evaluate Safety and Therapeutic Effect of Re-infusing Subjects Who Completed Participation in the VRX-496-USA-05-002 Trial with Autologous T Cells with VRX496

Table 2: Lentiviral vector trials.

Noteworthy is also the clinical trial of Manno et al. of hemophilia B patients who received intramuscular injections of adeno-associated viral (AAV) vectors expressing coagulation factor IX.[578] AAV vectors are a good choice for long-term therapy, because they are capable of genomic integration, albeit this is not a required step as in retroviral vectors.[579-581] These patients showed some clinical benefits, although only low levels of factor IX were detected.

The successes with retroviral and adeno-associated viral vectors contrast the problems encountered with the first vectors to enter human trials, adenoviral (Ad) vectors.

Potent immune responses to vectors and transduced tissue[582, 583] were encountered, the magnitude of which became apparent by the death of a participant of a phase I trial.[584]

A total of 11 gene therapy trials with lentiviral vectors are underway at this point. While most address HIV, four trials differ in that they employ HIV vectors in non-HIV positive subjects: US-758 for hematopoietic-directed gene therapy for mucopolysaccharidosis VII, US-791 for patients with locally advanced or metastatic melanoma treated with engineered lymphocytes, US-852 for the treatment of beta-thalassemia major with autologous progenitor cells and US-793 to redirect autologous T cells to refractory leukemia and lymphoma. Few details are published about these trials perhaps because of the commercial interests behind them.

More recently, the first ocular gene therapy trials have begun. US-589 is a Phase 1 study in glaucoma subjects receiving SCH 412499 (rAd-p21) administered as a single injection into the subconjunctival space prior to primary trabeculectomy. The concept behind this trial is less innovative as at least two well established anti-fibrotic agents are in use, mitomycin C and 5-fluorouracil that work very well.

Bainbridge et al. report that early results of a phase I ocular gene therapy trial for Leber's amaurosis, an early-onset, severe retinal dystrophy caused by mutations in the gene encoding retinal pigment epithelium–specific 65-kDa protein that is associated with poor vision at birth and complete loss of vision in early adulthood. The authors administered AAV vectors 2/2 expressing RPE65 complementary DNA (cDNA) under the control of a human RPE65 promoter to three young adults and observed in one patient significant improvement in visual function on microperimetry and on dark-adapted perimetry. This patient also showed improvement in a subjective test of visual mobility. This study was mainly concerned with safety and used adults with advanced disease and poor vision (below 20/120). It will be interesting to see how pediatric patient will benefit from the transfer as planned in the near future. Two additional trials started at Scheie's Center for Hereditary Retinal Degenerations, University of Pennsylvania and the University of Florida College of Medicine in Gainesville and the other at the University of Pennsylvania and Children's Hospital of Philadelphia.

6.3.5. Ocular Gene Transfer

The chronicity of the majority of eye diseases poses a distinct challenge to physician and patient, often demanding lifelong management and good compliance with complicated medication regimens. In addition, treatment of ocular tissue by current conservative means is most the time only indirect and non-specific. Most ocular cell types are terminally differentiated and non-dividing, which has further implications for disease outcomes in that degenerative diseases often are characterized by a permanent, cumulative loss of function and no therapy is available. Chronic, progressive ailments of the optic nerve and the outflow tract, of the retina and of the cornea constitute leading causes of blindness. The impact on quality of life for the individual is dramatic and the burden of health care expenses and loss of labor is very high.[585] Gene therapy of chronic eye diseases with a long-term expressing vector may offer a focused and cost-effective therapy option, but choice of vector is limited to ones that allow stable long-term expression for the therapeutic goal of cell preservation.

Other ocular diseases are characterized by proliferation, such as neovascularization of retina, choroid, or cornea and require an entirely different choice of therapeutic gene and vector system. Transient expression to induce controlled cell death or stasis is a common goal in these cases.

Gene transfer has the advantage over drug application that sustained expression can be achieved locally, while minimizing any risk of systemic adverse effects. Ocular gene transfer usually requires a surgical approach because systemic vector application does not result in targeting to ocular structures. This can be accomplished by standard procedures through subretinal, intravitreal or intracameral injection. Since ocular tissues are highly compartmentalized, the transduction pattern by a given vector is dependent on the site of its intraocular administration. While subretinal injection of vectors largely results in gene transfer to cells lining this space (retinal pigment epithelium and photoreceptors),[76, 279] intravitreally or intracamerally injected vectors follow the flow of aqueous humor along retinal ganglion cells, lens, ciliary and iris epithelium, the trabecular meshwork and the corneal endothelium.[324, 504, 586]

Host immune responses during ocular gene therapy are often limited because intraocular vectors are sequestered from the systemic circulation and additionally suppressed by anterior chamber-associated immune deviation (ACAID) or inhibition

of delayed-type hypersensitivity (DTH) in the subretinal space.[587, 588] This phenomenon can prevent development not only of cytotoxic T cells, but also of complement fixing antibodies. Other factors have been identified in the eye that ameliorate immune responses, such as transforming growth factor-β, Fas ligand, melanocyte-stimulating hormone, vasoactive intestinal peptide, and calcitonin gene-related peptide.[589-591]

6.3.5.1. Anterior Segment

6.3.5.1.1. Corneal Disease

Few vectors are able to achieve efficient and long-term transduction of structures of the anterior segment. Adenoviral vectors have been used extensively, but resulted only in short-term expression most the time,[592, 593] as did HSV[594] and lipopolysaccharide (LPS).[595] Transduction of cornea was limited to the endothelial layer[596-598] in most cases. Longer expression can be achieved with AAV[599] or lentiviral vectors.[278] Gene therapy of for corneal disease will be reviewed in the following in a more limited fashion as the main focus of this thesis is gene transfer to the outflow tract for future glaucoma therapy and the retinal pigment epithelium. The major topics of corneal gene therapy are corneal transplantation and graft rejection, herpetic stromal keratitis, corneal neovascularization, corneal haze and mucopolysaccharidosis VII. These diseases do not share many common features: while some are chronic or inherited, some are more acute. Most are leading causes of vision loss from corneal disease with exception of mucopolysacharidosis which is an attractive target because the genetics and molecular pathway is well understood and there are little therapeutic alternatives. Advantages of the cornea as a target tissue are that it many features of a live tissue culture: it is easily observable, spread out in a plane more than three dimensionally and transparent allowing for immediate inspection of the few layers present and non-invasive treatment. Because it is generally not vascularized corneal transgenes are less accessible by the immune system than in perfused organs. Sophisticated morphometric technology is available as a result of recent developments in cornea and refractive surgery. Potentially facilitating gene therapy is the ocular immune privilege that is the result of the mentioned blood-ocular barrier that physically prevents cellular infiltration, the low expression of major histocompatibility complex class I and II molecules and the lack

of lymphatic drainage. Active aspects of ocular immune privilege include the constitutive expression of inhibitors of complement activation by corneal endothelial cells and of Fas ligand (which induces apoptosis of activated T cells) by corneal cells. The aqueous humor further contributes to immune privilege as it contains immunosuppressive factors. The anterior chamber-associated immune deviation is a descriptive term applied to an immune response that is deficient of B cells that secrete complement-fixing antibodies and T cells that mediate delayed hypersensitivity. The result of ocular immune privilege is that immune defense takes place with no inflammation to preserve corneal clarity, a vitally important condition. Finally, the cornea itself takes an active role in immune protection of the structure and function of the eye surface in that corneal epithelial cells and keratocytes secrete cytokines.
First gene transfer studies to the cornea appeared in 1994.[600] Already in 1996 attempts were made to prevent graft rejection by ex vivo manipulation of the cornea prior to transplantation,[596]followed by Rouse et al. to treat HSK[601] and Rakoczy et al.[602] to address corneal neovascularization.
Graft rejection is the major reason for transplant failure.[603] Graft rejection is mediated by elevated levels of Th1 cytokines, while Th1 and Th2 cells are inhibitory. Many gene therapy approaches therefore attempt to support Th2 or inhibit Th1 pathway. Several studies have investigated corneal gene transfer of IL-4[604] and IL-10,[605] both of which are Th2 cytokines, and CTLA4-Ig[606] and P40 IL-12[604] which are antagonists of Th1 response. Other interesting immunomodulary molecules are viral IL-10, a homolog to the human IL-10 that exhibits the immunosuppressive properties but lacks the immunostimulatory effects of human IL-10[607] and indoleamine 2,3-dioxygenase, an intracellular enzyme that arrests activated T cells in the G1 phase.[608] Stout et al. used a different approach by suppressing activation of endothelial cells and neovascularization that are related to graft rejection.[609] Gene delivery of endostatin:kringle 5 of plasminogen, a fusion protein that prevents endothelial cell proliferation and migration and also has anti-angiogenic properties was transduced into rabbit cornea using HIV vectors. Graft survival from 14 and 18 days in the control group was extended to at least 39 days.

Different strategies that have been proposed to address *herpes simplex virus keratitis* include vaccination against a primary ocular HSV-1 infection, *prevention of recurrent HSV reactivation* and treatment of existing HSV keratitis symptoms as well as *anti-*

neovascular approaches. Neburn et al. used recombinant vaccinia virus as a means to vaccinate against viral envelope glycoproteins as early as 1990 but provided only a small amount of protection.[610] Recombinant HSV-1 virus encoding for cytokine adjuvants were used by Osorio et al.[611] Mice immunized with IL-4-expressing virus cleared the virus from their eyes more rapidly than mice immunized with IL-2- or IFN-gamma-expressing virus. The same author constructed and compared then recombinant HSV-1 viruses expressing IL-12p35 or IL-12p40 (subunits of IL12 with different biological activity) with the previous IL-4 expressing virus by intraperitoneally immunized BALB/c mice.[612] IL-12 had been shown to act as a molecular adjuvant by bridging both innate and adaptive immunity but toxicity was observed after systemic application in the past. IL-12 is a regulatory protein produced by activated hematopoietic phagocytic cells and dendritic cells. Biological activities of IL-12 include growth stimulation of activated $CD4^+$ and $CD8^+$ T cells and natural killer cells. HSV-I expressing IL12-p35 exhibited the lowest virus replication, more rapid virus clearance and the lowest level of reactivation in the eyes after virus challenge without the toxicity seen with IL-12.

Dahesia et al[613] and Wasmuth et al[614] attempted to attenuate or *prevent recurrence of HSV keratitis* and corneal symptoms in relative early stages by topical ocular administration of plasmid DNA encoding antigens and cytokines and application of TNF-alpha-antisense oligonucleotides. DNA encoding the cytokines IL-4 or IL-10, but not IL-2 or interferon-gamma, modulated the severity of the immunoinflammatory response to subsequent corneal infection with HSV. The antisense strategy diminished the release of TNF-alpha from lymphocytes in HSV-1-infected corneas, mitigating the course of HSV keratitis to some extent. Anti-neovascular therapy for HSV keratitis tries to prevent infiltration of CD4+ T cells into the stroma and derived from the observation that IL-12 can suppress corneal lesions via anti-angiogenesis. Various investigators have administered naked DNA encoding IL-18,[615] RNAi knockdown of VEGF[616] or MMP-9[617] to prevent neovascularization. All of these strategies worked in the short term decreasing neovascularization and reducing keratitis.

Corneal neovascularization can be caused by infection (such as the previously mentioned HSV keratitis), inflammation of various cause and trauma. Common animal models try to mimic these conditions by chemical, mechanical injury or

implantation of angiogenic pellets. Anti-VEGF strategies are prevailing among anti-neovascular gene therapy as VEGF is the most potent neovascular molecule known: Lai et al. used adenoviral vectors to express FLt1, a VEGF receptor that can function as a sink[602] resulting in protection of 92% of animals compared to control, while Stechschulte et al. found that naked plasmid cDNA alone injected under pressure in mouse cornea effectively prevented neovascularization.[618] Other authors have fused FLt23K, Flt24K, VEGF-binding domains of Flt1 with KDEL, an endoplasmic reticulum retention peptide or albumin polyplexes as vehicles for Flt23K DNA to inhibit VEGF intracellularly.[619, 620] RNAi[616] and adenovirally encoded antisense VEGF[621] successfully knocked down VEGF. IL-18 similarly suppressed neovascularization as previously mentioned.[615] Naked DNA administration of IL-1 receptor antagonist that was shown in a model of penetrating keratoplasty to reduce VEGF expression was unable to affect VEGF expression in a model of corneal neovascularization.[622] Another interesting recent study that has potential to work longer term is that of Cheng et al. who used an AAV vector expressing angiostatin for subconjunctival injection in a model of alkaline induced corneal neovascularization.[623] Surprisingly, angiostatin was found by PCR neither in the conjunctiva nor cornea but limited to the extraocular muscle insertion sites suggesting serotype specific transduction as seen at other vector injection sites. The authors nevertheless found significant reduction of corneal neovascularization in the area of injection. As the main criticism the authors label regression of neovascularization what in fact is prevention of neovascularization as transduction is performed 3 weeks ahead of the alkali burn rather than in the clinically realistic, reverse order.

Several gene therapy studies have been conducted to address corneal haze, clouding or deposits some of which have similar approaches. Corneal haze can be a complication of excimer laser procedures used in refractive surgery and are a result of fibroblast proliferation. Therapeutic transgenes used were the dominant negative mutant cyclin G1, a survival factor that triggers apoptosis in various proliferative cells,[624] or a suicide gene/prodrug combination of a retrovirus encoding the HSV thymidine kinase gene with ganciclovir.[625] HSV thymidine kinase transforms ganciclovir to a toxic metabolite in proliferating keratocytes killing them.

A different condition that is associated with corneal deposits is mucopolysaccharidosis VII, a lysosomal storage disease caused by deficiency of the

enzyme beta-glucuronidase and the least common one. Treatment of corneal opacities is more of academic interest because of the rarity of this disease and because potentially life threatening issues need to be addressed first. A study by Kamata et al. showed widespread transgene expression of adenoviral vector mediated beta-glucuronidase transfer either intracameral injection or intracorneal administration (lamellar keratotomy), and rapid elimination of the lysosomal storage in corneal keratocytes occurred. This study is striking in how efficiently such a severe metabolic disease can be cured in local tissue and that the pathology of adjacent tissue resolves as well.[626]

6.3.5.1.2. Glaucoma

Although glaucoma is a leading cause of blindness at an age that has a maximum impact on the most productive years and is generating more costs than other leading causes of blindness not to mention the personal tragedies, gene therapy of glaucoma is in its infancy. This is because the molecular pathophysiology is still not understood and in contrast to many degenerative retinal diseases, single genetic defects are the rare exception. Congenital glaucoma with single gene defects present with a developmental dysgenesis of the outflow tract that is already completed by the time or birth. This cannot be addressed by gene therapy anymore. Goals in gene therapy for the most common form of glaucoma, primary open angle glaucoma, are therefore to increase survival of retinal ganglion cells in the back of the eye or to facilitate outflow of aqueous humor in the front of the eye as well as to address issues of glaucoma surgery by adjunctive therapy (e.g. suppression of fibrosis in filtering blebs). The principle is to get an exogenous gene with a product that is therapeutically useful albeit not necessarily directly related to pathogenesis.

6.3.5.1.2.1. Outflow Tract Gene Transfer

Genetic modification of the aqueous humor outflow site of mice, rabbits, rats, monkeys and human donor eyes[244, 264, 592, 627-629] has been attempted before with a variety of vectors, but was mostly unspecific and short-lived, with exception of lentiviral vectors.[324, 504] Non-viral methods are generally impeded by low transfection efficiency and only transient expression. Hangai et al. used fusogenic liposomes from

hemagglutinating virus of Japan to transfer LacZ as well as fluorescein isothiocyanate (FITC)-labeled phosphorothioate oligonucleotides into the outflow tract of rats and rhesus monkeys. Interestingly, beta-galacosidase expression could be visualized longer than in adenoviral vector mediated similar transduction protocols perhaps due to lower immunogenicity. The authors report that expression could be followed for 60 days in rats and 30 days in monkeys. FITC fluorescence could be seen for as long at 14 days in rat and 7 days in monkeys. While this transfer system makes for a safe way of gene transfer, transfer efficiency is disappointing both in numbers of cells transduced and expression levels per single cell.[263]

Comes and Borras investigated whether naked siRNA could be delivered to human TM in anterior chamber cultures by direct perfusion.[630] SiRNAs were directed against the matrix Gla protein and the glucocorticoid receptor. With this simple and straightforward approach using readily available, unmodified siRNA, matrix Gla protein expression was silenced in the trabecular meshwork perfused with naked MGP siRNA by 95% and the glucocorticoid receptor by 93%, respectively. Pretreatment of glucocorticoid receptor siRNA followed by dexamethasone treatment caused a reduction of myocilin expression, a glaucoma associated gene, by 99%.

A follow up study to prior work in which accidental transduction of the anterior segment was seen,[631] Budenz et al. injected purified replication-deficient adenoviral vectors with a CMV-promoter driven beta-galactosidase expression cassette into the anterior chamber of adult CD-1 mice.[627] Mice were sacrificed and processed for beta-galactosidase expression histochemically from 2 to 21 days. Expression was seen in corneal endothelium and trabecular meshwork for only 14 days after injection. The authors noted that despite early loss of expression there was no toxicity observed in transduced tissue. The expression levels and extent of expression appear to be rather marginal in the data published.

Borras et al. came to similar conclusions with adenoviral gene transfer to the anterior segment but in contrast to Budenz et al. the authors did observe a severe inflammatory response. In this study, anterior segment adenoviral gene transfer was performed in rabbits. Rabbits were injected once with 20 µl containing 8×10^8 TU and evaluated 48 hours after injection. Beta-galactosidase expression was seen in corneal endothelium, the anterior endothelium of the iris and the trabecular meshwork. Transduction of lens endothelium led to endothelial decompensation with cell

detachment and corneal opacification highlighting the toxicity in some species of these first generation adenoviral vectors with E1 deletion and E3 inactivation. Inflammatory responses included a severe anterior uveitis in some animals requiring sacrifice. Borras later studied transduction of perfused anterior human segments and porcine anterior segments with the same adenoviral vector.[628] In contrast to the previously in vivo transduced rabbit eyes, transduction of these eyes ex vivo was tolerated much better at lower doses of 10^7, 10^6 and 10^5 TU and did not affect outflow facility. At 10^8 TU the outflow facility was reduced suggesting toxicity. Transduction of along the outflow pathway was observed that included the trabecular, juxtacanalicular trabecular meshwork, and the inner wall of Schlemm's canal. Expression of the reporter enzyme was seen at 7 days. Later studies by the same lead author in monkeys with an eGFP expressing vector led to gonioscopically observable fluorescence in the trabecular meshwork.[264] Ten to 100 fold more transducing units were used despite the previously determined toxicity threshold of below 10^7 TU in other species but similar eye size. Two monkeys were injected with 10^9 TU and two more with 10^7 TU due to anticipated difficulties visualizing fluorescence with a direct and insensitive detection system (personal communication). eGFP fluorescence was seen at both titers tested. One monkey received four consecutive injections into the same eye of 10^7 TU over a 7 month period. Expression lasted 3-4 weeks with little clinical signs of inflammation. In the monkey injected repeatedly, expression was again seen for 3-4 weeks but induced severe iritis and corneal decompensation on the fourth occasion. These results demonstrated the shortcomings of adenoviral gene transfer that is limited to a short amount of time likely due to the episomal state of the DNA and immunogenicity resulting in almost immediate failure with repeat injections. The study did not distinguish between potential immunogenic substances (adenoviral proteins versus eGFP) but eGFP expression has been observed long-term in various animals including monkeys[632] and was tolerated well in the past.

Kee et al. tried to take adenoviral gene transfer to the ocular outflow tract a step further by using a therapeutic gene, stromelysin.[629] MMP-3 (Stromelysin-1) can break down the extracellular matrix but has to be activated before that as other matrix metalloproteinases. Matrix metalloproteinases break down extracellular matrix during physiological processes such as embryogenesis, reproduction and tissue remodeling but also in disease processes such as arthritis and metastasis. Almost all MMPs are

secreted in an inactive zymogene form (proprotein) that requires activation by extracellular proteinases. MMP-3 degrades fibronectin, laminin, collagen III, IV, IX and X as well as cartilage proteoglycans.

Stromelysin perfusion has been demonstrated to increase outflow facility,[633] The authors injected vectors intracamerally in rat eyes and found stromelysin expression in trabecular meshwork, iris and the uveoscleral outflow pathway. This study was hampered by the lack of stromelysin activation and a resulting lack of outflow change. Outflow therapy with matrix metalloproteinase gene transfer remains an attractive option but attention must be paid to the complex biochemistry and interaction of these enzymes. Constitutively active matrix metalloproteinases have been described which may be more useful for this purpose.

In perfused human anterior segments, Ads carrying the dominant-negative RhoA effectively transduced the TM and increased outflow facility slightly.[634] In this study a CMV promoter driven dominant-negative form of RhoA with a single amino acid substitution of Thr19 to Asn was expressed by a replication-deficient adenoviral vector in perfused human anterior segment cultures. At 66 hours post transduction, anterior segments experienced an increase in outflow facility of 32.5%. TM cells showed a reduction in actin stress fibers and of the focal adhesion-containing protein, paxilin. The authors interpreted the increased outflow as a loosening of the cell-substrate and cell-cell attachments along the outflow pathway. The Rho family of proteins belongs to the larger Ras superfamily of GTP-binding proteins and has been shown to regulate a complex network of cytoskeleton-dependent cell functions. Manipulation of any content of this pathway harbors the risk of triggering cell migration and cell division ultimately resulting in cancer. Any vector with this potential should have a suicide gene cassette as well to allow ablation e.g. by HSV-tk conversion of acyclovir. This is still not a sufficient solution for non-integrating vectors as the cancer cells cannot be ablated anymore once the transient expression is extinguished.

In human TM cells, Ad carrying aquaporin I induced an 8.7% increase in resting cell volume that paralleled an 8% decrease in paracellular permeability of infected monolayers.[635] Conversely, aquaporin antisense adenoviral vector transduced cells had a reduced cell volume by 7.8%. It is possible that one way how prostaglandin analogues might increase conventional outflow is via an observed aquaporin

downregulation.[636] Because cell size is able to regulate outflow through the trabecular meshwork, gene therapeutic knockdown of aquaporin might increase outflow facility. Results of transduction of perfused anterior chambers have not been published yet. The original idea of this author that aquaporin is responsible for water passage from the anterior chamber directly through trabecular meshwork cells into Schlemm's canal[637] appears to be too simplistic and not applicable to glaucoma gene therapy.

Caldesmon is another protein that participates in the regulation of actin stress fibers and their manipulation is able to change outflow. Gabelt et al. over-expressed rat non-muscle caldesmon in human trabecular meshwork cells of cultured human and monkey anterior segments and found an increase of outflow facility by 43% at 66 hours (human) and 35% (monkey), respectively.[638] Histological studies showed that stress fibers gradually disappeared and novel actin structures were formed. Caldesmon is a calmodulin- and actin-binding protein that regulates smooth muscle and nonmuscle contraction. The conserved domain of this protein possesses the binding activities to Ca^{++}-calmodulin, actin, tropomyosin, myosin, and phospholipids. This protein is a potent tonical inhibitor of the actin-tropomyosin activated myosin Mg-ATPase, and serves as a mediating factor for Ca^{++}-dependent inhibition of smooth muscle contraction. Caldesmon over-expression prevents focal adhesion and stress fiber formation even if the cells constitutively active Rho suggesting that caldesmon is operating downstream of the Rho signaling pathway.

The same group also studied C3 transgene expression and its effect on actin and cellular adhesions in cultured human trabecular meshwork cells and on outflow facility of cultured anterior monkey segments.[639] C3 transferase is an exoenzyme from clostridium botulinum that targets Rho GTPases by specifically inactivating Rho through ADP-ribosylation. Similar to transduction with caldesmon, transduction with $1.2x10^8$ TU adenoviral vector expressing C3 resulted in a dose-dependent morphological change about 3 to 4 days later with partial retraction, rounding and elongation. The authors observed disruption of the actin cytoskeleton, reduced vinculin-positive focal adhesions and loss of beta-catenin as assessed by immunofluorescence. Outflow facility increased rather dramatically by 90% as corrected for GFP transduced control eyes.

As described in this thesis and discussed in detail below, use of lentiviral vectors for genetic modification of the ocular outflow tract is the only tool that has achieved stable long-term transduction.[324, 504, 586, 640, 641] Similar to the HIV and FIV vectors used in this thesis, Challa et al. used HIV vectors with an internal elongation factor 1 alpha (EF-1alpha) promoter driving eGFP expression.[640] In the later study authors found expression for three weeks at the study endpoint not only in the trabecular meshwork and the downstream outflow tract but also in the corneal endothelium. The authors speculate that frequent corneal neovascularization might be attributable to endothelial transduction and the fashion in which the needle is inserted (bevel up versus bevel down) but the lack of corneal infiltration or edema is inconsistent with this idea. More likely, this could be caused by the high titer used that were identical to the upper amount of TU used in the much larger feline eyes in our studies resulting in over-transduction with toxicity. Species differences may further result in different vector convection and exposure time. Balaggan et al. found the same using an equine infectious anemia virus (EIAV) in mice. In these even smaller eyes, high level transduction of TM and moderate transduction of corneal endothelium was observed after intracameral injection of approximately 2.8×10^7 TU.[642] When pseudotyped with the rabies-G rather than VSV-G transduction was poor. In some cases eGFP fluorescence was observed in the cornea in linear radial initial mid-stroma and central anterior stroma configuration that may be consistent with the pattern of neuronal innervations. Similarly, linear fluorescence was seen along the anterior border of the iris and within the ciliary body that may be following ciliary body nerves and the ciliary neuronal plexus. Prior studies found neuronal tropism of rabies-G pseudotyped vectors (VSV-G recognizes the ubiquitous phosphatidylserine, whereas rabies-G uses the neuronal cell adhesion molecule, nicotinic acetylcholine receptor and p75 preferentially).[643]

While most investigators have injected vectors and vehicles directly into the anterior chamber, Hudde et al. have described a way of achieving high multiplicities of infection and site specific targeting by direct injection into Schlemm's canal.[644] The authors performed surgical sclera unroofing of Schlemm's canal followed by direct injection of adenoviral vectors encoding MMP-3 (stromelysin). The authors found high transgene expression in the inner Schlemm's wall and trabecular meshwork but

failed to detect breakdown of the extracellular matrix. The same criticism of Kee et al.'s study discussed above applies here: although in cell culture MMP-3 appears to be active by zymographic assay, it is not clear whether MMP-3 is active in the ex vivo and in vivo experiments. A constitutively active form of MMP-3 should have been used. The authors confirm the intense immunogenicity of adenoviral vectors and find not only invasion of Schlemm's canal and trabecular meshwork by inflammatory cells but also keratic precipitates although the vector was not applied intracamerally.

Another way of limiting transgene expression is the use of trabecular meshwork specific promoters. Liton et al. used the chitinase 3-like 1 (Ch3L1) gene promoter after a comparative expression analysis of trabecular meshwork and Schlemm's canal cells to restrict adenoviral vector expression to the TM.[645] The authors transduced cultured cells and anterior human segments with 10^7 TU of adenoviral vectors that contained a Ch3L1 promoter driven lacZ cassette. Ch3L1 is a mammalian glycoprotein member of family 18 glycosyl hydrolases that is involved in tissue remodeling and inflammation and acts as a growth factor for connective tissue cells and as a potent migration factor for endothelial cells which could also play a role in both the normal physiology of the TM and the abnormalities that occur in glaucoma. Gonzales et al. found in a similar experiment by the same group that promoter fragments from the matrix Gla protein can specifically direct expression to the trabecular meshwork, while use of the vascular endothelin-cadherin gene promoter may allow differentiating between vascular and Schlemm's canal endothelial cells.[646]

A peculiar reverse observation is the complete inability of AAV vectors to achieve notable expression in the TM including primary cells cultures, organ cultures and living animals. AAV vectors have all the features that would make them highly desirable for long-term transduction of TM that apply to lentiviral vectors. Borras et al. studied the reasons for this restriction and found evidence for host downregulation of genes involved in cell cycle and DNA replication that require adenovirus coinfection for productive transduction.[647] This block can be overcome for the purpose of transduction with self-complementary AAV vectors which bypasses the required second-strand DNA synthesis to achieve a transcriptionally active AAV genome for gene expression.

Many variations of the idea of wound healing modulation after glaucoma filtration surgery have been described. Perkins et al. developed a gene therapy approach adjuvant to glaucoma filtering surgery, where an outflow shunts is created from the anterior chamber to a fluid reservoir under the conjunctiva.[648] While this procedure can lower intraocular pressure very effectively when the fluid reservoir functions properly, scar tissue formation and closure of the draining shunt and reservoir often result in failure. Ad encoding the cell cycle inhibitor protein p21 prevented scar formation to an extent comparable to the commonly used mitomycin C. p21 is the major transcriptional target of the tumor suppressor gene, p53; despite this, loss-of-function mutations in p21 - unlike p53 - do not accumulate in cancer nor do they predispose to cancer incidence. This gene encodes a potent cyclin-dependent kinase inhibitor that binds to cyclin-CDK2 or -CDK4 complexes, and thus functions as a regulator of cell cycle progression at G1. The protein can interact with proliferating cell nuclear antigen, a DNA polymerase accessory factor, and plays a regulatory role in S phase DNA replication and DNA damage repair. This protein is cleaved by CASP3-like caspases, which leads to activation of CDK2, and may participate in execution of apoptosis following caspase activation. Other groups have used very similar strategies with the same gene producing similar results (reviewed here[649]). Another approach to adjuvantive antifibrotic gene therapy is the use of RAD50, which is involved in the repair of mammalian DNA damage and antiproliferative activity that is p53-independent and p21-dependent.[650]

6.3.5.1.2.2. Retinal Ganglion Cells

Retinal ganglion cells (RGCs) represent the inner most cell layer of the neurosensory retina and their axons constitute the optic nerve. RGC death results irrevocably in optic nerve degeneration and loss of vision. Although technically easier to administer, gene transfer to retinal ganglion cells faces more significant barriers than subretinal injections targeting the RPE and outer neuroretina. Different from the liquefied, degenerated vitreous that is seen in patients with age related macular degeneration that allows easy diffusion and circulation of injected therapeutics, vitreous in experimental animals is without exception thick and gel like due to the relatively young age and perhaps species-difference. In contrast to the homogenous colloid structure of a gel, vitreous contains collagen strands that immobilize it and impede

circulation. The vitreous is surrounded by a membrane, the hyaloid face while the internal limiting membrane presents another barrier that vectors must overcome before making physical contact with retinal ganglion cells. As discussed below, these barriers proved to be insurmountable to pseudotyped FIV vector in our own experiments.[75] It is possible that surface charge and vector particle size are more favorable for parvoviral AAV vectors to overcome these barriers than the larger pseudotyped lentiviral vectors. As the focus of my studies was anterior gene transfer to the outflow tract rather than posterior neuroprotection, the cause of impaired gene transfer to retinal ganglion cells has not been examined in a scholarly fashion.

After noticeable absence of studies demonstrating efficient gene transfer to retina ganglion cells for many years, there are now several interesting ones that use AAV as the vector. Neurotrophic factors are now known to be problematic in many cases. For instance while BNDF is neutrotrophic on neurons, it causes up-regulation of nitric oxide synthase[651] or by suppressing the heat shock protein 27.[652] CNTF can produce rapid weight loss and death in mice.[653] BNDF is thought to be the most potent neuroprotective factor[654] but it also influences other neuronal cells of the retina such as amacrine cells, Müller glia, and cone photoreceptors.[655] Use of the extracellular signal-regulated kinase 1/2 (Erk1/2) and the phosphatidylinositol-3 kinase pathway represents an alternative strategy to target the intracellular events that lead to RGC survival thus bypassing the use of exogenous peptide factors.[656] This is what Zhou et al. chose to do: 8.5×10^7 TU of intravitreally injected AAV vectors were used to transduce retinal ganglion cells with the constitutively active or wild-type MAP2K1, the upstream activator of Erk1/2. After 5 weeks of ocular hypertension the dorsal retina RGC counts were almost twice as high as the control eyes. A major advantage of this approach over other strategies is that AAV serotype 2 mediates gene transfer to >70% of RGCs and a few displaced amacrine cells,[657] but not other retinal cell types, hence Erk1/2 activation is largely restricted to a target neuronal population. Although a difference of 50% compared to controls might not deem much, this is the threshold below which only subtle visual field impairment occurs while above 50% RGC loss results in noticeable, severe visual impairment in primates.[658]

The same senior investigator had previously used AAV vectors to transduce BDNF into RGCs by intravitreal injection. The protection against RGC loss was approximately 20% compared to control rats.[659] In an earlier study this senior author used AAV to transduce the chicken beta-actin driven human baculoviral IAP repeat-containing protein-4 (BIRC4), a potent caspase inhibitor, into RGCs of an ocular hypertensive rat. BIRC4 is an intriguing molecule the discovery of which began when it was found that the baculovirus caspase inhibitory gene p35 was able to rescue photoreceptors in retinal degeneration-mutant fruit flies.[660] Searches for homologs of p35 led to the discovery of inhibitors of apoptosis protein (IAP) genes, also found to be evolutionarily conserved in viruses, insects, and mammals.[660] IAPs are defined by baculovirus IAP repeat domains critical to apoptosis inhibition.[661] One member of the mammalian IAP family, BIRC4 (also known as XIAP or hILP), is a direct inhibitor of downstream cell death proteases.

Another study that used AAV mediated gene transfer or the basic fibroblast growth factor (bFGF) and BDNF found that intravitreally injected rats were protected against NMDA challenge compared to controls at 1 month post challenge.[662] The difference was relatively disappointing as BFGF achieved 18% protection and BDNF 12% in comparison to controls. Protection in the optic nerve crush model was only seen with bFGF and amounted 18%. Similarly, Ad mediated basic fibroblast growth factor (bFGF) expression rescued RGCs transiently.[663] In the later study only semiquantitation was performed by measuring optic nerve layer thickness making it difficult to judge outcome.

Leaver et al. used AAV-mediated gene transfer of CNTF to promote survival of axotomized retinal ganglion cells.[664] This effect was bigger in bcl-2 over-expressing mice after optic nerve crush. The authors injected $1.5x10^9$ TU of AAV vectors and observed an increase of viability of RGCs by about 50% in bcl-2 overexpressing mice while there was only a disappointing 7% increase in wild type mice. Leaver et al. used AAV-2 vectors to transduce either BNDF or CNTF into eyes with optic nerve crush or transection with an attachment of a peripheral nerve.[665] The authors found that only eyes with autologous peripheral nerve to optic nerve transplantation in combination with CNTF gene transfer would allow survival of about 25% at 7 weeks. Although these numbers are small overall, in a crush or transection model (as opposed

to the less drastic insult of ocular hypertension) it is remarkable that about 1/4th of retinal ganglion cells can survive the definite fate of apoptosis. In early gene transfer studies to retinal ganglion cells, Ad vectors were able to temporarily extend survival of Muller cells of rats with axotomized RGCs[666] by about 4.5 fold by transducing brain-derived neurotrophic factor (BDNF).

Again using an AAV vector, Wu et al. achieved long-term expression of glial cell line-derived neurotrophic factor to retinal ganglion cells after injecting 1.1×10^7 TU of AAV expressing GDNF intravitreally. The authors note the absence of inflammation, cell loss or change of electroretinogram latency and observed expression at the 1 year study endpoint.[667] As the main shortcoming, this study did not examine whether ganglion cell survival is improved in a glaucoma model. Ishikawa et al. also used GDNF but directly electroporated plasmids into RGCs after intravitreal injection. The authors find an improved survival of 50% of RGCs versus 15% in untreated controls at 2 weeks after optic nerve crush. The extent of survival is surprising given the relative inefficiency of gene transfer to only 24% of retinal ganglion cells.[668]

Malik et al. demonstrated that AAV2 mediated gene transfer of Bcl-XL is very effective in preventing cell death in 94% compared to 15% of RGCs compared to control eyes at 2 weeks and 46% at 8 weeks compared to 6% in controls after optic nerve crush.[669] Risks versus benefits must be carefully considered in gene transfer of members of the Bcl-2 family and other anti-apoptotic molecules. BCL-xl stands for "basal cell lymphoma-extra large" and has been isolated from cancer cells. Apoptosis serves a physiological purpose and manipulation of this mechanism could easily have the opposite effect. Bcl-xl is a transmembrane molecule in mitochondria that is involved in the signal transduction pathway of Fas ligand (FasL), itself a transmembrane protein that belongs to the tumor necrosis factor (TNF) family, the binding of which induces apoptosis.

Another approach to ganglion cell protection that is not directly related to glaucoma was demonstrated for experimental autoimmune encephalomyelitis, an autoimmune inflammatory disorder of primary central nervous system demyelination that has been frequently used as an animal model for testing treatments against multiple sclerosis.

The optic nerve is a frequent site of involvement in both experimental autoimmune encephalomyelitis and multiple sclerosis. Reactive oxygen species such as superoxide, hydrogen peroxide, nitric oxide, and peroxynitrite are mediators of demyelination and disruption of the blood-brain barrier in experimental autoimmune encephalomyelitis. Cellular defenses against reactive oxygen species include catalase and superoxide dismutase. Superoxide dismutase dismutes superoxide to hydrogen peroxide (H_2O_2), and catalase detoxifies the H_2O_2 to H_2O and O_2. Qi et al. cloned the human extracellular superoxide dismutase or catalase gene into AAV vectors and transduced mice by intravitreal injection.[670] Animals were then sensitized for EAE, followed by serial contrast-enhanced MRI for 6 months, and sacrifice. Western blot analysis of infected RGC-5 cells revealed that expression of dismutase increased 15-fold and that of catalase 3.5-fold. One month after intraocular injections, transgene expression increased 4-fold for dismutase and 3.3-fold for catalase. Six months after intraocular injections and EAE sensitization, combination therapy with dismutase and catalase decreased retinal ganglion cell loss by 29%, optic nerve demyelination by 36%, axonal loss by 44%, and cellular infiltration by 34% compared with the contralateral control eyes transduced with an eGFP expressing AAV vector.

6.3.5.2. Posterior Segment

6.3.5.2.1. Retinal Degeneration

The most experience in ocular gene therapy exists for retinal diseases, in particular for inherited retinal degeneration. The decoding of molecular mechanisms, identification of genetic defects and cloning of genes involved has dramatically advanced gene therapy in this area. Retinitis pigmentosa is a group of inherited photoreceptor defects that lead to incurable, progressive degeneration in about 1 in 3000 people.[671] There is a large number of natural or genetically engineered animal models with retinal degeneration analogous to human retinitis pigmentosa that can be used for development of preclinical therapy.

Retinal degeneration can involve lack-of-function mutations as well as gain of function mutations. Gene therapeutic replacement for a lack-of-function mutation is e.g. the premature stop codon of the beta subunit of the rod photoreceptor-specific cGMP phosphodiesterase (PDE-β). The defect is caused by a premature stop codon that affects only the homozygous, but not the heterozygous, which suggests that even

partial replacement of the defect might be sufficient. Rescue has been achieved in a mouse model (the rd mouse) with adenoviral,[672] AAV,[673] gutted adenoviral[674]and lentiviral vectors[281] carrying the same gene (PDEb).

Autosomal dominant retinitis pigmentosa is an example for *gain-of-function mutations*, which are more complex to treat. Defects may cause abnormal localization of proteins or altered function.[675, 676] AAV vectors have been used to deliver RNA-cleaving RNA molecules, ribozymes that leave the wild-type mRNA intact, while degrading the mutant RNA[677]and photoreceptor degeneration was slowed down for more than 3 months.

As described above in the therapeutic approaches for retinal ganglion cells in glaucoma, secondary strategies may consist of antiapoptotic[678, 679] or neurotrophic therapy of photoreceptors.[663, 680] Ad vector with rhodopsin promoter driven expression of bcl-2, an anti-apoptotic molecule, temporarily rescued photoreceptors in the rd mouse was able to rescue photoreceptors.[679] Rescue with AAV vectors expressing neurotrophic factors CNTF[320]or GDNF[681] resulted in improvement of retinal morphology in rats, but there was no functional ERG improvement with CNTF.[315]

Efficiency of non-viral transduction into the retina can be enhanced by simultaneous electroporation. Electroporated plasmids injected into the subretinal space can produce reporter gene expression for up to 50 days[682] but this can be extended to more than 4 months with cotransfection of phiC31 integrase to allow integrase-mediated recombination with attB sequences.[683] It is important that electroporation be optimized for each species as severe disruption of ocular structures can occur with inflammation, cataract formation, retinal degeneration and phthisis bulbi because of its physically violent nature.

Lentiviral vectors are an excellent choice for disorders that originate in the retinal pigment epithelium and can be applied to treat both degenerative as well as vaso-proliferative conditions. However, transduction of neuroretina is inefficient or impossible depending on the age and species. In our own experience as detailed below, FIV vectors only transduced retinal pigment epithelial cells even when injected into 5 day old rats. This contrasts to results with HIV vectors in mice that were injected at day 2 resulting in efficient transduction of neuroretina.[281] In all other studies lentiviral gene transfer to neuroretina was disappointing no matter what

promoter or pseudotype.[684] It is likely that this is the result of barriers and physical vector properties (charge, size) that may depend on species and animal maturity. Neuroretinal transduction can be improved by local trauma and enzymatic disruption of the inter-photoreceptor maxtrix.[278, 685, 686] Lentiviral vector mediated expression in the RPE has been reported for up to 2 years.[76, 687, 688] SIV and HIV vectors have been used successfully to treat retinal degeneration caused by a genetic defect of the RPE.[344, 688] Recent findings suggest that lentiviral vectors that are integrase defective can be used to achieve high enough expression levels to be therapeutic in RPE disease.[279, 488] Yanez-Munoz et al. show that $Rpe65^{rd12/rd12}$ mutant mice with a phenotype similar to that of individuals with Leber congenital amaurosis, a severe form of early-onset autosomal recessive retinitis pigmentosa that results from mutations in RPE65 can be rescued with HIV vectors that have a D64V mutation. Vectors can persist as episomal double-stranded DNA circles.[279]

AAV vectors are the common vectors used for gene transfer to the retinal pigment epithelium and the neuroretina. Although the majority of AAV vectors does not integrase but remains in the cell in the form of concatomers, transgene expression from AAV vectors has been followed for several years.[689-691]Tissue specificity as well as expression kinetics are surprisingly dependent on the vector serotype and ocular structure into which vectors are injected. Recent hybrid vectors in which AAV an AAV genome is packaged in a capsid from a different serotype have expanded the applicability. For instance, while AAV-2 vectors typically show a delayed onset of expression, slowly increasing expression after 2-4 months (which may be an advantage that allows gentle accumulation of a foreign transgene with less disruption of intracellular metabolism and immunogenicity), AAV-2/1, AAV-2/5 and AAV-5/5 vectors cause rather rapid expression as early 3 days after transduction. AAV-2/2 and AAV-2/5 transduce the RPE and photoreceptors, while AAV-4/4 and AAV-2/4 are restricted to the RPE.[691] Successful gene replacement has been achieved in both rodent and large animal models of inherited retinal degenerations with AAV-5 vectors.[691, 692] A novel serotype, AAV-2/8 can transduce photoreceptors and RPE even more efficiently than AAV-2/2 and AAV2/5. The self-complementary version of AAV-2/8, a strategy in which sense and antisense genomes are mixed in the final vector preparation, shows even faster and higher transgene expression than AAV-2/8.[693]

For both experimental and therapeutic purposes, gene regulation is a desirable feature. This has been accomplished in the retina with dual vector as well as single vector systems with both rapamycin and tetracycline-inducible systems.[694] Lebherz et al. achieved regulated long-term expression with a dimerizer-inducible expression system (rapamycin) in non-human primates for 2.5 years.[695] In an experimental model of uveitis tetracycline-inducible expression of IL-10 using a single AAV vector worked well.[696] Other researchers have used promoters that respond to environmental changes such as ischemia with mixed success.[697] The authors do not quantify the change of expression. The use of native promoters is of advantage as other inducible systems have been noted to be immunogenic (reviewed in[698]).

Proof-of-principle for gene replacement therapy has been demonstrated in several experimental models of inherited retinal degeneration resulting from loss-of-function mutations and is the most classical example of gene therapy. AAV vectors are the foremost vectors but not the only ones. In the rds mouse model peripherin, a membrane glycoprotein that is responsible for the formation and stability of photoreceptor outer segments can be replaced and restore function if done within 14 weeks. However, gene replacement is not maintained in the long term most likely because of the timing of intervention.[699] A protein anchored in the photoreceptor connecting cilia, the retinitis pigmentosa GTPase regulator interacting protein (RPGRIP), can be replaced as well and is able to preserve photoreceptors and function in a mouse model of Leber's congenital amourosis.[700]AAV-2 mediated expression of retinoschisin in a model of X-lined recessive juvenile retinoschisis allowed the electroretinographic improvement however, the retinal structure did not recover.[701] When younger animals were used in the same model functional and structural improvements were found for up to one year using AAV-5 vectors.[702] Another common murine model is the Royal College of Surgeons rat that is lacking Mertk, an RPE receptor tyrosine kinase involved in the phagocytosis of shed photoreceptor outer segments. Rescue of this model was achieved with both AAV2 and lentiviral vectors.[688, 703] HIV-vector mediated gene transfer was more efficient in this model, likely an effect of the RPE-specific tropism as well as the more rapid onset compared with AAV-2 vectors. Another interesting model is the murine model of ocular albinism in which gene replacement of OA1 has been performed, restoring the number of melanosomes and improving the electroretinographic abnormalities.[704]

RPE65 is another model of Leber's congenital amaurosis. RPE 65 is an RPE-specific visual cycle isomerase which is essential for the synthesis of 11-cis-retinal. Dejenka et al. performed in utero delivery of RPE65 in *RPE65-/-* knockout mice with resulting rescue.[705] By now several groups have treated Swedish Briard dogs which are homozygous for an RPE65 null mutation.[282, 692, 706-708] The phenotype in these dogs is similar to humans with very poor vision from early life and almost absent dark- and light adapted electroretinography.

The study of Acland et al.[282] was regarded a breakthrough because it was the first case in which actual visual function was restored through gene therapy: dogs with a genetic defect equivalent to Leber's amaurosis in humans (RPE65-deficiency with 4 bp deletion resulting in a premature stop codon) recovered already altered vision and retinal function in electroretinography (ERG) after a single subretinal injection of AAV expressing RPE65 wild type. Four months after injection, electroretinography (ERG) of the treated eyes as well as behavioral and visual assessment tests, demonstrated that the dog had recovered the ability to avoid objects only on the side of the treated eye. This represents the first case of restoring visual function by gene therapy. Gene transfer corrected this phenotype and noticeably changed the dogs' behavior for the 3 years these animals were followed.[692]

The first cone-target gene therapy was recently presented in which the authors corrected cone-mediated ERG function and restored visual acuity in an animal model of achromatopsia with AAV vectors that have an internal red/green cone rhodopsin promoter driving α-transducin expression.[709] Using adeno-associated virus (AAV) gene therapy, Alexander et al. further showed that it is possible to rescue visual acuity in the *Gnat2*^{cpfl3} mouse model[710] of achromatopsia. This study demonstrates the feasibility of targeting cones in order to treat many of the most prevalent disorders threatening vision in humans.

Henning et al. used a mouse model of mucopolysaccaridosis VII to study AAV-mediated gene replacement of beta-glucuronidase by intravitreal injection.[711] The authors found reduction of partially degraded gycosaminoglycans in RPE cells and improved retinographic responses.

Cleaving of mutant mRNA using ribozymes is an attractive solution for heterozygous genetic defects with a pathogenic gene product rather than simple lack of function. One rationale that has driven ribozyme use for retinal degenerations is the fact that it will be impossible to develop individual gene therapies for the over 100 different mutations that have been described for the rhodopsin gene alone in retinitis pigmentosa. Gorbatyuk demonstrated that this can be accomplished in combination with gene replacement of a ribozyme-resistant wild-type rhodopsin.[712] Small interfering RNA (RNAi) has revolutionized the field and as a result ribozyme use has fallen into disfavor. Paskowitz et al. elegantly show that RNAi mediated knock-down can be accomplished with both AAV and HIV vectors in rat RPE and suppress basic fibroblast growth factor within a few days after vector injection which remained stable throughout the study which concluded at 60 days.[713] Others have knocked down rhodopsin without yet providing wild-type substitution.[714] Because rhodopsin is produced in large amounts and rapidly, it is difficult to knock down entirely. This may be an insurmountable obstacle for aggressive dominant mutants such as the rhodopsin P23H mutation.[715]

6.3.5.2.2. Retinal and Choroidal Neovascularization

Choroidal and retinal neovascularization is a major cause for visual loss.[267-272] In view of limited efficacy and significant adverse effects of current treatments[277, 716, 717] novel strategies are needed. Stable long-term expression of anti-angiogenic proteins from gene therapeutic vectors have already produced first promising results with vectors expressing vascular endothelial growth factor (VEGF) receptor as a VEGF sink,[390, 718] angiostatin,[313] endostatin,[349] and pigment epithelium-derived factor (PEDF).[312, 314, 346, 347, 356]

Diabetic retinopathy and age-related macular degeneration are two major causes of blindness in developed countries and share ocular neovascularization as a central feature. Present novel therapy with small molecules requires repeated injection into the vitreous. Ocular gene transfer offers the opportunity of sustained and targeted delivery of angiostatic molecules preventing potential systemic complications such as thromboembolic events.

Murin oxygen induced retinopathy is a common model of ischemia-induced, VEGF-dependent retinal neovascularization. Adenoviral and AAV vectors have been used to express soluble fms-like tyrosine kinase (sFlt-1), a VEGF receptor.[718] After induction of proliferative retinopathy in mice by oxygen exposure, intravitreally injected adenoviral vectors resulted in a 56% reduction of neovascular endothelial cells and a 52% reduction in AAV injected eyes.

In lieu of an animal model of AMD, choroidal neovascularization models of laser-induced rupture of Bruch's membrane have been developed. Subretinal delivery of AAV vectors expressing sFlt-1 can successfully suppress such neovascularization.[390] Expression of PEDF[346] or angiostatin[313] can equally successful prevent choroidal neovascularization.

Lamartina et al. used helper dependent adenoviral vectors that the authors have previously used to express eGFP for up to one year previously to transfer sFlt-1 into a rat model of oxygen induced retinopathy.[719] Retinal neovascularization was inhibited by more than 60%. HD-Ad/GFP promoted long-lasting (up to 1 year) transgene expression in retinal Müller cells, in marked contrast with the short-term expression observed with FG-Ad/GFP.

Comparably fewer studies with lentiviral vectors delivering angiostatic proteins have been performed. Most noteworthy is Igarashi et al.'s use of HIV vectors expressing angiostatin to reduce neovascularization dramatically by 90%.[355] EIAV vectors also achieved impressive reduction in a laser model of choroidal neovascularization: EIAV vectors expressing endostatin resulted in an approximately 60% reduction in neovascularization area and angiostatin expressing vectors a 50% reduction.[720] Hyperpermeability was also assessed and was reduced by 26% with endostatin versus 24% with angiostatin.

6.3.5.3. Ocular Malignancies

Uveal melanomas (iris, ciliary body, and choroids) or retinoblastomas constitute potential targets for gene therapy that require an entirely different approach. The known problems of preferential tumor transduction, tumor penetration and avoidance of the delicate adjacent structures in the eye present difficult hurdles. The initial

optimism that gene therapy for ocular tumors will allow better treatment modalities has not materialized. In the contrary, it has become more obvious that classical methods of cancer therapy are preferable. For instance, retinoblastomas respond well to adjuvantive chemotherapy to shrink a tumor e.g. prior to laser therapy. This allows confining damage with excellent manual control in the hand of the treating surgeon. Any cytotoxic therapy in the eye can easily be detrimental to neighboring structures. Uveal melanomas in contrast can be treated with sutured radioactive plaques that can be applied directly above the lesion on the sclera and removed after destruction of the tumor.

Kimura et al. was one of the first ones to propose and demonstrate cytotoxic gene therapy to proliferating cells in the eye.[721] Originally thought out for proliferative vitreoretinopathy, this approach has been adopted to ocular malignancies later on. The authors took advantage of the trademark of type C retroviral vectors, selective transduction of dividing cells that distinguishes this vector type from others. Because type C retroviral vectors require cellular division to obtain access to the genome for integration, only the diseased tissue is affected. Rabbit with experimental proliferative vitreoretinopathy were transduced with retroviral MLV vectors, expressing the herpes simplex virus thymidine kinase (HSV-tk) gene, allowing for the selective killing of these cells after ganciclovir exposure. Unfortunately, in vivo transduction efficiency was low after intravitreal injection in with a relative transduction efficiency of approximately 2%. Despite this, transduction of HSV-tk was associated with a powerful bystander effect both in vitro and in vivo with significant effects even when HSV-tk-positive cells represented only 1% of the population. In vivo transduction followed by GCV significantly inhibited the development of proliferative vitreoretinopathy.

Hurwitz et al. popularized the idea of treating retinoblastoma with herpes simplex virus thymidine kinase.[722] This approach can result in efficient tumor ablation and has been approved for a phase 1 human clinical trial.[723] Because present treatment for large retinoblastoma are enucleation followed by radiation or chemotherapy (and secondary malignancies later in life), search for novel therapies is justified. The authors tested the hypothesis that gene therapy can reduce the tumor size sufficiently to allow local control by laser or cryo treatment in a murine model of retinoblastoma. Intravitreal injections of retinoblastoma Y79Rb cells in immunodeficient mice create

an aggressive, metastatic murine model of retinoblastoma. When these murine retinoblastomas were transduced in vivo with adenoviral vectors expressing HSV thymidine kinase followed by intraocular injection of ganciclovir, 70% showed a complete ablation of detectable tumor. Mice had a significantly longer progression-free survival compared with controls. A clinical trial was subsequently initiated to apply these results to patients with retinoblastoma that demonstrated the safety of vector application and remission in one patient.

The same group has now instigated a recently discovered picorna virus, Seneca Valley Virus, a conditionally replication competent virus that is not pathogenic to normal human cells but causes lysis in human retinoblastoma cells.[724] In the above mentioned xenograft murine model of metastatic retinoblastoma was injected with 10^{13} viral particles. Only 1 out of 20 animals showed invasive disease versus 7 out of 20 in the control group. CNS metastasis was prevented in all animals compared to 4 metastatic events in the control group. No adverse events were observed.: 18006805

Plasminogen activators are facilitating tumor metastatic by promoting invasion of tissue barriers. Uveal melanoma is the most common intraocular malignancy in adults and has a mortality of 50%. Ma et al.[725] explored the possibility of preventing the metastasis of intraocular melanomas by disrupting plasminogen activator function through gene transfer. A replication-deficient adenovirus vector was used for the in vivo transfer of plasminogen activator inhibitor type 1 by intraocular injection. The authors found transduction of more than 95% of human and murine uveal melanoma cells in the eyes of nude mice, a 50% reduction in the number of animals developing liver metastases and a 78% reduction in the metastatic tumor burden in animals that eventually developed metastases. Intravenous injections of this vector resulted in transduction of normal liver cells and culminated in a sharp reduction in the incidence of metastases and a significant prolongation of host survival. The effect seen in this study is rather dramatic and encouraging. As a significant difference to human melanomas, the tumors in this study are very small and high transduction rates can more readily be achieved than in the solid tumors of humans.

7. Materials and Methods

7.1. Materials

The following is a comprehensive list of materials and reagents used in the context of this thesis. The next chapter will provide details about their application and use.

7.1.1. Amplification of Plasmid DNA in Bacteria

Bacterial plasmid DNA

Competent E. coli One Shot Top10 high efficiency kit (Invitrogen, Carlsbad, California)

Competent E. coli Subcloning Efficiency Dh5alpha (Invitrogen, Carlsbad, California)

Waterbath

7.1.2. DNA Analysis

Restriction enzymes (New England Biolabs, Ipswich, MA)

7.1.3. Cloning using Plasmid Vectors

Restriction enzymes (New England Biolabs, Ipswich, MA): cutting of DNA

DNA ligase (New England Biolabs, Ipswich, MA): joining of DNA fragments

T4 Polynucleotide Kinase (New England Biolabs, Ipswich, MA): addition of 5′-phosphates to oligonucleotides to allow subsequent ligation

DNA Polymerase I, Large (Klenow) Fragment (New England Biolabs, Ipswich, MA)

7.1.4. Polymerase Chain Reaction

Taq PCR kit (New England Biolabs, Ipswich, MA)

High Fidelity PCR (Roche Applied Science, Indianapolis, IN)

Primers, custom made by Mayo Clinic Sequencing Core

7.1.5. DNA Sequencing

Primers, custom made by Mayo Clinic Sequencing Core

7.1.6. Cloning of Viral Vectors

Generally, current retroviral vectors systems such as the one used in the context of this thesis are replication-defective and tripartite. They consist of: 1. transfer vector, 2. packaging plasmid and 3. envelope plasmid. Same molar ratios of 3:3:1 apply but

might have to be optimized depending on the individual vector system. Components of the FIV vectors system are discussed in detail in the chapter "FIV Vectors".

7.1.6.1. Feline Immunodeficiency Virus (FIV) vectors

1. pMD.G: plasmid encoding VSV-G: 84 μg for CF10, 16.8 μg (CF2), or 1 μg (T75).

2. Transfer vector. pGiNWF: minimal bi-cistronic FIV transfer vector plasmid coding for EGFP and neomycin phosphotransferase neoR, containing WPRE and FIV central DNA flap; pCT26: lacZ-encoding second generation FIV plasmid or other FIV transfer vector: 252 μg for CF10, 50.4 μg (CF2), or 3 μg (T75). This vector also has the central DNA flap inserted between the end of the gag segment and RRE.

3. pFP93: minimal FIV packaging plasmid coding for structural and enzymatic proteins derived from the Gag/Pol precursor (matrix, capsid, nucleocapsid, protease, reverse transcriptase, RNase H, integrase, dUTPase) and Rev (regulator of expression of virion proteins): 252 μg for CF10, 50.4 μg (CF2), or 3 μg (T75).

Ratio of pMD.G/pGiNWF/pFP93 is 1/3/3. DNA used for vector preparation for in vivo applications must be sterile and endotoxin free to prevent toxic or inflammatory reactions in animals. There are several kits commercially available, EndoFree Plasmid Maxi Kit (Qiagen, cat. no. 2362).

7.1.6.2. Murine Leukemia Virus (MLV) beta-galactosidase expressing vector LZRNL[462]

1. 293GP-LZRNL cells (retrovirus packaging cell line 293GP expressing the Moloney *gag* and *pol* genes[462] and LZRNL provirus (LTR-lacZ-RSV-neoR-LTR)[726]

2. pCMV-G[462]

7.1.6.3. Human Immunodeficiency Virus (HIV) vectors[240, 250]

1. pHR9CMVlacZ[240, 250]

2. pCMVDR8.9[240, 250]

3. pCMV-G[462]

7.1.6.4. Adenoviral Vector

Ad.CMVlacZ[727-730]

7.1.7. Cell Cultures

7.1.7.1. Cell Cultures

The same culture materials as described in the following were used in all cell cultures that were part of this thesis unless otherwise mentioned. Materials and reagents are therefore not listed separately. All cell lines can be obtained from the American Type Culture Collection (ATCC) unless otherwise noted. Tissue culture techniques were performed in a tissue culture hood approved for biosafety level 2 + handling.

7.1.7.2. Cell Cultures for Retroviral Vector Production

1. 293T cells.
2. Adherent fibro-epithelial cell lines for titration: CrFK cells.
3. Dulbecco's modified Eagle medium with 10% fetal calf serum (DMEM-10), penicillin G sodium 100 units/mL, streptomycin sulfate 100 μg/mL and L-glutamine 2 mM.
4. Trypsin, tissue culture grade
5. PBS (phosphate-buffered saline), tissue culture grade.
6. Distilled water, sterile.
7. 70% isopropanol or ethanol.
8. 37°C humidified incubators, 5% CO2.
9. Nikon Coolpix 990 camera for digital image capture (Nikon, Melville, NY)
10. Nikon Eclipse TE300 microscope (Nikon, Melville, NY)

7.1.7.3. Cell Cultures for Production in Cell Factories

1. Cell Factory with desired number of layers (Nunc Cell Factory, available as 1-layer CF1, 2-layer CF2, 10-layer CF10, and 40-layer CF40).

2. Cell Factory start-up kit (cat. no. 170769) with the following components: HDPE connectors (cat. no. 171838), white Tyvek cover caps (cat. no. 171897), blue sealing caps (cat. no. 167652), Gelman 4210 bacterial air vent filter.

3. 2 L Kimax aspirator bottle (Kimble Glass, cat. no. 14607-2000) or similar bottle.

4. Funnels, sterile.

5. Cell strainers (BD Falcon, cat no. 352350)

7.1.7.4. Cell Cultures for Production in T75 Flasks

Appropriate number of T75 tissue culture flasks with gas-permeable cap.

7.1.7.5. Human Ocular Anterior Segment Cultures

Human donor eyes from the local eye bank

Custom made anterior chamber segment perfusion equipment as described by Douglas H. Johnson[731] consisting of:

1. Bottom chamber
2. Scleral sealing ring
3. Cover
4. Perfusion tubing
5. Pressure transducer
6. Pressure recording software
7. Microperfusion pump

7.1.8. Transfections

1. 2.5 M CaCl2.

2. 0.01 M Tris-HCl, pH 8.0.

3. 2X HBS (HEPES-buffered saline). Stock solution of dibasic Na_2HPO_4: 52.5g Na_2HPO_4, 5000 mL H_2O. 2X HBS: 80 g NaCl, 65 g N-2-hydroxyethylpiperazine- N-2-ethanesulfonic acid (HEPES) (sodium salt), 100 mL Na_2HPO_4 stock solution. Bring

volume to 5000 mL and adjust pH of 6.95, 7, and 7.05 with 1 N NaOH. Optimal pH needs to be determined (see Notes and recipes): pH 6.95, 7.00, or 7.05.

4. Fresh culture media.

7.1.8.1. Cell Factories

1. Sterile plastic bottle (CF2, 250 mL; CF10, 500 mL).

2. Waste beaker with same volume as culture media in use.

3. Sterile Cell Factory loading bottle with silicon tube and connector.

7.1.8.2. T75 Flasks

1. Clear polystyrene 5-mL tubes (Falcon, cat. no. 352058).

7.1.9. Vector Harvest

7.1.9.1. Cell Factories

1. 500-mL filter units, 0.22-μm pore size

2. Cryovials

3. -80 C freezer

7.1.9.2. T75 Flasks

1. Small filter unit (50 mL).

2. Cryovials

3. -80 C freezer

7.1.10. Vector Concentration

7.1.10.1. Cell Factories

1. 500-mL filter units, 0.22-μm pore size.

2. 250-mL polyallomer Oak Ridge ultracentrifuge bottles (Sorvall, cat. no. 54477) with fluorocarbon caps (Sorvall, cat. no. 54421) for A612 rotor (Sorvall, cat. no 11997).

3. Scale.

4. 36-mL disposable polyallomer ultracentrifuge tubes (Sorvall, cat. no. 03141) for SureSpin 630 rotor (Sorvall, cat. no. 79367).

5. 1.8-mL screw cap cryo vials, sterile.

6. 0.5- and 1.5-mL microcentrifuge tubes, sterile.

7. PBS, tissue culture grade/suitable for in vivo application.

8. 70% molecular grade ethanol in squeeze bottle.

7.1.10.2. T75 Flasks

1. Scale.

2. 36-mL disposable polyallomer ultracentrifuge tubes (Sorvall, cat. no. 03141) for SureSpin 630 rotor (Sorvall, cat. no. 79367).

3. 1.8-mL screw cap cryo vials, sterile.

4. 0.5- and 1.5-mL microcentrifuge tubes, sterile.

5. PBS, tissue culture grade/suitable for in vivo application.

5. 70% molecular grade ethanol in squeeze bottle.

7.1.11. In Vivo Applications

7.1.11.1. Animals

Specific pathogen-free domestic cats (Harlan, Indianapolis, IN)

Sprague-Dawley rats (Harlan Laboratories, Indianapolis, IN)

7.1.11.2. Imaging

1. Nikon digital microscopy camera DXM 1200 (Nikon, Melville, NY)
2. Nikon image capture software (Automatic Camera Tamer (ACT-1), Nikon, Melville, NY)
3. Custom made cat restrainer as detailed below
4. Zeiss gonioscope to visualize the trabecular meshwork
5. Tiletamine HCl/Zolazepam HCl (Telazol, Fort Dodge Laboratories Inc., Fort Dodge, IA)
6. Slit lamp (Haag-Streit, Mason, OH)

7. Gonioscope (Posner, Ocular Instruments, Bellevue, WA)
8. Microscope (Nikon Eclipse E400)
9. GFP-optimized filter (Nikon, EF-4 B-2E/C FITC, cat. 96107)

7.1.11.3. Pressure recording

Handheld pneumatonometer (Model 30 Classic, Medtronic, Fridley, MN) to determine IOP

7.1.11.4. Subretinal Injection in Rats

1. Custom needle (32 ga, 12° bevel, 7 mm length, Hamilton Co., Reno, NV)
2. 5 µl Hamilton microsyringe (Hamilton Co., Reno, NV)
3. Inhalation anesthesia with Metofane® (Schering-Plough Animal Health Corp, Union, NJ)

7.2. Methods

7.2.1. Manipulation of Vector Components

7.2.1.1. Cloning using Plasmid Vectors

Molecular cloning is the procedure of isolating a specific DNA sequence and copying it with techniques of molecular biology. Cloning is used to amplify a DNA sequence in order to change its ends (e.g. by adding restriction enzyme sites) and to link it to other DNA. Most the time DNA is amplified in E. coli in circular form as a plasmid and therefore needs an origin of replication. For selection of bacteria that contain the desired plasmid, an antibiotic resistance gene (e.g. for ampicillin resistance) is needed as well.

Cloning of a DNA fragment requires fragmentation with restriction enzymes, ligation with ligases (DNA linking enzymes), transformation into bacteria, selection with antibiotic resistance for successful transformation and screening with restriction enzymes and electrophoresis.

7.2.1.1.1. Creating DNA Fragments

DNA fragments can be created with single or combination of restriction enzymes as described above for diagnostic purposes. The difference here is the careful choice of

location of the restricted location in order not to destroy an intact feature (e.g. gene, promoter, internal ribosomal entry site, etc). This is often followed by gel electrophoresis to confirm the digest, to isolate and purify the desired insert.

7.2.1.1.2. Manipulation of Restriction Sites

Restriction sites can be manipulated with several other enzymes that are capable of removing 5' or 3' single strand overhangs or filling in of single strand overhangs. The enzymes below were used for molecular cloning as described in the cloning history.

Exonuclease T (Exo T) (cat. No. M0265S), also known as RNase T, is a single-stranded DNA or RNA specific nuclease that requires a free 3' terminus and removes nucleotides in the 3' → 5' direction. Exonuclease T can be used to generate blunt ends from a DNA molecule that has a 3' extension.

T7 Exonuclease (cat. No. M0263S) acts in the 5' to 3' direction, catalyzing the removal of 5' mononucleotides from duplex DNA. T7 Exonuclease is able to initiate nucleotide removal from the 5' termini or at gaps and nicks of double-stranded DNA. It will degrade both 5' phosphorylated or 5' dephosphorylated DNA. It has also been reported to degrade RNA and DNA from RNA/DNA hybrids in the 5' to 3' direction but is unable to degrade either double-stranded or single-stranded RNA. The protein is the product of T7 gene 6.

DNA Polymerase I, Large (Klenow) Fragment (cat. No. M0210S) is a proteolytic product of E. coli DNA Polymerase I which retains polymerization and 3'→ 5' exonuclease activity, but has lost 5'→ 3' exonuclease activity. Klenow retains the polymerization fidelity of the holoenzyme without degrading 5' termini.

7.2.1.1.3. Isolation of DNA Fragments from Agarose Gel

DNA fragments were extracted from agarose gel using the QIAquick Gel Extraction Kit (cat. No. 28704) using a microcentrifuge.

DNA fragment were excised from the agarose gel with a clean, sharp scalpel and weighed in a microcentrifuge tube. 3 volumes of Buffer QG to 1 volume of gel (100 mg ~ 100 µl) were added and incubated at 50°C for 10 min interrupted by frequent shaking to facilitated mixing. The QIAquick spin column was placed in a provided 2

ml collection tube, the sample was applied to the column and centrifuged for 1 minute. The flow-through was discarded and placed back in the QIAquick column. 0.75 ml of Buffer PE was added to the QIAquick column and centrifuge for 1 min for washing. The flow-through was discarded and the QIAquick column was centrifuged for an additional 1 min at 17,900 x g. The QIAquick column was placed into a clean 1.5 ml microcentrifuge tube, 50 µl of Buffer EB (10 mM Tris·Cl, pH 8.5) was added to the center of the QIAquick membrane and centrifuged for 1 min to elute DNA.

7.2.1.1.4. DNA ligation

A ligase catalyzes the formation of a phosphodiester bond between juxtaposed 5' phosphate and 3' hydroxyl termini of both blunt ends and cohesive end termini. Ligations were performed at room temperature using 1 µl of T4 DNA Ligase (cat. No. M0202T) in a 20 µl reaction for 10 minutes for cohesive ends. For blunt ends, 1 µl high concentration T4 DNA Ligase was used for 10 minutes (cat. No. M2200S). Cloned plasmids were then transformed into bacteria, extracted and analyzed as described in the following.

7.2.1.2. Amplification of Plasmid DNA in Bacteria

7.2.1.2.1. Transformation of Competent Bacterial Cells

Bacterial transformation is the uptake of DNA resulting in a stable genetic change. This uptake is only able in so called competent cells that are able to uptake exogenous DNA. In the laboratory, this competence is referred to as "artificial" because cells are made passively permeable to DNA by mechanisms that would not normally occur in nature. For plasmid DNA, cells are chilled and incubated with DNA to make the cell wall more permeable followed by a brief heat shock that causes the DNA to enter the cell. Electroporation would be another way of transformation but this method was not applied in this thesis and will not be discussed further.

A plasmid must contain an origin of replication to persist and be stably maintained in the cell. A gene coding for antibiotic resistance is also contained to allow selection to transformed cells from the abundant non-transformed cells.

For all transformations Invitrogen One Shot Top 10 cells (cat no C4040-6) were used. Transformation was started immediately following the thawing of the cells on ice and

mixed by swirling. Before starting the water bath was warmed to 42°C and both the vial of media and the plates were warmed to room temperature. One µl of each ligation reaction was added directly into the vial of competent cells and mixed by tapping. The vials were incubated for 30 minutes on ice followed by heat shock at 42°C in the water bath and placement on ice again. 250 µl of pre-warmed medium was added to each vial. The vials were placed on a shaker at 37°C for exactly 1 hour at 225 rpm. 20 µl of bacteria were then spread on a pre-warmed plate and placed inverted into an incubator overnight at 37°C. Colonies were picked, grown in minipreps and analyzed with restriction digest.

7.2.1.2.2. Amplification and Recovery of Recombinant Plasmid DNA

Ten clones from each agar plate were picked with disposable pipette plastic tips and dropped into 10 ml disposable media tubes that were filled with 1 ml lysogeny broth (LB). The minipreps were incubated on shaking incubators at 37C overnight.

LB media is a nutritionally rich medium that is primarily used for the growth of bacteria. It is also known as Luria broth or Luria-Bertani broth. LB media formulations have been an industry standard for the cultivation of Escherichia coli as far back as the 1950s. These media have been widely used in molecular microbiology applications for the preparation of plasmid DNA and recombinant proteins. It continues to be one of the most common media used for maintaining and cultivating recombinant strains of Escherichia coli. There are several common formulations of LB. Although they are different, they generally share a somewhat similar composition of ingredients used to promote growth, including peptides and casein peptones, vitamins, trace elements (e.g. nitrogen, sulfur, magnesium) and minerals. Peptides and peptones are provided by tryptone. Vitamins and certain trace elements are provided by yeast extract. Sodium ions for transport and osmotic balance are provided by sodium chloride. Bacto-tryptone is used to provide essential amino acids to the growing bacteria, while the bacto-yeast extract is used to provide a plethora of organic compounds helpful for bacterial growth.

For 1 liter of LB 10g tryptone, 5g yeast extract and 10g NaCl were mixed and suspended in 800 ml of distilled water. Further water was added to make for a total of

1 liter. The mix was autoclaved at 121°C and stored at 4°C. Immediately prior to use ampicillin was added to 100 mg/ml to allow selection of plasmids.

For miniprep cultures, 1 ml of LB media with ampicillin was used to grow picked clones overnight while for maxiprep cultures 150 ml or more was grown once the proper clone was confirmed. Cultures were incubated at 37C overnight.

To extract plasmid DNA from miniprep picked clones, DNA was isolated using a Miniprep kit (QIAprep Spin Miniprep Kit, Cat. No. 27104; Qiagen, Hilden, Germany) and a microcentrifuge.

This protocol was designed for purification of up to 20 µg of high-copy plasmid DNA from 1 ml overnight cultures of E. coli in LB medium. The bacterial cells were harvested by centrifugation at 6800 x g in a conventional table-top microcentrifuge for 3 min at room temperature in microcentrifuge tubes. Bacterial pellets were resuspended in 250 µl Buffer P1 and transferred to a microcentrifuge tube. RNase A had been added to Buffer P1. No cell clumps were visible after re-suspension of the pellet. Bacteria were resuspended completely by pipetting up and down until no cell clumps remained. 250 µl Buffer P2 was added and mixed thoroughly by inverting the tube 4–6 times. The lysis reaction was not allowed proceed for more than 5 min. 350 µl Buffer N3 was added and mixed immediately and thoroughly by inverting the tube 4–6 times. Tubes were centrifuged for 10 min at 17,900 x g in a table-top microcentrifuge and a white pellet formed. The supernatants from were applied to the QIAprep spin columns by pipetting and centrifuged for 30–60 s, the flow-through was discarded. QIAprep spin columns were washed by adding 0.75 ml Buffer PE and centrifuged for 30–60 s. The flow-through was discarded and centrifugation was continued for an additional 1 min to remove residual wash buffer. The QIAprep column was placed in a clean 1.5 ml microcentrifuge tube. To elute DNA, 50 µl Buffer EB (10 mM TrisCl, pH 8.5) was added, let stand for 1 min, and centrifuged for 1 min.

7.2.1.2.3. Quantification of Nucleic Acid

Because DNA and RNA absorb ultraviolet light with an absorption peak at 260 nm, a UV spectrophotometer could be used to calculate DNA concentration using the Beer Lambert Law. DNA was diluted in water at a ratio of 1:10 or above till reliable

readouts were obtained. DNA purity was estimated using the absorption ratio at 260:280 nm and only samples with 90% purity or above were accepted.

7.2.1.3. DNA Analysis

7.2.1.3.1. Restriction Enzyme Digestion of Plasmid DNA

Restriction enzyme digests were used to analyze DNA. This technique uses restriction enzymes that are capable of cutting DNA into shorter fragments that can be visualized in gel electrophoresis. A restriction enzyme cuts DNA segments with a highly specific nucleotide recognition sequence that typically consists of six, to twelve nucleotides. Because of the limited number by which these sequences can occur along a DNA the distance at which a cut occurs is very characteristic for a DNA of interest. The same technique was used not only to identify correct orientation of inserts in vector plasmids used in this thesis but also for cloning as DNA fragments with corresponding cut sequences can be ligated back together. The enzymes used in this thesis are listed in the FIV cloning history. DNA was analyzed by digesting with commercially available restriction enzymes. All restriction enzyme digests used in this thesis were from New England Biolabs (New England Biolabs, Ipswich, MA) and followed the New England Biolabs protocols. A restriction digest was performed using 1 microliter of enzyme solution at 37C for 1-2 hours in a volume of 10 to 20 microliter. Solutions that allow restriction to occur consist of the plasmid DNA, an enzyme optimized buffer that allows the reaction to occur, the restriction enzyme and water to bring the reaction volume to 10 microliter.

7.2.1.3.2. Gel Electrophoresis of DNA

Agarose gel electrophoresis is a method to separate DNA. Nucleic acid is negatively charged and migrates at different speed based on molecule size through the agarose gel grid following an electric field towards the (positively charged) cathode. Shorter molecules move faster and migrate farther than longer ones. Increasing the agarose concentration of a gel reduces the migration speed and enables separation of smaller DNA molecules. Migration speed increased with increasing voltage but resolution might suffer. In order to visualize the DNA gels are stained with ethidium bromide which fluoresces under UV light when intercalated with DNA. As ethidium bromide is a carcinogen it has to be handled carefully.

7.2.1.4. Polymerase Chain Reaction

Polymerase chain reaction (PCR) is used to amplify a specific region of a DNA strand. The PCR applications in this thesis employed a heat-stable DNA polymerase from Thermus aquaticus, Taq polymerase. This DNA polymerase enzymatically assembles a new DNA strand from nucleotides, using single-stranded DNA as the template and DNA primers required for initiation of synthesis. This is achieved by thermal cycling to a defined series of temperature steps. The selectivity of a PCR is primarily due to highly complementary primers to the DNA region targeted for amplification and to the thermal cycling conditions.

Any PCR requires a DNA template that contains the DNA region to be amplified, one or more primers, which are complementary to the 5' and 3' ends of the DNA region, a polymerase with a temperature optimum around 70°C, deoxynucleoside triphosphates (dNTPs), a buffer solution, magnesium and monovalent cation potassium ions.

The PCR protocol typically 20 to 35 repeated temperature cycles with 2-3 discrete temperature steps each. The cycling is preceded by a single temperature step at a high temperature to meld DNA at above 90°C. Temperature and the length of time depend on the enzyme used and the melting temperature of the primers.

In the initialization step the reaction is heated to 94°C and held for about 5 minutes for a so called hot-start. The denaturation step is the first regular cycling event that consists of heating to 94C for 20-30 seconds resulting in DNA template and primer melting by disrupting hydrogen bonds between complementary bases and yields single strands of DNA. During the subsequent annealing the temperature is lowered to 50-65°C for 20-40 seconds allowing annealing of the primers to the single-stranded DNA template. Typically the annealing temperature is about 3-5 degrees Celsius below the Tm of the primers used. The polymerase binds to the primer-template hybrid and begins DNA synthesis. In the extension phase the temperature is increased to the optimum activity temperature of about 72C for Taq. At this step the DNA polymerase synthesizes a new DNA strand complementary to the DNA template strand by adding dNTPs that are complementary to the template in 5' to 3' direction, condensing the 5'-phosphate group of the dNTPs with the 3'-hydroxyl group at the end of the nascent (extending) DNA strand. The extension time depends both on the DNA

polymerase used and on the length of the DNA fragment to be amplified (typically 1000 bases/minute). Because the amount of DNA target is doubled each cycle the amplification is exponential. During final elongation at 70-74°C for 5-15 minutes, the remaining single-stranded DNA is fully extended. Usually a final hold at 4C is added after this for short-term storage.

7.2.1.5. DNA Sequencing

DNA sequencing is the process of determining the nucleotide order of a given DNA fragment. The classical technique developed by Frederick Sanger uses sequence-specific termination of a DNA synthesis reaction using modified nucleotide substrates. Sequencing is initiated at a specific site on the template DNA by using a short oligonucleotide 'primer' complementary to the template at that region and extended using a DNA polymerase. The sequencing reaction contains the four deoxynucleoside bases in addition to the primer and DNA polymerase, along with a low concentration of a chain terminating nucleotide. Limited incorporation of the chain terminating nucleotide by the DNA polymerase results in a series of related DNA fragments that are terminated only at positions where that particular nucleotide is used. The fragments are then size-separated by electrophoresis in a slab polyacrylamide gel or in a glass capillary filled with a viscous polymer. The primers used for sequencing of FIV vectors are described in the cloning history where appropriate.

7.2.1.6. FIV Vector Components

7.2.1.6.1. Glossary of Lentiviral Vector Components

The ***LTR (Long Terminal Repeat)*** comprises ***U3-R-U5*** (5'to 3') and measures 300 to 1800 base pairs composed. LTRs are located at both ends of the unintegrated and integrated proviral linear DNA. The LTRs are also found in closed circular forms of retroviral DNA that can contain one or two LTRs.

R (Repeat) is a nucleotide sequence at both ends genomic RNA that measures only 15 to 250 nucleotides. The boundaries are defined by the RNA transcription initiation and polyadenylation (AAUAAA). R is present in both LTRs between ***U3*** and ***U5***. In HIV, R is the binding site for the transactivator Tat.

U5 (Unique 5') is located between ***R*** and the primer binding site, ***PBS***. In the viral RNA genome it is only present once but in the in integrated provirus also copied to the 3' end as part of the LTR.

PBS (Primer-binding Site) is a very short sequence that usually starts with 5'TGG and measures 18 nucleotides. PBS binds tRNA and initiates reverse transcription. It therefore has to be specific to the host tRNA.

gag is one of the retroviral genes that are found in all retroviruses. It encodes the group specific antigen, Gag that is subsequently cleaved into ***matrix (MA), capsid (CA)*** and ***nucleocapsid (NC)*** that form the virus core.

The polyprotein ***pro*** is cleaved from Gag-Pro-Pol into a ***protease (PR)*** and ***dUTPase*** (DU).

pol codes for ***reverse transcriptase (RT)*** and ***integrase (IN)***.

env encodes for an envelope precursor protein that is further processed to ***surface (SU)*** and ***transmembrane (TM)*** structural proteins.

The ***SD (Splice Donor Site)*** is a site where an upstream 5' RNA is joined to the splice acceptor (SA) 3' RNA.

RRE (Rev Response Element) is a binding site for the ***Rev*** protein to aid the export of unspliced RNA from the nucleus.

The ***PPT (Polypurine Tract)*** is a purine-rich sequence of 7–18 nucleotides immediately upstream of U3 that is cleaved during reverse transcription to produce the RNA primer for synthesis of the plus (+) strand of viral DNA. Lentiviruses use an additional ***central polypurine*** tract to form a three dimensional structure that participates in nuclear import and facilitates transduction of non-dividing cells.

U3 (Unique 3') is a sequence of ~190 to 1200 nucleotides that are positioned between PPT and R near the 3′end of viral RNA and is present once in viral genome RNA but twice in viral DNA as part of the LTR. U3 contains promoter-enhancer sequences that control viral RNA transcription from the 5′LTR.

Poly (A) Tract is consists of 50–200 adenylic acid residues following the R sequence at the 3′end of the viral RNA. It is added posttranscriptionally and not encoded in the viral genome. A signal for polyadenylation (AAUAAA) is generally present about 15–20 nucleotides upstream (5′) of the site of polyadenylation within R.

The ***IR (Inverted Repeat or att site)*** are short sequences of 3 to 25 bp that form inverted repeats at the ends of the LTR providing recognition sites for the integrase.

CMV (cytomegalovirus) immediate early promoter is a strong promoter with a broad host range that functions in most eukaryotic cells.

IRES (internal ribosome entry site) allows for cap independent translation initiation in the middle of an mRNA. In vectors this allows for expression of two proteins (cap-mediated and IRES mediated) from the same transcript.

VSV-G (vesicular stomatitis virus G protein) is one of five major proteins of VSV, a member of the vesiculovirus genera of the rhabdovirus family. It enables viral entry by mediating attachment and fusion of the viral envelope with the endosomal membrane after endocytosis. It provides broad tropism and has sufficient stability to survive ultracentrifugation.

WPRE (woodchuck hepatitis virus posttranscription regulatory element) enhances transcription through an unknown mechanism

7.2.1.6.2. FIV Packaging Constructs

The first packaging construct, CF1Δenv,[1] was cloned by ***Eric M. Poeschla*** in whose laboratory I conducted my studies. It was made by blunting the AcI-BlpI fragment containing most of the viral genome into the polylinker of a human cytomegalovirus immediate early gene promoter expression plasmid and then deleting a 0.9 kb fragment of the env gene (Figure 12, Top and Middle). ***Roman Barraza*** further reduced significant overlap with cis-acting transfer vector sequences in CF1Δenv, the 5' LTR (U3, R, and U5 elements) by additionally deleting 154 nt of the FIV leader upstream of SacI, leaving 119 nt of leader upstream of gag including the interval between the major splice donor and gag. Viral sequences terminated 37 nt downstream of the second exon of Rev and most of U3 (all of R and U5 are missing) at the 3' end, the dispensable vif gene is intact. During a series of modifications, ***Roman Barraza*** deleted cis-acting sequences and unneeded viral coding sequences while preserving Gag/Pol expression. In contrast to CF1Δenv, the resulting construct, pFP93, lacks all viral leader sequences, as well as vif, and contains less residual *env* sequence (Figure 12, Bottom). At the 3' end, viral sequences terminate with the stop codon of Rev.

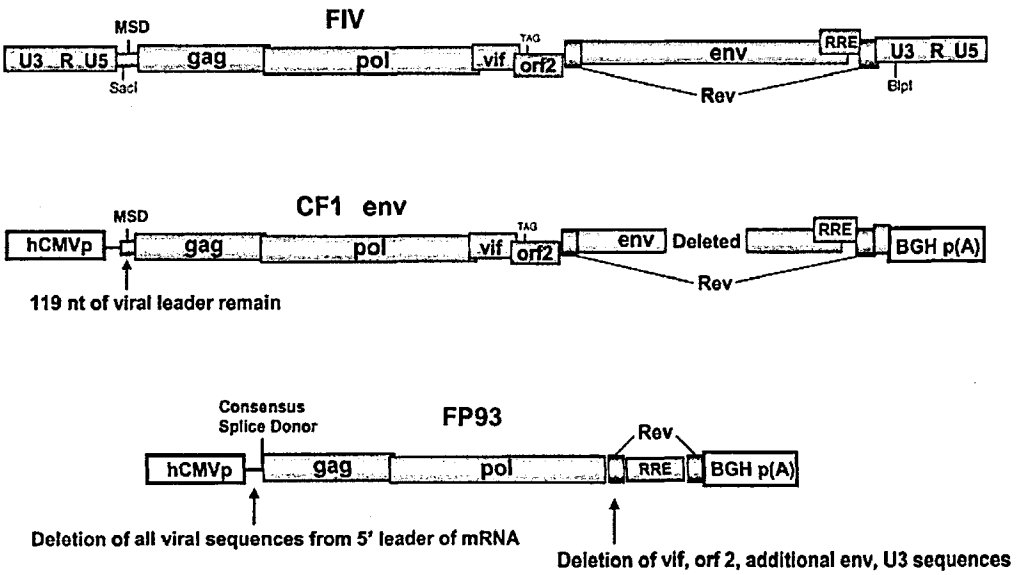

Figure 12: Genomic structure of FIV and derivative packaging constructs. Top: Genome of FIV34TF10. LTR is long terminal repeat; U3, 3'-unique region of LTR; U5, 5'-unique region of LTR; R, repeat element of LTR; SD, major splice donor; Gag, group antigen (encodes structural components of virion core particle); Pol encodes a polyprotein that is cleaved by the viral protease into the five enzymatic activities: reverse transcriptase, integrase, RNAse H, protease, and dUTPase; Vif, virion infectivity factor; SU, surface envelope glycoprotein; TM, transmembrane portion of the envelope glycoprotein; RRE, rev response element. Orf2 is open reading frame 2. The Orf2 gene product may have LTR transactivating activity similar to HIV-1 Tat. However, ORF2 is not expressed by FIV 34TF10 because of the illustrated premature stop codon, and in any case, the vector system dispenses with the promoter activity of the FIV U3 element entirely by using a CMV promoter substitution and fusion at the TATA box (explained below). Middle: First generation packaging construct pCF1delta*env*. Bottom: Second generation packaging construct pFP93. Note deletions of *vif*, *Orf2*, additional *env* sequences, and removal of all viral sequences upstream of *gag*. Deletions of *vif* and *orf 2* are attenuating to FIV in vivo.

7.2.1.6.2.1. Deletion of Leader Sequence and Nonstructural Genes

Roman Barraza replaced all FIV sequences upstream of the gag gene with a 9 nt canonical splice donor sequence. Vif, additional env, and U3 sequences were also removed. Splice donor and acceptor sites were selectively inserted between pol and rev to permit splicing.

7.2.1.6.2.2. Packaging Signal Exclusion

Iris Kemler mapped encapsidation (packaging) determinants in FIV genomic mRNA using RNAse protection.[493] Her data demonstrated that the packaging constructs lacked the necessary encapsidation determinants.

7.2.1.6.2.3. Development of Class I Integrase Mutants for Control Vectors

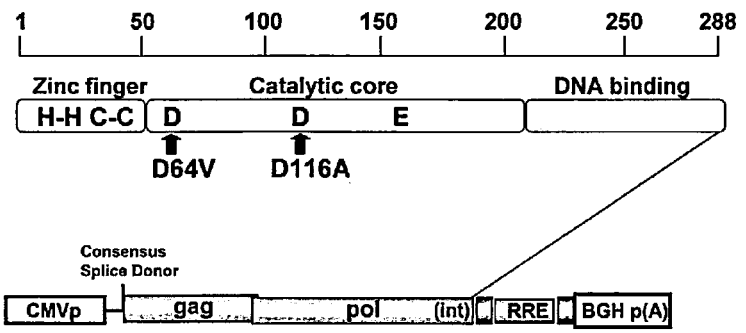

Figure 13: Class I FIV integrase mutations. The three universally conserved amino acids (D64, D116, and E152) that are required for function of the integrase catalytic center are illustrated. The aspartic acid (D) at position 64 was mutated to valine (V) by site-directed mutagenesis. Subsequently, addition of a second mutation (D116A) has been shown to preserve class I properties.

To establish that transgene expression in vivo occurs from integrated vector DNA and to provide a control for pseudotransduction, I constructed a single amino acid mutant of FIV integrase (D64V, Figure 13). Pseudotransduction is false-positive transduction caused by carryover of preformed protein present in the vector preparation. This source of artifactual transduction needs to be considered in all lentiviral vector experiments. 293T cells cotransfected with VSV-G, a vesiculating protein, can release large amounts of preformed marker gene protein into the supernatant. Generally this results in a mottled, nonuniform appearance of the target cell, but this distinction is not always reliable, and in vivo in tissues it can be hard to distinguish from genuine de novo synthesis. Although enhanced green fluorescent protein (EGFP) can occasionally produce this problem, β-galactosidase (lacZ) is more likely to confound. Two controls for pseudotransduction can be used. First, the packaging plasmid can be omitted during vector production (transfer vector and VSV-G are transfected). This "mock" vector should be processed in parallel with the real vector. The second, more elegant, control is a class I integrase mutant packaging plasmid.

The aspartic acid residue at position 64 is required for integrase catalytic activity that consists of DNA cleaving and joining. It is a universally conserved participant in the catalytic center of retroviral integrases.[732] I performed site-directed mutagenesis of FIV integrase in three steps to create a D64V-requivalent (amino acid D66V (aspartic acid to valine) in FIV), selectively integration deficient FIV vector as a control for experiments. This allowed generating control vectors that only became available at the end of the present thesis. Other controls were used in prior experiments. A 1.8 kbp integrase fragment of FIV *pol* was generated by PCR using FIV packaging plasmid CF1Δenv,[1] as the template using sense primer 5'-ATATACTAGTTCTAGAGAAGCCTGGGAATC-3' and antisense primer 5'-ATATGAATTCTCCGGAGGTAGCCTAG-3'. The restriction sites EcoRI and SpeI introduced by these primers were then used to subclone the integrase fragment into pCI (Promega, Madison, WI). The GAT encoding aspartic acid at position 66 of the integrase was changed to GTA (valine) by mutagenesis (QuikChange, Stratagene, La Jolla, CA) with sense primer 5'-GCCTGGTATCTGGCAAATGGTATGCACACACTTTGATGGC-3' and antisense primer 5'-GCCATCAAAGTGTGTGCATACCATTTGCCAGATACCAGGC-3'. The mutation, and lack of introduction of inadvertent second-site mutations in the insert, was confirmed by sequencing. Finally, the fragment was excised with internal BspE1 and Bsu36I sites and ligated between BspE1 and Bsu36I in CF1Δenv to form packaging plasmid CF1Δenv.D66V. RT activity was determined in triplicate for both CT25 and the integrase mutant CT25.D66V.[76] Experiments were conducted with equal RT units of each vector. The measurements or RT activity were carried out by **Dyana T. Saenz** and **Mary Peretz**.

7.2.1.6.3. FIV Transfer Vectors

Eric Poeschla found in his first studies of FIV vectors that fusion of the hCMV promoter to the R repeat permitted high-level expression of FIV proteins and production of infectious virus in human cells.[1, 261] This hybrid LTR is the basis of all other transfer vectors that I will describe in the following.

7.2.1.6.3.1. Minimal Packaging Signal Inclusion

Complementary to the packaging construct changes, only 311 nt of the 1353 bp of gag were included in the transfer vector to reduce potential recombination with the packaging plasmid. I minimized gag by following analogy to other lentiviral vectors and found them to be fully functional in preliminary transduction experiments. ***Iris Kemler*** subsequently investigated encapsidation requirements of FIV and established that a smaller gag fragment enhanced encapsidation compared to the original vector.[493]

7.2.1.6.3.2. Central DNA Flap

Todd Whitwam demonstrated that the FIV central polypurine tract (cPPT) and central termination sequence (CTS) act as cis-acting elements[492] as seen in other lentiviruses to enhance transduction of non-dividing cells or progenitor cells.[249] This feature has only a relatively small impact on FIV vector performance however its presence suggests some evolutionary advantage and was maintained in FIV vectors since its discovery to match other current lentiviral vectors systems. Todd Whitwam has to be acknowledged for integrating the cPPT and CTS into FIV vectors that I later used in my studies.

Todd Whitwam inserted the central polypurine tract (cPPT) into pCT26 by PCR amplifying the cPPT-CTS from FIV 34 Tf10 with sense primer 5'-aaaaCCTTCAAGAGGctgcagaaacaacctccttggataatgcc- 3' and antisense primer 5'-atataCCTTCAAGAGGtctagactctccttatgtgtctcctagg-3'. The cPPT-CTS combination is also referred to as the central DNA flap, because the strand initiations and terminations that occur at these loci result in a triple stranded DNA flap structure at the completion of FIV reverse transcription. The amplicon was blunted into the EcoNI site of pCT25 downstream of the RRE. CT26 therefore contains, from 5' to 3', the hybrid promoter, R repeat, U5, leader, 311 bp of gag, RRE, central DNA flap, human CMV immediate early promoter lacZ, and 3' LTR.

7.2.1.6.3.3. Woodchuck Hepatitis Virus Posttranscriptional Regulatory Element (WPRE)

The woodchuck hepatitis virus posttranscriptional regulatory element (WPRE) is an RNA transport element that enhances transgene expression[733, 734] I inserted it

upstream of the polypurine tract at the 3'-LTR by sticky-end cloning into a single ClaI site using the WPRE flanking ClaI sites. WPRE was derived from plasmid pCLNTluc-W[734] which contained WPRE flanked by two ClaI sites of plasmid pCLNCX after substituting a *Bam*HI-*Hin*dIII thymidine kinase (TK)-luciferase cassette for the CMV promoter.[735]

7.2.1.6.3.4. Plasmid Construction of eGFP and β-galactosidase FIV Transfer Vectors

β-galactosidase expressing ***CT25***[504] contains, in series from 59 to 39, the hybrid U3-substituted promoter of pCT5;[1] the FIV R repeat, U5 element, and leader sequence; the first 311 bp of the gag open reading frame (ORF); the Rev response element; an internal cytomegalovirus (CMV)-lacZ cassette; and the 39 long terminal repeat (LTR).

pCT25, a lacZ transfer vector, was parental to a sequentially constructed series of eGFP-containing plasmids eventuating in ***pGiNWF***: pGiN (also called CT25.eGFP.ires.neo), pGiNW, pGiNWcPPT-CTS, and pGiNWF. To first construct pGiN, peGFP-1 (BDE Biosciences-Clontech, Palo Alto, CA) was cleaved with NotI, blunted with Klenow fragment, and then cleaved with BamHI. The resultant 0.74-kb fragment was inserted into an MLV retroviral vector between BamHI and HpaI, yielding the EcoRI-containing sequence GCGGCCAACGAATTC at the 3'- junction. This eGFP insert was then excised with BamHI and EcoRI and inserted into the BamHI-EcoRI–cleaved backbone of pCT25, thus replacing lacZ and generating pCT25.eGFP.

A 1.49-kb Sal-Nhe fragment containing the internal ribosome entry site and neoR gene from pJZ30814 was then inserted by blunt-end ligation into the EcoRI site of pCT25.eGFP, generating ***pGiN*** (pCT25.egfp. ires.neo).

pGinW was constructed by inserting the WPRE by blunt insertion of an EcoRV-XhoI fragment of pBluescriptIISK'WPRE-B1112 into the BspEI site of pGiN (yielding a regenerated BspEI site that is blocked by dam methylation). Finally, the central DNA flap was inserted in several steps as follows. A 279-nt amplicon containing the FIV cPPT-CTS was synthesized by PCR, by using a sense primer tailed with a BstBI site (5'-

ATATTTCGAATCAAATCAAACTAATAAAGTATGTATTGTGAAACAACCTC CTTGGATAATGCC- 3') and an antisense primer tailed with an Xba site (5'-ATATACCTCTTTTAGGTCTAGACTCTCATGTGTCTCCTAGG- 3'). The sense primer fuses the cPPT with the 3' end of the FIV RRE and deletes an unneeded splice acceptor. This BstB1-Xba amplicon was inserted into the corresponding sites of pGiNW, generating pGiNWcPPT-CTS. The latter maneuver removed the internal CMV promoter from pGinW and inserted the cPPT-CTS. To restore this promoter, the BamHI-XhoI fragment of pGiNW was inserted into the XhoI-BamHI backbone of pCR2.1 (Invitrogen, San Diego, CA). An XbaI linker (GCTCTAGAGC) was inserted into the Klenow-treated AflII site of this intermediate plasmid, and the 614-nt XbaI-XbaI fragment was then inserted into the Xba site of pGiNWcPPT-CTS, generating pGiNWF. GiNWF contains, from 5' to 3', a hybrid U3-substituted promoter derived from pCT5,[1] the FIV R repeat, U5 element, leader sequence, the first 311-bp of the gag gene, the Rev response element (RRE, nucleotides 8537–8952 of the FIV 34TF10 genome), a sequence (FIV nt 4904–5191) containing the FIV central polypurine tract (cPPT), and the central termination sequence (CTS), the CMVp, eGFP, an internal ribosomal entry site (IRES) neoR, the woodchuck hepatitis virus posttranscriptional regulatory element (WPRE),12 and the 3' long terminal repeat (LTR).

7.2.1.6.3.5. Bi-cistronic Vectors Utilizing an Internal Ribosomal Entry Site (IRES)

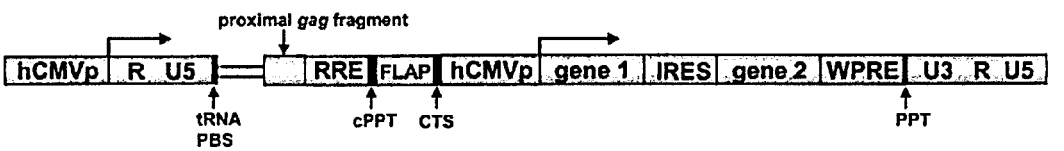

Figure 14: Second-generation bicistronic transfer vector. The central DNA flap[492] and WPRE[733] have been inserted, and *gag* has been reduced to 311 nt.

I created a bi-cistronic expression cassette was created that contains an internal ribosomal entry site (IRES), a picornavirus element that mediates cap-independent translation (Figure 14). The choice of transgene position influences the expression level achievable and is typically between 10 to 20-fold lower from the second position than from the first position when a standard ECMV IRES is used.[736]

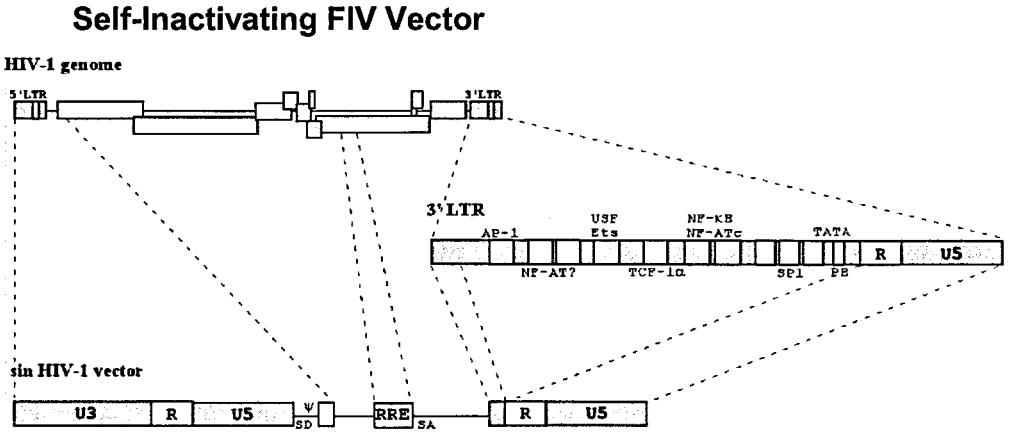

Figure 15: HIV vector with self-inactivating (SIN) LTR modification (after ref. [737]).

In parallel to HIV vectors,[737-740] I constructed a new series of FIV SIN vectors by deleting 172 bp in the U3 region of the 3' LTR, including the TATA box and binding sites for transcription factors (NFκB, NF-ATc, SP1) (**Figure 15**). Self-inactivating (SIN) lentiviral vectors improve significantly the biosafety by reducing the likelihood that replication competent retroviruses will originate in the vector producer and target cells. Although FIV LTR promoter function is minimal in non-feline cells, any residual promoter activity from either 5'- or 3'-LTR should be avoided. While 3'-LTR promoter activity could lead to expression of open reading frames downstream of the insertion site, 5'-LTR promoter activity may generate antigenic peptides from Δgag. The U3 deletion of the 3'-LTR SIN design is copied to the 5'-LTR during reverse transcription and inactivates both LTRs of the integrated vector (**Figure 7**).

pFSIN-MCS, a minimal FIV SIN vector with a large multiple cloning site and only 230 bp of *gag* was generated as follows: pGINWF served as the template to delete 171 bp of the 3'-U3 by overlapping primer extension. A first PCRs amplified the WPRE and the most 5' part of the 3'-U3 (first PCR sense primer: 5'-tatatctagatccggatcaagcttatcg-3' and antisense primer 5'-CACTGGTTAGCTAGCTTCAGGGTTCCAATACTCATCCC-3') and a second PCR amplified the most 3' part of the 3'-U3, R, and U5 (second PCR sense primer 5'-ccctgaagctagcgtgctttgtgaaacttcgaggagt-3' and antisense primer 5'-TATAAAGCTCTCGACGC-3'; bold = overlap). PCR products were then combined and amplified with the most 5' and 3' primer to complete the deletion by fusion in a third PCR. The final product was digested with XbaI and NotI and cloned into pGINWF-G230 (pGINWF with only 230bp gag) to form FSIN. A directly synthesized

multiple cloning site (MCS) of 90 bp length with 19 unique restriction sites was then inserted into the XbaI and BspeI sites of pFSIN generating pFSIN-MCS. The eGFP cassette of pGINWF was subsequently cloned into this vector and used for studies in cats.

7.2.1.6.4. Retroviral Transfer Vectors for Outflow Tract and Retinal Experiments

Two lentiviral vectors (FIV based and HIV-1 based), an MuLV vector (LZRNL),[462] and an adenoviral vector[741] were evaluated. Vesicular stomatitis virus glycoprotein G (VSV-G) pseudotypes for FIV, HIV, and MuLV lacZ vectors were prepared by transient plasmid transfection as previously described.[1, 462] Plasmids used to generate FIV vectors were a minimal transfer vector (pCT25), packaging construct pCF1Δenv,[1] and a VSV-G expression construct, pCMV-G.[462] pCT25 contains, in series from 59 to 39, the hybrid U3-substituted promoter of pCT5[1]; the FIV R repeat, U5 element, and leader sequence; the first 311 bp of the gag open reading frame (ORF); the Rev response element; an internal cytomegalovirus (CMV)-lacZ cassette; and the 39 long terminal repeat (LTR). HIV-1 vectors were generated with pHR9CMVlacZ and pCMVDR8.9[240, 250] plus pCMV-G. Adenovirus lacZ vector (Ad.CMVLacZ) was prepared as described.[741]

All retroviral vectors were filtered through a 0.45-mm pore size filter, concentrated by ultracentrifugation, resuspended, centrifuged at low speed to remove particulates, and titered on CrFK cells.[1, 462] For transduction of cultured human eyes, high-titer stocks of each of the lacZ-encoding vectors were generated and adjusted to 1 x 10^8 CrFK-transducing units (TU)/ml. As a control for pseudotransduction, a mock FIV vector was prepared by transient transfection into 293T cells of the same amounts of pCT25 DNA and pCMV-G DNA used for generation of transducing vector, while omitting the packaging plasmid. Plasmid transfection efficiency was evaluated by 5-bromo-4-chloro-3-indolyl-β-D-galactopyranoside (X-Gal) staining and was greater than 80% for the transfected 293T producer cells for both mock and packaged CT25 vectors. 39-Azido-29,39-dideoxythymidine (AZT, 50 mM; Sigma, St. Louis, MO) was used as an additional control for pseudotransduction in both cultured cells and perfused eyes. Reverse transcriptase measurements with a ^{32}P based assay were performed as previously described.[1] Before normalization to 10^8 TU/ml, vector titers were 4.6 x 10^8

TU/ml for FIV, 1.2 x 10^8 TU/ml for HIV, 2.4 x 10^8 TU/ml for MuLV, and 1.1 x 10^{11} TU/ml for Ad.CMVlacZ.

7.2.1.6.5. History of Beta-Galactosidase Expressing Murine Leukemia Viral Vector LZRNL

The murine leukemia viral (MLV) vector LZRNL was a vector plasmid stably transfected into MLV packaging cell line 293GP forming the cell line 293GP-LZRNL[462] and was generously *provided by* ***J. C. Burns.*** 293GP-LZRNL cells express the Moloney *gag* and *pol* genes as well as the LZRNL MLV provirus and only need to be transfected with an envelope plasmid. The vesicular stomatitis G protein was used in my experiments for this purpose. The MLV provirus contains from 5' to 3' the MLV LTR driving lacZ (beta-galactosidase) and further RSV-neoR-LTR.[726]

7.2.1.6.6. Cloning of Human Immunodeficiency Viral Vectors

Human immunodeficiency viral vector plasmid pHR9CMVlacZ and HIV packaging plasmid PCMVDR8.9 was a generous *gift by* ***Luigi Naldini.*** PHR9CMVlacZ contains a beta-galactosidase expressing cassette driven by a CMV promoter.[240, 250] Packaging plasmid pCMVDR8.9 contains HIV gag and pol genes under control of a CMV promoter.[240, 250]

7.2.1.6.7. History of Adenoviral Vector

The adenoviral vector used in this thesis was a generous *gift by* ***Robert D. Simari*** at the Mayo Clinic. It expressed β-galactosidase directed by the same human cytomegalovirus immediate-early promoter/enhancer[742, 743] as the FIV vector used here. This adenoviral vector (Ad.CMVlacZ)[727-730] was derived from adenovirus-5 serotype and contains deletions in regions E1a spanning 1.0 to 9.2 map units and E3 spanning 78.4 to 86 map units, rendering it replication-deficient. The CMV-lacZ cassette was inserted into the E1 deletion of Ad.E1Δ that was parental to Ad.CMVlacZ.[727] Ad.CMVlacZ was a kind gift of J. Wilson[727, 728] to R. Simari and Z. Katusic.[729]

7.2.2. Cell Cultures

7.2.2.1.1. Cell Lines

7.2.2.1.1.1. 293T Cells

293T cells were readily available in the laboratory where the studies were conducted. 293T cells are a highly transfectable derivative of the 293 cell line (also known as HEK or human embryonic kidney 293 cells) into which the temperature sensitive gene for SV40 T-antigen had been inserted. Because these cells are so easily transfectable, they are the standard cell line for retroviral vector production when transient transfection is used (as opposed to inducible producer cell lines).

Historically, HEK 293 cells were generated by transformation of cultures of normal human embryonic kidney cells with sheared adenovirus 5 DNA in the laboratory of Alex Van der Eb in Leiden, Holland in the early 70s. The human embryonic kidney cells were obtained from a healthy aborted fetus and originally cultured by Van der Eb himself, and the transformation by adenovirus was performed by Frank Graham who published his findings in the late 1970s.[428] The number 293 indicates the investigator's 293rd experiment. Subsequent analysis showed that the transformation was brought about by an insert consisting of 4.5 kb from the adenoviral genome, which became incorporated into human chromosome 19.[744] For many years it was assumed that HEK 293 cells were generated by transformation of either a renal fibroblastic, endothelial or epithelial cell. Recently, Shaw et al. demonstrated that HEK 293 cells have properties of immature neurons rather than epithelial properties.[745]

On Day –1 of a respective experiment 3 x 10^6 293T cells per T75 flask, 5 x 10^7 of the above 293T cells into a CF2s or 2.5 x 10^8 per CF10. The detailed transfection protocol is discussed below.

7.2.2.1.1.2. CRFK Cells

The CRFK feline kidney cell line was established by Rees A. Crandell from the renal cortex of a 12-week-old female domestic cat.[746] These cells exhibit typical epithelial morphology and are often utilized in viral research and in the production of vaccines.

Crandell feline kidney (CrFK) cells are robust, rapidly dividing cells that experience moderate contact inhibition at high confluency resulting in slower division. These

cells were used for titration of transducing units of vector preparations and to determine vector differences upon cell cycle arrest with aphidicolin. As with other cells, 2.5 x 10^5 cells were seeded into each well of a 6-well plate one day prior to titration. On day 0, 4 h before transduction, old media was replaced with 2 mL fresh media per well.

7.2.2.1.1.3. Primary Human Trabecular Meshwork Cells

Human trabecular meshwork (TM) cells were kindly *provided by* ***Terete Borras*** who obtained them from a normal human eye at autopsy within 24 hours and treated as follows: The TM had been isolated by microdissection and digested with collagenase. Isolated cells were grown in 24-well plates for 2 weeks to near confluence in Dulbecco's modified Eagle's medium (DMEM) with 10% fetal calf serum (FCS). Doubling time was approximately 4 days.

I received a frozen vial of *human TM cells from* ***Douglas H. Johnson*** at the Mayo Clinic after these cells had been expanded by 2 passages in T25 flasks and frozen down in liquid nitrogen.

Primary human trabecular meshwork cells were treated and propagated in analogy to 293T cells except that the passage time was twice as long. These cells were used primarily to test for transduction differences of various vector types. One day prior to titration, 2.5 x 10^5 cells were seeded into each well of a 6-well plate. On day 0, 4 h before transduction, old media was replaced with 2 mL fresh media per well.

7.2.2.1.2. Culture Techniques

Cells were thawed in a 37C waterbath, washed with DMEM containing 10% FCS and antibiotic, spun down at 300 rpm for 3 minutes and seeded again in a T25 flask. Cells were grown again to confluency, DMEM was removed, cells were washed with phosphate buffered saline (PBS) and trypsinized with 1 ml of tissue culture grade trypsin for 3 minutes at 37 C in an incubator. Cells were then suspended in 8 ml of PBS, pipetted up and down while resting the tip of the pipette agains the bottom of the T25 flask to break up cell clumps. Cells were then spun down again with the above settings, supernatant was decanted and the cell pellet was suspended in DMEM with 10% FCS and antibiotic.

7.2.2.1.3. Transduction Techquiques

7.2.2.1.3.1. Transduction of Primary Human Trabecular Meshwork Cells

Cells were then transduced with 300 ml of unconcentrated supernatant containing a 2.5 x 10^6-TU/ml concentration of MuLV or FIV lacZ vectors with or without 24 hr of prior growth arrest with aphidicolin (15 mg/ml). The transduction was carried out for 6 hr before replacement with fresh medium. Aphidicolin (15 mg/ml) was maintained in all media overlying growth-arrested cells throughout the experiment, and was replenished daily until fixation and staining for β-galactosidase activity at 48 hr after transduction. G1/S growth arrest was verified by flow cytometric analysis with propidium iodide. Percent transduction was calculated by counting 10 visual fields per well at 340 magnification. No background β-galactosidase activity was detected in TM cells at any time point.

7.2.2.1.3.2. Cultured TM Cell Transduction

Primary human TM cells (***gift of T. Borras***, University of North Carolina Chapel Hill) were transduced with an escalating multiplicity of infection (m.o.i) of GINWF to test for potential GFP toxicity in vitro prior to in vivo experimentation. Doses were chosen to have an equivalent m.o.i to that in a feline eye injected with a bolus of 10^6, 10^7, 10^8 and 10^9 TU.[747, 748] The medium was replaced weekly and TM cell layers were photographed (Nikon Coolpix 990 and Nikon Eclipse TE300, Nikon, Melville, NY) at the experimental endpoint of one month.

7.2.2.1.3.3. Human Eyes

Pairs of human eyes were obtained from the Minnesota Lions Eye Bank (Minneapolis, MN). Eyes were from individuals without any known eye disease (median age, 65 years) and were cultured within 36 hr of death. Eyes were sectioned along the equator, dissected to remove retina, iris, and lens, and cultured as described previously.[731] Briefly, the sectioned specimens were sealed at the equator into a custom-built culture vessel as shown (**Figure 17**). The culture vessel was placed in an incubator (37°C, 5% CO2), and connected to a microinfusion pump that perfused the eye with medium at the normal human anterior chamber rate of 2.5 ml/min. A dose of 1 x 10^8 TU, or a range of doses for the dose–response experiments, was injected as a

bolus into the afferent perfusate. AZT (50 mM) was included in the perfusate in some control experiments. Generally, eyes were cultured for 3 to 21 days. For the initial characterization of transduction by FIV, HIV, MuLV, adenoviral, and mock vectors, all eyes were injected and perfused with a randomly assigned vector, whereas the fellow eye was not injected and served as a control for potential endogenous β-galactosidase activity. Pairwise comparisons of FIV to MuLV vector and of FIV to HIV vector were performed, using the left and right fellow eyes of human donors. Three pairs of randomly assigned eyes were transduced by injection of 1×10^8 TU of FIV vector in one eye and 1×10^8 TU of MuLV vector in the other eye of the pair, and three pairs were transduced in a separate experimental set with 1×10^8 TU of FIV and HIV vector, respectively. Eyes were fixed and stained for β-galactosidase activity on day 7 after transduction. The ratio of transduced to total TM cells was determined by counting all TM cells in each of four sections per eye (one from each quadrant).

7.2.2.2. Trypsinizing Cells

In order to propagate cells, media of established cell cultures in T75 bottles were removed by vacuum aspiration and washed twice with 5 ml of phosphate buffered saline (PBS). 2.5 ml trypsin solution was added and evenly spread across the cell monolayer by tilting. The culture bottles were placed back into the incubator to provide the ideal temperature for the enzymatic action of trypsin. At about 3 minutes the culture bottle was removed from the incubator, rocked to dislodge adherent cells, placed back in the incubator and trypsinization allowed to continue for another 2 minutes. Bottles were removed from the incubator and opened in the tissue culture hood. The cell suspension was aspirated with an automatic pipette and forcefully ejected while creating a moderate seal with the counter pressure from the wall at the bottle end to break up remaining cell clumps that had not completely trypsinized. A volume of 7.5 ml Dulbecco's modified Eagle medium with 10% fetal calf serum (DMEM-10), penicillin G sodium 100 units/mL, streptomycin sulfate 100 µg/mL and L-glutamine 2 mM (DMEM) was added to stop trypsinization and provide appropriate culture environment.

7.2.2.3. Counting Cells

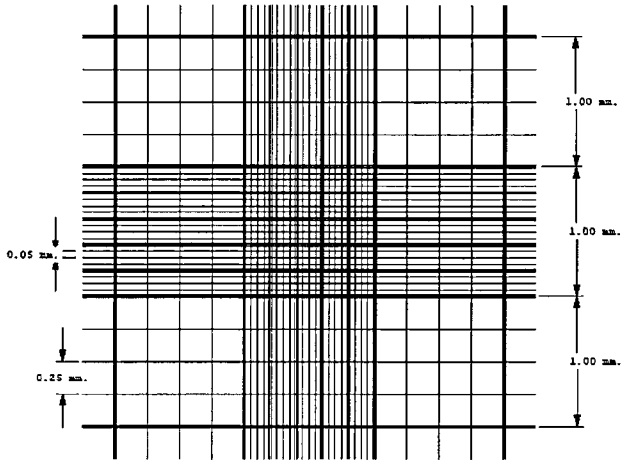

Figure 16: Hematocytometer counting chamber. Rulings cover 9 square millimeters. Boundary lines of the Neubauer ruling are the center lines of the groups of three. (These are indicated in the illustration below.) The central square millimeter is ruled into 25 groups of 16 small squares, each group separated by triple lines, the middle one of which is the boundary. The ruled surface is 0.10mm below the cover glass, so that the volume over each of the 16 small squares is .00025 cubic mm.

After trypsinization as described above, suspended cells were counted with an improved Neubauer hemocytometer (cat. No. 3100, Hausser Scientific, Horsham, PA, USA) and a counter. This device has two separate cell counting areas, one of which is shown above (Figure 16). The volume above each square contains 0.1 mm^3 of sample when covered by a cover slip (1 x 1 x 0.1 mm^3). A cover slip mounts on two ground glass bars to form the top of the two chambers. The cell suspension that had to be counted was transferred to each chamber with a pipette resulting in the suspension being drawn into the chamber by capillary action. For proper counting both sides of the chamber have to be filled and counted. Fine rulings on the floor of each chamber provide grids to help count the number of cells in suspension. There are nine large squares on each side of the hemocytometer. Cells were counted in three big squares. The number of cells per milliliter was calculated as the average number per square times 10^4. Cells that were lying at the top and left hand lines of each box were included in the count but not the ones on the lower and right hand line. On average, 100 to 300 cells were counted per chamber to increase accuracy. The same procedure was repeated in the second chamber. The appropriate volume was then added to the desired culture vessel and filled up with DMEM to the recommended volume as described below.

7.2.2.4. Seeding and Growing Cells

7.2.2.4.1. 293T Cell Cultures for Retroviral Vector Production by Transfection

1. 293T cells.
2. Adherent fibro-epithelial cell lines for titration: CrFK cells.
3. Dulbecco's modified Eagle medium with 10% fetal calf serum (DMEM-10), penicillin G sodium 100 units/mL, streptomycin sulfate 100 µg/mL and L-glutamine 2 mM.
4. Trypsin, tissue culture grade.
5. PBS (phosphate-buffered saline), tissue culture grade.
6. Distilled water, sterile.
7. 70% isopropanol or ethanol.
8. 37°C humidified incubators, 5% CO2.
9. Nikon Coolpix 990 camera for digital image capture (Nikon, Melville, NY)
10. Nikon Eclipse TE300 microscope (Nikon, Melville, NY)

7.2.2.4.1.1. T75Flask

On Day –1 of a respective experiment 3 x 10^6 293T cells per T75 flask were seeded. On day 0, 4 h before transfection, old media was replaced with 10 mL fresh media

7.2.2.4.1.2. Cell Factory CF2

1. Day –4: CF2: seeding each of 4 T75 flasks with 3 x 10^6 293T cells.

2. Day –2: Trypsinizing and seeding a CF2 with 5 x 10^7 of the above 293T cells.

3. Day –1: Trypsinizing and reseeding 5 x 10^7 of the above 293T cells into a CF2s. If desired and if full doubling occurred over from day –2 to day –1, a second CF2 can be seeded.

4. Day 0: Transfection.

7.2.2.4.1.3. Cell Factory CF10

1. Day –6: Seeding of 4 x 10^6 293T cells into each of 4 T75 flasks.

2. Day –4: Trypsinizing and seeding 6.3 x 10^7 of the above 293T cells into a CF2.

3. Day –2: Trypsinizing and seeding a CF10 with 2.5 x 10^8 of the above 293T cells.

4. Day –1: Trypsinizing the CF10 and reseeding 2.5 x 10^8 of these 293T cells into the same CF10 (i.e., the original CF10 is reused).

5. Day 0: Transfection.

7.2.2.4.2. Human Ocular Anterior Segment Cultures

Human donor eyes from the local eye bank

Custom made anterior chamber segment perfusion equipment as described by Douglas H. Johnson[731] consisting of:

1. Bottom chamber
2. Scleral sealing ring
3. Cover
4. Perfusion tubing
5. Pressure transducer
6. Pressure recording software
7. Microperfusion pump

7.2.3. Generation of Vectors

7.2.3.1. Feline Immunodeficiency Virus Vectors

I generated replication defective feline immunodeficiency viral (FIV) vectors with the technical help of ***Mary Peretz*** and ***Wu-Lin Teo***. Several different derivatives were created in the course of this thesis as detailed in the cloning history. Plasmids used to generate initial FIV vectors were a minimal transfer vector (pCT25), packaging construct pCF1Δenv,[1] and a VSV-G expression construct, pCMV-G.[462] pCT25 contains, in series from 59 to 39, the hybrid U3-substituted promoter of pCT5[1]; the FIV R repeat, U5 element, and leader sequence; the first 311 bp of the gag open reading frame (ORF); the Rev response element; an internal cytomegalovirus (CMV)-lacZ cassette; and the 39 long terminal repeat (LTR).

7.2.3.1.1. Transfection

The amount of DNA was adjusted to 1 µg pCMV-G[462], 3 µg of pCT25[504] and 3 µg of packaging plasmid pCF1Δenv.[1] The volume was brought to 800 µl with 0.01 M Tris-HCl (pH 8.0) and 800 µl of 2.5 M $CaCl_2$ were added while vortexing at middle speed. The mix was allowed to precipitate for exactly 3 min and then pipetted at once into media pooled at the end of the tilted T75. Further mixing was achieved by turning the tilted flask back and forth around its longitudinal axis without dislodging cells. Bottles were placed in incubators and left undisturbed until the medium was changed 18 h later.

7.2.3.1.2. Harvest

Supernatants were collected 48 h after removal of the transfection mix, filtered through a 0.22-µm filter and aliquoted into cryovials. Aliquots were frozen at -80 C.

7.2.3.2. Feline Immunodeficiency Virus Mock Vectors

Mock vectors are not vector particles but allow comparing true transduction with proteins expressed from transduced genes to proteins that are present in the collected supernatants. A false positive result from unintentionally transferred of proteins is also known as pseudotransduction. Mock vectors were made with omission of packaging plasmids. Because there negligible transduction of trabecular meshwork cells in vitro or in ex vivo organ cultures, no mock vectors were needed in the experiments discussed below. HIV mock vectors were not generated because no pseudotransduction was found with FIV mock vectors and studies were designed to compare FIV to HIV mediated transduction while excluding pseudotransduction. Experiments also had to be designed with a limited number of human donor eyes.

7.2.3.2.1. Transfection

The amount of DNA was adjusted to 1 µg pCMV-G[462], 3 µg of pCT25[504] while packaging plasmid pCF1Δenv,[1] was left out. The volume was brought to 800 µl with 0.01 M Tris-HCl (pH 8.0) and 800 µl of 2.5 M $CaCl_2$ were added while vortexing at middle speed. The mix was allowed to precipitate for exactly 3 min and then pipetted at once into media pooled at the end of the tilted T75. Further mixing was achieved by

turning the tilted flask back and forth around its longitudinal axis without dislodging cells. Bottles were placed in incubators and left undisturbed until the medium was changed 18 h later.

7.2.3.2.2. Harvest

Supernatants were collected 48 h after removal of the transfection mix, filtered through a 0.22-μm filter and aliquoted into cryovials. Aliquots were frozen at -80 C.

7.2.3.3. Adenovirus Vectors

The adenoviral vector used in this study was a generous gift by ***Robert D. Simari.*** It was generated as described before.[749, 750] Briefly, subconfluent 293 cells were infected with crude viral lysate, the supernatant was collected and purified twice by cesium chloride ultracentrifugation. The viral band was collected and desalted by dialysis, equilibrated with 0.01 M Tris pH 8, 0.01 M MgCl2 and 10% glycerol. Viral titers were determined and recorded as transducing units by infecting Crandell feline kidney (CrFK) cells. The absence of replication-competent virus was confirmed by testing the vector preparation on 293 cells at a multiplicity of infection of 10.

7.2.3.4. Murine Leukemia Virus Vectors

I generated beta-galactosidase expressing murine leukemia virus (MLV) vector LZRNL[462] as published[462, 504] and detailed in the following. ***Mary Peretz*** provided technical assistance with vector production. All materials as listed in the materials and reagents section were present in ***Eric Poeschla's*** laboratory where I conducted my studies.

7.2.3.4.1. Transfection

The amount of DNA of VSV-G expressing plasmid was adjusted to 1 μg. The volume was brought to 800 μl with 0.01 M Tris-HCl (pH 8.0) and 800 μl of 2.5 M $CaCl_2$ were added while vortexing at middle speed. The mix was allowed to precipitate for exactly 3 min and then pipetted at once into media pooled at the end of the tilted T75. Further mixing was achieved by turning the tilted flask back and forth around its longitudinal

axis without dislodging cells. Bottles were placed in incubators and left undisturbed until the medium was changed 18 h later.

7.2.3.4.2. Harvest

Supernatants were collected 48 h after removal of the transfection mix, filtered through a 0.22-μm filter and aliquoted into cryovials. Aliquots were frozen at -80 C.

7.2.3.5. Human Immunodeficiency Virus Vectors

I produced the replication defective human immunodeficiency viral (HIV) vectors[240, 250] with the technical help of ***Mary Peretz***. Production was similar to that of MLV and HIV vectors.

7.2.3.5.1. Transfection

The amount of DNA was adjusted to 1 μg pCMV-G[462], 3 μg of pHR9CMVlacZ[240, 250] and 3 μg of packaging plasmid pCMVDR8.9.[240, 250] The volume was brought to 800 μl with 0.01 M Tris-HCl (pH 8.0) and 800 μl of 2.5 M $CaCl_2$ were added while vortexing at middle speed. The mix was allowed to precipitate for exactly 3 min and then pipetted at once into media pooled at the end of the tilted T75. Further mixing was achieved by turning the tilted flask back and forth around its longitudinal axis without dislodging cells. Bottles were placed in incubators and left undisturbed until the medium was changed 18 h later.

7.2.3.5.2. Harvest

Supernatants were collected 48 h after removal of the transfection mix, filtered through a 0.22-μm filter and aliquoted into cryovials. Aliquots were frozen at -80 C.

7.2.4. Scaled-up Lentiviral Vector Production

Use of larger animals in the course of this thesis required larger volumes of vector and made development of a protocol for scaled up lentiviral vector production necessary. I established this protocol with the technical help of ***Wu-Lin Teo*** which has been

published.[321] Depending on the amount of vectors needed, either larger volume cell factories (CF10) were used or smaller ones (CF2).

7.2.4.1. Production of High-Titer FIV Vector Stocks by Transient Transfection of 293T Cells

7.2.4.1.1. Transfection and Vector Production

1. I adjusted the DNA amount of the three plasmids pMD.G/pFP93/pGINWF to a ratio of 1/3/3. For CF10, use 84.5/253.5/253.5 μg in a 500-mL sterile plastic bottle, bring volume to 60.5 mL with 0.01 M Tris-HCl (pH 8.0), add 6.5 mL of 2.5 M CaCl2, and mix by bubbling air into transfection mix with pipette. For CF2, use 16.9/50.7/50.7 μg in a 250-mL sterile plastic bottle, brought volume to 12.1 mL with 0.01 M Tris-HCl (pH 8.0), add 1.3 mL of 2.5 M CaCl2, and bubbled with pipette.

2. I tilted the bottle to gather contents in corner of bottle and added 67 mL (CF10) or 13.4 mL (CF2) of 2X HBS by rapid pipetting. Bubbled air through the mix and shake for 10 s. Vortexing was found to be less desirable because contents were not mixed immediately. Set aside and let precipitate for exactly 3 min. I found that small DNA amounts used in this protocol resulted in fewer condensation nuclei during precipitation and faster growth of crystals than large DNA amounts.

3. While the precipitation continued, I emptied Cell Factory into waste beaker, wiped inlets again with 70% ethanol-soaked Kimwipe, and connect loading bottle with silicon tube and connector to Cell Factory. Filled loading bottle with 100 mL of fresh culture media per layer (total of 1000 mL in CF10 or 200 mL in CF2) without letting media run into Cell Factory.

4. At 3 min, stopped precipitation by pouring transfection mix straight into media in loading bottle. Shook and bubbled vigorously for even distribution.

5. I placed the Cell Factory on its side and filled by elevating loading bottle. Made sure chambers of Cell Factory contain equal media levels; lifted Cell Factory at connector end while still placed on side to prevent media of upper chambers from leaking into lower chambers. Rolled back into horizontal orientation. Put Cell Factory back into incubator in a precisely horizontal orientation.

6. Removed media 18 h later and replaced with fresh media.

7.2.4.1.2. Vector Harvest

1. On day 3, i.e., 48 h after replacement of transfection mixed with fresh media, collected supernatant in large beaker, stirred, and let sit for 3 min to allow detached cells to settle.

2. Filtered through 0.22-μm filter into 500-mL filter units. Aliquoted filtered vector supernatant into appropriate number of 1.8-mL cryovials.

7.2.4.2. Concentration by Large Volume Ultracentrifugation

Generation of larger volumes of vector required new ways of concentration. Therefore, I developed a fixed, large volume rotor protocol. This was done by extrapolating and estimating parameters from the swinging bucket rotor concentration protocol.

1. I washed insides of 250-mL centrifuge buckets and lids with 70% ethanol. Aspirated dry with vacuum. Always filled buckets to top mark and used additional PBS if necessary. Balanced tubes on scale together with lids and closed tightly.
2. Spun at 67,000g_{rmax} for 6 h at 4°C. A brownish vector pellet was visible at the outer bottom rim of the bucket.
3. Decanted buckets, placed on ice at 45° angle with pellet pointing upward, let sit on ice for 2 min, and sucked up collected liquid at bottom. Rotated pellet to bottom and add 5 mL PBS if two rounds of concentration were planned. Used smaller volume if only one round of centrifugation is desired.
4. Started re-suspension with 5-mL pipette by washing down the whole outer wall to which pellet was attached, along with the entire bottom and the outer rim. Directed the wash jet toward the pellet. This process took more than 5 min per bucket. Undispersed fragments are pipetted into 25-mL tubes for second round of concentration together with fully dispersed vector.
5. Washed insides of 36-mL centrifuge tubes, as well as buckets and lids of swinging bucket rotor with 70% ethanol. Sucked dry with vacuum. Filled buckets to the maximum level with resuspended vector from first round.

Added PBS if necessary. Balanced tubes on scale together with lids and closed tightly.

6. Spun at 67,000g_{rmax}, 31,000g_{rmin} for 1 h 30 min at 4°C. A brown vector pellet was visible at the bottom of the bucket.
7. Resuspended pellet in 500 µl PBS by washing the entire bottom with jets for 5 min. Set pipette to 250 µL and kept tip submerged to prevent bubbles and foam. Pipetted resuspended vector into 1.5-mL microcentrifuge tube and spun for 3 min at 3000g to remove large unsuspended particles.
8. Aliquoted vector in 50-µL fractions in tubes with narrow bottoms; freeze at –80°C.
9. Washed Cell Factories twice with dH2O inside the hood. Seal and store at 4°C if reuse was desired for production of same vector in next days.

7.2.5. Titration of Transducing Units

1. I seeded 2.5 x 10^5 CrFK into each well of a 6-well plate.

2. Twenty-four hours later, thawed vector stocks and made 10-fold serial dilutions.

3. Removed media from 6-well plate and added each mixture to a well of the 6-well plate, either changing the tip each time or moving from most dilute to least dilute. Left one well untransduced as a control.

4. After 6 h, replaced supernatant with fresh media.

7.2.5.1. Enhanced (eGFP) and Renilia (rGFP) Green Fluorescent Protein Transducing Units

CrFK and TM cells were transduced as described above with enhanced (eGFP) or Renilla (rGFP) green fluorescent protein expressing vectors. Cells were trypsinized 48 h after start of transduction following the same protocol as for "Seeding and Growing Cells", washed with PBS, resuspended in PBS, and fixed with 1% formalin in PBS. The suspension was analyzed for the percentage of transduced cells with fluorescence-activated cell sorter flow cytometry (FACS).

7.2.5.2. Beta-Galactosidase Transducing Units

48 h after transduction, fixed cells with 1% glutaraldehyde for 3 min, washed with PBS, and incubated overnight at 37°C with 5-bromo-4-chloro- 3-indoxyl-β-D-galactopyranoside (X-Gal) staining solution. Washed once with PBS and replaced with 1% glutaraldehyde. Used a transparent 2-mm x 2-mm-square counting grid and determined number of squares per well. Counted positive foci in 10 random squares at 100x magnification and determined the number of positive colonies per well. Multiplied count by dilution factor to obtain TU/mL. E.g. for a volume of 1 mL the titer = total number of β-galactosidase positive colonies per well x dilution factor = transducing units per milliliter.

7.2.6. In Vitro and Ex Vivo Methods

7.2.6.1. In Vitro Human Trabecular Meshwork Cells

Human trabecular meshwork (TM) cells (***gift from T. Borras***) were derived from a normal human eye obtained at autopsy and seeded as described above. Transduction was carried out for 6 hr before replacement with fresh medium. Half the 6 wells with TM cells were incubated with aphidicolin (15 mg/ml) to achieve growth arrest which was maintained in all media overlying growth-arrested cells throughout the experiment. Media was replenished daily until fixation and staining for β-galactosidase activity at 48 hr after transduction. G1/S growth arrest was verified by flow cytometric analysis with propidium iodide. Percent transduction was calculated by counting 10 visual fields per well at 340-fold magnification. Beta-galactosidase staining was performed as described in the section "Titration". No background β-galactosidase activity was detected in TM cells at any time point.

For the experiments seeking to enable real-time non-invasive monitoring, GFP-expressing vectors were the principal focus. To preliminarily assess feasibility and potential toxicity of GFP expression, cultured primary human TM cells were transduced with a 4-log range of FIV vector input. Transduction was carried out for 6 hours before replacement with fresh medium and subsequently changed every 3 days. Fluorescence and viability of cells was confirmed by observation for one month with a tissue culture microscope with fluorescence equipment.

7.2.6.2. Ex Vivo Human Donor Eyes

7.2.6.2.1. Human Organ-Perfusion Culture

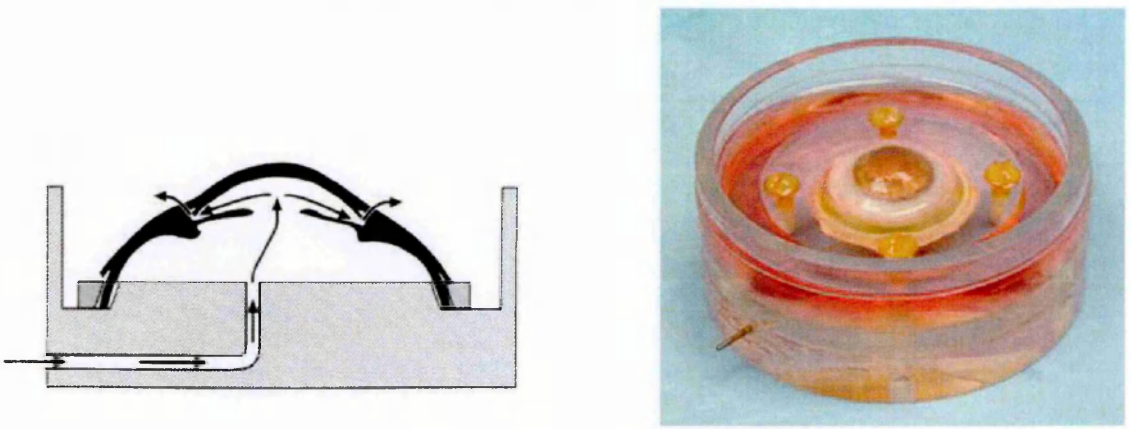

Figure 17: Anterior chamber perfusion model.[751] Left: Schematic side view. Media enters hemidisected eye centrally and exits following the natural route through the TM and episcleral veins collecting in the well surrounding the eye. A pressure transducer to measure IOP is also connected to the anterior chamber and enters from underneath (not shown). Right: Top view of open culture chamber.

The Minnesota Lions Eye Bank (Minneapolis, MN) provided pairs of human eyes. Eyes were used in accordance with Mayo Clinic Institutional Review Board guidelines and according to the tenets of the Declaration of Helsinki. All were from donors (median age, 76.5 years, $n = 6$) without known eye disease and were placed in perfusion culture within 24 hours of death, as previously described.[731, 751] In this system, a human eye is obtained shortly postmortem and hemisectioned at the equator, the entire posterior pole, retina and choroid, iris and lens are removed. The anterior half is sealed posteriorly with an apparatus that maintains the aqueous circulation with fidelity to natural parameters (**Figure 17**). Medium is perfused with DMEM and antibiotics at the physiological rate of 2.5 microliter per minute and 37 C through the anterior chamber and exits the eye through the normal conventional outflow pathway (trabecular meshwork, Schlemm's canal, collector channels, and episcleral veins). The cultures were maintained in 5% CO2 in an incubator. Eyes cultured in this fashion remain viable for up to 4 weeks, during which outflow tract structures and trabecular meshwork cells maintain normal morphology.[751] Intraocular pressure was measured every 60 seconds for 5 days and recorded as averages per hour.

7.2.6.2.2. Intraocular Application of Vectors

One anterior segment of each pair ($n = 3$) was injected with a bolus of 1 x 10^8 transduction units (TU) CT26 vector in a volume of 500 µL DMEM, and the fellow eyes received an equivalent volume of CT26 mock vector. Similarly, 1 x 10^8 TU of GiNWF vector in 500 µL DMEM was injected into one anterior segment of a pair ($n = 3$), whereas the control fellow eye received the same volume of medium without vector.

For comparison of HIV, FIV and MLV vectors, a dose of 1 x 10^8 TU, or a range of doses for the dose–response experiments, was injected as a bolus into the afferent perfusate. AZT (50 mM) was included in the perfusate in some control experiments. Generally, eyes were cultured for 3 to 21 days. For the initial characterization of transduction by FIV, HIV, MuLV, adenoviral, and mock vectors, all eyes were injected and perfused with a randomly assigned vector, whereas the fellow eye was not injected and served as a control for potential endogenous β-galactosidase activity. Pairwise comparisons of FIV to MuLV vector and of FIV to HIV vector were performed, using the left and right fellow eyes of human donors. Three pairs of randomly assigned eyes were transduced by injection of 1 x 10^8 TU of FIV vector in one eye and 1 x 10^8 TU of MuLV vector in the other eye of the pair, and three pairs were transduced in a separate experimental set with 1 x 10^8 TU of FIV and HIV vector, respectively. Eyes were fixed and stained for β-galactosidase activity on day 7 after transduction. The ratio of transduced to total TM cells was determined by counting all TM cells in each of four sections per eye (one from each quadrant).

7.2.6.2.3. Time course of Expression

To evaluate the time course of expression, the TM of eyes in the vector comparison study (FIV, HIV, MLV) was biopsied 3 days after transduction, while the eyes were kept in culture for 16 days. For this, a standard surgical trabeculectomy was performed on two quadrants 90 degrees apart on day 3. Histological assessment of the entire meshwork was done at the end of the culture period, on day 16 after transduction.

7.2.7. Tissue Processing and Marker Detection

7.2.7.1. Beta-Galactosidase Detection with the X-Gal Assay

7.2.7.1.1. X-Gal Assay in Human Eyes

Eyes were rinsed in phosphate-buffered saline (PBS) and cut into quadrants. From each quadrant, one corneoscleral wedge was taken for antibody labeling, while an adjacent wedge was fixed for 15 min in 4% paraformaldehyde, rinsed in PBS, and stained for 16 hr in X-Gal solution, rinsed with PBS, and embedded in paraffin or JB-4 plastic medium. Sections (6 mm) were obtained from unstained and stained paraffin blocks for antibody labeling. Nuclear fast red was used as a nuclear counterstain. JB4 embedding and staining was performed by ***Cindy Bahler***.

7.2.7.1.2. X-Gal Assay in Cat Eyes

Eyes of sacrificed animals that were injected with beta-galactosidase expressing FIV vector CT26 were enucleated. Only one random quadrant was removed from the anterior segment for X-Gal-staining, while the remaining 3 were used for eGFP detection because the in vivo study focused on detailed assessment of a live marker. Eyes were X-Gal stained overnight, photographed with an operating microscope (Nikon, SMZ800, and DXM 1200, ACT-1 software), and embedded in paraffin by the Histopathology Core Facility of the Mayo Clinic. Sections were counterstained with fast nuclear red.

7.2.7.1.3. X-Gal Assay in Rat Eyes

To assess gene expression for the comparison of subretinal and intravitreal injection techniques, half of the neonatal rats in each litter injected with CT25 in right eyes, were sacrificed at 2 days post-injection and the other half at 7 days post-injection. Time points 2 and 7 days were chosen because neovascularization is maximal in the ROP model during this period.[752] In the long-term expression/integration study comparing FIV WT integrase and mutant integrase vectors, 10 animals were sacrificed at 2 months, 10 animals at 3 months and the rest of 17 animals at the experimental endpoint of 7 months. After sacrifice and enucleation, eyes were fixed in 10% formalin at 4°C for 90 minutes and cornea and lens were removed. To detect expression of the marker gene, eye cups were incubated in X-gal reagent overnight at

37°C. Eyes were then send to the Histopathology core at the Mayo Clinic for paraffin embedding and counterstaining with nuclear fast red.

For cross-sectional histology of eyes transduced with FIV or adenoviral vectors, two representative pairs of eye cups from each time point were processed as above, embedded in paraffin, sectioned at 6 μm through the transduced area and counterstained with either neutral red or nuclear fast red. To assess the histology in a masked manner, all slides were examined by an ophthalmic pathologist (JDC) who was unaware of the experimental group.

7.2.7.2. Beta-Galactosidase Detection by Anti-Body Labeling

7.2.7.2.1. Antibody Labeling of Beta-Galactosidase in Human Eyes

For labeling with anti-β-galactosidase antibodies, 6- mm sections were mounted on slides at 60°C, deparaffinized with HemoD (Fisherbrand; Fisher Scientific, Pittsburgh, PA), rehydrated through stepped ethanol–water baths, and placed for 30 min into a steamer with 0.1 M piperazine-N,N9-bis(2-ethanesulfonic acid) (PIPES, pH 8.0) to maximize antigen retrieval. Nonspecific binding was blocked by a 1-hr incubation with bovine serum albumin, followed by two 5-min washes with PBS, a 1-hr incubation with a polyclonal rabbit anti-β-galactosidase antibody (Molecular Probes, Eugene, OR) at a dilution of 1:50, washing, and a 30-min incubation with a secondary photostable, pH-independent, green fluorophore-conjugated goat anti-rabbit antibody (Alexa Fluor 488, Molecular Probes; fluorescence absorption peak at 495 nm, emission peak at 539 nm) at a concentration of 1:300. A 5-min incubation with diamidinophenylindole (DAPI; Molecular Probes) was used to stain nuclei.

7.2.7.2.2. Antibody Labeling of Beta-Galactosidase in Rat eyes

In the study comparing FIV WT and integrase mutant vectors, an additional expanded litter of 25 rats was used to assess localization of transgene expression using immunohistochemistry with anti-β-galactosidase antibodies.[504] All right eyes received subretinal injections of CT25 vector as described above. Left eyes were treated as one of three controls as described above. Prefixed eyecups were soaked in 20% sucrose overnight, embedded in OCT, and snap frozen in liquid nitrogen. 10 μm cryosections

were rehydrated with PBS for 10 minutes and blocked with 3% bovine serum albumin and 0.1% Tween in PBS for 1 hour. Sections were then washed twice with PBS for 5 minutes, exposed to the primary antibody (rabbit anti-β-galactosidase antibody, Molecular Probes, A-11132) at a dilution of 1:100 in PBS for 60 minutes, washed twice with PBS for 5 minutes, incubated with the secondary antibody (goat anti-rabbit antibody Alexa Fluor 488 labeled, Molecular Probes, A-11008) at a dilution of 1:300 in PBS for 90 minutes, and washed twice for 5 minutes each in PBS. Cell nuclei were stained with a 300 nM DAPI solution in PBS.

7.2.7.3. Antibody Labeling of Enhanced Green Fluorescent Protein (EGFP)

7.2.7.3.1. Antibody Labeling of EGFP in Human Eyes

Localization and extent of expression of eGFP were confirmed with specific antibody labeling in human eyes. Six micron paraffin-embedded sections from two quadrants of each eye were deparaffinized (22-143975; Citrisolv; Fisherbrand, Fair Lawn, NJ) and rehydrated with decreasing concentrations of ethanol, and antigens were retrieved for 5 minutes in a steam chamber with piperazine-*N*-*N*'-bis(2-ethanesulfonic acid) (PIPES) buffer. Sections were incubated for 60 minutes with a primary rabbit anti-eGFP antibody (1:200 dilution, NB 600-303; Novus Biologicals, Littleton, CO) and for 30 minutes with a fluorescent phalloidin-labeled secondary goat anti-rabbit antibody (1:200 dilution, A-11088, Alexa 488; Molecular Probes). Nuclei were stained with a 1:1000 dilution of 4',6'-diamino-2-phenylindole (DAPI; D-1306; Molecular Probes).

7.2.7.3.2. Antibody Labeling of EGFP in Cat Eyes

For a more sensitive assessment of the extent of transduction with GINWF other eyes were labeled with an anti-GFP antibody following the exact same protocol as above.

7.2.7.3.3. Antibody Labeling of Feline Macrophages and T-Cells

7.2.7.3.3.1. Feline Macrophages

Anterior segment sections from cats that had developed an iritis after GFP over-expression were analyzed for presence of feline macrophages with a primary murine

anti-myeloid/histiocyte antibody (1:50 dilution, MAC 387, M0747, DAKO)[753-755] and a secondary Alexa 488-labeled goat anti-mouse antibody (1:100 dilution, A-11001, Molecular Probes). Specifically, sections were pretreated with a pre-made solution of proteinase K (DAKO, product number S3020) for 10 minutes, blocked with DAKO blocking solution (DAKO, product number S200189) and incubated with MAC 387 for 1 hour followed by washing with PBS for 5 minutes in the presence of blocking solution. Sections were then incubated with the secondary Alexa 488-labeled goat anti-mouse antibody for 1 hour followed by PBS washing for 10 minutes. MAC 387 detects the myeloid/histiocyte antigen, a calcium-binding molecule, which predominantly consists of different polypeptide chains adding up to an Mr of ~36 500 protein complex.[756] The complex contains at least two different subunits, which have molecular masses of 8 and 14 kDa.[757] It belongs to the S100 family,[757] which is a large subfamily of EF-hand proteins.[758] The myeloid/histiocyte antigen is expressed by circulating (and emigrated) neutrophils and monocytes, as well as a subset of reactive tissue macrophages and many tissue eosinophils.

7.2.7.3.3.2. Feline T-Cells

To detect feline T-cells,[753, 754, 759] sections were incubated with peroxidase-conjugated anti-CD3 (Anti-CD3/HRP, U0026, DAKO) according to manufacturer protocol. Tissue sections were deparaffinized (22-143975; Citrisolv; Fisherbrand, Fair Lawn, NJ) and rehydrated, followed by incubation with 3% hydrogen peroxide in distilled water for 5 minutes. Sections were then rinsed with Tris-buffered saline (TBS) for 5 minutes and incubated with proteinase K (DAKO, product number S3020) for 5 minutes. Sections were again rinsed in TBS for 5 minutes. Specimen were then covered with 2-3 drops of DAKO EPOS Anti-CD3/HRP and incubated for 60 minutes at room temperature. A horseradish peroxidase-labeled immunoglobulin mix (DAKO EPOS Negative Control solution, U0951) was used as a control: sections were rinsed in TBS for 5 minutes, incubated with DAKO Liquid DAB Plus (code Nos K 3467/K 3468), a chromogenic substrate solution, for 5-15 minutes. Slides were rinsed with water and counterstained and mounted with a cover slip.

Sera of cats with proven iritis infiltrate were analyzed for antibodies against GFP and VSV-G. A 10% SDS-PAGE gel with a continuous well was loaded with GFP protein produced by transient transfection of 293T cells and transferred. Membrane strips

were incubated with serum before transduction and 4 weeks after animals had developed an iritis. A rabbit anti-GFP antibody (1:1000 dilution, Novus Biologicals, NB 600-303) and a monoclonal mouse anti-VSV-glycoprotein antibody (1:1000 dilution, protein clone P5D4, C-7706, Sigma, St. Louis, MO) served as a positive control. After washing, wells with cat serum as the primary incubation were incubated with a secondary peroxidase conjugated goat anti-cat antibody (1:1000 dilution, cat. 55293, IGN Pharmaceuticals, Aurora, OH). A peroxidase conjugated goat anti-rabbit antibody (1:1000 dilution, Calbiochem, San Diego, CA) served as a secondary antibody for GFP detection and a peroxidase conjugated goat anti-mouse antibody (1:1000 dilution, Calbiochem) as the secondary antibody to the anti-VSV-G antibody. The same protocol was used to detect anti-VSV-G antibodies except that 293T cells were transfected with VSV-G expression plasmid pMD-G.

7.2.8. Animal Handling and Vector Application

7.2.8.1. Animals

All animals in used in this thesis were handled in accordance to the Institutional Animal Care and Use Committee and the ARVO Statement for the Use of Animals in Ophthalmic and Vision Research.

7.2.8.1.1. Long-Term Outflow Tract Modification in the Cat

Because the anterior chamber perfusion model is artificial in many respects, such as short viability with consequent inability to assess long-term outcomes, substitution of the complex aqueous humor with synthetic medium, and the complete lack of a systemic immune response. In rodents, the outflow tract is too rudimentary to permit robust comparisons. I therefore proceeded to assess the possibility of long-term targeted gene expression with the required characteristics in the cat, a readily available larger animal with an outflow tract that is anatomically and physiologically similar to that of humans.

Experiments were conducted with specific pathogen-free domestic cats (Harlan, Indianapolis, IN). Ten days before vector application, cats were anesthetized with 10 mg/kg intramuscular Tiletamine HCl/Zolazepam HCl (Telazol, Fort Dodge Laboratories Inc., Fort Dodge, IA) for ocular examination with slit lamp (Haag-Streit,

Mason, OH) and a handheld pneumatonometer (Model 30 Classic, Medtronic, Fridley, MN) to determine IOP. Fluorescence of transduced trabecular meshwork was observed with a standard gonioscope (Posner, Ocular Instruments, Bellevue, WA) and a microscope (Nikon Eclipse E400) equipped with a GFP-optimized filter (Nikon, EF-4 B-2E/C FITC, cat. 96107). Two days before vector application, two initial pilot cats received a bilateral conjunctival injection of 200 µl Kenalog-40 (Bristol-Myers Squibb, Princeton, NJ) to blunt nonspecific iritis during initial intraocular procedures as seen after saline injection in pilot studies. However, this procedure was abandoned in subsequent animals when no iritis occurred in two further cats.

Twelve subsequent animals were assigned to dosing groups (group 1: 10^8 TU, group 2: 10^8 TU, group 3: 10^7 TU, group 4: 10^6 TU) in which each group of 3 animals was transcorneally injected with different vectors (see **Table 4** for vector identities) in each eye but without Kenalog.

7.2.8.1.2. Subretinal versus Intravitreal Injection Route Study in the Rat

To characterize transduction after different types of intraocular injection of FIV vectors, I chose subretinal and intravitreal routes in seven day old rats. Expanded litters were assembled that are commonly used in models of oxygen-induced retinopathy resulting in retinal neovascularization similar to retinopathy of prematurity. For this, 100 newborn Sprague-Dawley rats (Harlan Laboratories, Indianapolis, IN) were randomly assigned at birth to 4 expanded litters of 25,[329-331, 333] and raised in room air. 77 of the original 100 animals survived to the day of injection (day 7), an expected attrition rate due to the expanded litter design.[329] For comparison of injection techniques, right eyes of 39 rats received subretinal injections and right eyes of 38 rats intravitreal injections of CT25 on day 7 of life, while left eyes were assigned to one of three control groups: 1) FIV mock vector (n = 13 subretinal, n = 13 intravitreal), 2) DMEM+10% FCS (n = 13 subretinal, n = 12 intravitreal) and 3) no injection (n = 26). DMEM+10%FCS was chosen as a control because vectors were produced in this medium. In the injection route study, 4 µl of 4.6×10^8 TU/ml (1.8×10^6 TU total) of CT25 or control was delivered by either subretinal or intravitreal injection.

7.2.8.1.3. Comparison of Long-Term Expression in the Rat with FIV and Adenoviral Vectors

In a second experiment, I tested whether genomic integration of FIV vectors is of advantage for long-term expression compared to non-integrating adenoviral vectors.[76] In the long-term expression study, 60 five-day-old Sprague-Dawley rats received subretinal injections of 2 x 10^5 TU FIV vector into right eyes and 2 x 10^5 TU Ad vector into left eyes. An additional 10 animals served as non-injected grading controls. At 1 week, 1 month, 3 months and 6 months, 10 injected animals and 2 non-injected controls were sacrificed for analysis of transgene expression. Ten injected animals and 1 non-injected control were sacrificed at 12 months. Deaths by normal senescence (n = 3) began to occur at 16 months, so the remaining animals (7 injected and one non-injected control) were sacrificed at that time point.

7.2.8.1.4. Retinal Long-Term Expression and Integration Study In the Rat with Wild-Type versus Mutant Integrase FIV Vectors

50 rats were raised in expanded litters as described above. At 7 days, right eyes of the 37 surviving were injected subretinally with 2 µl of 4.6×10^8 TU/ml of CT25 and left eyes were injected with the integrase mutant vector (CT25.D66V).

7.2.8.2. Anesthesia

7.2.8.2.1. Cats

Cats were anesthetized with 10 mg/kg intramuscular Tiletamine HCl/Zolazepam HCl (Telazol, Fort Dodge Laboratories Inc., Fort Dodge, IA)

7.2.8.2.2. Neonatal Rats

In the FIV versus FIV integrase mutant vector study, seven-day-old pups underwent inhalation anesthesia with Metofane® (methoxy urane, Schering-Plough Animal Health Corp, Union, NJ) and were placed under an operating microscope. The anesthetic was delivered by placing a soaked sponge into the cover of a syringe and placing the open end over the nose of the animal. Metofane had the advantage that it did not require a vaporizer or doser. Although it has been very popular it is no longer available for use because of its carcinogenic and nephrotoxic potential in humans.

In the study that compared FIV with adenoviral vectors, rat pups underwent inhalation anesthesia with isoflurane (isoflurane, USP; Abbott Laboratories, North Chicago, IL) and were placed under an operating microscope. Isoflurane was delivered as above metofane.

7.2.8.3. intraocular Application of Vectors

7.2.8.3.1. Intracameral Vector Application Technique in the Cat

A 1 microliter syringe with a 30 gauge needle was used to inject anterior chambers of cat eyes under an operating microscope with a bolus of 50 µl of PBS (DPBS, Cellgro, Mediatech, Herndon, VA) containing 10^8 TU, 10^7 TU, or 10^6 TU of vectors RGWF, GINWF, CT26 or FGINSIN. Good vector circulation was achieved by aspirating 100 microliter a total of 3 times. Circulation of the highly concentrated vector suspension was visualized and even distribution confirmed.

7.2.8.3.2. Subretinal and Intravitreal Vector Application Technique in the Neonatal Rat

Harvested vector supernatant of producer cells must be concentrated for subretinal or intravitreal injection because of the limited volume that can be introduced (**Figure 18**). I developed a novel subretinal injection technique. Because of the small size of the eye of newborn rats (**Figure 19** A), subretinal injections are difficult and good microsurgical skills are required.

The eyelid was cleaned with a cotton wool swap soaked with 70% alcohol. Alcohol must not contain any additional substances or be denatured to avoid remanescence and interference with the injected vector. After canthotomy with extension of the lateral palpebral lid fissure by 1 mm (**Figure 19** B), a latex membrane with a 1 mm central slit was placed on top of the eye and spread open with curved forceps. The eye was prolapsed through the membrane with a gentle backward movement toward the orbit (**Figure 19** C).

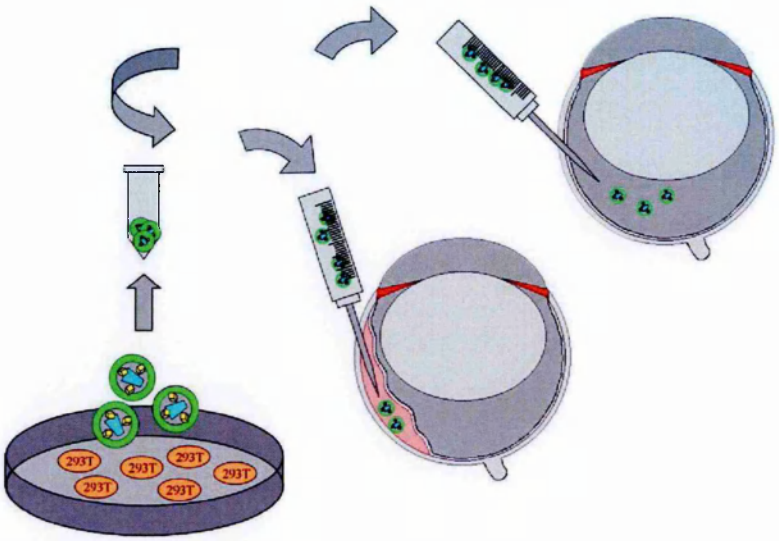

Figure 18: Vector production, concentration, and injection. Supernatants of transfected 293T cells are collected, filtered, and concentrated by ultracentrifugation. For a subretinal injection, the needle is inserted through a sclera tunnel with the bevel of the needle facing the center of the eye (middle). An intravitreal injection requires a steeper angle and the bevel is rotated outwards (right). Injury of the large rodent lens must be avoided to prevent cataract formation.

7.2.8.3.2.1. Subretinal Injection

The subretinal injection was carried out in two steps: first, a 30ga needle was used to create a sclerotomy incision at the superior pars plana 1 mm back from the limbus (**Figure 19** D). Because the latex membrane exercised slight pressure to the back of the eye, good hemostasis was achieved. A small volume of aqueous humor usually leaked and made room for the vector bolus. Precaution was taken not to injure the lens during the initial incision that aims toward the center of the eye. The 33ga needle of a custom made Hamilton syringe was advanced in a flat, tangential angle through the first incision, which directed the needle into the subretinal space (**Figure 19** E). It was crucial to turn the needle with the open side and bevel facing the center of the eye for proper guidance. Successful subretinal injection formed a detachment that could be seen through the translucent sclera of non- to medium pigmented animals (**Figure 19** F). In contrast, misplacement of the needle in the subconjunctival space caused outward bulging and could be recognized immediately. The needle was withdrawn, the latex membrane was stretched to open the central slit and removed.

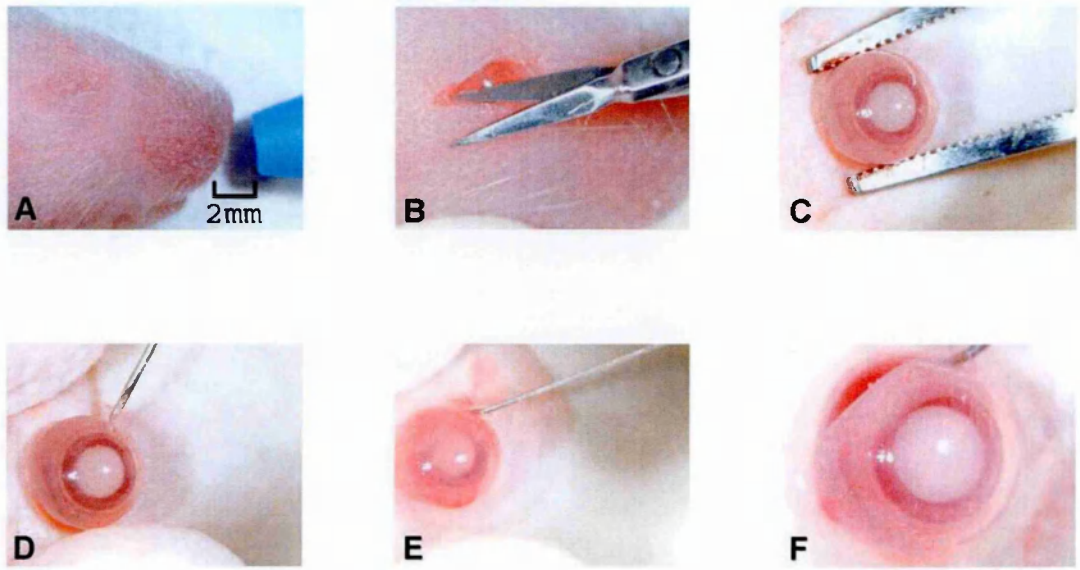

Figure 19: Subretinal injection technique. (A) Size of a 7 day old rat in comparison to the tip of a pen. (B) When full anesthesia is reached, lids are spread open with forceps and the lateral palpebral fissure is extended by 1 mm. (C) A latex membrane with a central cut of 2 mm is placed on top of the eye and the eye prolapsed with curved forceps in a backward motion while the slit is stretched open. (D) Creation of a sclera tunnel using a 30ga hypodermic needle. (E) Tangential insertion of a 33ga needle mounted on a custom made Hamilton syringe through the sclera tunnel. (F) A forming retinal detachment can be seen as a translucent crescent in animals without dark pigmentation.

7.2.8.3.2.2. Intravitreal Injection

Similar to subretinal injections, the intraretinal injection was carried out in two steps: first, a 30ga needle was used to create a sclerotomy incision at the superior pars plana 1 mm back from the limbus (**Figure 19** D). Because the latex membrane exercised slight pressure to the back of the eye, good hemostasis was achieved. Leakage of a small volume of aqueous humor was observed that made room for the vector bolus. Precaution was taken not to injure the lens during the initial incision that aims toward the center of the eye. The 33ga needle of a custom made Hamilton syringe was now directed into the vitreous, anterior to the optic nerve, the vector bolus was injected and the needle retracted.

7.2.9. Ex Vivo and In vivo Imaging of Transduced Cells Expressing Fluorescent Proteins

7.2.9.1. Ex Vivo Imaging

7.2.9.1.1. Imaging of Anterior Human Segments

Transduction efficiency was determined as the mean percentage of transduced cells in four quadrants. Eyes in the eGFP group were divided into four quadrants, and 2-mm wedges were removed, rinsed in PBS, and placed into phenol red–free Dulbecco's modified Eagle's medium with 0.1% Hoechst 33342 (H-3570; Molecular Probes, Eugene, OR) for in vivo staining of nuclei. Expression of eGFP in freshly dissected, unfixed anterior segments was visualized by a frontal view toward the TM and a sagittal view of wedges mounted on their sides, by a microscope with a fluorescent light source (Eclipse E400; Nikon, Melville, NY) and by confocal microscopy (LSM 510; Carl Zeiss, Thornwood, NY). To measure transduction efficiency with GiNWF, eGFP-positive TM cell bodies and stained nuclei were manually counted at 400x magnification in microscopic fields comprising an area of 0.24 mm^2 in each of the four quadrants. Transduction efficiency is expressed as the mean percentage of eGFP-expressing cells versus stained nuclei ± SD. Medium-injected fellow eyes served as the control.

7.2.9.1.2. Imaging of Enucleated Cat Eyes

Cats were sacrificed with an injection of 175 mg/kg pentobarbital sodium IV (Sleepaway, Fort Dodge Laboratories, Sligo, Ireland) and eyes were enucleated. To correlate gonioscopic expression grades with transduction efficiency, 3 quadrants in one eye per expression grade were analyzed. One random quadrant was removed from the anterior segment for X-Gal-staining, while the remaining 3 were incubated with PBS and 1000-fold diluted Hoechst 33342 (Molecular Probes, Eugene, OR) to counter stain nuclei of living cells. The transduction efficiency was determined by counting GFP positive, living TM cells, and Hoechst 33342-positive nuclei in the same visual field at 100-fold magnification with a histology microscope (Nikon Eclipse E400). This required that the focus be moved up and down to count cells lining along the three-dimensional structure of the trabecular meshwork.

7.2.9.2. Non-Invasive In Vivo Monitoring of Enhanced (eGFP) and Renilla (rGFP) Green Fluorescent Protein Expression in the Cat Eye

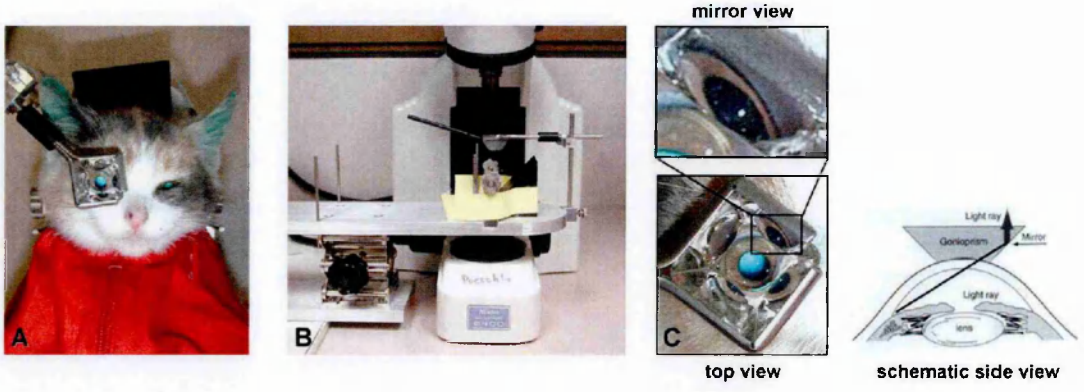

Figure 20: Top view of anesthetized cat on restrainer (A) and side view of restrainer under modified microscope (B). The trabecular meshwork can be seen as a black ring in the mirror of the gonioscope that is placed on the cornea (C).

Anesthetized cats were examined with slit lamp, pneumatonometer, and biomicroscopy at the day after arrival, 3 days before, at day of, and 3 days after vector application, then weekly for 2 months, bi-weekly for 4 months and monthly thereafter. IOP was always measured at the same time of the day, three readings per eye were taken and averaged. The entire TM circumference was inspected. Photographs of fluorescent TM were taken at each examination and grades determined in a masked manner by two observers rating independently, using the scale photographs shown in Fig. 1b. A digital microscopy camera (DXM 1200, Nikon, Melville, NY) was used, with 2 second exposures and image capture software (Automatic Camera Tamer (ACT-1), Nikon, Melville, NY).

During the examination, animals were secured in a bag (red bag in **Figure 20** A) and placed on a custom made restrainer looking upwards. I designed this restrainer and had it manufactured by the Engineering Department of the Mayo Clinic. A Posner gonioscope mounted on a holder that could be moved around the head was positioned on top of the open eye without use of a contact gel.

7.2.10. Quantification and Statistics

7.2.10.1.1. Quantification and Statistics of Human Eyes of Perfused Anterior Segment Cultures

The ratios of β-galactosidase-positive TM cells to total TM cells present in random 6-mm sections from each quadrant of an eye were determined by counting the labeled and unlabeled cells and calculating the mean value for each quadrant. Colocalized nuclear staining (nuclear fast red) and cytoplasmic β-galactosidase staining was counted as a transduced cell. A paired Student t test was used for statistical analysis.

7.2.10.1.2. Quantification and Statistics of Expression in Feline Eyes

In vivo TM fluorescence as seen during gonioscopy was graded on a scale of 0 to 4, with representative photographs shown in **Figure 23** B. Grade 0 was defined as no detectable fluorescence, grade 1 as single fluorescent spots in the TM, grade 2 as numerous nonconfluent fluorescent spots with some confluent areas, grade 3 as extensive, mostly confluent, mid-level transduction and grade 4 as extensive, high level and completely confluent fluorescence. Because of the high linear correlation, expression grades were handled as continuous data during the statistical comparison of marker protein accumulation. To determine whether the rate of fluorescent marker protein accumulation (V_F) influenced the duration of expression, V_F was measured as the change from initial expression grade ($grade_I$) to peak expression grade ($grade_P$) over time from the first examination (t_I) to the time point of peak expression (t_P): $V_F = \Delta grade/\Delta time = (grade_P - grade_I)/(t_P - t_I)$. Time was measured in days. A large increase in expression grade over a short period of time would result in a larger V_F than a small increase in the same period of time. IOP readings before vector injection were compared to peak pressures of the same eye as well as to the experimental endpoint using the paired student's t-test.

7.2.10.1.3. Blinded Assessment and Statistics of Expression In Rat Eyes Transduced with Normal or Integrase Mutant Vectors

X-Gal-stained eye cups were graded in random order for transduction, and scored as positive if β-galactosidase expressing cells could be identified in at least one retinal quadrant by an independent observer in a masked manner using a Zeiss operating

microscope. Eyes were finally scored before the random number code was broken. The proportions of eyes transduced after intravitreal and subretinal injection were compared at 2 and 7 days post injection using a chi-square test. Statistical significance was defined as a p value ≤ 0.05.

7.2.10.1.4. Assessment of Incidence and Extent of Transduction of FIV and Adenoviral Vectors after Intravitreal or Subretinal Injection

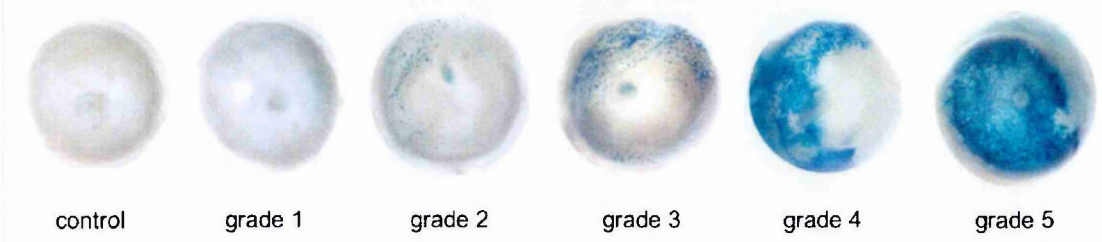

Figure 21: Grading system for β-galactosidase expression. Grades were defined prospectively on a scale with a range from 0 to 5. Grade 5 = confluent transduction of entire retinal surface area, grade 4 = large confluent areas of at least half of retinal surface area, grade 3 = confluent areas with less than half the retinal surface area, grade 2 = large areas of non-confluent transduced cells, grade 1 = isolated, discrete transduced cells, grade 0 = no detectable β-galactosidase activity.

After sacrifice, eyes were enucleated and fixed for 90 minutes in 10% formalin at 4°C. The cornea and lens were then removed and eye cups were stained overnight in X-gal solution to detect β-galactosidase expression. All eye cups were evaluated in a masked manner by an observer unaware of the experimental group for extent of transduction using a Zeiss stereo operating microscope (Zeiss OPMI MD; Carl Zeiss Surgical, Inc., Thornwood, NY). I used a prospectively defined grading scale to quantify the extent of retinal transgene expression, with a range from 0 to 5 (**Figure 21**). Grade 5 was defined as confluent transduction of the entire retinal surface area, grade 4 as large confluent areas of transduction involving at least half of the retinal surface area, and grade 3 as confluent areas of transduction but involving less than half the retinal surface area. Grade 2 was defined as large areas of non-confluent transduced cells, grade 1 as the presence of isolated, discrete transduced cells and grade 0 as no detectable β-galactosidase activity.

Incidence and extent of transduction at each time point, and overall, were compared using McNemar's tests and Wilcoxon signed-rank tests.

8. Results

8.1. Transgenesis of the Ocular Outflow Tract with Lentiviral Vectors as a Basis for Gene Therapy of Glaucoma

8.1.1. FIV transfer vectors and Production Procedures

8.1.1.1. Transfer Vector Modification

The original beta-galactosidase expressing FIV vector, CTRZLb,[251] was modified to minimize the risk of recombination with the packaging plasmids. The resulting minimal transfer vector, CT25, contained no sequences derived from viral coding regions except for the initial 311 nucleotides of the gag ORF, and a 250-nucleotide 39 env fragment encoding the Rev response element. Reporter gene (lacZ) transcription was promoted internally by the human CMV immediate- early promoter-enhancer. Unconcentrated CT25 vector pseudotyped with VSV-G yielded mean titers of 1.6 (±0.74) x 10^6 TU/ml (n = 12 preparations). After concentration by ultracentrifugation, mean titers were 2.2 (±1.8) x 10^8 TU/ml (n = 4 preparations). These were at least equivalent to titers obtained with FIV vector CTRZLb, which contained an additional 938 nucleotides of gag that ***Iris Kemler*** found to be dispensable for efficient FIV genome encapsidation.[493] Vectors with this truncated *gag* segment are in fact packaged into virions at higher efficiency than those with the longer *gag* segment contained in the original vectors.[493] Reverse transcriptase (RT) measurements performed by ***Iris Kemler*** confirmed equivalence: transducing units per counts per minute of RT activity for CT25 and CTRZLb vectors were 2.89 and 1.18, respectively (n = 3). Two rounds of concentration of CT25 vector increased titer from 4.8 x 10^6 TU/ml to 2.3 x 10^{10} TU/ml (79% yield).

Subsequent eGFP transfer vectors also contained new transgenes (*eGFP* and *neoR*) and additional viral elements that are involved in reverse transcription and viral nuclear import (cPPT)[492] or that enhance transgene mRNA levels (WPRE).[733]

8.1.1.2. Production Procedures

To enhance scalability of vector production, I developed a modified procedure that uses a much smaller amounts of plasmid DNA than in previously described protocols[240] (10 times less in micrograms of DNA per square centimeter of 293T cell monolayer), as well as high-surface-area vessels (Cell Factory, Nunc) and large

volume ultracentrifugation. Large-scale vector supernatants produced with these methods in cell factories averaged $2.8 \pm 1.5 \times 10^6$ TU/mL ($n = 8$). The first round of ultracentrifugation resulted in vector recoveries of 60% to 80%, the second round in recovery of 40% to 60%, and maximum titers of 2.5×10^9 TU/mL. Vector preparations used for the organ perfusion experiments contained 6.83×10^8 TU/mL (GiNWF) and 2.5×10^9 TU/mL (CT26) and were diluted for injection of 1×10^8 TU in a volume of 500 µL. For bicistronic vector preparations, *eGFP* and *neoR* titers correlated within 50% of each other and more than 95% of G418-stable colonies expressed *eGFP*, indicating good function of the internal ribosomal entry site.

8.1.2. Transduction of Primary Human Trabecular Meshwork Cells with FIV LacZ Transfer Vector CT25

The CT25 FIV vector was tested for its ability to transduce primary TM cells derived from human trabecular meshwork. CT25 was compared with an MuLV-based lacZ vector also pseudotyped with VSV-G; for this and all comparisons in this study, vector preparations were normalized to equal transducing units after titration under identical conditions. The lentiviral vector transduced both proliferating cells and cells growth-arrested in G1/S phase with aphidicolin (**Figure 22**). In contrast, growth arrest prevented transduction by the MuLV vector. No background β-galactosidase activity was detected in TM cells, no transduction was seen with a mock FIV vector, and transduction by both vectors was completely blocked by 50 mM AZT, an inhibitor of reverse transcriptase.

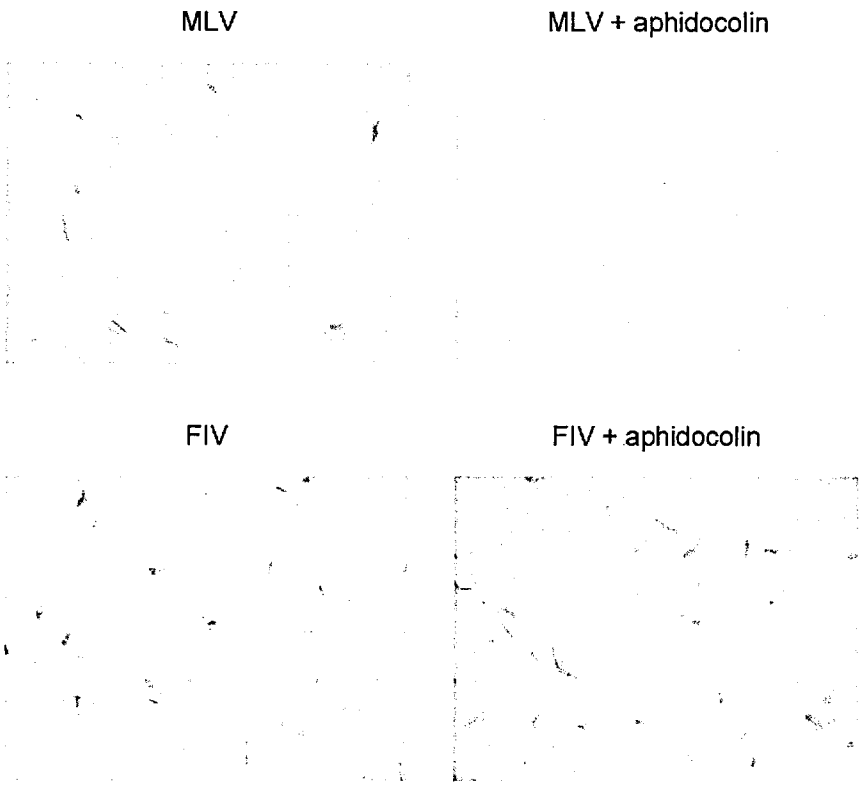

percentage of transduced TM cells

	no aphidocolin	aphidocolin
MLV	31%	4%
FIV	40%	43%

Figure 22: Primary trabecular meshwork cell transduction and effect of growth arrest. Cells isolated from human trabecular meshwork and plated in 24-well plates were transduced with 300 *m*l of unconcentrated supernatant containing a 2.5 x 10^6-TU/ml concentration of MuLV vector (*top*) or FIV *lacZ* vector (*bottom*). Growth arrest with aphidicolin (15 *m*g/ml, right-hand side) blocked MuLV but not FIV transduction. Percent transduction is shown at the bottom.

8.1.3. Transduction of Primary Human Trabecular Meshwork Cells with FIV eGFP Transfer Vector GINWF

Because enabling real-time non-invasive monitoring was a central goal, GFP-expressing vectors were the principal focus of the study. To preliminarily assess feasibility and potential toxicity of GFP expression, cultured primary human TM cells were transduced with a 4-log range of FIV vector input (**Figure 23**a). Transduction at the highest multiplicity of infection (m.o.i), which I estimated to be the approximate equivalent of ten times the maximum in vivo multiplicity used in the animal experiments that follow, produced marked GFP over-expression in all TM cells

(**Figure 23**) without morphological change, detachment, vacuolization, change in doubling time, or other evidence of vector or transgene toxicity. The plateau of GFP fluorescence was reached within 24 to 48 hours. As shown by the one-month post-transduction results in **Figure 23**, this transgene expression was stable. When Renilla GFP (from the sea pansy[760, 761]) was substituted for Aequoria[760, 762] GFP, cells transduced with equivalent m.o.i appeared paler and reached peak fluorescence later, at 48 to 72 hours. Unless otherwise specified below, GFP designates the Aequorea protein. Similar to in vivo TM cells, cultured primary TM cells experience strong contact inhibition and stop dividing when a certain culture density is reached. Cells were viable for at least 2 months under these conditions.

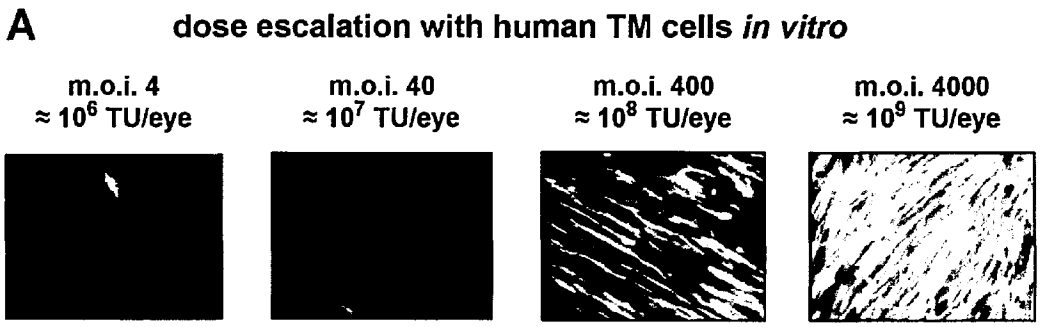

Figure 23: Vector dose escalation experiments. (a) Dose-escalation experiment with GINWF in primary cultured human TM cells. Shown are contact-inhibited TM cells at 1 month post transduction. The vector encodes enhanced (codon-humanized) green fluorescent protein (GFP) under the transcriptional control of the human CMV promoter. No toxicity was observed at any dose.

8.1.4. Transduction of Human TM

8.1.4.1. Transduction of Cultured Human Eyes: Extent and Time Course of Transgene Expression in the Trabecuiar Meshwork

Efficient transduction of growth-arrested primary human TM cells with the FIV vector provided a basis for proceeding to the human organ perfusion model. Initial experiments were performed to assess the comparative capabilities of the MuLV vector, an adenoviral vector, and two different lentiviral vectors: the CT25 FIV vector and an HIV-1 vector, pHR9CMVlacZ.[240, 250] Vectors were administered as a single bolus injection of 1 x 10^8 TU into the afferent perfusion chamber. No polycations or other enhancers of virion–cell binding were added, as Polybrene was highly toxic at concentrations (4 mg/ml) that enhanced transduction of cultured cell lines (data not shown). The MuLV vector produced minimal transduction of the TM at both days 3 and 16 (Figure 24). Only occasional blue cells were seen in stained histological sections. In contrast, both FIV and HIV lentiviral vectors consistently transduced more than 60% of TM cells when examined on day 3; staining intensity was increased by day 16 (Figure 24). Transduction was distributed throughout the TM, including the juxtacanalicular portion, and extended to the endothelium of Schlemm's canal. As previously shown,[244] the adenoviral lacZ vector also transduced the majority of TM cells at both time points. The majority of lentiviral transduction was seen in the TM, although some lacZ-transduced cells could also be detected in portions of the ciliary body, corneal endothelium, Schlemm's canal, and downstream collector channels. For example, day 3 trabecular biopsies and day 16 chamber angle views in lentivirally-transduced eyes in Figure 24 show patchy β-galactosidase activity in the corneal endothelium adjacent to the heavily transduced TM. The results were confirmed by the more sensitive method of antibody labeling, which detected β-galactosidase protein in TM cells after transduction with either of the lentiviral vectors, but not after oncoretroviral transduction (Figure 26). Controls using either preimmune rabbit serum as the primary antibody or only the secondary antibody were negative, as was an untransduced control eye using both antibodies. Furthermore, mock FIV vector-injected eyes showed no X-Gal staining or antibody labeling, and 50 mM AZT blocked TM transduction completely, confirming that both endogenous LacZ staining and pseudotransduction were absent.

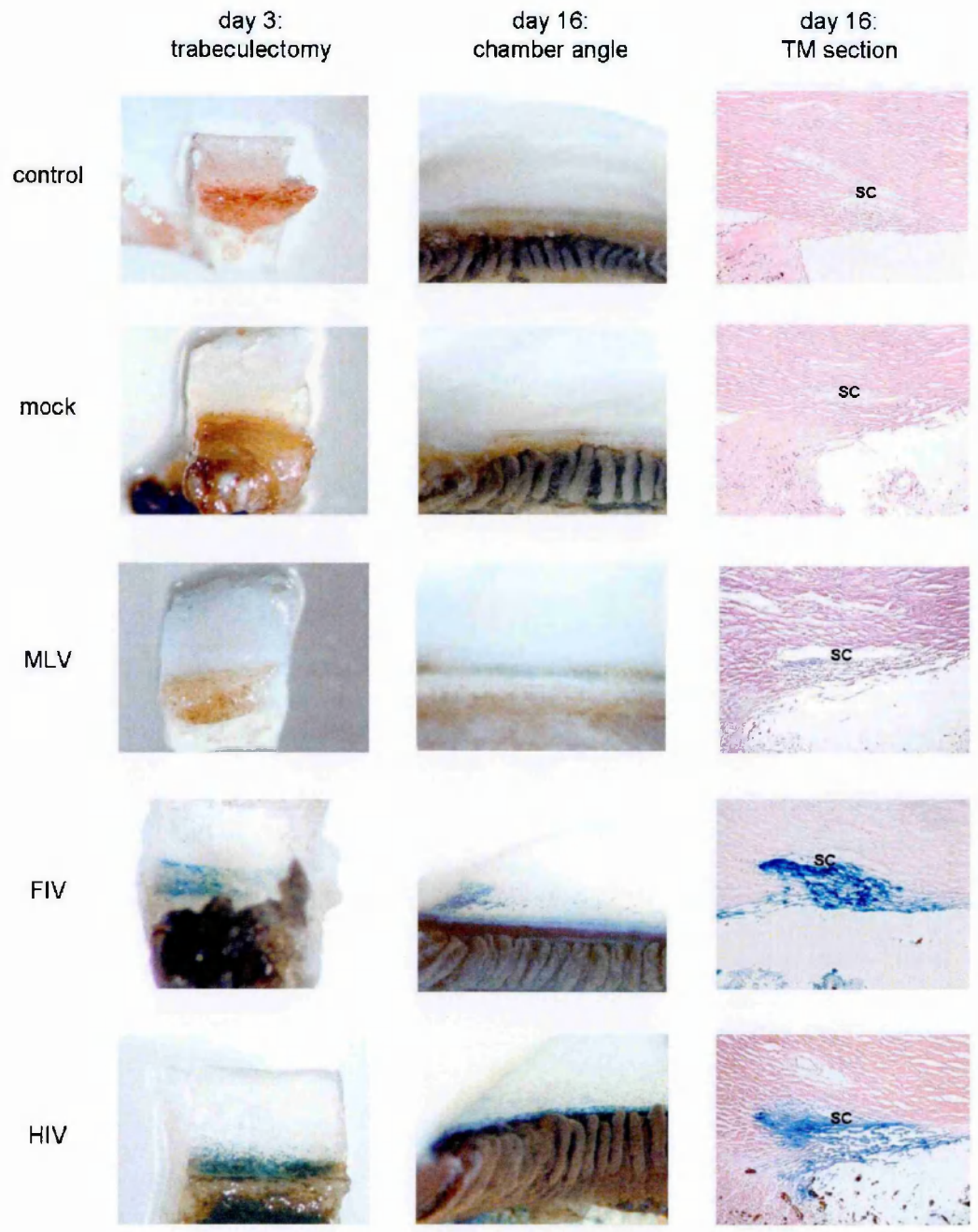

Figure 24: Transduction of human trabecular meshwork. *Left*: Representative TM biopsies obtained on day 3 after transduction. *Middle* and *right*: Representative chamber angles and histological sections, respectively, from eyes evaluated for reporter gene expression 16 days after transduction. TM, Trabecular meshwork; SC, Schlemm's canal.

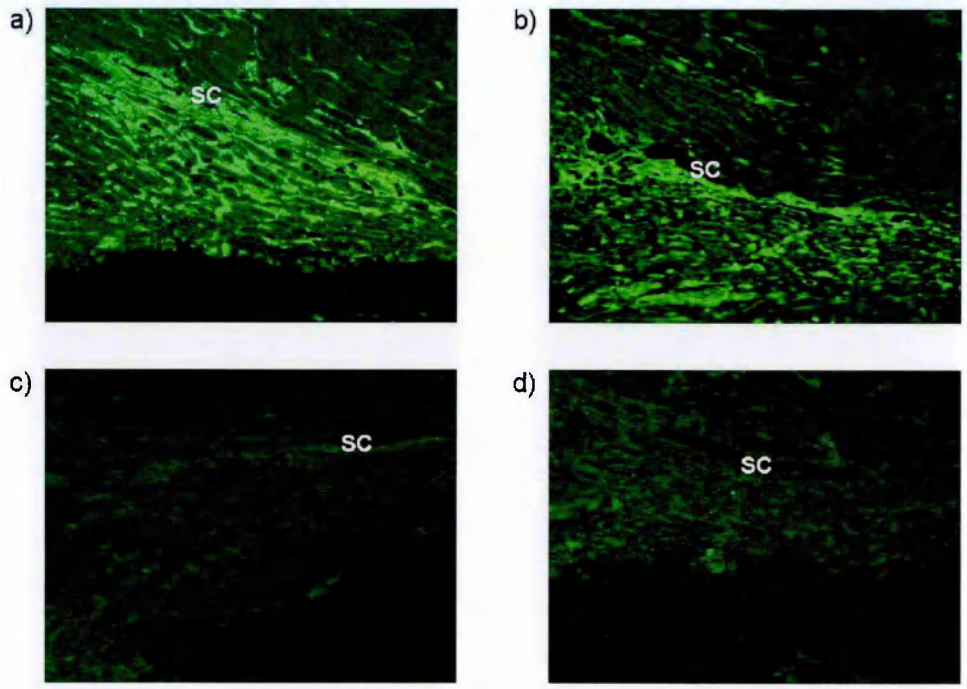

Figure 25: Fluorophore-labeled anti-β-galactosidase antibody labeling of the trabecular meshwork 16 days after injection of 10^8 TU of FIV vector (a), 10^8 TU of HIV-1 vector (b), or 10^8 TU of MuLV vector (c) or mock FIV vector (d). SC, Schlemm's canal.

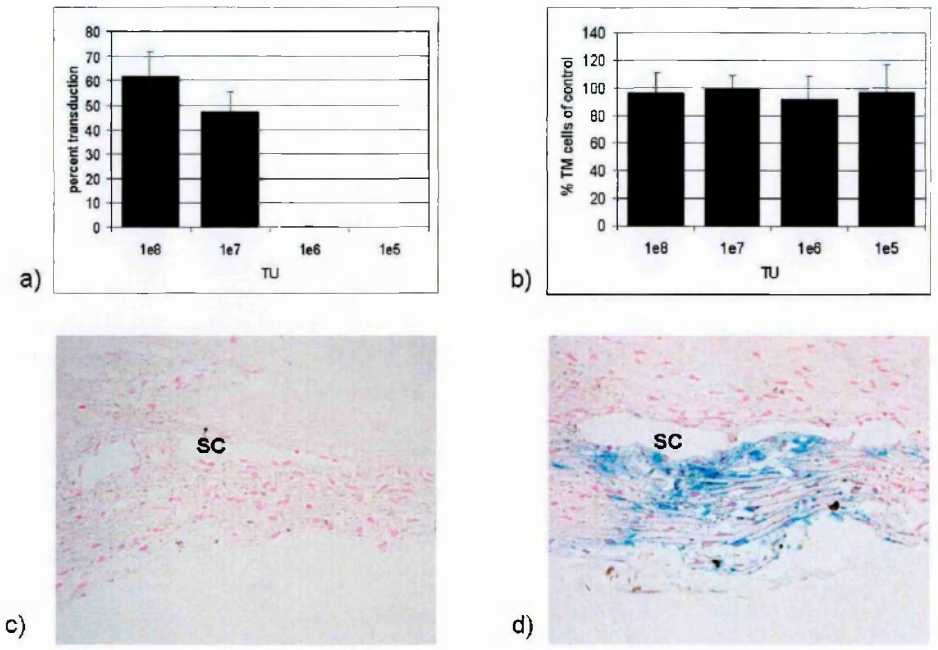

Figure 26: Dose response and trabecular meshwork preservation. Percent transduction (a) and total trabecular cells (b) in four eye pairs perfused with the indicated doses of vector. A section from each quadrant of an eye was counted and the mean was compared with the simultaneously perfused and untransduced fellow eye. Bars represent the SD. (c and d) TMs from a pair of fellow eyes perfused with medium alone (c) or 10^8 TU of FIV vector (d).

8.1.4.2. Dose Response

A dose-response study for FIV vector was then performed (**Figure 26**). Significant transduction of TM cells was seen after administration of 10^8 and 10^7 TU, but not at lower vector doses (**Figure 26**). Fellow control eyes from each human donor in this series received no vector and displayed no β-galactosidase activity (data not shown). TM structure was intact in fellow eyes perfused with medium alone (**Figure 26**) or 10^8 TU of FIV vector (**Figure 26**). TM lamellae, extracellular matrix, and cellularity were preserved after transduction. Thin, blue-staining cytoplasm extended along trabecular beams from counterstained TM cell nuclei (**Figure 26**). No significant differences in cellularity were found between transduced eyes and untransduced fellow eyes from the same donor (**Figure 26**).

8.1.4.3. Pairwise Comparison of Trabecular Meshwork Transduction by Oncoretroviral and Lentiviral Vectors

Direct, pairwise comparisons of FIV vector with MuLV vector and separately with HIV vector were performed, using the left and right fellow eyes of human donors (**Table 3**). Three pairs of eyes were used for each comparison. Quantitation of the meshwork cells expressing β-galactosidase showed that MuLV vector-perfused eyes had no transduced TM cells, compared with transduction of 68 ± 3% of TM cells with the FIV vector ($p = 0.0005$, $n = 3$). The separate, FIV/HIV-1 vector comparison in eyes from three donors resulted in 75 ± 4% transduced cells for the FIV eyes and 79 ± 11% for HIV eyes; this difference was not statistically significant ($p = 0.67$). Transduction was uniform around the circumference of each TM (**Table 3**, standard deviations for quadrant counts), indicating even dispersal of vector.

	Paired comparison I	
	FIV	*HIV*
Donor 1	79 ± 6 (R)[a]	66 ± 3 (L)
Donor 2	71 ± 4 (L)	84 ± 7 (R)
Donor 3	74 ± 15 (L)	87 ± 3 (R)
Mean ± SEM:	**75 ± 2**[b]	**79 ± 6**

	Paired comparison II	
	FIV	*MLV*
Donor 4	70 ± 5 (L)	<1 (R)
Donor 5	65 ± 22 (R)	<1 (L)
Donor 6	69 ± 20 (L)	<1 (R)
Mean ± SEM:	**68 ± 2**	**<1**

Table 3: Paired comparison of retroviral vectors – percent transduction after injection of 10^8 TU per eye. a) Percent transduction values for the individual eyes represent means 6 SD of counts from four TM sections, one from each eye quadrant. b) Aggregate mean 6 SEM was derived for each three-eye set.

8.1.4.4. Expression of eGFP and β-Galactosidase in Human Trabecuiar Meshwork

GiNWF vector injection into cultured anterior segments produced efficient TM transduction, as determined by visualization of expression of eGFP (**Figure 27**). Transduction was limited to the TM, with the exception of occasional eGFP-positive

cells elsewhere within the outflow pathway (corneal endothelium in proximity to the TM, Schlemm's canal, collector channels). Cell counts performed with nuclear counterstaining revealed that a mean of 82% ± 4% of TM cells were eGFP positive and no cell loss was apparent ($P = 0.94$ for comparison with control eyes, $n = 3$). Staining of tissue sections with anti-eGFP antibodies confirmed the extent and location of expression of eGFP (data not shown). Plastic-embedded sections showed preserved TM morphology and cellularity. Transduction of two unpaired eyes with a version of GiNWF without the central DNA flap or WPRE (pGiN) showed less efficient transduction (data not shown).

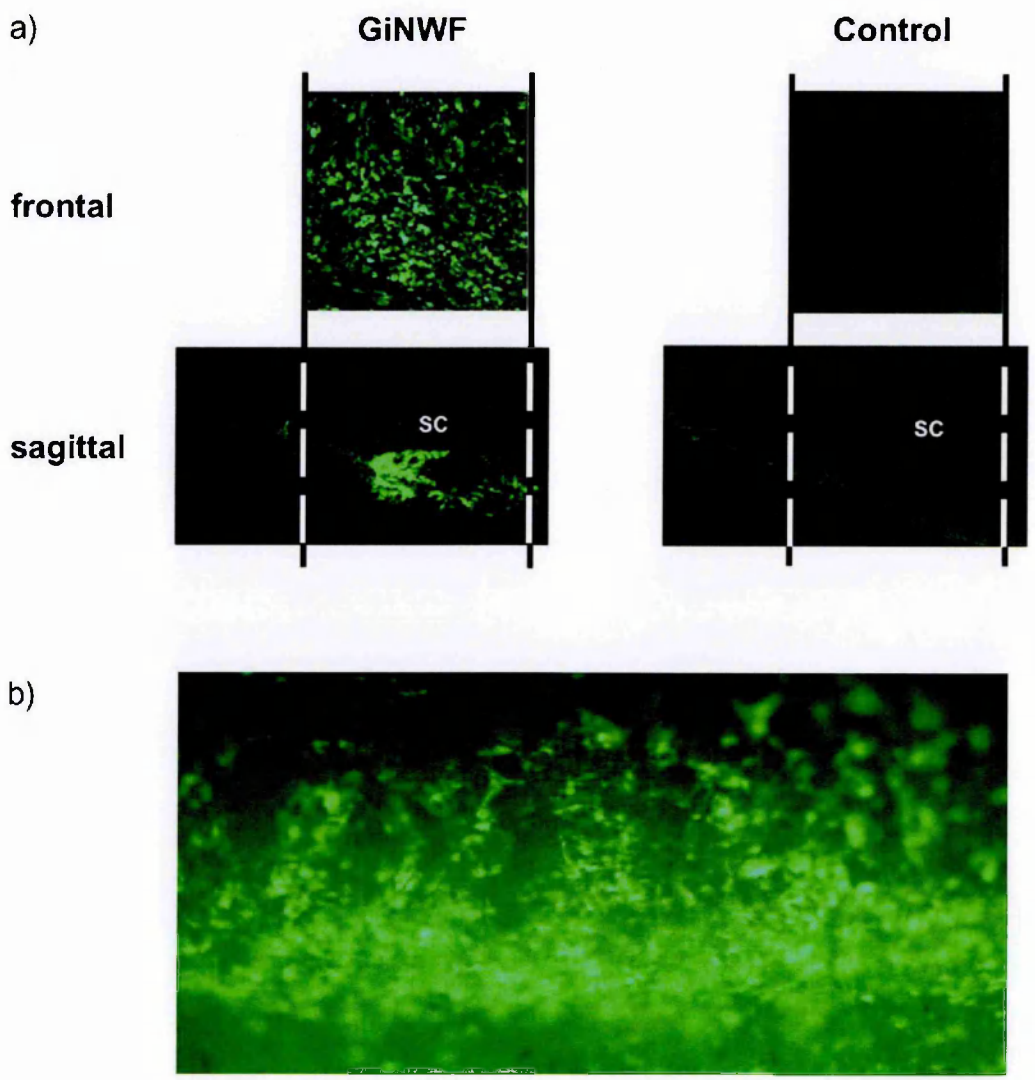

Figure 27: (a) Confocal microscopy view with frontal and sagittal view of TM 5 days after transduction with GiNWF and the TM in the fellow control eye. Imaging depth of 20 µm with wide pinhole. (b) Conventional fluorescence microscopic view. 400x magnification.

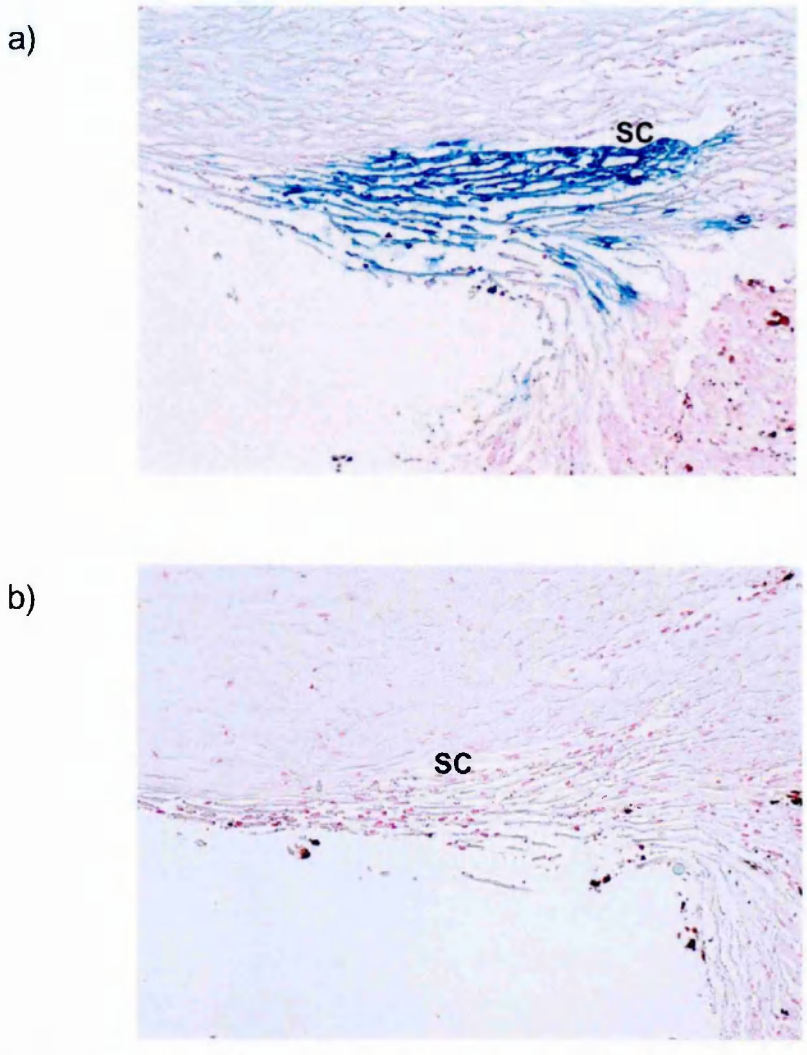

Figure 28: Chamber angles 5 days after injection of CT26 (a), and CT26.mock vector (b). Sections are stained with X-Gal to detect expression of β-galactosidase. SC, Schlemm's canal.

Transduction with the *lacZ*-encoding CT26 vector also resulted in high-level transduction (79% ± 15%) of TM cells (**Figure 28**). The fellow eyes injected with the CT26.mock vector did not stain positively for ß-galactosidase, confirming absence of pseudotransduction.[763] Comparison of total cell numbers showed no significant cell loss ($P = 0.18$ for comparison with control eyes, $n = 3$) and the morphology was well-preserved (data not shown). Expression of ß-galactosidase was mainly observed in TM, although a few corneal endothelial cells in proximity to the TM and occasional cells in the endothelia of Schlemm's canal and the collector channels were also transduced.

8.1.5. Effects on Outflow Facility

Despite the extensive transduction and high levels of marker gene expression in both sets of eye pairs, only slight and transient changes in outflow facility were observed (**Figure 29**). In six eyes with high (79% or greater) transduction of TM cells with *lacZ* or *eGFP*, a mean 30% ± 22% ($P = 0.02$) peak reduction in outflow facility was observed. This minimal decrease in outflow facility was followed by stable return to preinjection levels by approximately 48 to 72 hours. The experiments were terminated at 5 days. The mean peak decreases were not significantly different between the *lacZ* and *eGFP* groups (25% ± 30% and 36% ± 17%, respectively, $P = 0.6$, $n = 3$ per group). CT26.mock vector–injected eyes did not show a significant change in outflow facility compared with medium-injected control eyes.

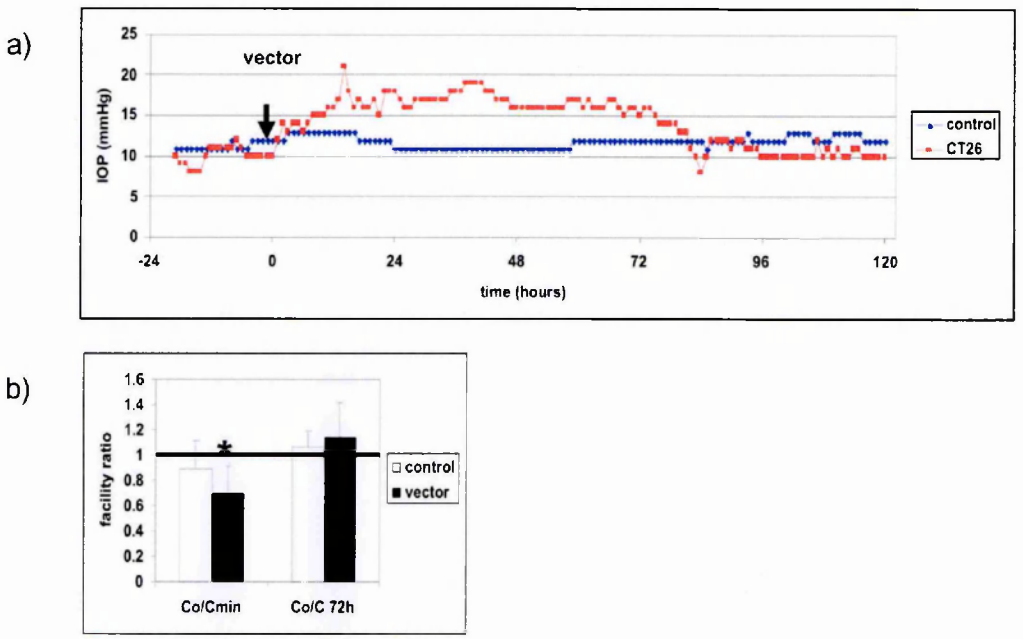

Figure 29: Intraocular pressure. (a) Recording of eye injected with CT26 and CT26.mock vector control. (b) Ratio of outflow facility (1/R) before transduction (C_0) and at recorded minimum (Cmin) and C0 and 72 hours after transduction (C72h). Outflow facility ratio of transduced eyes was significantly different from the control at the recorded minimum (*$P = 0.02$), but returned to stable baseline at 72 hours.

8.1.6. Transgene Expression In Vivo

A total of 19 domestic cats were used in this study. 7 were used as pilot animals to establish techniques and assess feasibility of gene transfer with eGFP vector, using what was later established to be a highly effective dose (10^8 TU per eye). When these animals showed extensive expression of GFP in the TM, 12 more cats were assigned to groups organized by dose level and marker gene in a design that utilized

comparisons of different marker transgenes in right and left eyes of the same animal (see Methods and Table 1 for animal group assignments). Vectors were injected transcorneally into the anterior chambers of lightly anaesthetized animals via single 50 µl bolus injections through a 27-gauge needle. Animals injected with $10^7$and 10^8 TU of GFP-transducing vector developed high grade (grade 4; see **Figure 23**b for grading scale), persistent GFP expression in the TM that was readily visualized and photographed through a conventional gonioscope (**Figure 31**& 2). Notably, expression was confined to the TM. Numerical results are summarized by group in Table 1. GFP expression in the TM steadily increased after transduction, reaching a maximum within days to weeks. It then was observed in most animals to plateau at the same or a lower grade, where it persisted for at least ten months, at which time the animals were sacrificed (**Figure 32**a, Aequorea GFP panels). There was a high linear correlation ($R^2 = 0.9$) of gonioscopic expression grade and histologically determined transduction efficiency, with antibody labeling for GFP confirming that expression was limited to the TM (**Figure 33**). Overlay with DAPI (nuclear) staining demonstrated normal cellularity in both highly transduced and untransduced TM in the same animal (**Figure 33**). Of note, the expression grade data in this study were scored in a masked manner by 2 independent observers who used the scale photographs shown in Fig. 1b, did not participate in the experiments, and were blinded to vector assignments. The robustness of this rating scale is evident in the outcome that both of the masked observers agreed independently on each scored expression grade, except for one point in which a grade of 2 was assigned by one observer and 3 by the other. In this one instance, a grade of 2 was scored.

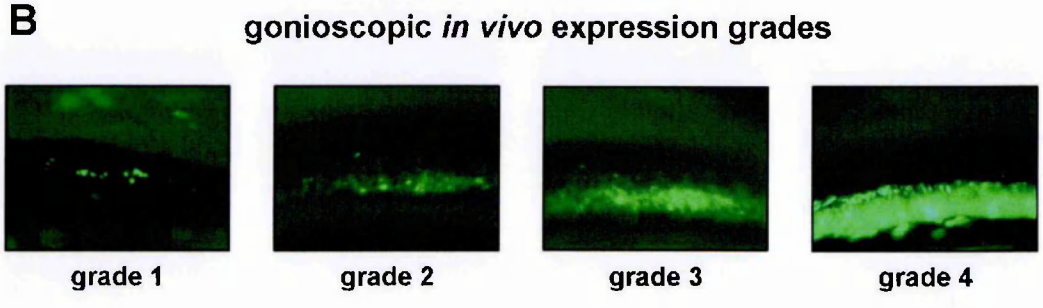

Figure 30: Gonioscopic in vivo expression grades. GFP fluorescence in the TM of living cats was serially photographed and graded by direct gonioscopy (a cornea-shaped lens with a mirror is used to enable visualization of the anterior chamber angle). There was a high linear correlation ($R^2 = 0.9$) between expression grade and histological transduction efficiency (grade 1, 2% ± 0.3%; grade 2, 21% ± 1%; grade , 39% ± 3%; and grade 4, 94% ± 5%).

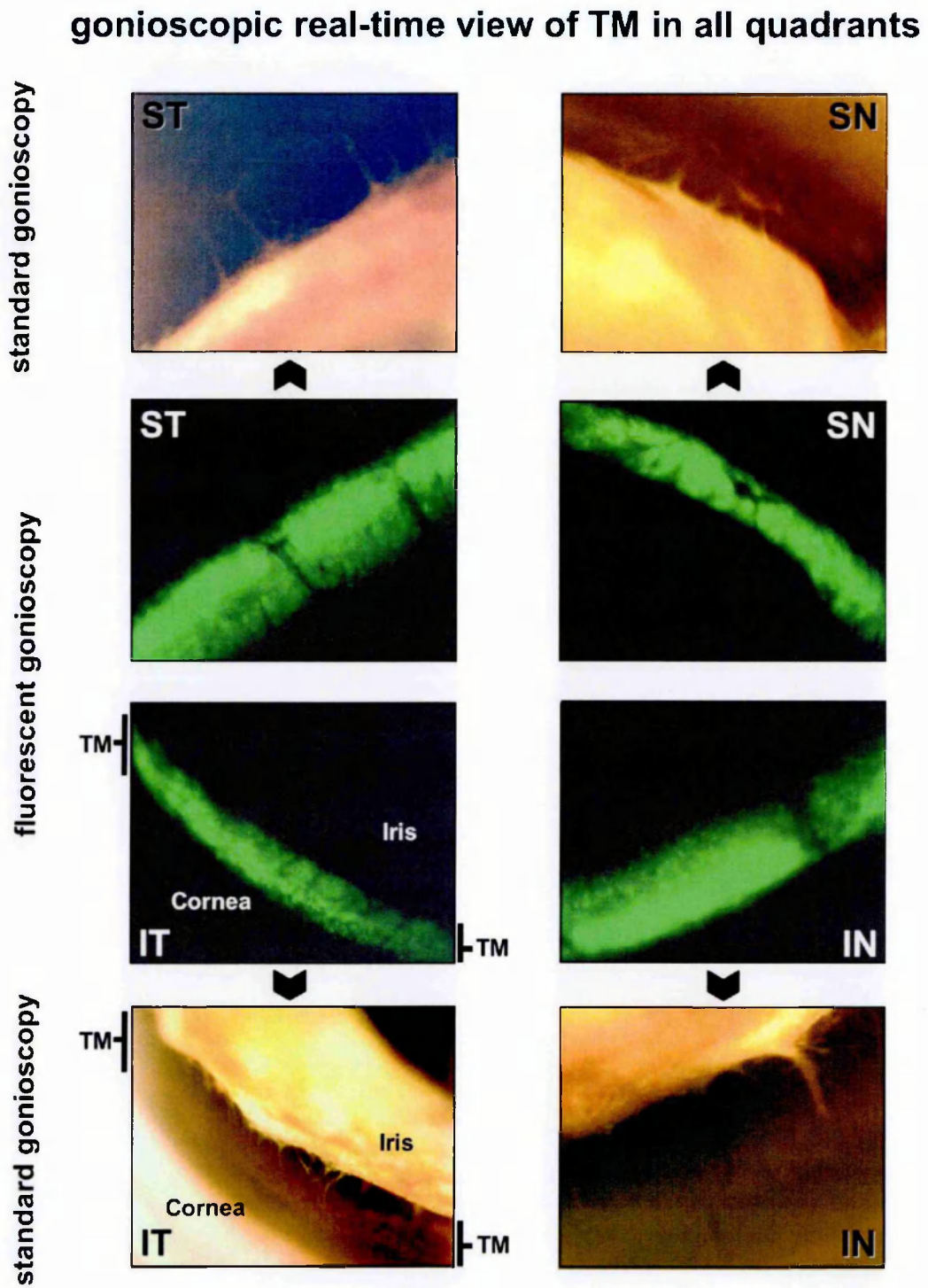

Figure 31: View of trabecular meshwork in living animal in standard (top and bottom) and corresponding UV light gonioscopic views (center). All four quadrants from an eye with grade 4 expression after transduction with 10^8 TU are shown (SN = superonasal, IN = inferonasal, IT = inferotemporal, ST = superotemporal). Transduction was virtually complete and was confined to the TM.

Temporal and spatial patterns of cats in Group 1, which were injected with 10^8 TU GFP vector in one eye and 10^8 TU Renilla GFP vector in the other eye were consistent with the human TM cell culture outcomes described above. Companion eyes were initially similar (**Figure 32** and **Figure 34** A). However, eyes expressing Renilla GFP showed smaller median expression (maximum grade 2 compared to 4 in the GFP injected eye of the same animal, $p = 0.04$, Table 1). Renilla GFP expression was also shorter lived than GFP expression (35±22 days versus more than 10 months). High level GFP expression remained stable in two of the three Group 1 animals (grade 2 in one, grade 3 in the other) to the endpoint of the study (i.e., sacrifice at 10 months). The third animal also had grade 4 GFP expression initially. Strikingly however, the intense GFP fluorescence was observed to disappear abruptly on day 38, concurrent with a brief iritis (discussed further below). Rate of marker protein accumulation VF, expressed as Δgrade/time was 0.2±0.1 grades/day for GFP and 0.2±0.1 grades/day ($p = 0.4$) for Renilla GFP (**Figure 32**).

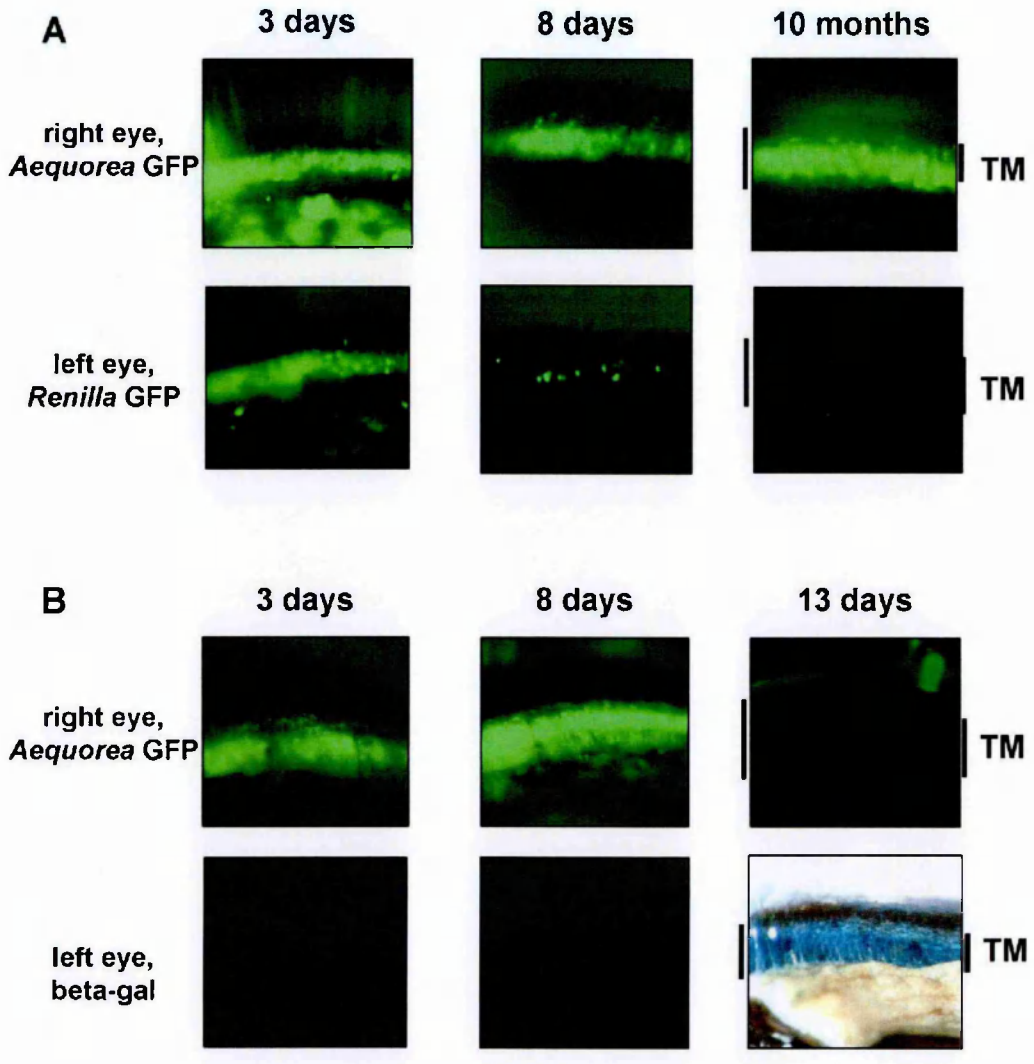

Figure 32: Representative examples of reporter gene expression in animals in group 1 and 2. (a) Renilla GFP (right eye) and GFP (left eye) expression in group 1. (b) Paired comparison of GFP (right eye) and ß-galactosidase expression (left eye) in group 2. Shown are photos of TM as seen via UV light gonioscopy (the 13 day ß-galactosidase eye was fixed and stained with X-gal after sacrifice). Detectable Renilla GFP expression was always shorter-lived than that of GFP, while ß-galactosidase expression persisted longer than GFP only at the highest dose, when over-expression toxicity of GFP was observed.

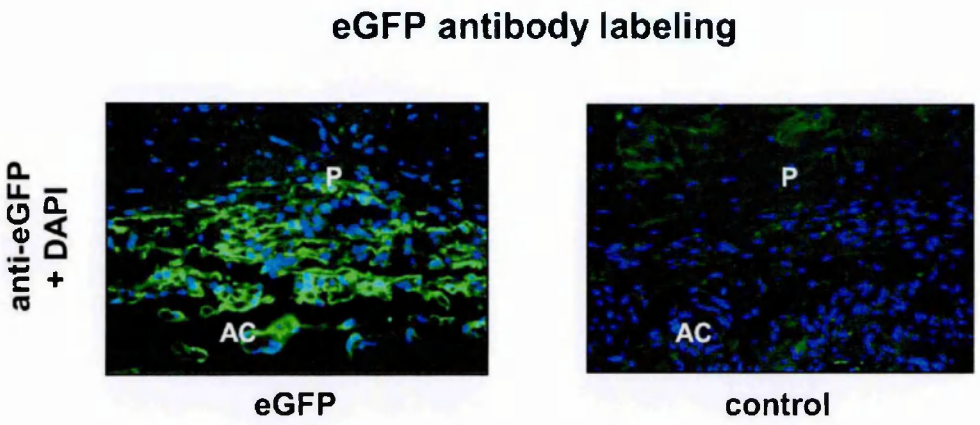

Figure 33: Antibody labeling for GFP confirms gonioscopic extent of transduction. GFP expression was limited to the TM and collector channels. Comparison DAPI staining of transduced TM (left) and control TM (right) demonstrates preserved cellularity in GFP-expressing TM. AC = anterior chamber, P = plexus.

group	number of cats	vector	median expression grades max.	median expression grades final	duration	V_E= Δ grade / day	IOP_{start} vs. IOP_{end}
1	n = 3	R = 10^8 TU GFP	4	2*	> 10 months*	0.2±0.1	p = 0.93
		L = 10^8 TU Renilla GFP	2	0	35±22 days	0.2±0.1	p = 0.06
2	n = 3	R = 10^8 TU GFP	4	0	12±5 days	1.1±0.5	p = 0.88
		L = 10^8 TU beta-gal	n.a.	n.a.	> 12±5 days	n.a.	p = 0.07
3	n = 3	R = 10^7 TU GFP	4	4	> 10 months	0.2±0.03	p = 0.41
		L = 10^7 TU beta-gal	n.a.	n.a.	> 10 months	n.a.	p = 0.08
4	n = 3	R = 10^6 TU GFP	3	2	> 10 months	0.1±0.1	p = 0.20
		L = 10^6 TU beta-gal	n.a.	n.a.	> 10 months	n.a.	p = 0.03

* One animal terminated expression at 38 days.

Table 4: Characteristics of transgene expression imaged serially in vivo.

These results indicated that quite high level and sustained transgene expression focused to the TM was feasible after a single transcorneal injection, that it could be monitored gonioscopically, and that GFP (from Aequorea) was preferable to Renilla GFP. Because of the high level of GFP expression achieved with 10^8 TU, the loss of expression in one of these maximally-transduced animals might be due to the previously reported phenomenon of GFP-specific over-expression toxicity.[760, 762, 764-770] I therefore proceeded to examine further the parameters affecting GFP expression

in dose response studies, this time using ß-galactosidase vector[324] as a control in the companion eye rather than Renilla GFP vector (Table 4). In Group 2 (10^8 TU for each vector), the extent of GFP and ß-galactosidase expression were comparable (Figure 32), and all animals developed sustained grade 4 GFP expression. They attained the plateau of GFP expression 5-fold faster (Figure 32, Figure 34) than the animals of group 1 ($p = 0.03$). Here, the rate of marker protein accumulation VF was 1.1±0.5 grades/day. Consistent with toxicity from rapid GFP over-expression, the intense fluorescence in all Group 2 animals was observed to terminate abruptly after a mean of 12±5 days, concurrent with a brief iritis. In contrast, and consistent with the results of ß-galactosidase vector transduction in human eyes,[324, 504] high-level ß-galactosidase expression was found in the same animals at sacrifice after GFP expression had disappeared in the other eye (Figure 32). Thus, the cytotoxicity observed was marker protein-specific and the result of rapidly developing GFP over-expression. Immunolabeling with leukocyte lineage-specific antibodies in histological sections of eyes from cats experiencing this short-lived GFP over-expression showed numerous T cells, but not neutrophils or macrophages, in the TM, as well as loss of TM cells (Figure 35). Sections of Renilla GFP expressing eyes also demonstrated occasional T-cells. No infiltrates were present in companion eyes expressing ß-galactosidase. Sera of cats with short-term expression did not react in immunoblots with GFP, which was readily detected with commercial anti-GFP sera (data not shown).

These results were encouraging because they indicated that the method was effective enough to enable marked protein over-expression in the TM. Because of that, I injected reduced vector doses (animal groups 3 and 4, receiving 10^7 and 10^6 TUs respectively, again via single transcorneal injections). 10^7 TU also produced a median expression grade of 4, which was not significantly different from group 2 ($p = 0.37$). Importantly, however, at this lower dose, the grade 4 GFP expression was reached noticeably slower than in group 2 (VF was 0.2±0.03 grades/day, Table 1). A clear difference with Groups 1 and 2 was that GFP expression persisted until sacrifice at the 10 month-post injection endpoint of the study, and remained Grade 4 throughout. Thus, 10^7 TUs emerged as the optimal dose for the GFP vector, while ß-galactosidase was tolerated well at 10^8 TUs. Group 4 animals (10^6 TU GFP vs. ß-galactosidase vector, or 2 logs less vector input than animals in groups 1 and 2) corroborated these results and clarified dose requirements. They had a maximum median expression

grade of 3, with a VF of only 0.1±0.1. The expression persisted at grade 2 until sacrifice at 10 months. The results indicate that an optimal GFP vector dose substantially below the peak of the achievable dynamic range can be selected (10^7 TUs in the case of this GFP vector) to achieve long-term gene expression in the TM.

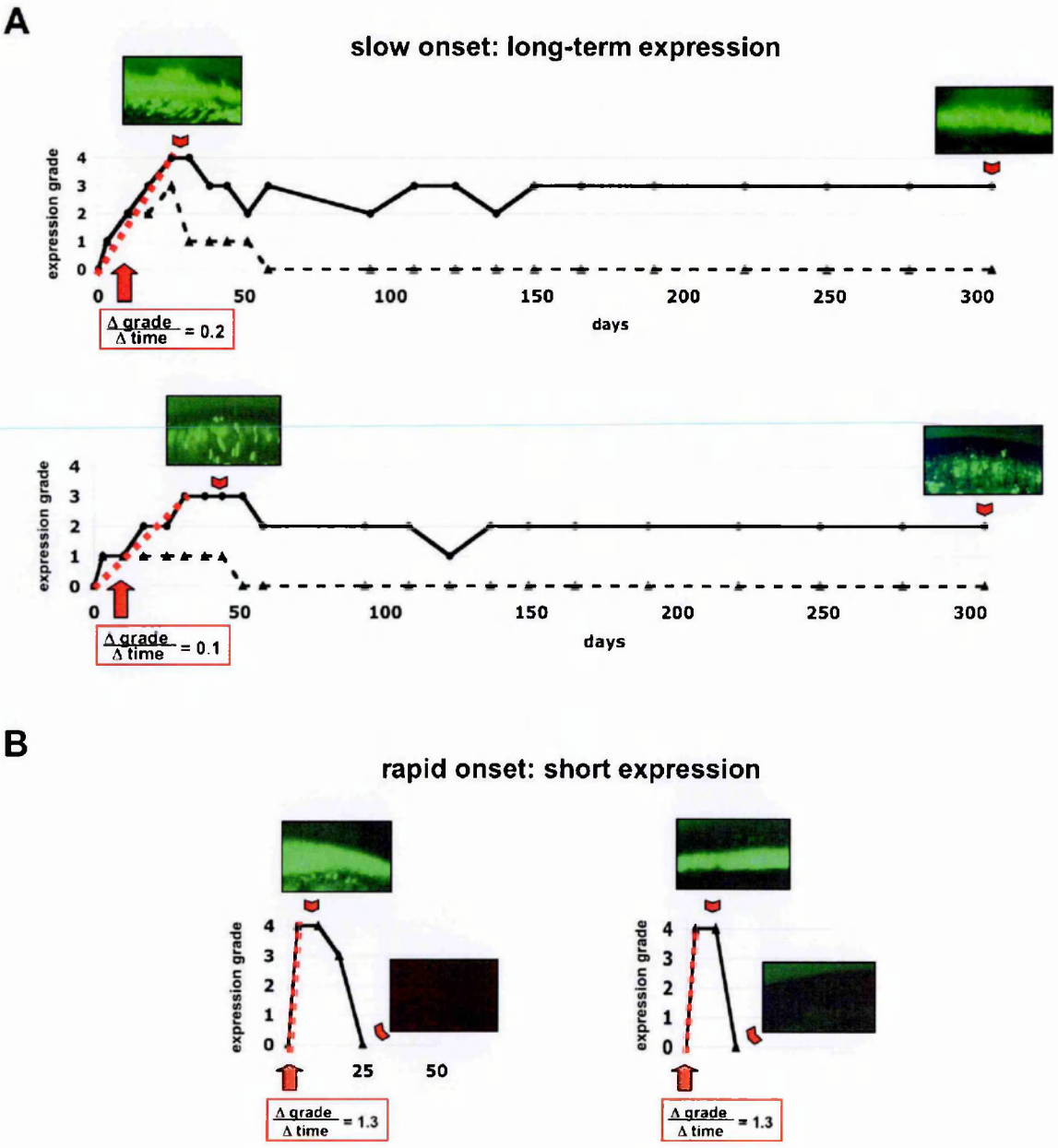

Figure 34: Rate of initial GFP accumulation determines whether successful long-term GFP expression is established. (a) Expression slowly reached peak levels in two cats from group 1 transduced with 10^8 TU GFP vector (right eye) and Renilla GFP vector (left eye), resulting in stable fluorescence of GFP, but not Renilla GFP. (b) Rapid GFP over-expression in animals of group 3 that were also transduced with 10^8 TU GFP vector triggered an iritis that eliminated transduced cells. Dotted red line illustrates onset of expression. Inserted photos show actual gonioscopic view of TM as indicated.

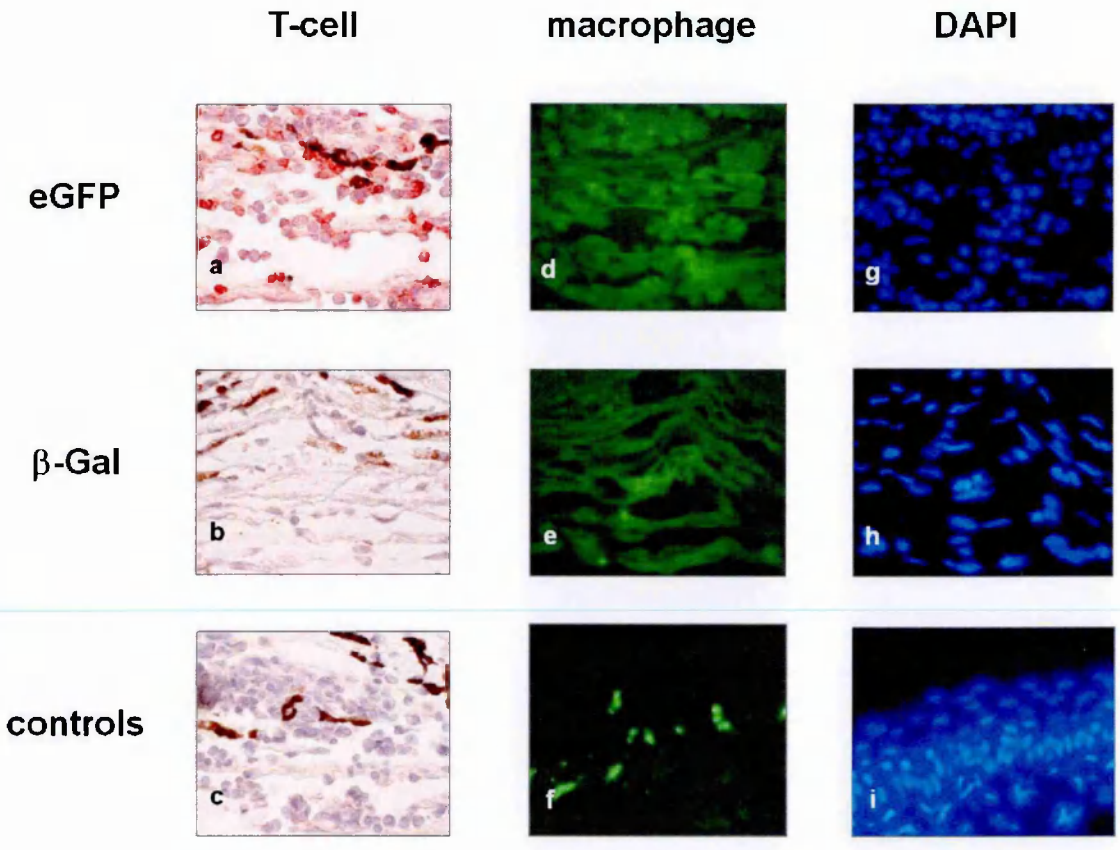

Figure 35: Antibody staining for T-cells (anti-CD3: a, b and c), macrophages (anti-myelomoncyte: d, e and f) and DAPI staining (g, h and i). Shown are sections from a TM transduced with eGFP (a, d and g) after loss of expression and the β-galactosidase transduced partner eye (b, e, h). Only the eGFP transduced TM is infiltrated by T-cells (a), but not macrophages (d), while there is no infiltrate in the other eye. Control c is an isotype control section from the same eGFP eye (c). Control f the corneo-conjunctival junction where macrophages are expected (f and i).

8.1.6.1.1. Intraocular Pressure

The initial IOP of all transduced eyes was not different from IOP at the end of the study ($p = 0.4$). Days to weeks after application, cats had a brief increase in IOP ($33\pm34\%$, $p<0.01$) followed by return to normal pressures, which may be consistent with corticosteroid induced ocular hypertension.[771, 772] In support of this inference, IOP change in non-premedicated pilot animals was minimal with GFP vector ($n = 3$, IOP change = $3\pm5\%$, $p = 0.4$) or ß-galactosidase vector ($n = 3$, IOP change = $1\pm1\%$, $p = 0.4$).

8.1.6.1.2. SIN Modification

	CMV.eGFP.IRES.neo	
	GINWF	FGINSIN
eGFP TU/ml	1.6 x10^6	7.8 x10^5
cpm/ml	4.0 x10^6	1.5 x10^6
ratio	40:100	50:100

Table 5: Differences of eGFP expression. SIN modification of the FIV-LTR slightly improves eGFP expression levels from internal CMV.eGFP.IRES.neo cassette. Cpm/ml = counts per minute per ml in RT assay, eGFP TU/ml = eGFP transducing units per ml determined with flow cytometry, GINWF = internal CMV.eGFP.IRES.neo cassette, FGINSIN = internal CMV.eGFP.IRES.neo cassette.

SIN vector FGINSIN had a slightly higher ratio of eGFP TU per RT than GINWF-G230 (50:100 vs. 40:100, **Table 5**). In conclusion, the SIN deletion of the FIV 3'-LTR did not negatively affect vector function.

8.2. Transgenesis of the Retinal Pigment Epithelium with FIV Vectors as a Basis for Gene Therapy of Retinal and Choroidal Diseases

8.2.1. Comparison of Wild-Type and Class I Integrase Mutant-FIV Vectors in the Retina Demonstrates Sustained Expression of Integrated Transgenes in Retinal Pigment Epithelium

8.2.1.1. Results

8.2.1.1.1. Eyes Analyzed

For the comparison of subretinal and intravitreal injections, all injected animals were available for analysis at the conclusion of the study (n = 39 in the subretinal group, and 38 in the intravitreal group). In the intravitreal group, six pairs of eyes were unreadable due to problems in tissue processing, leaving 32 pairs for analysis. Therefore, 39 right eyes subretinally injected with the β-galactosidase-encoding FIV vector, CT25, and 32 right eyes intravitreally injected with CT25 could be analyzed. Control left eyes were treated as follows: (1) FIV mock vector (n = 13 subretinal, n = 11 intravitreal), (2) DMEM+10% FCS (n = 13 subretinal, n = 10 intravitreal), and (3) no injection (n = 24). For the long-term expression/integration study, all 37 animals survived from injection to outcome. Ten animals injected subretinally were analyzed at 2 months, 10 at 3 months, and the remaining 17 at 7 months. All eyes in all groups were evaluated and scored in random sequence by an observer blinded to injection assignment.

8.2.1.1.2. Comparison of Subretinal and Intravitreal Injection

VSV-G-pseudotyped FIV vectors were injected either subretinally or intravitreally. Following subretinal injection, *β*-galactosidase expression was found in 15 of 19 retinae (79%) at 2 days and in 19 of 20 (95%) retinae at 7 days (**Figure 36**) and expression was widespread (**Figure 37** a), with some eyes showing nearly complete transduction of the retina. Cross-sectional histology revealed extensive *β*-galactosidase activity in the retinal pigment epithelium (RPE) (eyes from representative animals are shown in **Figure 38** a and 3b), with more than half of RPE cells expressing the marker gene. Antibody labeling for *β*- galactosidase in one additional litter confirmed transduction of the RPE in eyes injected subretinally (**Figure 38** c and d). No transgene activity was detected in noninjected control eyes or control eyes injected subretinally with mock FIV vector or DMEM+10% FCS.

Occasionally, endogenous β-galactosidase activity was observed in the ciliary body (**Figure 37**); this was equivalent in uninjected and injected animals, and at a histological level was not confined to cell bodies. No other ocular tissues showed such endogenous activity, and no inflammation or virus-induced pathology was observed.

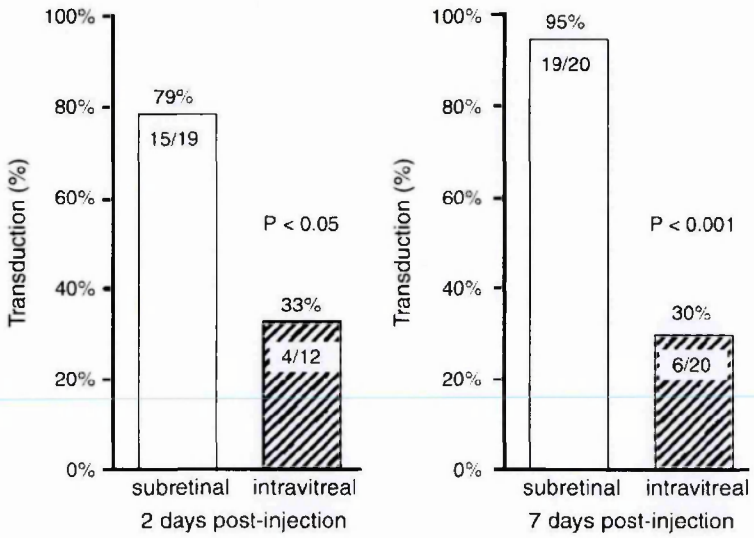

Figure 36: Proportion of eyes transduced 2 and 7 days after either subretinal or intravitreal injection.

In contrast to subretinal injections, reporter transgene expression was found in only 4 of 12 eyes (33%) at 2 days following intravitreal injection of the same volume of vector and 6 of 20 (30%) eyes at 7 days (**Figure 36**). Also, in clear contrast, expression in eyes receiving intravitreal injections was limited to a small area of retina directly adjacent to the injection site (**Figure 37**c). As in control eyes for subretinal injections, no reporter transgene activity was detected in control eyes intravitreally injected with mock vector or DMEM + 10% FCS, or in non-injected eyes, and no inflammation or pathological change was seen. In summary, subretinal injections resulted in a significantly greater proportion of transduced retinae than intravitreal injections at both 2 and 7 days following injection ($p < 0.05$ and <0.001, respectively). Subretinal injections also caused transduction of a larger retinal area compared with intravitreal injections. Subretinal injections resulted in virtually complete RPE transduction, while only patchy transduction was observed near the injection site of intravitreally injected eyes.

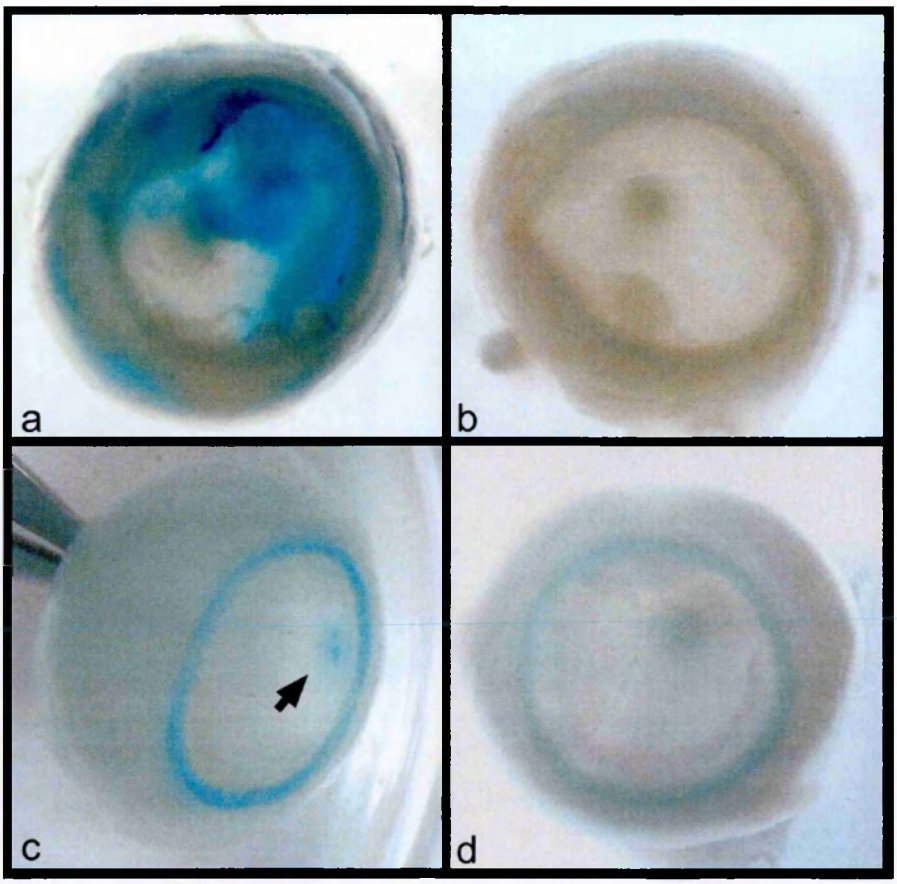

Figure 37: Representative eyes injected *subretinally* with (a) CT25 vector and (b) subretinal injection control, or injected *intravitreally* with (c) CT25 vector and (d) intravitreal injection control. Note the larger area of transduced retina with subretinal injection (a versus c, arrow). Endogenous β-galactosidase activity in the ciliary body was occasionally observed, and was equivalent in both uninjected and injected eyes, as seen in panels (b)–(d) (blue ring).

8.2.1.1.3. Long-term Expression and Integration

In the second group of experiments, I examined duration of expression, compared wild-type, and class I integrase-mutant vectors. Right eyes of 37 rats were injected subretinally with CT25 and left eyes were injected with CT25.D66V. Preparation of CT25.D66V was identical to the preparation of the integrase-competent CT25 with the exception of using packaging plasmid CF1Δenv.D66V, in which the only change from CF1Δenv is the single amino acid in integrase. Class I properties (selective block to integrase catalytic function without disruption of other Gag/Pol functions, equivalent to those described for HIV-1 integrase D64V) have been systematically validated in tissue culture studies for this mutant of FIV integrase and were reported

elsewhere.[279] Reverse transcriptase (RT) activity was determined in triplicate as described for both CT25 and the integrase mutant CT25.D66V and animals were injected with equal RT units of each vector.[261]

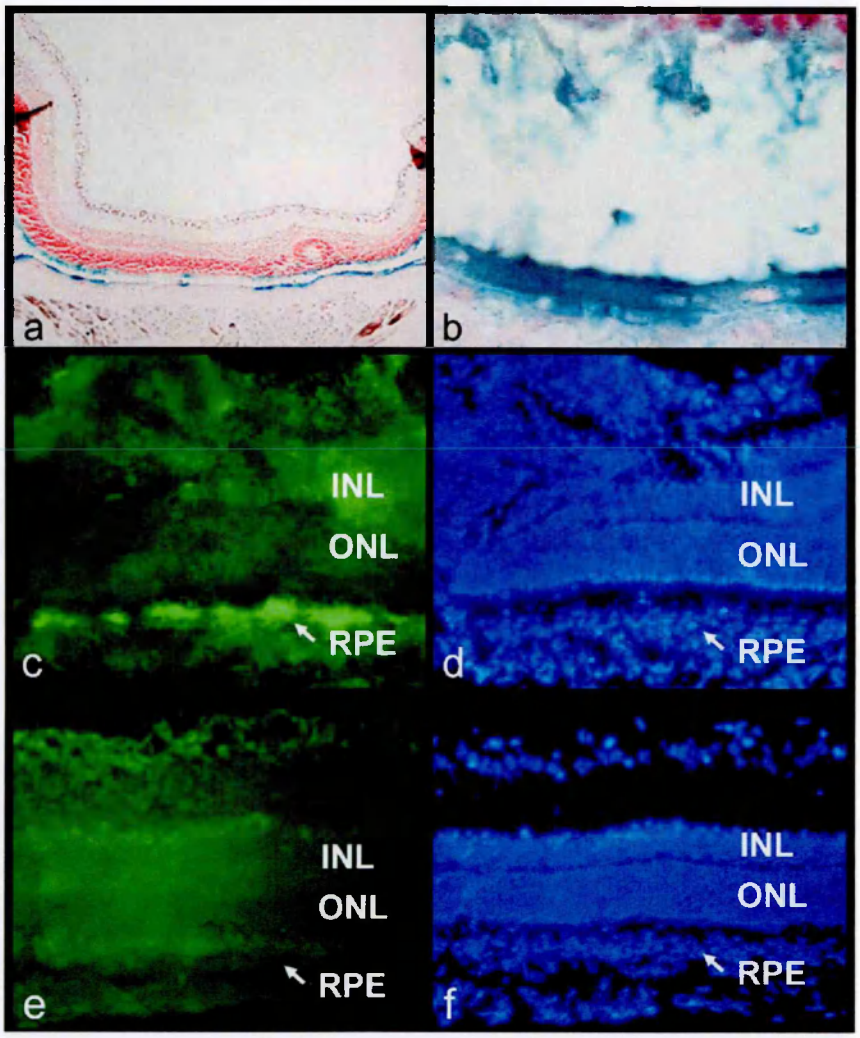

Figure 38: Examples of representative cross-sectional histology confirming transduction of the RPE. Paraffin sections (a and b) counterstained with neutral red showing β-galactosidase activity as blue stain within the RPE at both low power (a, 65x) and high power (b, 1100x). Antibody labeling for β-galactosidase confirmed limitation of marker gene expression to the RPE (400x; INL = inner nuclear layer, ONL = outer nuclear layer, RPE = retinal pigment epithelium). CT25 injected eye with (c) anti-β-galactosidase antibody staining and (d) DAPI counter stain. (e, f) Non-injected control eye.

10 animals were evaluated at 2 months, 10 were evaluated at 3 months, and 17 were evaluated at 7 months post-injection. All eyes injected subretinally with CT25 demonstrated extensive, confluent areas of β-galactosidase expression in the RPE

(**Figure 39**). At the longest time period (7 months), 60% of eyes demonstrated such expression in more than half of the total area of the retina (**Figure 39** e), with the remainder ranging from a punctate distribution in one quadrant up to 50% or less of the total retinal area. In addition, occasional cells in inner retinal layers expressed β-galactosidase at 3 and 7 months (**Figure 39** a and d). In contrast to CT25- injected eyes, fellow eyes injected with CT25.D66V vector had no or only very rare cells expressing β-galactosidase (**Figure 39** c and f). Incidence and extent of expression at 2, 3, and 7 months were the same, with widespread areas of transduction after CT25 injection and only very sparse, punctate staining with the integrase mutant CT25.D66V.

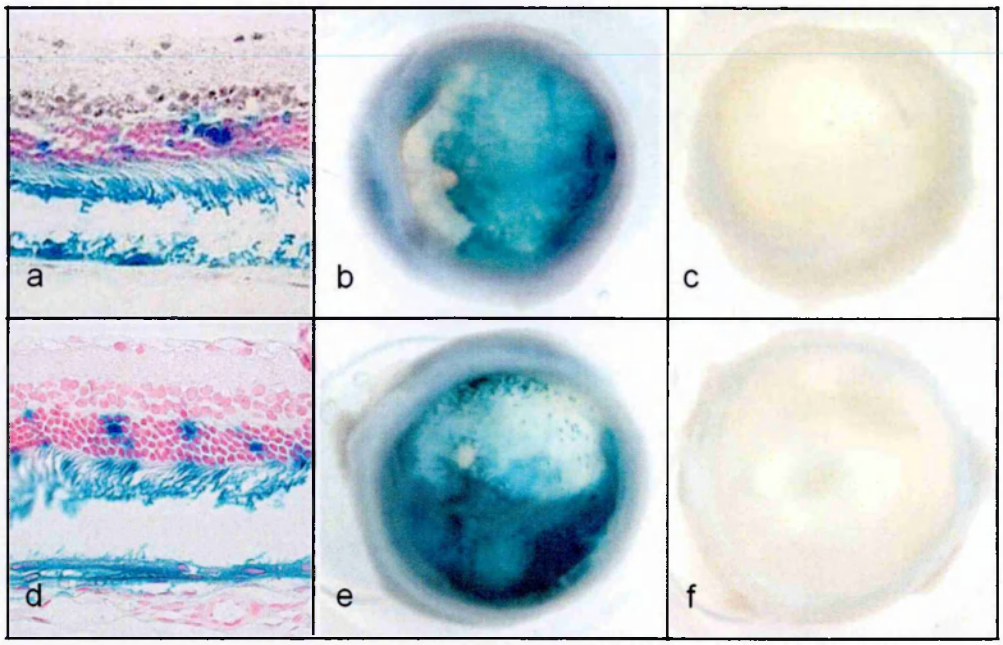

Figure 39: Cross-sectional histology (a and d) and whole eye cups (b, c and e, f) of representative eyes 3 (a–c) and 7 months (d–f) after subretinal injection with CT25 vector (b and e), and CT25.D66V (c and f). Vector particles, which differ in only one amino acid, were normalized to equal RT units.

8.2.2. Long-Term Retinal Transgene Expression with FIV versus Adenoviral Vectors

8.2.2.1. Results

8.2.2.1.1. Dose-Response Study

To determine the optimum vector dose for the subsequent long-term expression study, eyes injected subretinally with 3 different doses of FIV and Ad vectors were assessed at 2 days post injection for β-galactosidase expression.

At the highest dose of 2×10^5 TU, all animals survived to the study endpoint. All 14 FIV vector injected eyes and 13 of 14 Ad vector injected eyes showed transduction with a median grade of 3 with each vector ($p = 1$). In contrast, at a dose of 2×10^4 TU, 9 of 13 (69%) FIV vector injected eyes showed expression, compared to 5 of 13 (38%) Ad vector injected eyes. The median grade of transduction was greater in eyes injected with 2×10^4 TU FIV vector, but this was not statistically significant (median grade 2 versus 0; $p = 0.22$). Only 2 of 12 (17%) eyes injected with 2×10^3 TU FIV vector and 4 of 12 (33%) eyes injected with Ad vector showed expression. One rat injected with 2×10^4 TU, and two rats injected with 2×10^3 TU, died prior to sacrifice, and therefore were not analyzed. None of eyes from non-injected control animals showed transduction. Based on these results, 2×10^5 TU was chosen for the following long-term expression study.

8.2.2.1.2. Long-Term Expression Study

Nearly all eyes (96%) through all time points of the study showed some degree of transduction (**Figure 40**). Analyzing data from all eyes across the entire 16 month study, FIV vector produced a higher distribution of grade of expression than Ad (**Figure 40**, $p = 0.01$, Wilcoxon signed-rank). Analyzing each time point separately, differences in expression grade were statistically significant at 6 months, when FIV vector transduced eyes had a higher grade than Ad eyes ($p < 0.05$) (**Figure 40**). At all other time points beyond one week, FIV vector transduced eyes had higher grades of transduction than Ad eyes (**Figure 40**), though these differences were not statistically significant due to low statistical power. For example, at sixteen months, 4 of 7 FIV vector transduced eyes were grades 3-4, while none of the Ad eyes achieved this degree of transduction, but individual time point comparisons were limited by low statistical power.

Grades of expression across the 16 months suggested that FIV vector expression increased to a maximal level at 3 months, with some subsequent reduction in extent (**Figure 40**). In contrast, Ad vectors appeared to yield more immediate expression, peaking at 1 week, with a decline thereafter (**Figure 40**).

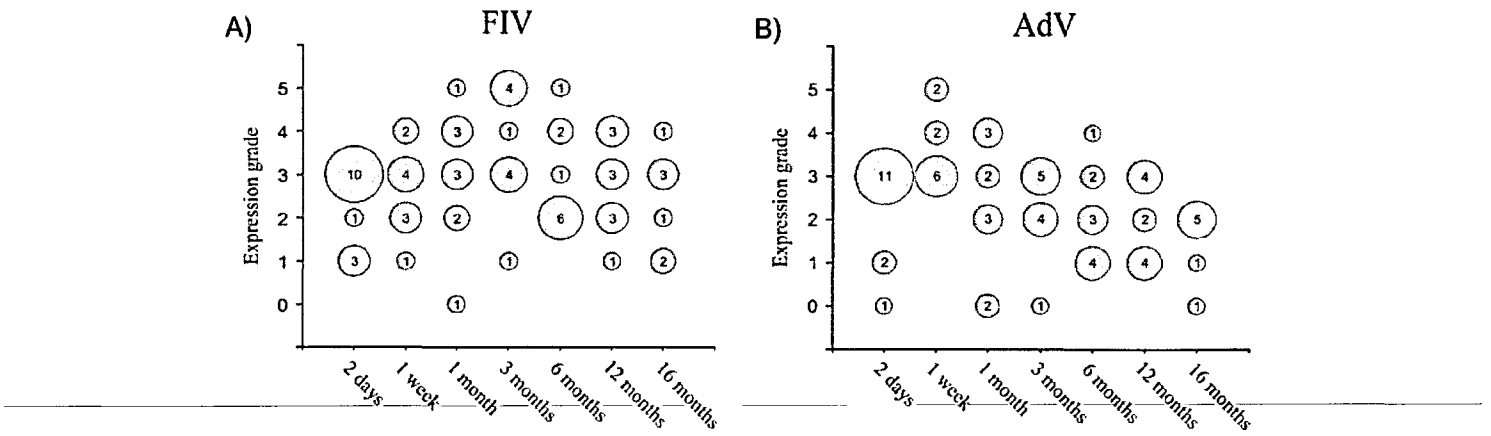

Figure 40: Time course of β-galactosidase expression. FIV is shown in panel A, and Ad vectors are shown in panel B. Circle sizes represent the number of animals at each grade. FIV expression reached a maximum extent at 3 months and then decreased, while expression from Ad vectors reached its maximum extent at 1 week.

When cross-sectional histology was examined, the retinal pigment epithelium showed β-galactosidase expression with both vectors at day 2 (**Figure 41**). In eye cups that had lower grade of transduction the staining was greatest in the quadrant that corresponded to the site of injection. The retinae had multiple folds (not shown), similar to our findings in previous studies using subretinal injection. At day 7, expression was similar to day 2 (**Figure 41**).

At 1 month, extensive β-galactosidase staining could be seen throughout the retinal pigment epithelium, associated with staining of the adjacent photoreceptor outer segments (**Figure 41**). Some individual cells in the inner retinal layers in both FIV- and Ad vector injected eyes were transduced. In Ad injected eyes, there was evidence of infiltration by large cells morphologically consistent with macrophages (**Figure 41**, see insert shown in 16 month section) and extracellular β-galactosidase staining was prominent. The shallow retinal folds seen earlier with both FIV and Ad persisted, presumably secondary to subretinal injection and there were isolated areas of

intraretinal microcyst formation (not shown). Retinae from both groups showed areas of attenuation, consistent with resolving focal traumatic retinopathy (not shown), while the remaining retinal architecture remained intact.

At 3 months, 6 months and 12 months, FIV vector-injected eyes were similar to those at 1 month with the exception of the time-dependent increase of cells in the outer nuclear layer staining positive for β-galactosidase. In Ad vector injected eyes, the intensity of RPE staining for β-galactosidase decreased over time. Transduced areas in Ad injected eyes often accumulated a focal cellular infiltrate and the previously normal retinal architecture appeared disrupted.

At the conclusion of the study (16 months), β-galactosidase positive cells were found in the RPE and occasionally in the inner and outer nuclear layers of FIV vector-injected eyes. There was focal traumatic retinopathy, while the rest of the retina showed normal retinal morphology. Ad vector injected eyes still expressed β-galactosidase, but were less extensively transduced and had larger areas with disrupted retinal architecture (**Figure 41**).

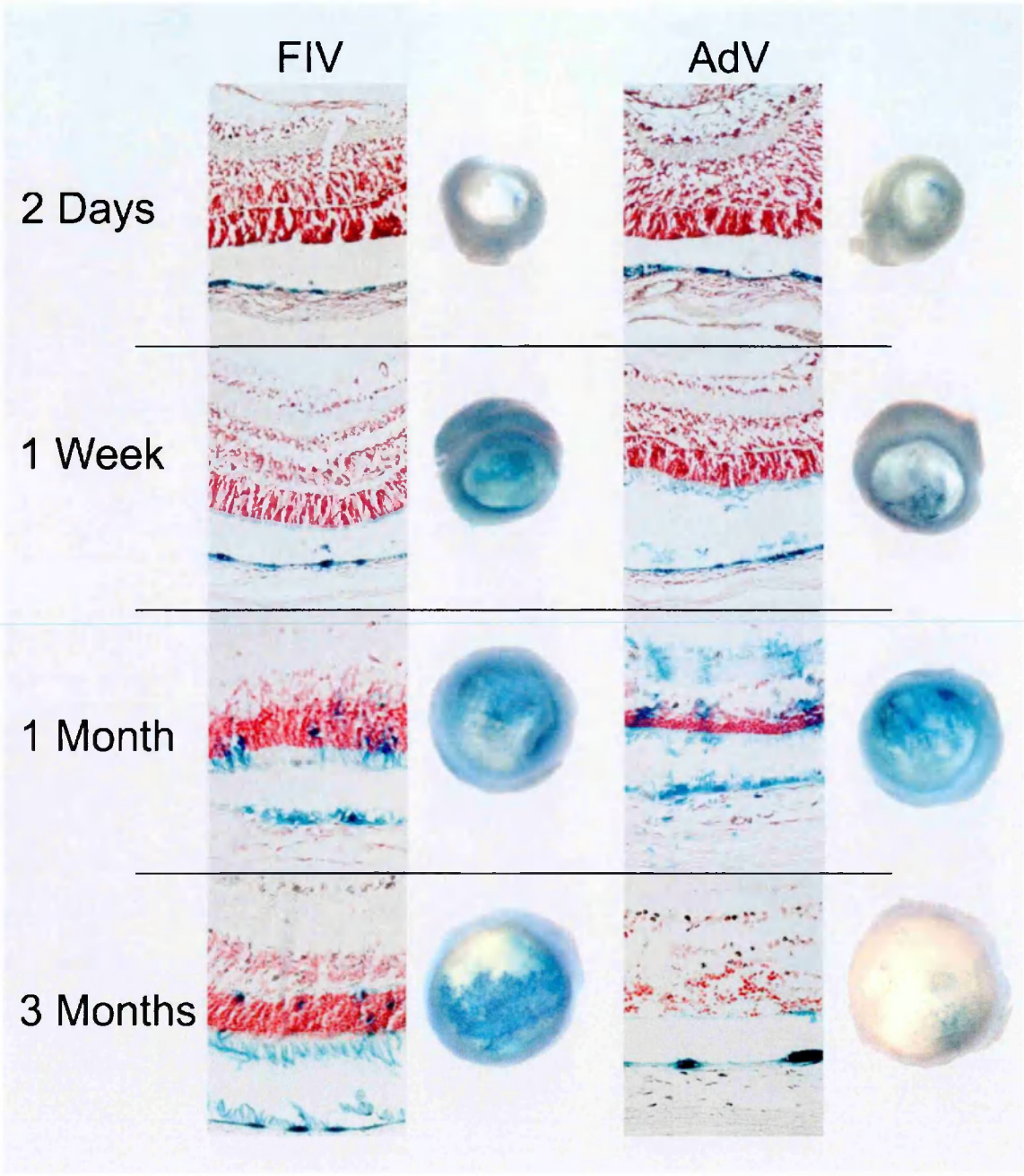
FIV
AdV
2 Days
1 Week
1 Month
3 Months

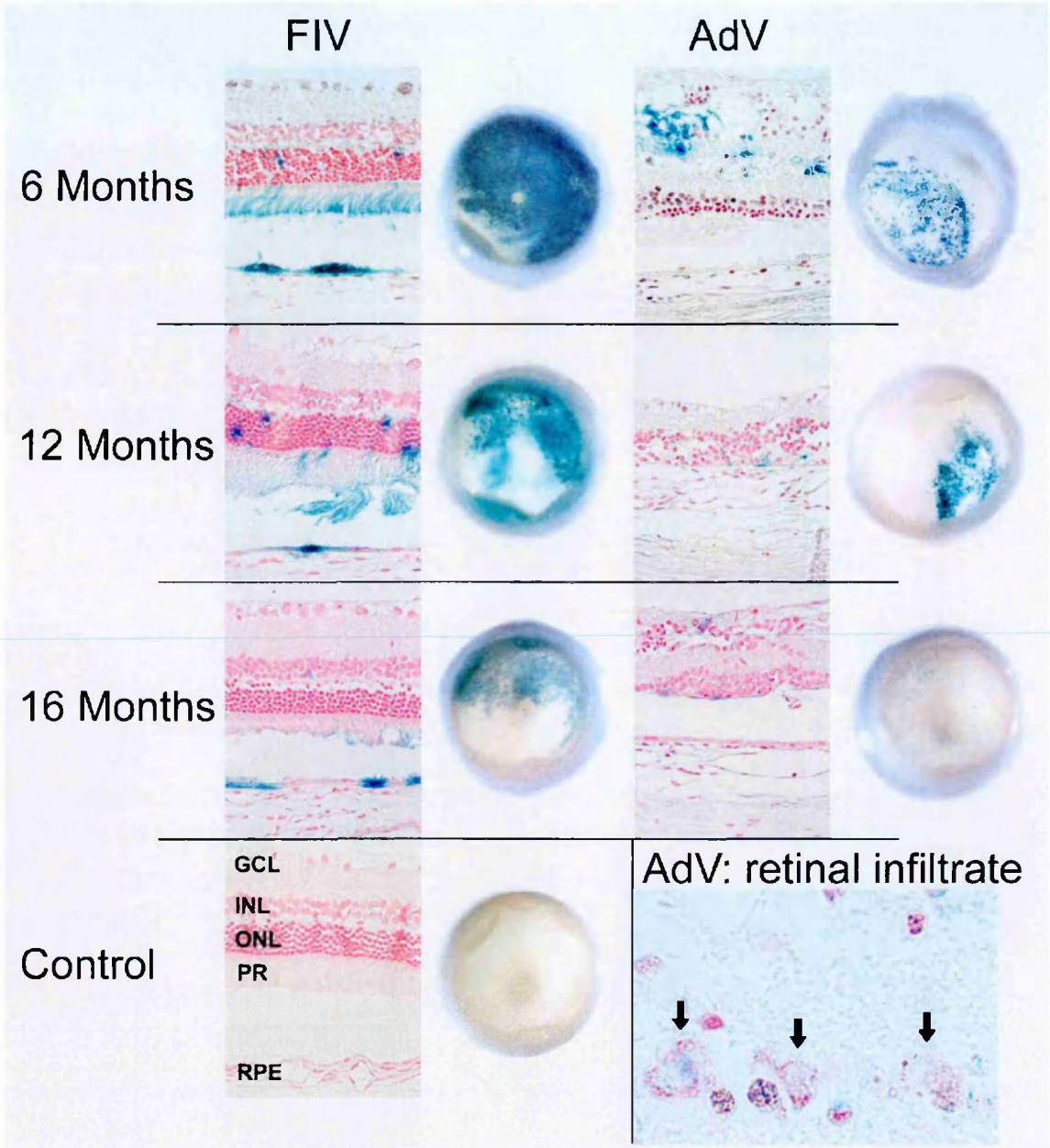

Figure 41: Representative eye cups and histological sections through the transduced retina of eye pairs from the same animal. Right eyes were injected with FIV, left eyes with Ad vector. When a retinal detachment was present in the section, images of neurosensory retina and RPE are shown in their normal spatial relationship. Insert: large, macrophage-like cells with abundant cytoplasm appeared to contain phagocytosed β-galactosidase positive material (arrows). Macrophage infiltrates were often seen in Ad transduced eyes after 3 months. Abbreviations (for control eye section): GCL = retinal ganglion cell layer, INL = inner nuclear cell layer, ONL = outer nuclear layer, PR = photoreceptor outer segments, RPE = retinal pigment epithelium.

9. Discussion

9.1. Transgenesis of the Ocular Outflow Tract with Lentiviral Vectors as a Basis for Gene Therapy of Glaucoma

9.1.1. Genetic Modification of Human Trabecular Meshwork with Lentiviral and Adenoviral Vectors versus Type-C Retroviral Vectors

The results demonstrate that lentiviral vectors effectively transduce the human trabecular meshwork in situ. The direct, controlled comparisons of vector systems using normalized vectors in the present work also demonstrated for the first time that lentiviral vectors derived from FIV can perform as effectively as a well-validated vector derived from a human lentivirus for transduction of a mitotically quiescent, differentiated human tissue. The consistently efficient transduction of trabecular cells with two different lentiviral vectors but not with equal numbers of transducing units of a murine leukemia virus vector establishes vector properties needed to achieve genetic modification of the meshwork, and is consistent with evidence that turnover of TM cells is minimal in vivo.[235, 242, 243] For example, gross injury from laser trabeculoplasty stimulates [^{3}H]thymidine labeling of TM cells, but processes often associated with decreased outflow facility and glaucoma (such as increased phagocytosis, inflammation, and hyphema) do not.[235, 242, 243] The finding that lentiretroviral vectors but not onco-retroviral vectors transduce the trabecular meshwork is additional evidence that trabecular cells are mitotically quiescent in vivo.

Anterior chamber injection is a routine ophthalmologic procedure that requires only local anesthesia. The present results suggest that administration of lentiviral vectors into the anterior chamber circulation has potential to deliver therapeutic genes to the trabecular meshwork. The preferential transduction of the TM over other outflow tract structures may be an in vivo correlate of the enhancement of transduction that is produced by perpendicular convective flow of retroviral vector supernatants through target cell monolayers grown on porous substrates.[773] This targeting effect was not completely selective, because a few β-galactosidase-expressing cells could also be detected in some eyes in the outflow pathway both downstream (Schlemm's canal and collector channels) and upstream (corneal endothelium in proximity to the TM, and the transition zone between ciliary muscle and TM). Additional strategies, for example, transcriptional targeting, may be useful in this regard. This has been

successfully demonstrated by Liton et al.[645] The authors used the chitinase 3-like 1 (Ch3L1) gene promoter after a comparative expression analysis of trabecular meshwork and Schlemm's canal cells to restrict adenoviral vector expression to the TM of adenoviral vectors that contained a Ch3L1 promoter driven lacZ cassette. Ch3L1 is a mammalian glycoprotein member of family 18 glycosyl hydrolases that is involved in tissue remodeling and inflammation and acts as a growth factor for connective tissue cells and as a potent migration factor for endothelial cells which could also play a role in both the normal physiology of the TM and the abnormalities that occur in glaucoma. Gonzales et al. found in a similar experiment by the same group that promoter fragments from the matrix Gla protein can specifically direct expression to the trabecular meshwork, while use of the vascular endothelin-cadherin gene promoter even allows differentiating between vascular and Schlemm's canal endothelial cells.[646]

Vectors that transduce nondividing cells but do not predictably integrate into the cellular genome also have potential to express transgenes in the human TM, as found here and previously.[244] However, glaucoma is a chronic disease. Aqueous outflow impairment requires long-term control, which is best addressed by a vector that stably integrates as an obligate part of the transduction process. In addition, adenovirus vectors can trigger marked inflammation, which could exacerbate glaucoma. The importance of investigating long-term expression is underscored by work that identified a stably abnormal gene expression profile in the glaucomatous TM.[150] Although a gene mutation has been associated with glaucoma,[143] a therapeutic gene has yet to be described. Lentiviral vectors will facilitate study of candidate genes in the human organ perfusion model and in animals.

9.1.2. Preservation of Aqueous Outflow Facility after FIV-Mediated Transduction of Anterior Segments of Human Eyes

The goal of glaucoma gene therapy directed to the anterior chamber is to restore and preserve aqueous outflow through the TM. For therapeutic transgenes to be validated and for eventual clinical application to proceed, a method not only has to be stable but non-toxic modification is needed that does cause intraocular pressure to be dangerously high during or immediately after transduction. This capability is necessary for experimental evaluation of candidate therapeutic genes and for eventual

use of those genes in therapy. In particular, the method of gene transfer must not cause counterproductive disruption of aqueous outflow through the TM. My histological analyses in transduction experiments of human eyes with FIV, HIV, MLV and adenoviral vectors proved that cellularity is well preserved and that lentiviral vector transduction is minimally toxic. In the next set of experiments I extended these results by demonstrating that *eGFP* can also be used as an effective marker gene and that the extensive transduction observed with these vectors does not significantly impair outflow facility. I used more refined, second-generation vectors that incorporated the FIV central DNA flap that Todd Whitwam identified[492] and cloned into the eGFP vector I had engineered and WPRE, as had been demonstrated to improve transgene expression levels in other lentiviral vector systems.[734]

Aqueous humor outflow is a complex process that is not completely understood. The unique architecture of the TM, the phagocytic biology of the cells, their arrangement within a collagenous lattice and the extracellular matrix they populate are all believed to play important roles. A final regulatory step may occur at the interface of the TM with Schlemm's canal, where bulk flow occurs through large outpouchings (giant vacuoles) in the endothelium.[774] A potential concern for gene therapy is that gene transfer methods might disrupt the physiology of this structure. Despite a high level of transgene expression, FIV vector–mediated gene transfer caused only transient, slight (mean of 30%) declines in outflow facility, with stable return to normal baseline levels from 48 to 72 hours after transduction until the end of the experiment at 5 days. These results compare favorably with those obtained by Borrás et al.[774] in the same model after injection of adenoviral vectors. After injection of 1×10^8 TU of adenoviral vectors, outflow facility declined 13% compared with control eyes within the first 4 hours, and was reduced by 54% after 12 hours. Subsequently, baseline outflow facility was reached at 36 hours and continued to increase to approximately 20% higher than baseline until the end of the experiment at 48 hours.[628] As in my previous experiments,[504] I observed preferential transduction of TM. Targeted transduction prevents unwanted effects of transgene expression on neighboring structures. This is of particular importance in ocular gene therapy, in which anatomic structures in close proximity serve highly specialized functions.

9.1.3. Long-Term Genetic Modification of the Outflow Tract Coupled with Non-Invasive Imaging of Gene Expression In Vivo

Any gene therapy for glaucoma and the proper investigation of glaucoma associated genetic mutations requires a method that is simple to administer and can provide long-term, stable, high-grade, and properly targeted transgene expression within the anterior chamber. The experiments with domestic cats demonstrated that long-term, serial in vivo imaging of transgene expression is possible and that transduction can lead to stable genetic modification in living animals for 10 months. The effectiveness of gene transfer was so high that at the highest doses rapidly accumulating GFP expression resulted in toxicity from overtransduction. In contrast, administration of equivalent ß-galactosidase vector also produced high level expression but without toxicity. Toxicity of GFP is well-described, particularly at maximal expression levels, and appears to be cell-type-dependent.[760, 762, 764-770] Since eGFP is not amplifiable (one molecule equals one fluorophore, whereas enzymatic markers can convert many molecules of substrate to detectable dye), at least 10^5 molecules per cell are needed for the cell to yield twice the background fluorescence.[762] This estimate is a lower boundary as it assumes perfect eGFP maturation; incomplete maturation would raise the threshold higher.[762] Undoubtedly, many more than 10^5 molecules per cell are needed to image through the cornea and to produce the high grade fluorescence observed here. As the same applies to the titration of FIV vectors, it is possible that the same number of transducing units of eGFP expressing vectors is a much higher number of physical vectors particles and a higher m.o.i. than with ß-galactosidase vectors. That lower doses circumvented this problem while resulting in GFP expression that was still readily imaged in the living animal makes clear that a high dynamic range of gene delivery and expression was achieved. Consistent with results of others,[761] the use of Renilla GFP did not offer advantages in the TM. Renilla GFP was originally advertised as a fluorescent molecule with better biocompatibility but this has not been solidified in a stringent way and may represent company-intern findings by the vendor.

As seen in human eyes, I again observed preferential transduction of TM over other ocular structures in cats which is consistent with the results in perfused human anterior chambers.[324, 504] This targeting may be an in vivo correlate of the enhancement produced by perpendicular convective flow of retroviral vector

supernatants through target cell monolayers grown on porous substrates.[775] In addition, the tropism of these VSV-G pseudotyped lentiviral vectors may favor certain cell types, as seen for example in the subretinal space where the retinal pigment epithelium is preferentially transduced. Thus aqueous humor flow dynamics and cell-specific permissiveness to transduction by these vectors may both be factors. Strict targeting in these larger eyes has not been seen by two other groups who used rodent eyes, the mouse[278, 642] and the rat.[640] It is possible that this is a species specific observation and a result of lentiviral restriction in corneal endothelial cells.[776] On the other hand, it is unlikely that the large amount of lentiviral vectors does not cause saturation of restricting factors[776] in corneal endothelial cells but does so in trabecular meshwork cells. More likely, convection and flow are different in small rodent eyes: in the cat and in human eyes the central cornea is further away from the draining structure, the trabecular meshwork than in rodent eyes (**Figure 17**). Occasionally injected air bubbles may have contributed to protection of corneal endothelium as is commonly done prior to surgery of mature cataracts when trypan blue is injected underneath air to only stain the anterior surface of the lens immediately before capsulorhexis. As of note, I observed some transduction of corneal endothelial cells directly adjacent to TM (Figure 24). Another possibility is that manipulation of small rodent eyes creates more corneal warping and stretching compared to the larger eyes which may induce endothelial cell cycling of this non-dividing cell. It is known that cell division facilitates lentiviral transduction[777] although these vectors have a evolved a specialized mechanism that allows transduction of non-dividing cells, a feature that distinguishes them from type-C retroviral vectors.

As in human donor eyes,[324, 504] high level transduction could be performed without detriment to aqueous humor outflow or the histological fine structure, indicating that these replication-defective lentiviral vectors have favorable toxicity profiles for further investigation of glaucoma gene therapy. This was reflected in an only moderate and transient change of intraocular pressure.

There is a critical need for a realistic animal model for glaucoma. The results establish that prolonged, targeted, and multi-grade expression of transgenes in the disease-relevant tissue is possible. After completion of the studies for this thesis, we have explored this in the cat model that I developed here using myocilin and myocilin

mutant expressing vectors.[641] However, co-expression with enhanced GFP of myocilin or a juvenile glaucoma-associated mutant myocilin did not elevate IOP.

The association of myocilin gene mutations with familial glaucoma was recognized a decade ago;[143] a number of disease-associated mutations have been identified.[177, 778] Since various studies suggest that the heterozygous state for many of these mutations is associated with POAG,[779] we hypothesized that prolonged expression of a glaucoma-associated mutant (and possibly even additional wild-type protein expression) might produce elevated IOP in cats. It is possible that the feline outflow pathway may not be vulnerable to myocilin-related pathophysiology or the feline Y423H mutant chosen for study may differ from the human Y437H mutant protein in structure or other aspects. However, feline myocilin did behave similarly to human myocilin with respect to intracellular trafficking, with the Y423H mutant retained in the cell similar to human Y437H and the wild-type proteins undergoing export. The lack of significant IOP elevation we observed could be due to inadequate expression, or lack of uniform expression in all cells, since our immunofluorescence analyses using an epitope-tag do not establish the degree of expression of the exogenous myocilins relative to endogenous levels. However, consistent with our study, transgenic mice with uniform Y423H expression also do not develop IOP elevation or glaucoma.[780] Taken together with clinical and epidemiological data, existing animal data suggest that development of IOP elevation is dependent on other factors in addition to a mutant myocilin protein. Finally, since the clinical time course of human genetic glaucomas is quite variable, and disease can take many years to become evident, our study may simply lack the necessary duration for detecting an effect on IOP despite its relatively long follow-up period. Although the Y437H has a relatively early onset phenotype in humans, these individuals do not develop glaucoma at 1–2 years of age (the term of our study) and the period of follow-up in the cats may well have been too short to detect an effect. The lentiviral vector feline model has the potential to produce a reliable, realistic animal model of POAG, but this will possibly also require alternative transgene approaches that can induce a realistic POAG-like state. While surgical or laser injuries to the full circumference of the TM can raise IOP,[781] such approaches cannot recapitulate the subtle outflow resistance problem in POAG and the gross injury destroys the therapeutic target, the TM.

The lack of a high fidelity full disease model of POAG with IOP elevation that can be followed to the endpoint of retinal ganglion cell death, should not prove to be an impediment of any great degree to pre-clinical therapeutic transgene testing. Small molecule therapies in current practice appear to utilize physiological mechanisms that are also available in the normal outflow pathway (reviewed in[782]). Normotensive eyes are currently used for pre-clinical animal studies of candidate IOP-reducing POAG therapeutics which have often used the domestic cat; this is because IOP reductions in normotensive eyes are predictive of efficacy in POAG and the minimal variation between eyes at baseline facilitates paired left to right eye comparison designs.[782]

9.1.4. Conclusions from Studies of Genetic Modification of the Outflow Tract and Future Directions

I have shown that lenti-retroviral, but not oncoretroviral, vectors allow the specific transduction of trabecular meshwork in human donor eyes and established a dose-response curve over 4 logs between injected vector number and transduction efficiency.[504] Despite high transduction efficiencies the outflow facility was affected only transiently and to a minor degree.[324] The fine structure of the trabecular meshwork remained unaltered.[324, 504] In the cat, a similar transduction efficiency and effect on outflow facility was observed. Vector function could be followed in real time for the entire study of 10 months.[586]

FIV-mediated transgenesis is a highly effective method to reprogram the outflow tract permanently. This opens entirely new options to develop realistic glaucoma animal models by injecting vectors into the anterior chamber that transduce a desired genotype.

Our results with myocilin mutants cast doubt on the idea that mutations are responsible for intracellular deposits of proteins that are undegradable by the proteasome and are essentially the equivalent of a neurodegenerative disease of the outflow tract. Ongoing in vivo experiments with feline myocilin mutants in the cat will help to better understand the pathomechanism that leads to the glaucoma phenotype.

Long-term genetic modifications for therapeutic purposes appear to be possible. This is the first basis for a gene therapy of glaucoma that can adequately address the

chronicity of glaucoma. Because transduction is targeted to the outflow structures, the choice of potential therapeutic transgene is also limited to proteins responsible for its regulation, which limits for instance regulation of aqueous humor production by the ciliary body. A variety of transgenes has been suggested for the therapeutic modification of TM. Transduction of stromelysin[629] to modify the extracellular matrix is attractive in theory, but will require well controlled expression to avoid autodigestion of the cellular network. Matrixmetalloproteinases also require activation by a complex system of other metalloproteinsases. Simple delivery of e.g. stromelysin cDNA ignores this fact[629] resulting in expression of inactive pro-stromelysin.

An attractive transgene for gene therapy is the small guanosine triphosphatase (GTP) Rho that regulates remodeling of the actin cytoskeleton during cell morphogenesis and motility. Rao et al. investigated the role of Rho kinase in the modulation of aqueous humor outflow facility.[783] The treatment of human trabecular meshwork and canal of Schlemm cells with a Rho kinase-specific inhibitor led to significant but reversible changes in cell shape and decreased actin stress fibers, focal adhesions, and protein phosphotyrosine staining. Based on the Rho kinase inhibitor-induced changes in myosin light chain phosphorylation and actomyosin organization, the authors suggested that cellular relaxation and loss of cell-substratum adhesions in the human trabecular meshwork and canal of Schlemm cells could result in either increased paracellular fluid flow across the canal of Schlemm or altered flow pathway through the juxtacanalicular tissue, thereby lowering resistance to outflow. Rho kinase is a potential target for the development of drugs to modulate intraocular pressure in glaucoma patients. However, adenoviral vector mediated transduction of TM with the RhoA gene's dominant-negative mutant protein showed only minor effects.[634]

C3 transferase could be of use as a therapeutic transgene because it selectively ADP-ribozylates Rho in its effector-binding domain on asparagine residue 41 and thereby abolishes its biological function.[784, 785]

Caldesmon is another protein with therapeutic potential as an actomyosin regulatory protein found in smooth muscle and nonmuscle cells.[786] Domain mapping and physical studies suggested that caldesmon is an elongated molecule with an N-terminal myosin/calmodulin-binding domain and a C-terminal tropomyosin/actin/calmodulin-binding domain separated by a 40-nm-long central helix.

A different approach is the transduction of enzymes that produce pro-inflammatory substances, e.g. cyclooxygenase catalyzing the first two steps in prostaglandin, thromboxane, and prostacycline synthesis from arachnidonic acid. Some of the most successful intraocular pressure lowering drugs mimic the effect of prostaglandin F_{2a} (latanoprost).[787] However, the effect of prostaglandins produced by cyclooxygenase, while potent, are not specific. It may be possible to cotransduce the appropriate receptor to make the effect specific. In order to create a production site of cyclooxygenase for the generation of prostaglandins, the jet during intracameral injection can be directed at different targets and repeatedly washed. The receptor should be expressed by the outflow structures and intraocular injection techniques would not have to be modified.

A more radical idea that I would like to pursue and have recently submitted for funding is trabeculoablative gene therapy to improve outflow and to create a model to study repopulation dynamics of the trabecular meshwork. The site of the highest resistance to outflow of aqueous humor is the juxtacanalicular trabecular meshwork[28, 136] and the principal site of pathology in primary open angle glaucoma (POAG).[137, 220, 221] Traditional therapies for advanced glaucoma attempt to lower intraocular pressure surgically by circumventing the outflow resistance of the TM by shunting aqueous humor to the subtenon space (e.g. *trabeculectomy*, *glaucoma drainage device*).[222] These filtering procedures have a high rate of complication and failure[226] despite the introduction of antimetabolites and improvement of drainage device design, respectively. The complete disruption of the TM and wall of Schlemm's canal has recently been achieved with the *trabectome*,[224] but this disruption is irreversible creating a permanently open connection to the downstream drainage system. Instead, trackable FIV vectors that co-express eGFP and herpes simplex virus thymidine kinase for selective ablation of the juxtacanalicular trabecular meshwork by ganciclovir[788] may offer a solution. HSV-tk converts the antiviral prodrug of nucleotide analogs such as ganciclovir to the diphosphorylated form, which is then converted by endogenous cellular kinases to the toxic triphosphate form that competes with normal nucleosides for DNA replication. After incorporation into DNA elongation is inhibited leading to apoptosis.

HSV-tk suicide gene therapy[789, 790] is a well established method of cytoreduction (reviewed in [791]). *Yang et al.* have recently demonstrated that an HIV vector co-

expressing both HSV-tk and eGFP can be generated and is highly successful in killing human lens epithelial cells.[788] Because of selective transduction of the trabecular meshwork with FIV vectors and minimal bystander effect of HSV-tk, this approach will leave the supporting structures (trabecular beams, corneal endothelium, iris) intact and allow regeneration from adjacent tissues. This strategy has the advantage of (a) being simple as it is using an already established model with proved transgenes, (b) the chief pathology of POAG of an abnormally high outflow resistance is addressed in its core and (c) a new model to study TM regeneration and repopulation will be created. Another desirable safety feature for potential therapeutic application is that cells that were permanently genetically altered by an integrating vector can be visualized and reliably ablated.

Finally, trabecular meshwork transgenesis must be evaluated in eyes that are even more similar to that of humans, e.g. that of macaques. Cats are different in that they have a more wide-spread trabecular meshwork and a plexus of collector channels, while primates have a more confined, wedge-shaped TM and one occasionally doubled collecting Schlemm's canal. I have participated in studies with Dr. Paul Kaufman by setting up the imaging system, producing the vector and teaching vector application techniques. These findings have been presented at the 2006 meeting of the Association for Research in Vision and Ophthalmology in Fort Lauderdale. Preliminary results of trabecular meshwork transduction in macaques have demonstrated that the prior results in cultured human and live feline eyes can be replicated.

9.2. Transgenesis of the Retinal Pigment Epithelium with FIV Vectors as a Basis for Gene Therapy of Retinal and Choroidal Diseases

9.2.1. Comparison of Wild-Type and Class I Integrase Mutant-FIV Vectors in the Retina Demonstrates Sustained Expression of Integrated Transgenes in Retinal Pigment Epithelium

My studies followed retinal transgene expression for the longest reported time. Experiments with pseudotyped lentiviral vector systems in retina prior to mine reported expression in rodents only up to post-injection day 42,[278] 84,[280, 335, 336] 140[337] and 168.[281] My studies also involved the unbiased reporting of results from all animals enrolled in a prospective design, and were scored by observers masked to injection status minimizing observer influence.

Intravitreal injections resulted in relatively poor transduction efficiency compared to subretinal injections, using the same volume for delivery. In contrast, subretinal injections of a similar volume caused extensive transduction of the RPE, indicating broad dissemination of the vector within the subretinal space. It is possible that the extent of transduction in eyes injected by the intravitreal route would be different at later time points, which were not examined in the injection route comparisons. However, most published studies agree with mine that the inner retinal layers block significant access of lentiviral vectors and other vectors to the RPE from the vitreous.[266, 278, 334, 336-338, 720]

I found extensive transgene expression in the RPE, at 2, 3, and 7 months, and in only occasional cells of other inner and outer retinal layers. It was limited to the RPE at early time points (2 and 7 days). Transduction of neonatal rat neurosensory retina, in addition to the RPE, has been observed using subretinal injection of HIV vectors by other investigators.[280] An important distinction is that the latter study was limited to rats injected earlier in post-partum development (2-5 days) than the rats in our study (7 days). The very rapid developmental changes occurring at these early time points are likely to influence permissivity. My findings are therefore consistent with the results of a number of studies that have found that in rodents older than 5 days post-natal, and in adult rabbits, expression has been largely limited to the RPE, whether administered subretinally or intravitreally.[266, 278, 334, 336-338] VSV-G is believed to mediate entry via ubiquitous plasma lemma lipid molecules, thereby giving the vectors broad entry specificity.[792] Varying distribution of these molecules between

cell types, and differential vector particle diffusion, might also contribute to preferential transduction of RPE. Duisit et al. saw only RPE transduction in a large series of rats injected with SIV vectors pseudotyped with 5 different viral envelopes, including VSV-G and Mokola-G,[266] and a study with bovine immunodeficiency virus vectors showed targeted, high-level RPE expression in mice.[337] One group saw reporter protein localization in both RPE and photoreceptors in 5-7 week old mice after HIV-1 vector injection; pseudotyping with the Mokola-G rather than VSV-G restricted transduction to the RPE.[335] In contrast, in non-human primates injected at the macula, FIV vector-mediated expression was reported to be variably detectable in Müller cells and photoreceptors in some animals.[339] Transduction of RPE cells is facilitated by vector uptake at their phagocytotically active, apical site.[793] Other factors influencing differential expression between cell types include distance of and barriers to diffusion as well as varying metabolism rates of neurosensory retina and RPE.

The class I integrase mutant vector data in my study suggests that integration is necessary for long-term transgene expression by this lentiviral vector. This has been confirmed in later collaborative studies with Dyana T. Saenz who has explored factors involved with integration[279, 794] and species-dependent resistance of transduction in more detail.[776] I observed substantial, sustained transgene expression after subretinal injection of wild-type FIV vector (for at least 7 months); this was blocked when the D66V vector was used. D66 is the most amino-terminal of the three invariant acidic residues in the conserved catalytic core domain of integrases ($DX_{39-58}DX_{35}E$).[795] The residues are highly conserved in eukaryotic retro-element integrases as well as in bacterial transposons.[796-798] A D64V substitution in the HIV-1 integrase results in dramatically lower to undetectable transduction in rat brains[240, 250, 799] and has been shown to be "class I" in that it specifically blocks the integration reaction while leaving all of the multiple other functions of Gag/Pol precursor-derived proteins undisturbed.[732, 795, 800-802] In contrast, simple deletions, frame shifts, and most other point mutations in integrase yield "class II" phenotypes in which particles are pleiotropically aberrant in non-integrase functions.[795, 803] In vector experiments, this elegant control has the virtue of comparing particles that differ only in a single amino acid in a single enzyme that forms a very small molar fraction of the virion.[240, 250, 799] Class I integrase mutants had not been described for FIV, or tested in the eye for any

lentiviral vector. My results with FIV vectors demonstrate long-term transgene expression in retina from an FIV vector and show that preventing integration prevents sustained expression. This single amino acid variant of FIV integrase provides a useful control for future studies using FIV vectors; pseudotransduction might in part account for some of the previously reported discrepancies in retinal layer targeting.

It is remarkable that Yanez-Munoz et al. found high level transduction with a non-integrating HIV vector in mice.[488] My own studies employed a rat model and FIV vectors as did Naldini et al. in brain transduction experiments.[250] However, Park et al. transduced mouse liver and were unable to detect transduction with non-integrating vectors.[804] It is possible that this is a species barrier or perhaps that the mode of application resulted in more cell cycling and attrition of non-integrated vector circles as the same author has demonstrated before.[777]

The high transgene expression seen at days 2 to 7 after injection of CT25 correlates temporally with the peak of neovascularization in ROP models.[752] It will be of interest to use FIV vectors to deliver candidate therapeutic genes to the retina of neonatal rats under conditions of oxygen-induced retinopathy in a model for ROP. This may provide a tool to understand the pathogenesis of neovascular diseases and allow exploration of novel therapies for clinically approachable diseases such as age-related macular degeneration. The ability to obtain preferential gene expression in the RPE is desirable. Endogenous angiostatic factors, such as pigment epithelium derived factor (PEDF), are produced in these cells, and diffuse from the RPE into the adjacent retinal and choroidal layers.[286] Adeno-associated virus vectors have shown promise for retinal expression of pigment epithelium derived factor; however, they do not limit expression of this protein to its physiological origin, the RPE.[312] RPE-targeted gene therapy using FIV or other lentiviral vectors may be useful in treating diseases characterized by abnormal retinal angiogenesis. Other lentiviral vectors have now been successfully used to express anti-angiogenic substances: Igarashi et al. used HIV vectors expressing angiostatin to reduce neovascularization dramatically by 90%.[355] EIAV vectors also achieved reduction of neovascularization in a laser model by expressing endostatin. Approximately 60% of the neovascularization area was reduced with endostatin versus 50% with angiostatin.[720]

9.2.2. Long-Term Retinal Transgene Expression with FIV versus Adenoviral Vectors

I found similar location, extent and duration of transgene expression in neonatal rat eyes subretinally injected with FIV and Ad vectors expressing β-galactosidase under transcriptional control of the human CMV immediate-early promoter/enhancer. Expression with each vector was present at 16 months post injection. There was a higher overall extent of expression with FIV, which peaked later than Ad (3 months vs. 1 week). Histology revealed greater cellular infiltrate and disruption of normal retinal architecture with Ad.

Preferential transduction of RPE over other retinal cell types was again seen by VSV-G pseudotyped lentiviral vectors as reported.[76, 266, 278, 334, 336, 338] Ad vectors appear to have a similar tropism within the retina.[328, 631, 805, 806] In contrast, only occasional expression in the post-mitotic, terminally differentiated, neurosensory retina occurred at 1 month post-injection and beyond with both FIV and Ad vectors. While this might limit applicability to neovascularization of inner retinal layers, choroidal neovascularization and degeneration of the RPE, as seen in wet macular degeneration, are good targets. Limiting expression to the RPE is desirable in degenerative diseases of the retinal pigment epithelium that result also in degeneration of photoreceptors from death of RPE cells.[282] In wet macular degeneration, the combination of neuroprotective and anti-angiogenic action of PEDF would be highly desirable to prevent photoreceptor death and progressive vessel growth and exudation.

The extent and duration of expression with FIV vectors has implications for future therapy: lentiviral vectors are advantageous for long-term expression over other vectors because of their ability to integrate into the host cell genome. In my own studies, this was supported by the use of a single amino acid mutation in the catalytic core domain of the FIV integrase (D66V) blocked efficient transduction, while vectors with intact integrase expressed for 7 months.[76]

The duration of expression from a first generation Ad vector was unexpected. Marker gene expression from subretinally injected Ad vector in an immunocompetent host often lasts between 1 to 3 months.[327, 328, 631, 807] Ad vectors lack any mechanism for integration, leaving them more vulnerable to attrition by intracellular metabolism and dilution during cell division. Although adenoviral vectors may integrate in 0.1% to

1% of infected cells,[808, 809] this mechanism cannot explain the extent and duration observed in the present study. Most likely, the low mitotic rate of RPE cells contributes to long-term persistence of Ad vectors in this cell type.

Immunogenicity is a disadvantage of first generation Ad vectors.[325, 328, 582, 810, 811] I confirmed that Ad vectors induce a long-term cellular response, associated with disruption of the normal retinal architecture in our model. This retinal disruption limits the clinical application of first generation Ad vectors in treating retinal disease. In contrast, retinal architecture was preserved in eyes injected with FIV vectors, with the exception of small areas of atrophy directly adjacent to the injection site.

Based on light microscopy, my experiments suggest minimal toxicity of FIV vectors following subretinal injection. Others have confirmed normal retina function with technically highly specialized assessment with electroretinography after lentiviral vector gene transfer to the subretinal space.[344, 688]

10. Conclusion

The central goal to engineer FIV vectors into a more modular platform for long-term ocular gene therapy could be accomplished by separating envelope, packaging and transfer function.[321] While this was a collaborative approach between several individuals (mostly Todd Whitwam, Iris Kemler, Roman Barraza) in Eric Poeschla's laboratory, I contributed by transfer vector optimization. FIV mediated gene transfer to the aqueous humor outflow tract[324, 504, 586] and to the retina[75, 76, 279] was established and long-term vector function and biocompatibility were assessed.[75, 76, 586] Transduction of the outflow tract was highly efficient and resulted in genetic modification of nearly the entire trabecular meshwork.[324, 504, 586] I developed methods for administration and more sensitive monitoring of FIV vectors in the anterior chamber[586] and a novel subretinal injection technique.[75, 76, 279]

Bicistronic FIV vectors generated high levels of two different transgenes eGFP and β-galactosidase, which allowed live in vivo tracking[324, 586, 641] and sensitive yet specific cell labeling in tissue specimen, respectively.[75, 76, 504] In eGFP vectors, I disabled the LTR promoter function of integrated vectors through a SIN modification in analogy to HIV vectors.[738-740] This vector was used in later studies in which I participated to deliver myocilin mutants to the outflow tract in vivo to generate an in vivo glaucoma model.[641] The above studies and subsequent experiments that I have participated in and co-published published recently[641] establish that durable transgene expression is readily achievable and is well tolerated, exceeding 2 years. This model has been recreated by other investigators in other species[640, 642] as well as with a collaborator, Paul Kaufman, in macaques. Future directions that I will pursue include development of trabeculoablative gene therapy and creation of a model to study trabecular meshwork repopulation dynamics and cell based therapy.

I also cloned an integrase mutant control vector that differed in only one amino acid while preserving all other biochemical properties.[76, 279] While I observed no transduction in vivo,[76] later studies have shown that there is significant transgene expression in non-dividing cells in vitro experiments.[794] Unfortunately, more recent results with HIV integrase mutant vectors where full rescue could be achieved question the usefulness of this control unless the observed effect is HIV and rodent specific.[488]

With the technical assistance of Teo Wu-Lin I developed a novel protocol for scaled-up production of these vectors using cell factories and large-volume concentration that proved useful in subsequent animal studies.[75, 76, 279, 321, 324, 504, 586] Especially the results achieved in the larger animal model, the domestic cat, validate the protocol for large-scale production. Transient transfection of 10 times less DNA in 293T cells within high surface area slides and high volume, fixed-angle ultracentrifugation resulted in high titer vectors that were effective in the eye. Standard protocols use 5 to 10 times as much transfection DNA, which is expensive and time consuming to produce, and generally concentrate vectors in smaller volumes.[1, 240, 504] Although inducible vector production cell lines are very useful,[812-814] they do not have the versatility of transient transfection that allows readily adjustment and swapping of vector components.

Further preclinical studies will have to be conducted to evaluate vector safety and immunology. Although FIV is unable to actively infect and replicate in human cells, the domestic cat as the natural host will be used as a model to evaluate chances of generating replication competent retroviruses that could emerge in theory. For the actual clinical application, FIV vector producing cell lines will have to be generated and well characterized to fulfill regulations of Good Manufacturing Practices.

11. References

1. Poeschla E, Wong-Staal F, Looney D. Efficient transduction of nondividing cells by feline immunodeficiency virus lentiviral vectors. *Nat Med* 1998;4:354-357.
2. Haddad A, De Almeida JC, Laicine EM, Fife RS, Pelletier G. The origin of the intrinsic glycoproteins of the rabbit vitreous body: an immunohistochemical and autoradiographic study. *Exp Eye Res* 1990;50:555-561.
3. Morrison JC, Van Buskirk EM. Anterior collateral circulation in the primate eye. *Ophthalmology* 1983;90:707-715.
4. Morrison JC, Van Buskirk EM. Ciliary process microvasculature of the primate eye. *Am J Ophthalmol* 1984;97:372-383.
5. Funk R, Rohen JW. SEM studies of the functional morphology of the ciliary process vasculature in the cynomolgus monkey: reactions after application of epinephrine. *Exp Eye Res* 1988;47:653-663.
6. Funk R, Rohen JW. Scanning electron microscopic study on the vasculature of the human anterior eye segment, especially with respect to the ciliary processes. *Exp Eye Res* 1990;51:651-661.
7. Freddo TF. Shifting the paradigm of the blood-aqueous barrier. *Exp Eye Res* 2001;73:581-592.
8. Raviola G, Raviola E. Intercellular junctions in the ciliary epithelium. *Invest Ophthalmol Vis Sci* 1978;17:958-981.
9. Hirsch M, Montcourrier P, Arguillere P, Keller N. The structure of tight junctions in the ciliary epithelium. *Curr Eye Res* 1985;4:493-501.
10. Flugel C, Lutjen-Drecoll E. Presence and distribution of Na+/K+-ATPase in the ciliary epithelium of the rabbit. *Histochemistry* 1988;88:613-621.
11. Lutjen-Drecoll E, Lonnerholm G, Eichhorn M. Carbonic anhydrase distribution in the human and monkey eye by light and electron microscopy. *Graefes Arch Clin Exp Ophthalmol* 1983;220:285-291.
12. Lippa EA, Carlson LE, Ehinger B, et al. Dose response and duration of action of dorzolamide, a topical carbonic anhydrase inhibitor. *Arch Ophthalmol* 1992;110:495-499.
13. Reddy DV, Rosenberg C, Kinsey VE. Steady state distribution of free amino acids in the aqueous humours, vitreous body and plasma of the rabbit. *Exp Eye Res* 1961;1:175-191.
14. Freddo TF. Intercellular junctions of the ciliary epithelium in anterior uveitis. *Invest Ophthalmol Vis Sci* 1987;28:320-329.
15. Green K, Bountra C, Georgiou P, House CR. An electrophysiologic study of rabbit ciliary epithelium. *Invest Ophthalmol Vis Sci* 1985;26:371-381.
16. Edelman JL, Sachs G, Adorante JS. Ion transport asymmetry and functional coupling in bovine pigmented and nonpigmented ciliary epithelial cells. *Am J Physiol* 1994;266:C1210-1221.
17. Bill A, Phillips CI. Uveoscleral drainage of aqueous humour in human eyes. *Exp Eye Res* 1971;12:275-281.
18. Weinreb RN. Uveoscleral outflow: the other outflow pathway. *Journal of glaucoma* 2000;9:343-345.
19. Bill A. Some thoughts on the pressure dependence of uveoscleral flow. *Journal of glaucoma* 2003;12:88-89; author reply 93-84.
20. Schachtschabel U, Lindsey JD, Weinreb RN. The mechanism of action of prostaglandins on uveoscleral outflow. *Current opinion in ophthalmology* 2000;11:112-115.

21. Lutjen-Drecoll E, Tamm E. Morphological study of the anterior segment of cynomolgus monkey eyes following treatment with prostaglandin F2 alpha. *Exp Eye Res* 1988;47:761-769.

22. Rohen JW, van der Zypen E. The phagocytic activity of the trabecularmeshwork endothelium. An electron-microscopic study of the vervet (Cercopithecus aethiops). *Albrecht Von Graefes Arch Klin Exp Ophthalmol* 1968;175:143-160.

23. Fruttiger M. Development of the retinal vasculature. *Angiogenesis* 2007;10:77-88.

24. Alvarado J, Murphy C, Juster R. Trabecular meshwork cellularity in primary open-angle glaucoma and nonglaucomatous normals. *Ophthalmology* 1984;91:564-579.

25. Grierson I, Howes RC. Age-related depletion of the cell population in the human trabecular meshwork. *Eye* 1987;1 (Pt 2):204-210.

26. Camp JJ, Hann CR, Johnson DH, Tarara JE, Robb RA. Three-dimensional reconstruction of aqueous channels in human trabecular meshwork using light microscopy and confocal microscopy. *Scanning* 1997;19:258-263.

27. Rohen JW, Futa R, Lutjen-Drecoll E. The fine structure of the cribriform meshwork in normal and glaucomatous eyes as seen in tangential sections. *Invest Ophthalmol Vis Sci* 1981;21:574-585.

28. Maepea O, Bill A. Pressures in the juxtacanalicular tissue and Schlemm's canal in monkeys. *Exp Eye Res* 1992;54:879-883.

29. Knepper PA, Farbman AI, Telser AG. Aqueous outflow pathway glycosaminoglycans. *Exp Eye Res* 1981;32:265-277.

30. Gong H, Ye W, Freddo TF, Hernandez MR. Hyaluronic acid in the normal and glaucomatous optic nerve. *Exp Eye Res* 1997;64:587-595.

31. Knepper PA, Goossens W, Hvizd M, Palmberg PF. Glycosaminoglycans of the human trabecular meshwork in primary open-angle glaucoma. *Invest Ophthalmol Vis Sci* 1996;37:1360-1367.

32. Grierson I, Lee WR. Pressure-induced changes in the ultrastructure of the endothelium lining Schlemm's canal. *Am J Ophthalmol* 1975;80:863-884.

33. Ethier CR, Coloma FM, Sit AJ, Johnson M. Two pore types in the inner-wall endothelium of Schlemm's canal. *Invest Ophthalmol Vis Sci* 1998;39:2041-2048.

34. de Kater AW, Spurr-Michaud SJ, Gipson IK. Localization of smooth muscle myosin-containing cells in the aqueous outflow pathway. *Invest Ophthalmol Vis Sci* 1990;31:347-353.

35. Ascher KW. Aqueous veins and their significance for pathogenesis of glaucoma. *Archives of ophthalmology* 1949;42:66-76.

36. Harrington DO. Differential diagnosis of the arcuate scotoma. *Invest Ophthalmol* 1969;8:96-105.

37. Hoyt WF, Luis O. Visual fiber anatomy in the infrageniculate pathway of the primate. *Arch Ophthalmol* 1962;68:94-106.

38. Hoyt WF, Luis O. The primate chiasm. Details of visual fiber organization studied by silver impregnation techniques. *Arch Ophthalmol* 1963;70:69-85.

39. Hoyt WF. Anatomic considerations of arcuate scotomas associated with lesions of the optic nerve and chiasm. A nauta axon degeneration study in the monkey. *Bulletin of the Johns Hopkins Hospital* 1962;111:57-71.

40. Radius RL, Anderson DR. The histology of retinal nerve fiber layer bundles and bundle defects. *Arch Ophthalmol* 1979;97:948-950.

41. Radius RL, Anderson DR. The course of axons through the retina and optic nerve head. *Arch Ophthalmol* 1979;97:1154-1158.

42. Minckler DS. The organization of nerve fiber bundles in the primate optic nerve head. *Arch Ophthalmol* 1980;98:1630-1636.

43. Radius RL, de Bruin J. Anatomy of the retinal nerve fiber layer. *Invest Ophthalmol Vis Sci* 1981;21:745-749.

44. Ogden TE. Nerve fiber layer of the primate retina: morphometric analysis. *Invest Ophthalmol Vis Sci* 1984;25:19-29.

45. Ogden TE. Nerve fiber layer of the macaque retina: retinotopic organization. *Invest Ophthalmol Vis Sci* 1983;24:85-98.

46. Hoyt WF, Frisen L, Newman NM. Fundoscopy of nerve fiber layer defects in glaucoma. *Invest Ophthalmol* 1973;12:814-829.

47. Weinreb RN, Dreher AW, Coleman A, Quigley H, Shaw B, Reiter K. Histopathologic validation of Fourier-ellipsometry measurements of retinal nerve fiber layer thickness. *Arch Ophthalmol* 1990;108:557-560.

48. Weinreb RN, Shakiba S, Zangwill L. Scanning laser polarimetry to measure the nerve fiber layer of normal and glaucomatous eyes. *Am J Ophthalmol* 1995;119:627-636.

49. Radius RL. Thickness of the retinal nerve fiber layer in primate eyes. *Arch Ophthalmol* 1980;98:1625-1629.

50. Quigley HA, Addicks EM. Quantitative studies of retinal nerve fiber layer defects. *Arch Ophthalmol* 1982;100:807-814.

51. Hoyt WF, Schlicke B, Eckelhoff RJ. Fundoscopic appearance of a nerve-fibre-bundle defect. *Br J Ophthalmol* 1972;56:577-583.

52. Sommer A, Miller NR, Pollack I, Maumenee AE, George T. The nerve fiber layer in the diagnosis of glaucoma. *Arch Ophthalmol* 1977;95:2149-2156.

53. Quigley HA, Miller NR, George T. Clinical evaluation of nerve fiber layer atrophy as an indicator of glaucomatous optic nerve damage. *Arch Ophthalmol* 1980;98:1564-1571.

54. Airaksinen PJ, Nieminen H, Mustonen E. Retinal nerve fibre layer photography with a wide angle fundus camera. *Acta ophthalmologica* 1982;60:362-368.

55. Huang XR, Knighton RW. Linear birefringence of the retinal nerve fiber layer measured in vitro with a multispectral imaging micropolarimeter. *Journal of biomedical optics* 2002;7:199-204.

56. Knighton RW, Huang XR. Directional and spectral reflectance of the rat retinal nerve fiber layer. *Invest Ophthalmol Vis Sci* 1999;40:639-647.

57. Huang XR, Knighton RW, Cavuoto LN. Microtubule contribution to the reflectance of the retinal nerve fiber layer. *Invest Ophthalmol Vis Sci* 2006;47:5363-5367.

58. Teal PK, Morin JD, McCulloch C. Assessment of the normal disc. *Transactions of the American Ophthalmological Society* 1972;70:164-177.

59. Savini G, Zanini M, Carelli V, Sadun AA, Ross-Cisneros FN, Barboni P. Optic nerve structure in healthy subjects. *Arch Ophthalmol* 2006;124:1507; author reply 1508-1509.

60. Kirsch RE, Anderson DR. Clinical recognition of glaucomatous cupping. *Am J Ophthalmol* 1973;75:442-454.

61. Harizman N, Oliveira C, Chiang A, et al. The ISNT rule and differentiation of normal from glaucomatous eyes. *Arch Ophthalmol* 2006;124:1579-1583.

62. Heijl A, Leske MC, Bengtsson B, Hyman L, Bengtsson B, Hussein M. Reduction of intraocular pressure and glaucoma progression: results from the Early Manifest Glaucoma Trial. *Arch Ophthalmol* 2002;120:1268-1279.

63. Kass MA, Heuer DK, Higginbotham EJ, et al. The Ocular Hypertension Treatment Study: a randomized trial determines that topical ocular hypotensive medication delays or prevents the onset of primary open-angle glaucoma. *Arch Ophthalmol* 2002;120:701-713; discussion 829-730.

64. Kerrigan LA, Zack DJ, Quigley HA, Smith SD, Pease ME. TUNEL-positive ganglion cells in human primary open-angle glaucoma. *Arch Ophthalmol* 1997;115:1031-1035.

65. Kamal D, Hitchings R. Normal tension glaucoma--a practical approach. *Br J Ophthalmol* 1998;82:835-840.

66. Gordon MO, Beiser JA, Brandt JD, et al. The Ocular Hypertension Treatment Study: baseline factors that predict the onset of primary open-angle glaucoma. *Arch Ophthalmol* 2002;120:714-720; discussion 829-730.

67. Anderson DR, Davis EB. Glaucoma, capillaries and pericytes. 5. Preliminary evidence that carbon dioxide relaxes pericyte contractile tone. *Ophthalmologica* 1996;210:280-284.

68. Flammer J, Orgul S, Costa VP, et al. The impact of ocular blood flow in glaucoma. *Prog Retin Eye Res* 2002;21:359-393.

69. Pillunat LE, Anderson DR, Knighton RW, Joos KM, Feuer WJ. Autoregulation of human optic nerve head circulation in response to increased intraocular pressure. *Exp Eye Res* 1997;64:737-744.

70. Matsugi T, Chen Q, Anderson DR. Suppression of CO2-induced relaxation of bovine retinal pericytes by angiotensin II. *Invest Ophthalmol Vis Sci* 1997;38:652-657.

71. Drance SM, Begg IS. Sector haemorrhage--a probable acute ischaemic disc change in chronic simple glaucoma. *Canadian journal of ophthalmology* 1970;5:137-141.

72. Airaksinen PJ, Mustonen E, Alanko HI. Optic disc haemorrhages precede retinal nerve fibre layer defects in ocular hypertension. *Acta ophthalmologica* 1981;59:627-641.

73. Pederson JE, Anderson DR. The mode of progressive disc cupping in ocular hypertension and glaucoma. *Arch Ophthalmol* 1980;98:490-495.

74. Sample PA, Bosworth CF, Weinreb RN. The loss of visual function in glaucoma. *Seminars in ophthalmology* 2000;15:182-193.

75. Loewen N, Leske DA, Cameron JD, et al. Long-term retinal transgene expression with FIV versus adenoviral vectors. *Molecular vision* 2004;10:272-280.

76. Loewen N, Leske DA, Chen Y, et al. Comparison of wild-type and class I integrase mutant-FIV vectors in retina demonstrates sustained expression of integrated transgenes in retinal pigment epithelium. *The journal of gene medicine* 2003;5:1009-1017.

77. Gekeler F, Szurman P, Grisanti S, et al. Compound subretinal prostheses with extra-ocular parts designed for human trials: successful long-term implantation in pigs. *Graefes Arch Clin Exp Ophthalmol* 2007;245:230-241.

78. Montezuma SR, Loewenstein J, Scholz C, Rizzo JF, 3rd. Biocompatibility of materials implanted into the subretinal space of Yucatan pigs. *Invest Ophthalmol Vis Sci* 2006;47:3514-3522.

79. Salzmann J, Linderholm OP, Guyomard JL, et al. Subretinal electrode implantation in the P23H rat for chronic stimulations. *Br J Ophthalmol* 2006;90:1183-1187.

80. Joseph DP, Thomas MA. Present indications for removal of choroidal neovascular membranes. *Current opinion in ophthalmology* 1998;9:23-30.

81. Abdel-Meguid A, Lappas A, Hartmann K, et al. One year follow up of macular translocation with 360 degree retinotomy in patients with age related macular degeneration. *Br J Ophthalmol* 2003;87:615-621.

82. Smith BT, Park CH, Federman JL, Sarin LK, Martidis A. Efficient total detachment of the retina for full macular translocation. *Retina (Philadelphia, Pa* 2006;26:580-583.

83. Travis GH, Golczak M, Moise AR, Palczewski K. Diseases caused by defects in the visual cycle: retinoids as potential therapeutic agents. *Annual review of pharmacology and toxicology* 2007;47:469-512.

84. Marmor MF. Structure, function, and disease of the retinal pigment epithelium. In: Marmor MF, Wofensberger T.J. (ed), *The Retinal Pigment Epithelium.* New York: Oxford University Press; 1998:3-9.

85. Hjelmeland LM, Cristofolo VJ, Funk W, Rakoczy E, Katz ML. Senescence of the retinal pigment epithelium. *Molecular vision* 1999;5:33.

86. Bunt-Milam AH, Saari JC, Klock IB, Garwin GG. Zonulae adherentes pore size in the external limiting membrane of the rabbit retina. *Invest Ophthalmol Vis Sci* 1985;26:1377-1380.

87. Hageman GS KM. Biology of the interphotoreceptor matrix-retinal pigment epithelium-retina interface. In: Marmor MF, Wofensberger T.J. (ed), *The Retinal Pigment Epithelium.* New York: Oxford University Press; 1998:361-391.

88. Dacey DM, Packer OS. Colour coding in the primate retina: diverse cell types and cone-specific circuitry. *Current opinion in neurobiology* 2003;13:421-427.

89. Curcio CA, Sloan KR, Kalina RE, Hendrickson AE. Human photoreceptor topography. *The Journal of comparative neurology* 1990;292:497-523.

90. Curcio CA, Allen KA, Sloan KR, et al. Distribution and morphology of human cone photoreceptors stained with anti-blue opsin. *The Journal of comparative neurology* 1991;312:610-624.

91. Eckmiller MS. Renewal of the ciliary axoneme in cone outer segments of the retina of Xenopus laevis. *Cell and tissue research* 1996;285:165-169.

92. Hogan MJ, Alvarado, J.A., Weddell, J.E. *Histology of the Human Eye*. Philadelphia: WB Saunders; 1971.

93. Fine BS, Zimmerman LE. Muller's cells and the "middle limiting membrane" of the human retina. An electron microscopic study. *Invest Ophthalmol* 1962;1:304-326.

94. Kolb H, Fernandez E, Schouten J, Ahnelt P, Linberg KA, Fisher SK. Are there three types of horizontal cell in the human retina? *The Journal of comparative neurology* 1994;343:370-386.

95. Primate retina: cell types, circuits and colour opponency by D.M. Dacey. Progress In retinal eye research 18 (1999), 737-763. *Prog Retin Eye Res* 2000;19:647-648.

96. Wassle H, Dacey DM, Haun T, Haverkamp S, Grunert U, Boycott BB. The mosaic of horizontal cells in the macaque monkey retina: with a comment on biplexiform ganglion cells. *Visual neuroscience* 2000;17:591-608.

97. Kolb H. The organization of the outer plexiform layer in the retina of the cat: electron microscopic observations. *Journal of neurocytology* 1977;6:131-153.

98. Kolb H. The architecture of functional neural circuits in the vertebrate retina. The Proctor Lecture. *Invest Ophthalmol Vis Sci* 1994;35:2385-2404.

99. Mariani AP. Bipolar cells in monkey retina selective for the cones likely to be blue-sensitive. *Nature* 1984;308:184-186.

100. Linberg KA, Fisher SK. An ultrastructural study of interplexiform cell synapses in the human retina. *The Journal of comparative neurology* 1986;243:561-576.

101. Curcio CA, Allen KA. Topography of ganglion cells in human retina. *The Journal of comparative neurology* 1990;300:5-25.

102. Dacey DM. Parallel pathways for spectral coding in primate retina. *Annual review of neuroscience* 2000;23:743-775.

103. Bringmann A, Francke M, Pannicke T, et al. Role of glial K(+) channels in ontogeny and gliosis: a hypothesis based upon studies on Muller cells. *Glia* 2000;29:35-44.

104. Provis JM, Diaz CM, Penfold PL. Microglia in human retina: a heterogeneous population with distinct ontogenies. *Perspectives on developmental neurobiology* 1996;3:213-222.

105. Ma N, Streilein JW. T cell immunity induced by allogeneic microglia in relation to neuronal retina transplantation. *J Immunol* 1999;162:4482-4489.

106. Provis JM. Development of the primate retinal vasculature. *Prog Retin Eye Res* 2001;20:799-821.

107. Ophthalmology AAo. Preferred practice pattern: primary open-angle glaucoma., *American Academy of Ophthalmology.* San Francisco, California; 2000.

108. Caprioli J. Clinical evaluation of the optic nerve in glaucoma. *Transactions of the American Ophthalmological Society* 1994;92:589-641.

109. Quigley HA, Addicks EM, Green WR. Optic nerve damage in human glaucoma. III. Quantitative correlation of nerve fiber loss and visual field defect in glaucoma, ischemic neuropathy, papilledema, and toxic neuropathy. *Arch Ophthalmol* 1982;100:135-146.

110. Quigley HA. Number of people with glaucoma worldwide. *Br J Ophthalmol* 1996;80:389-393.

111. Quigley HA. Proportion of those with open-angle glaucoma who become blind. *Ophthalmology* 1999;106:2039-2041.

112. Hattenhauer MG, Johnson DH, Ing HH, et al. The probability of blindness from open-angle glaucoma. *Ophthalmology* 1998;105:2099-2104.

113. Quigley HA. Open-angle glaucoma. *The New England journal of medicine* 1993;328:1097-1106.

114. Guzman G, Javitt J, Glick H, Tielsch JM, McDonald R. Glaucoma in the United States population: The economic burden of illness. *Invest Ophthalmol Vis Sci* 1992;33:759.

115. Dielemans I, Vingerling JR, Wolfs RC, Hofman A, Grobbee DE, de Jong PT. The prevalence of primary open-angle glaucoma in a population-based study in The Netherlands. The Rotterdam Study. *Ophthalmology* 1994;101:1851-1855.

116. Mitchell P, Smith W, Attebo K, Healey PR. Prevalence of open-angle glaucoma in Australia. The Blue Mountains Eye Study. *Ophthalmology* 1996;103:1661-1669.

117. Tielsch JM, Sommer A, Katz J, Royall RM, Quigley HA, Javitt J. Racial variations in the prevalence of primary open-angle glaucoma. The Baltimore Eye Survey. *Jama* 1991;266:369-374.

118. Sommer A, Tielsch JM, Katz J, et al. Relationship between intraocular pressure and primary open angle glaucoma among white and black Americans. The Baltimore Eye Survey. *Arch Ophthalmol* 1991;109:1090-1095.

119. Hollows FC, Graham PA. Intra-ocular pressure, glaucoma, and glaucoma suspects in a defined population. *Br J Ophthalmol* 1966;50:570-586.

120. Davanger M. Low-pressure glaucoma and the concept of the IOP tolerance distribution curve. *Acta ophthalmologica* 1989;67:256-260.

121. Davanger M, Ringvold A, Blika S. The frequency distribution of the glaucoma tolerance limit. *Acta ophthalmologica* 1991;69:782-785.

122. Davanger M, Ringvold A, Blika S. The probability of having glaucoma at different IOP levels. *Acta ophthalmologica* 1991;69:565-568.

123. Comparison of glaucomatous progression between untreated patients with normal-tension glaucoma and patients with therapeutically reduced intraocular pressures. Collaborative Normal-Tension Glaucoma Study Group. *Am J Ophthalmol* 1998;126:487-497.

124. The effectiveness of intraocular pressure reduction in the treatment of normal-tension glaucoma. Collaborative Normal-Tension Glaucoma Study Group. *Am J Ophthalmol* 1998;126:498-505.

125. Kass MA, Kolker AE, Becker B. Prognostic factors in glaucomatous visual field loss. *Arch Ophthalmol* 1976;94:1274-1276.

126. Quigley HA, Tielsch JM, Katz J, Sommer A. Rate of progression in open-angle glaucoma estimated from cross-sectional prevalence of visual field damage. *Am J Ophthalmol* 1996;122:355-363.

127. Mao LK, Stewart WC, Shields MB. Correlation between intraocular pressure control and progressive glaucomatous damage in primary open-angle glaucoma. *Am J Ophthalmol* 1991;111:51-55.

128. Erie JC, Hodge DO, Gray DT. The incidence of primary angle-closure glaucoma in Olmsted County, Minnesota. *Arch Ophthalmol* 1997;115:177-181.

129. Kington R, Rogowski J, Lillard L, Lee PP. Functional associations of "trouble seeing". *J Gen Intern Med* 1997;12:125-128.

130. Altangerel U, Spaeth GL, Rhee DJ. Visual function, disability, and psychological impact of glaucoma. *Current opinion in ophthalmology* 2003;14:100-105.

131. Green J, Siddall H, Murdoch I. Learning to live with glaucoma: a qualitative study of diagnosis and the impact of sight loss. *Soc Sci Med* 2002;55:257-267.

132. Tinetti ME, Speechley M, Ginter SF. Risk factors for falls among elderly persons living in the community. *The New England journal of medicine* 1988;319:1701-1707.

133. Steinberg EP, Tielsch JM, Schein OD, et al. The VF-14. An index of functional impairment in patients with cataract. *Arch Ophthalmol* 1994;112:630-638.

134. Parrish RK, 2nd. Visual impairment, visual functioning, and quality of life assessments in patients with glaucoma. *Transactions of the American Ophthalmological Society* 1996;94:919-1028.

135. Gutierrez P, Wilson MR, Johnson C, et al. Influence of glaucomatous visual field loss on health-related quality of life. *Arch Ophthalmol* 1997;115:777-784.

136. Grant WM. Experimental aqueous perfusion in enucleated human eyes. *Archives of ophthalmology* 1963;69:783-801.

137. Rohen JW. Why is intraocular pressure elevated in chronic simple glaucoma? Anatomical considerations. *Ophthalmology* 1983;90:758-765.

138. Krupin T. Special considerations in low-tension glaucoma. *Canadian journal of ophthalmology* 2007;42:414-417.

139. Miller KM, Quigley HA. The clinical appearance of the lamina cribrosa as a function of the extent of glaucomatous optic nerve damage. *Ophthalmology* 1988;95:135-138.

140. Quigley HA, Hohman RM, Addicks EM, Massof RW, Green WR. Morphologic changes in the lamina cribrosa correlated with neural loss in open-angle glaucoma. *Am J Ophthalmol* 1983;95:673-691.

141. Quigley HA, Addicks EM. Regional differences in the structure of the lamina cribrosa and their relation to glaucomatous optic nerve damage. *Arch Ophthalmol* 1981;99:137-143.

142. Danias J, Lee KC, Zamora MF, et al. Quantitative analysis of retinal ganglion cell (RGC) loss in aging DBA/2NNia glaucomatous mice: comparison with RGC loss in aging C57/BL6 mice. *Invest Ophthalmol Vis Sci* 2003;44:5151-5162.

143. Stone EM, Fingert JH, Alward WLM, et al. Identification of a gene that causes primary open angle glaucoma. *Science (New York, NY* 1997;275:668-670.

144. Tamm ER, Russell P, Epstein DL, Johnson DH, Piatigorsky J. Modulation of myocilin/TIGR expression in human trabecular meshwork. *Invest Ophthalmol Vis Sci* 1999;40:2577-2582.

145. Zimmerman CC, Lingappa VR, Richards JE, Rozsa FW, Lichter PR, Polansky JR. A trabecular meshwork glucocorticoid response (TIGR) gene mutation affects translocational processing. *Molecular vision* 1999;5:19.

146. Johnson DH. Myocilin and glaucoma: A TIGR by the tail? *Arch Ophthalmol* 2000;118:974-978.

147. Polansky JR, Fauss DJ, Zimmerman CC. Regulation of TIGR/MYOC gene expression in human trabecular meshwork cells. *Eye* 2000;14:503-514.

148. Sarfarazi M, Stoilov I. Molecular genetics of primary congenital glaucoma. *Eye* 2000;14:422-428.

149. Wang X, Johnson DH. mRNA in situ hybridization of TIGR/MYOC in human trabecular meshwork. *Invest Ophthalmol Vis Sci* 2000;41:1724-1729.

150. Wang N, Chintala S, Fini ME, Schuman JS. Activation of a tissue-specific stress response in the aqueous outflow pathway of the eye defines the glaucoma disease phenotype. *Nature Medcine* 2001;7:304-309.

151. Sit AJ, Coloma FM, Ethier CR, Johnson M. Factors affecting the pores of the inner wall endothelium of Schlemm's canal. *Invest Ophthalmol Vis Sci* 1997;38:1517-1525.

152. Johnson M, Chan D, Read AT, Christensen C, Sit A, Ethier CR. The pore density in the inner wall endothelium of Schlemm's canal of glaucomatous eyes. *Invest Ophthalmol Vis Sci* 2002;43:2950-2955.

153. Brilakis HS, Johnson DH. Giant vacuole survival time and implications for aqueous humor outflow. *Journal of glaucoma* 2001;10:277-283.

154. Aplin AE, Howe A, Alahari SK, Juliano RL. Signal transduction and signal modulation by cell adhesion receptors: the role of integrins, cadherins, immunoglobulin-cell adhesion molecules, and selectins. *Pharmacological reviews* 1998;50:197-263.

155. Bornstein P, Sage EH. Matricellular proteins: extracellular modulators of cell function. *Current opinion in cell biology* 2002;14:608-616.

156. Rhee DJ, Fariss RN, Brekken R, Sage EH, Russell P. The matricellular protein SPARC is expressed in human trabecular meshwork. *Exp Eye Res* 2003;77:601-607.

157. Flugel-Koch C, Ohlmann A, Fuchshofer R, Welge-Lussen U, Tamm ER. Thrombospondin-1 in the trabecular meshwork: localization in normal and glaucomatous eyes, and induction by TGF-beta1 and dexamethasone in vitro. *Exp Eye Res* 2004;79:649-663.

158. Maroudas A. Biophysical chemistry of cartilaginous tissues with special reference to solute and fluid transport. *Biorheology* 1975;12:233-248.

159. Bahler CK, Hann CR, Fautsch MP, Johnson DH. Pharmacologic disruption of Schlemm's canal cells and outflow facility in anterior segments of human eyes. *Invest Ophthalmol Vis Sci* 2004;45:2246-2254.

160. Santas AJ, Bahler C, Peterson JA, et al. Effect of heparin II domain of fibronectin on aqueous outflow in cultured anterior segments of human eyes. *Invest Ophthalmol Vis Sci* 2003;44:4796-4804.

161. Bill A. Conventional and uveo-scleral drainage of aqueous humour in the cynomolgus monkey (Macaca irus) at normal and high intraocular pressures. *Exp Eye Res* 1966;5:45-54.

162. Aihara M, Lindsey JD, Weinreb RN. Aqueous humor dynamics in mice. *Invest Ophthalmol Vis Sci* 2003;44:5168-5173.

163. Toris CB, Koepsell SA, Yablonski ME, Camras CB. Aqueous humor dynamics in ocular hypertensive patients. *Journal of glaucoma* 2002;11:253-258.

164. Weinreb RN, Toris CB, Gabelt BT, Lindsey JD, Kaufman PL. Effects of prostaglandins on the aqueous humor outflow pathways. *Surv Ophthalmol* 2002;47 Suppl 1:S53-64.

165. Bhattacharya SK, Rockwood EJ, Smith SD, et al. Proteomics reveal Cochlin deposits associated with glaucomatous trabecular meshwork. *J Biol Chem* 2005;280:6080-6084.

166. Hu DN, Ritch R, Liebmann J, Liu Y, Cheng B, Hu MS. Vascular endothelial growth factor is increased in aqueous humor of glaucomatous eyes. *Journal of glaucoma* 2002;11:406-410.

167. Tripathi RC, Li J, Chan WF, Tripathi BJ. Aqueous humor in glaucomatous eyes contains an increased level of TGF-beta 2. *Exp Eye Res* 1994;59:723-727.

168. Tezel G, Kass MA, Kolker AE, Becker B, Wax MB. Plasma and aqueous humor endothelin levels in primary open-angle glaucoma. *Journal of glaucoma* 1997;6:83-89.

169. Dan J, Belyea D, Gertner G, Leshem I, Lusky M, Miskin R. Plasminogen activator inhibitor-1 in the aqueous humor of patients with and without glaucoma. *Arch Ophthalmol* 2005;123:220-224.

170. Knepper PA, Mayanil CS, Goossens W, et al. Aqueous humor in primary open-angle glaucoma contains an increased level of CD44S. *Invest Ophthalmol Vis Sci* 2002;43:133-139.

171. Gottanka J, Chan D, Eichhorn M, Lutjen-Drecoll E, Ethier CR. Effects of TGF-beta2 in perfused human eyes. *Invest Ophthalmol Vis Sci* 2004;45:153-158.

172. Sacca SC, Izzotti A, Rossi P, Traverso C. Glaucomatous outflow pathway and oxidative stress. *Exp Eye Res* 2007;84:389-399.

173. Welge-Lussen U, May CA, Lutjen-Drecoll E. Induction of tissue transglutaminase in the trabecular meshwork by TGF-beta1 and TGF-beta2. *Invest Ophthalmol Vis Sci* 2000;41:2229-2238.

174. Polansky JR, Fauss DJ, Chen P, et al. Cellular pharmacology and molecular biology of the trabecular meshwork inducible glucocorticoid response gene product. *Ophthalmologica* 1997;211:126-139.

175. Nguyen TD, Chen P, Huang WD, Chen H, Johnson D, Polansky JR. Gene structure and properties of TIGR, an olfactomedin-related glycoprotein cloned from glucocorticoid-induced trabecular meshwork cells. *J Biol Chem* 1998;273:6341-6350.

176. Adam MF, Belmouden A, Binisti P, et al. Recurrent mutations in a single exon encoding the evolutionarily conserved olfactomedin-homology domain of TIGR in familial open-angle glaucoma. *Human molecular genetics* 1997;6:2091-2097.

177. Alward WL, Fingert JH, Coote MA, et al. Clinical features associated with mutations in the chromosome 1 open- angle glaucoma gene (GLC1A). *The New England journal of medicine* 1998;338:1022-1027.

178. Suzuki Y, Shirato S, Taniguchi F, Ohara K, Nishimaki K, Ohta S. Mutations in the TIGR gene in familial primary open-angle glaucoma in Japan. *American journal of human genetics* 1997;61:1202-1204.

179. Wiggs JL, Allingham RR, Vollrath D, et al. Prevalence of mutations in TIGR/Myocilin in patients with adult and juvenile primary open-angle glaucoma. *American journal of human genetics* 1998;63:1549-1552.

180. Stoilova D, Child A, Brice G, Crick RP, Fleck BW, Sarfarazi M. Identification of a new 'TIGR' mutation in a family with juvenile-onset primary open angle glaucoma. *Ophthalmic Genet* 1997;18:109-118.

181. Fingert JH, Heon E, Liebmann JM, et al. Analysis of myocilin mutations in 1703 glaucoma patients from five different populations. *Human molecular genetics* 1999;8:899-905.

182. Shimizu S, Lichter PR, Johnson AT, et al. Age-dependent prevalence of mutations at the GLC1A locus in primary open-angle glaucoma. *Am J Ophthalmol* 2000;130:165-177.

183. Fautsch MP, Bahler CK, Jewison DJ, Johnson DH. Recombinant TIGR/MYOC increases outflow resistance in the human anterior segment. *Invest Ophthalmol Vis Sci* 2000;41:4163-4168.

184. Fautsch MP, Johnson DH. Characterization of myocilin-myocilin interactions. *Invest Ophthalmol Vis Sci* 2001;42:2324-2331.

185. Tawara A, Okada Y, Kubota T, et al. Immunohistochemical localization of MYOC/TIGR protein in the trabecular tissue of normal and glaucomatous eyes. *Curr Eye Res* 2000;21:934-943.

186. Ueda J, Wentz-Hunter KK, Cheng EL, Fukuchi T, Abe H, Yue BY. Ultrastructural localization of myocilin in human trabecular meshwork cells and tissues. *J Histochem Cytochem* 2000;48:1321-1330.

187. Karali A, Russell P, Stefani FH, Tamm ER. Localization of myocilin/trabecular meshwork--inducible glucocorticoid response protein in the human eye. *Invest Ophthalmol Vis Sci* 2000;41:729-740.

188. Ueda J, Wentz-Hunter K, Yue BY. Distribution of myocilin and extracellular matrix components in the juxtacanalicular tissue of human eyes. *Invest Ophthalmol Vis Sci* 2002;43:1068-1076.

189. Filla MS, Liu X, Nguyen TD, et al. In vitro localization of TIGR/MYOC in trabecular meshwork extracellular matrix and binding to fibronectin. *Invest Ophthalmol Vis Sci* 2002;43:151-161.

190. Sohn S, Hur W, Joe MK, et al. Expression of wild-type and truncated myocilins in trabecular meshwork cells: their subcellular localizations and cytotoxicities. *Investigative Ophthalmology & Visual Science* 2002;43:3680-3685.

191. Rao PV, Allingham RR, Epstein DL. TIGR/myocilin in human aqueous humor. *Exp Eye Res* 2000;71:637-641.

192. Swiderski RE, Ross JL, Fingert JH, et al. Localization of MYOC transcripts in human eye and optic nerve by in situ hybridization. *Invest Ophthalmol Vis Sci* 2000;41:3420-3428.

193. Huang W, Jaroszewski J, Ortego J, Escribano J, Coca-Prados M. Expression of the TIGR gene in the iris, ciliary body, and trabecular meshwork of the human eye. *Ophthalmic Genet* 2000;21:155-169.

194. Noda S, Mashima Y, Obazawa M, et al. Myocilin expression in the astrocytes of the optic nerve head. *Biochem Biophys Res Commun* 2000;276:1129-1135.

195. Ricard CS, Agapova OA, Salvador-Silva M, Kaufman PL, Hernandez MR. Expression of myocilin/TIGR in normal and glaucomatous primate optic nerves. *Exp Eye Res* 2001;73:433-447.

196. Clark AF, Kawase K, English-Wright S, et al. Expression of the glaucoma gene myocilin (MYOC) in the human optic nerve head. *Faseb J* 2001;15:1251-1253.

197. Clark AF, Steely HT, Dickerson JE, Jr., et al. Glucocorticoid induction of the glaucoma gene MYOC in human and monkey trabecular meshwork cells and tissues. *Invest Ophthalmol Vis Sci* 2001;42:1769-1780.

198. Eddy DM, Sanders LE, Eddy JF. The value of screening for glaucoma with tonometry. *Surv Ophthalmol* 1983;28:194-205.

199. Meyerhof M. *Ali at-Tabari's 'Paradise of Wisdom,' One of the Oldest Arabic Compendiums of Medicine*. Cambridge: Cambridge University Press; 1921:37-40.

200. Sorsby A. *Modern Ophthalmology*. Washington, DC: Butterworth; 1963.

201. Drance SM, Sweeney VP, Morgan RW, Feldman F. Studies of factors involved in the production of low tension glaucoma. *Arch Ophthalmol* 1973;89:457-465.

202. Leske MC, Connell AM, Wu SY, Hyman LG, Schachat AP. Risk factors for open-angle glaucoma. The Barbados Eye Study. *Arch Ophthalmol* 1995;113:918-924.

203. Armaly MF, Krueger DE, Maunder L, et al. Biostatistical analysis of the collaborative glaucoma study. I. Summary report of the risk factors for glaucomatous visual-field defects. *Arch Ophthalmol* 1980;98:2163-2171.

204. Gordon MO, Kass MA. The Ocular Hypertension Treatment Study: design and baseline description of the participants. *Arch Ophthalmol* 1999;117:573-583.

205. Leske MC, Heijl A, Hyman L, Bengtsson B. Early Manifest Glaucoma Trial: design and baseline data. *Ophthalmology* 1999;106:2144-2153.

206. Ritch R. Complementary therapy for the treatment of glaucoma: a perspective. *Ophthalmology clinics of North America* 2005;18:597-609.

207. Liu S, Araujo SV, Spaeth GL, Katz LJ, Smith M. Lack of effect of calcium channel blockers on open-angle glaucoma. *Journal of glaucoma* 1996;5:187-190.

208. Yucel YH, Gupta N, Zhang Q, Mizisin AP, Kalichman MW, Weinreb RN. Memantine protects neurons from shrinkage in the lateral geniculate nucleus in experimental glaucoma. *Arch Ophthalmol* 2006;124:217-225.

209. Hare WA, WoldeMussie E, Lai RK, et al. Efficacy and safety of memantine treatment for reduction of changes associated with experimental glaucoma in monkey, I: Functional measures. *Invest Ophthalmol Vis Sci* 2004;45:2625-2639.

210. Hare WA, WoldeMussie E, Weinreb RN, et al. Efficacy and safety of memantine treatment for reduction of changes associated with experimental glaucoma in monkey, II: Structural measures. *Invest Ophthalmol Vis Sci* 2004;45:2640-2651.

211. Sheldon WG, Warbritton AR, Bucci TJ, Turturro A. Glaucoma in food-restricted and ad libitum-fed DBA/2NNia mice. *Laboratory animal science* 1995;45:508-518.

212. Rhee DJ, Katz LJ, Spaeth GL, Myers JS. Complementary and alternative medicine for glaucoma. *Surv Ophthalmol* 2001;46:43-55.

213. Goldmann H. [Out-flow pressure, minute volume and resistance of the anterior chamber flow in man.]. *Documenta ophthalmologica* 1951;5-6:278-356.

214. Bill A. Uveoscleral drainage of aqueous humor: physiology and pharmacology. *Prog Clin Biol Res* 1989;312:417-427.

215. Bill A. Some aspects of aqueous humour drainage. *Eye* 1993;7 (Pt 1):14-19.

216. Jocson VL, Sears ML. Experimental aqueous perfusion in enucleated human eyes. Results after obstruction of Schlemm's canal. *Arch Ophthalmol* 1971;86:65-71.

217. Kymes SM, Kass MA, Anderson DR, Miller JP, Gordon MO. Management of ocular hypertension: a cost-effectiveness approach from the Ocular Hypertension Treatment Study. *Am J Ophthalmol* 2006;141:997-1008.

218. Anderson DR. Collaborative normal tension glaucoma study. *Current opinion in ophthalmology* 2003;14:86-90.

219. Oliver JE, Hattenhauer MG, Herman D, et al. Blindness and glaucoma: a comparison of patients progressing to blindness from glaucoma with patients maintaining vision. *Am J Ophthalmol* 2002;133:764-772.

220. Grant WM. Clinical measurements of aqueous outflow. *Am J Ophthalmol* 1951;34:1603-1605.

221. Brubaker RF. Measurement with fluorophotometry: I. Plasma binding. II. Anterior segment, and III. Aqueous humor flow. *Graefes Arch Clin Exp Ophthalmol* 1985;222:190-193.

222. Gedde SJ, Schiffman JC, Feuer WJ, Herndon LW, Brandt JD, Budenz DL. Treatment outcomes in the tube versus trabeculectomy study after one year of follow-up. *Am J Ophthalmol* 2007;143:9-22.

223. Rolim de Moura C, Paranhos A, Jr., Wormald R. Laser trabeculoplasty for open angle glaucoma. *Cochrane database of systematic reviews (Online)* 2007;CD003919.

224. Francis BA, See RF, Rao NA, Minckler DS, Baerveldt G. Ab interno trabeculectomy: development of a novel device (Trabectome) and surgery for open-angle glaucoma. *Journal of glaucoma* 2006;15:68-73.

225. Alward WL. Medical management of glaucoma. *The New England journal of medicine* 1998;339:1298-1307.

226. Edmunds B, Thompson JR, Salmon JF, Wormald RP. The National Survey of Trabeculectomy. III. Early and late complications. *Eye* 2002;16:297-303.

227. Grierson I, Lee WR, Abraham S. The effects of topical pilocarpine on the morphology of the outflow apparatus of the baboon (Papio cynocephalus). *Invest Ophthalmol Vis Sci* 1979;18:346-355.

228. Frezzotti R. The glaucoma mystery from ancient times to the 21st century. The glaucoma mystery: ancient concepts. *Acta ophthalmologica Scandinavica* 2000;14-18.

229. Alvarado JA, Wood I, Polansky JR. Human trabecular cells. II. Growth pattern and ultrastructural characteristics. *Invest Ophthalmol Vis Sci* 1982;23:464-478.

230. Polansky JR, Weinreb RN, Baxter JD, Alvarado J. Human trabecular cells. I. Establishment in tissue culture and growth characteristics. *Invest Ophthalmol Vis Sci* 1979;18:1043-1049.

231. Polansky JR, Wood IS, Maglio MT, Alvarado JA. Trabecular meshwork cell culture in glaucoma research: evaluation of biological activity and structural properties of human trabecular cells in vitro. *Ophthalmology* 1984;91:580-595.

232. Kermani O, Lubatschowski H, Ertmer W, Krieglstein GK. Internal ablative sinostomy using a fiber delivered Q-switched CTE: YAG laser (2.69 microns). *International ophthalmology* 1993;17:211-215.

233. Gaasterland DE, Bonney CH, 3rd, Rodrigues MM, Kuwabara T. Long-term effects of Q-switched ruby laser on monkey anterior chamber angle. *Invest Ophthalmol Vis Sci* 1985;26:129-135.

234. Kramer TR, Noecker RJ. Comparison of the morphologic changes after selective laser trabeculoplasty and argon laser trabeculoplasty in human eye bank eyes. *Ophthalmology* 2001;108:773-779.

235. Dueker DK, Norberg M, Johnson DH, Tschumper RC, Feeney-Burns L. Stimulation of cell division by argon and Nd:YAG laser trabeculoplasty in cynomolgus monkeys. *Invest Ophthalmol Vis Sci* 1990;31:115-124.

236. Kaufman PL, Jia WW, Tan J, et al. A perspective of gene therapy in the glaucomas. *Surv Ophthalmol* 1999;43 Suppl 1:S91-97.

237. Rezaie T, Child A, Hitchings R, et al. Adult-onset primary open-angle glaucoma caused by mutations in optineurin. *Science (New York, NY* 2002;295:1077-1079.

238. Ray K, Mukhopadhyay A, Acharya M. Recent advances in molecular genetics of glaucoma. *Mol Cell Biochem* 2003;253:223-231.

239. Weinreb RN, Levin LA. Is neuroprotection a viable therapy for glaucoma? *Arch Ophthalmol* 1999;117:1540-1544.

240. Naldini L, Bloemer U, Gallay P, et al. In vivo gene delivery and stable transduction of nondividing cells by a lentiviral vector. *Science (New York, NY* 1996;272:263-267.

241. Kaufman PL, Gabelt BT, Cynader M. Introductory comments on neuroprotection. *Surv Ophthalmol* 1999;43 Suppl 1:S89-90.

242. Acott TS, Samples JR, Bradley JM, Bacon DR, Bylsma SS, Van Buskirk EM. Trabecular repopulation by anterior trabecular meshwork cells after laser trabeculoplasty. *Am J Ophthalmol* 1989;107:1-6.

243. Kimpel MW, Johnson DH. Factors influencing in vivo trabecular cell replication as determined by 3H-thymidine labelling; an autoradiographic study in cats. *Curr Eye Res* 1992;11:297-306.

244. Borras T, Matsumoto Y, Epstein DL, Johnson DH. Gene transfer to the human trabecular meshwork by anterior segment perfusion. *Invest Ophthalmol Vis Sci* 1998;39:1503-1507.

245. Liu X, Brandt CR, Gabelt BT, Bryar PJ, Smith ME, Kaufman PL. Herpes simplex virus mediated gene transfer to primate ocular tissues. *Exp Eye Res* 1999;69:385-395.

246. Miller DG, Adam MA, Miller AD. Gene transfer by retrovirus vectors occurs only in cells that are actively replicating at the time of infection. *Molecular and Cellular Biology* 1990;10:4239-4242.

247. Lewis PF, Emerman M. Passage through mitosis is required for oncoretroviruses but not for the human immunodeficiency virus. *Journal of virology* 1994;68:510-516.

248. Fouchier RA, Malim MH. Nuclear import of human immunodeficiency virus type-1 preintegration complexes. *Adv Virus Res* 1999;52:275-299.

249. Zennou V, Petit C, Guetard D, Nerhbass U, Montagnier L, Charneau P. HIV-1 genome nuclear import is mediated by a central DNA flap. *Cell* 2000;101:173-185.

250. Naldini L, Blomer U, Gage FH, Trono D, Verma IM. Efficient transfer, integration, and sustained long-term expression of the transgene in adult rat brains injected with a lentiviral vector. *Proceedings of the National Academy of Sciences of the United States of America* 1996;93:11382-11388.

251. Poeschla E, Gilbert J, Li X, Huang S, Ho A, Wong-Staal F. Identification of a human immunodeficiency virus type 2 (HIV-2) encapsidation determinant and transduction of nondividing human cells by HIV-2-based lentivirus vectors. *Journal of virology* 1998;72:6527-6536.

252. White SM, Renda M, Nam NY, et al. Lentivirus vectors using human and simian immunodeficiency virus elements. *Journal of virology* 1999;73:2832-2840.

253. Mangeot PE, Negre D, Dubois B, et al. Development of minimal lentivirus vectors derived from simian immunodeficiency virus (SIVmac251) and their use for gene transfer into human dendritic cells. *Journal of virology* 2000;74:8307-8315.

254. Naldini L, Verma IM. Lentiviral vectors. *Adv Virus Res* 2000;55:599-609.

255. Schnell T, Foley P, Wirth M, Munch J, Uberla K. Development of a self-inactivating, minimal lentivirus vector based on simian immunodeficiency virus. *Human gene therapy* 2000;11:439-447.

256. Kim SS, Kothari N, You XJ, et al. Generation of replication-defective helper-free vectors based on simian immunodeficiency virus. *Virology* 2001;282:154-167.

257. Olsen JC. Gene transfer vectors derived from equine infectious anemia virus. *Gene therapy* 1998;5:1481-1487.

258. Johnston JC, Gasmi M, Lim LE, et al. Minimum requirements for efficient transduction of dividing and nondividing cells by feline immunodeficiency virus vectors. *Journal of virology* 1999;73:4991-5000.

259. Mitrophanous K, Yoon S, Rohll J, et al. Stable gene transfer to the nervous system using a non-primate lentiviral vector. *Gene therapy* 1999;6:1808-1818.

260. Curran MA, Kaiser SM, Achacoso PL, Nolan GP. Efficient transduction of nondividing cells by optimized feline immunodeficiency virus vectors. *Molecular Therapy* 2000;1:31-38.

261. Poeschla E, Looney D. CXCR4 is required by a non-primate lentivirus: heterologous expression of feline immunodeficiency virus in human, rodent and feline cells. *Journal of virology* 1998;72:6858-6866.

262. Cavazzana-Calvo M, Hacein-Bey S, de Saint Basile G, et al. Gene therapy of human severe combined immunodeficiency (SCID)-X1 disease. *Science (New York, NY* 2000;288:669-672.

263. Hangai M, Tanihara H, Honda Y, Kaneda Y. Introduction of DNA into the rat and primate trabecular meshwork by fusogenic liposomes. *Investigative Ophthalmology & Visual Science* 1998;39:509-516.

264. Borras T, Gabelt BT, Klintworth GK, Peterson JC, Kaufman PL. Non-invasive observation of repeated adenoviral GFP gene delivery to the anterior segment of the monkey eye in vivo. *The journal of gene medicine* 2001;3:437-449.

265. Borras T, Brandt CR, Nickells R, Ritch R. Gene therapy for glaucoma: treating a multifaceted, chronic disease. *Investigative Ophthalmology & Visual Science* 2002;43:2513-2518.

266. Duisit G, Conrath H, Saleun S, et al. Five recombinant simian immunodeficiency virus pseudotypes lead to exclusive transduction of retinal pigmented epithelium in rat. *Mol Ther* 2002;6:446-454.

267. Steinkuller PG, Du L, Gilbert C, Foster A, Collins ML, Coats DK. Childhood blindness. *J Aapos* 1999;3:26-32.

268. Rahmani B, Tielsch JM, Katz J, et al. The cause-specific prevalence of visual impairment in an urban population. The Baltimore Eye Survey. *Ophthalmology* 1996;103:1721-1726.

269. Bressler NM, Bressler SB. Preventative ophthalmology. Age-related macular degeneration. *Ophthalmology* 1995;102:1206-1211.

270. Lee P, Wang CC, Adamis AP. Ocular neovascularization: an epidemiologic review. *Surv Ophthalmol* 1998;43:245-269.

271. Argon laser photocoagulation for neovascular maculopathy. Five-year results from randomized clinical trials. Macular Photocoagulation Study Group. *Arch Ophthalmol* 1991;109:1109-1114.

272. Klein R, Klein BE, Moss SE, Davis MD, DeMets DL. The Wisconsin epidemiologic study of diabetic retinopathy. IV. Diabetic macular edema. *Ophthalmology* 1984;91:1464-1474.

273. Ohno-Matsui K, Morita I, Tombran-Tink J, et al. Novel mechanism for age-related macular degeneration: an equilibrium shift between the angiogenesis factors VEGF and PEDF. *J Cell Physiol* 2001;189:323-333.

274. Campochiaro PA. Retinal and choroidal neovascularization. *J Cell Physiol* 2000;184:301-310.

275. Fong DS, Ferris FL, 3rd, Davis MD, Chew EY. Causes of severe visual loss in the early treatment diabetic retinopathy study: ETDRS report no. 24. Early Treatment Diabetic Retinopathy Study Research Group. *Am J Ophthalmol* 1999;127:137-141.

276. Early photocoagulation for diabetic retinopathy. ETDRS report number 9. Early Treatment Diabetic Retinopathy Study Research Group. *Ophthalmology* 1991;98:766-785.

277. Pelzek C, Lim JI. Diabetic macular edema: review and update. *Ophthalmology clinics of North America* 2002;15:555-563.

278. Bainbridge JW, Stephens C, Parsley K, et al. In vivo gene transfer to the mouse eye using an HIV-based lentiviral vector; efficient long-term transduction of corneal endothelium and retinal pigment epithelium. *Gene therapy* 2001;8:1665-1668.

279. Saenz DT, Loewen N, Peretz M, et al. Unintegrated lentivirus DNA persistence and accessibility to expression in nondividing cells: analysis with class I integrase mutants. *Journal of virology* 2004;78:2906-2920.

280. Miyoshi H, Takahashi M, Gage FH, Verma IM. Stable and efficient gene transfer into the retina using an HIV-based lentiviral vector. *Proc Natl Acad Sci U S A* 1997;94:10319-10323.

281. Takahashi M, Miyoshi H, Verma IM, Gage FH. Rescue from photoreceptor degeneration in the rd mouse by human immunodeficiency virus vector-mediated gene transfer. *Journal of virology* 1999;73:7812-7816.

282. Acland GM, Aguirre GD, Ray J, et al. Gene therapy restores vision in a canine model of childhood blindness. *Nat Genet* 2001;28:92-95.

283. Yanoff M. *Ocular Pathology*. 4th ed: Mosby Year Book; 1996.

284. Hunter DG, Repka MX. Diode laser photocoagulation for threshold retinopathy of prematurity. A randomized study. *Ophthalmology* 1993;100:238-244.

285. Pierce EA, Foley ED, Smith LE. Regulation of vascular endothelial growth factor by oxygen in a model of retinopathy of prematurity [see comments] [published erratum appears in Arch Ophthalmol 1997 Mar;115(3):427]. *Arch Ophthalmol* 1996;114:1219-1228.

286. Dawson DW, Volpert OV, Gillis P, et al. Pigment epithelium-derived factor: a potent inhibitor of angiogenesis. *Science (New York, NY* 1999;285:245-248.

287. Lashkari K, Hirose T, Yazdany J, McMeel JW, Kazlauskas A, Rahimi N. Vascular endothelial growth factor and hepatocyte growth factor levels are differentially elevated in patients with advanced retinopathy of prematurity. *The American journal of pathology* 2000;156:1337-1344.

288. Sone H, Kawakami Y, Segawa T, et al. Effects of intraocular or systemic administration of neutralizing antibody against vascular endothelial growth factor on the murine experimental model of retinopathy. *Life Sci* 1999;65:2573-2580.

289. Young TL, Anthony DC, Pierce E, Foley E, Smith LE. Histopathology and vascular endothelial growth factor in untreated and diode laser-treated retinopathy of prematurity. *J Aapos* 1997;1:105-110.

290. Multicenter Trial of Cryotherapy for Retinopathy of Prematurity: ophthalmological outcomes at 10 years. *Arch Ophthalmol* 2001;119:1110-1118.

291. Archer DB. Bowman Lecture 1998. Diabetic retinopathy: some cellular, molecular and therapeutic considerations. *Eye* 1999;13 (Pt 4):497-523.

292. Ferris FL, 3rd. Photocoagulation for diabetic retinopathy. Early Treatment Diabetic Retinopathy Study Research Group. *Jama* 1991;266:1263-1265.

293. Ogata N, Tombran-Tink J, Nishikawa M, et al. Pigment epithelium-derived factor in the vitreous is low in diabetic retinopathy and high in rhegmatogenous retinal detachment. *Am J Ophthalmol* 2001;132:378-382.

294. Spranger J, Osterhoff M, Reimann M, et al. Loss of the antiangiogenic pigment epithelium-derived factor in patients with angiogenic eye disease. *Diabetes* 2001;50:2641-2645.

295. Abdelsalam A, Del Priore L, Zarbin MA. Drusen in age-related macular degeneration: pathogenesis, natural course, and laser photocoagulation-induced regression. *Surv Ophthalmol* 1999;44:1-29.

296. Grunwald JE, Hariprasad SM, DuPont J, et al. Foveolar choroidal blood flow in age-related macular degeneration. *Invest Ophthalmol Vis Sci* 1998;39:385-390.

297. Ross RD, Barofsky JM, Cohen G, Baber WB, Palao SW, Gitter KA. Presumed macular choroidal watershed vascular filling, choroidal neovascularization, and systemic vascular disease in patients with age-related macular degeneration. *Am J Ophthalmol* 1998;125:71-80.

298. Spraul CW, Lang GE, Grossniklaus HE. Morphometric analysis of the choroid, Bruch's membrane, and retinal pigment epithelium in eyes with age-related macular degeneration. *Invest Ophthalmol Vis Sci* 1996;37:2724-2735.

299. Campochiaro PA, Soloway P, Ryan SJ, Miller JW. The pathogenesis of choroidal neovascularization in patients with age-related macular degeneration. *Molecular vision* 1999;5:34.

300. Mousa SA, Lorelli W, Campochiaro PA. Role of hypoxia and extracellular matrix-integrin binding in the modulation of angiogenic growth factors secretion by retinal pigmented epithelial cells. *J Cell Biochem* 1999;74:135-143.

301. Ferris FL, 3rd, Fine SL, Hyman L. Age-related macular degeneration and blindness due to neovascular maculopathy. *Arch Ophthalmol* 1984;102:1640-1642.

302. Ferris FL, 3rd. Senile macular degeneration: review of epidemiologic features. *Am J Epidemiol* 1983;118:132-151.

303. Ciulla TA, Danis RP, Harris A. Age-related macular degeneration: a review of experimental treatments. *Surv Ophthalmol* 1998;43:134-146.

304. Photodynamic therapy of subfoveal choroidal neovascularization in age-related macular degeneration with verteporfin: one-year results of 2 randomized clinical trials--TAP report. Treatment of age-related macular degeneration with photodynamic therapy (TAP) Study Group. *Arch Ophthalmol* 1999;117:1329-1345.

305. Verteporfin therapy of subfoveal choroidal neovascularization in age-related macular degeneration: two-year results of a randomized clinical trial including lesions with occult with no classic choroidal neovascularization--verteporfin in photodynamic therapy report 2. *Am J Ophthalmol* 2001;131:541-560.

306. Laser photocoagulation of subfoveal recurrent neovascular lesions in age-related macular degeneration. Results of a randomized clinical trial. Macular Photocoagulation Study Group. *Arch Ophthalmol* 1991;109:1232-1241.

307. Persistent and recurrent neovascularization after laser photocoagulation for subfoveal choroidal neovascularization of age-related macular degeneration. Macular Photocoagulation Study Group. *Arch Ophthalmol* 1994;112:489-499.

308. Recurrent choroidal neovascularization after argon laser photocoagulation for neovascular maculopathy. Macular Photocoagulation Study Group. *Arch Ophthalmol* 1986;104:503-512.

309. Cremers FP, Sankila EM, Brunsmann F, et al. Deletions in patients with classical choroideremia vary in size from 45 kb to several megabases. *American journal of human genetics* 1990;47:622-628.

310. van den Hurk JA, van de Pol TJ, Molloy CM, et al. Detection and characterization of point mutations in the choroideremia candidate gene by PCR-SSCP analysis and direct DNA sequencing. *American journal of human genetics* 1992;50:1195-1202.

311. Tolmachova T, Anders R, Abrink M, et al. Independent degeneration of photoreceptors and retinal pigment epithelium in conditional knockout mouse models of choroideremia. *J Clin Invest* 2006;116:386-394.

312. Mori K, Gehlbach P, Yamamoto S, et al. AAV-mediated gene transfer of pigment epithelium-derived factor inhibits choroidal neovascularization. *Invest Ophthalmol Vis Sci* 2002;43:1994-2000.

313. Lai CC, Wu WC, Chen SL, et al. Suppression of choroidal neovascularization by adeno-associated virus vector expressing angiostatin. *Invest Ophthalmol Vis Sci* 2001;42:2401-2407.

314. Auricchio A, Behling KC, Maguire AM, et al. Inhibition of retinal neovascularization by intraocular viral-mediated delivery of anti-angiogenic agents. *Mol Ther* 2002;6:490-494.

315. Liang FQ, Aleman TS, Dejneka NS, et al. Long-term protection of retinal structure but not function using RAAV.CNTF in animal models of retinitis pigmentosa. *Mol Ther* 2001;4:461-472.

316. Vollrath D, Feng W, Duncan JL, et al. Correction of the retinal dystrophy phenotype of the RCS rat by viral gene transfer of Mertk. *Proc Natl Acad Sci U S A* 2001;98:12584-12589.

317. Lau D, McGee LH, Zhou S, et al. Retinal degeneration is slowed in transgenic rats by AAV-mediated delivery of FGF-2. *Invest Ophthalmol Vis Sci* 2000;41:3622-3633.

318. McNally N, Kenna P, Humphries MM, et al. Structural and functional rescue of murine rod photoreceptors by human rhodopsin transgene. *Human molecular genetics* 1999;8:1309-1312.

319. Ali RR, Sarra GM, Stephens C, et al. Restoration of photoreceptor ultrastructure and function in retinal degeneration slow mice by gene therapy. *Nat Genet* 2000;25:306-310.

320. Liang FQ, Dejneka NS, Cohen DR, et al. AAV-mediated delivery of ciliary neurotrophic factor prolongs photoreceptor survival in the rhodopsin knockout mouse. *Mol Ther* 2001;3:241-248.

321. Loewen N, Barraza R, Whitwam T, Saenz D, Kemler I, Poeschla E. FIV Vectors. In: Federico M (ed), *Lentivirus Gene Engineering Protocols.* New York: Humana Press; 2003:251-271.

322. Tsui LV, Kelly M, Zayek N, et al. Production of human clotting Factor IX without toxicity in mice after vascular delivery of a lentiviral vector. *Nature biotechnology* 2002;20:53-57.

323. Pan D, Gunther R, Duan W, et al. Biodistribution and toxicity studies of VSVG-pseudotyped lentiviral vector after intravenous administration in mice with the observation of in vivo transduction of bone marrow. *Mol Ther* 2002;6:19-29.

324. Loewen N, Bahler C, Teo W, et al. Preservation of aqueous outflow facility after second-generation FIV vector-mediated expression of marker genes in anterior segments of human eyes. *Invest Ophthalmol Vis Sci* 2002;43:3686-3690.

325. Zhang Y, Chirmule N, Gao GP, et al. Acute cytokine response to systemic adenoviral vectors in mice is mediated by dendritic cells and macrophages. *Mol Ther* 2001;3:697-707.

326. Schnell MA, Zhang Y, Tazelaar J, et al. Activation of innate immunity in nonhuman primates following intraportal administration of adenoviral vectors. *Mol Ther* 2001;3:708-722.

327. Li T, Adamian M, Roof DJ, et al. In vivo transfer of a reporter gene to the retina mediated by an adenoviral vector. *Invest Ophthalmol Vis Sci* 1994;35:2543-2549.

328. Ali RR, Reichel MB, Byrnes AP, et al. Co-injection of adenovirus expressing CTLA4-Ig prolongs adenovirally mediated lacZ reporter gene expression in the mouse retina. *Gene therapy* 1998;5:1561-1565.

329. Holmes JM, Duffner LA. The effect of postnatal growth retardation on abnormal neovascularization in the oxygen exposed neonatal rat. *Curr Eye Res* 1996;15:403-409.

330. Holmes JM, Zhang S, Leske DA, Lanier WL. Carbon dioxide-induced retinopathy in the neonatal rat. *Curr Eye Res* 1998;17:608-616.

331. Holmes JM, Zhang S, Leske DA, Lanier WL. Metabolic acidosis-induced retinopathy in the neonatal rat. *Invest Ophthalmol Vis Sci* 1999;40:804-809.

332. Penn JS, Tolman BL, Lowery LA. Variable oxygen exposure causes preretinal neovascularization in the newborn rat. *Invest Ophthalmol Vis Sci* 1993;34:576-585.

333. Zhang S, Leske DA, Lanier WL, Berkowitz BA, Holmes JM. Preretinal neovascularization associated with acetazolamide-induced systemic acidosis in the neonatal rat. *Invest Ophthalmol Vis Sci* 2001;42:1066-1071.

334. Timmers AM, Nguyen T, Saban D, Grant MB. Viral vectors for efficient gene delivery to RPE cells. *Invest Ophthalmol Vis Sci* 2001;42:S125.

335. Auricchio A, Kobinger G, Anand V, et al. Exchange of surface proteins impacts on viral vector cellular specificity and transduction characteristics: the retina as a model. *Human molecular genetics* 2001;10:3075-3081.

336. Derksen TA, Sauter SL, Davidson BL. Feline immunodeficiency virus vectors. Gene transfer to mouse retina following intravitreal injection. *The journal of gene medicine* 2002;4:463-469.

337. Takahashi K, Luo T, Saishin Y, et al. Sustained transduction of ocular cells with a bovine immunodeficiency viral vector. *Human gene therapy* 2002;13:1305-1316.

338. Doi K, Hargitai J, Kong J, et al. Lentiviral transduction of green fluorescent protein in retinal epithelium: evidence of rejection. *Vision research* 2002;42:551-558.

339. Lotery AJ, Derksen TA, Russell SR, et al. Gene transfer to the nonhuman primate retina with recombinant feline immunodeficiency virus vectors. *Human gene therapy* 2002;13:689-696.

340. Hanahan D, Folkman J. Patterns and emerging mechanisms of the angiogenic switch during tumorigenesis. *Cell* 1996;86:353-364.

341. Smith LE. Pathogenesis of retinopathy of prematurity. *Semin Neonatol* 2003;8:469-473.

342. Lambooij AC, van Wely KH, Lindenbergh-Kortleve DJ, Kuijpers RW, Kliffen M, Mooy CM. Insulin-like growth factor-I and its receptor in neovascular age-related macular degeneration. *Invest Ophthalmol Vis Sci* 2003;44:2192-2198.

343. Takita H, Yoneya S, Gehlbach PL, Duh EJ, Wei LL, Mori K. Retinal neuroprotection against ischemic injury mediated by intraocular gene transfer of pigment epithelium-derived factor. *Invest Ophthalmol Vis Sci* 2003;44:4497-4504.

344. Miyazaki M, Ikeda Y, Yonemitsu Y, et al. Simian lentiviral vector-mediated retinal gene transfer of pigment epithelium-derived factor protects retinal degeneration and electrical defect in Royal College of Surgeons rats. *Gene therapy* 2003;10:1503-1511.

345. Gehlbach P, Demetriades AM, Yamamoto S, et al. Periocular gene transfer of sFlt-1 suppresses ocular neovascularization and vascular endothelial growth factor-induced breakdown of the blood-retinal barrier. *Human gene therapy* 2003;14:129-141.

346. Mori K, Gehlbach P, Ando A, McVey D, Wei L, Campochiaro PA. Regression of ocular neovascularization in response to increased expression of pigment epithelium-derived factor. *Invest Ophthalmol Vis Sci* 2002;43:2428-2434.

347. Rasmussen H, Chu KW, Campochiaro P, et al. Clinical protocol. An open-label, phase I, single administration, dose-escalation study of ADGVPEDF.11D (ADPEDF) in neovascular age-related macular degeneration (AMD). *Human gene therapy* 2001;12:2029-2032.

348. Mori K, Duh E, Gehlbach P, et al. Pigment epithelium-derived factor inhibits retinal and choroidal neovascularization. *J Cell Physiol* 2001;188:253-263.

349. Mori K, Ando A, Gehlbach P, et al. Inhibition of choroidal neovascularization by intravenous injection of adenoviral vectors expressing secretable endostatin. *The American journal of pathology* 2001;159:313-320.

350. Plantner JJ, Jiang C, Smine A. Increase in interphotoreceptor matrix gelatinase A (MMP-2) associated with age-related macular degeneration. *Exp Eye Res* 1998;67:637-645.

351. Kvanta A, Shen WY, Sarman S, Seregard S, Steen B, Rakoczy E. Matrix metalloproteinase (MMP) expression in experimental choroidal neovascularization. *Curr Eye Res* 2000;21:684-690.

352. Salzmann J, Limb GA, Khaw PT, et al. Matrix metalloproteinases and their natural inhibitors in fibrovascular membranes of proliferative diabetic retinopathy. *Br J Ophthalmol* 2000;84:1091-1096.

353. Das A, McLamore A, Song W, McGuire PG. Retinal neovascularization is suppressed with a matrix metalloproteinase inhibitor. *Arch Ophthalmol* 1999;117:498-503.

354. Majka S, McGuire P, Colombo S, Das A. The balance between proteinases and inhibitors in a murine model of proliferative retinopathy. *Invest Ophthalmol Vis Sci* 2001;42:210-215.

355. Igarashi T, Miyake K, Kato K, et al. Lentivirus-mediated expression of angiostatin efficiently inhibits neovascularization in a murine proliferative retinopathy model. *Gene therapy* 2003;10:219-226.

356. Raisler BJ, Berns KI, Grant MB, Beliaev D, Hauswirth WW. Adeno-associated virus type-2 expression of pigmented epithelium-derived factor or Kringles 1-3 of angiostatin reduce retinal neovascularization. *Proc Natl Acad Sci U S A* 2002;99:8909-8914.

357. Le Gat L, Gogat K, Bouquet C, et al. In vivo adenovirus-mediated delivery of a uPA/uPAR antagonist reduces retinal neovascularization in a mouse model of retinopathy. *Gene therapy* 2003;10:2098-2103.

358. Takahashi K, Saishin Y, Silva RL, et al. Intraocular expression of endostatin reduces VEGF-induced retinal vascular permeability, neovascularization, and retinal detachment. *Faseb J* 2003;17:896-898.

359. Aiello LP. Vascular endothelial growth factor and the eye: biochemical mechanisms of action and implications for novel therapies. *Ophthalmic Res* 1997;29:354-362.

360. Ozaki H, Seo MS, Ozaki K, et al. Blockade of vascular endothelial cell growth factor receptor signaling is sufficient to completely prevent retinal neovascularization. *The American journal of pathology* 2000;156:697-707.

361. Pierce EA, Avery RL, Foley ED, Aiello LP, Smith LE. Vascular endothelial growth factor/vascular permeability factor expression in a mouse model of retinal neovascularization. *Proc Natl Acad Sci U S A* 1995;92:905-909.

362. Shima DT, Gougos A, Miller JW, et al. Cloning and mRNA expression of vascular endothelial growth factor in ischemic retinas of Macaca fascicularis. *Invest Ophthalmol Vis Sci* 1996;37:1334-1340.

363. Yi X, Mai LC, Uyama M, Yew DT. Time-course expression of vascular endothelial growth factor as related to the development of the retinochoroidal vasculature in rats. *Exp Brain Res* 1998;118:155-160.

364. Shweiki D, Itin A, Soffer D, Keshet E. Vascular endothelial growth factor induced by hypoxia may mediate hypoxia-initiated angiogenesis. *Nature* 1992;359:843-845.

365. Mazure NM, Chen EY, Laderoute KR, Giaccia AJ. Induction of vascular endothelial growth factor by hypoxia is modulated by a phosphatidylinositol 3-kinase/Akt signaling pathway in Ha-ras-transformed cells through a hypoxia inducible factor-1 transcriptional element. *Blood* 1997;90:3322-3331.

366. Adamis AP, Miller JW, Bernal MT, et al. Increased vascular endothelial growth factor levels in the vitreous of eyes with proliferative diabetic retinopathy. *Am J Ophthalmol* 1994;118:445-450.

367. Aiello LP, Avery RL, Arrigg PG, et al. Vascular endothelial growth factor in ocular fluid of patients with diabetic retinopathy and other retinal disorders. *The New England journal of medicine* 1994;331:1480-1487.

368. Boulton M, Gregor Z, McLeod D, et al. Intravitreal growth factors in proliferative diabetic retinopathy: correlation with neovascular activity and glycaemic management. *Br J Ophthalmol* 1997;81:228-233.

369. Miller JW, Adamis AP, Shima DT, et al. Vascular endothelial growth factor/vascular permeability factor is temporally and spatially correlated with ocular angiogenesis in a primate model. *The American journal of pathology* 1994;145:574-584.

370. Adamis AP, Shima DT, Tolentino MJ, et al. Inhibition of vascular endothelial growth factor prevents retinal ischemia-associated iris neovascularization in a nonhuman primate. *Arch Ophthalmol* 1996;114:66-71.

371. Krzystolik MG, Afshari MA, Adamis AP, et al. Prevention of experimental choroidal neovascularization with intravitreal anti-vascular endothelial growth factor antibody fragment. *Arch Ophthalmol* 2002;120:338-346.

372. Aiello LP, Pierce EA, Foley ED, et al. Suppression of retinal neovascularization in vivo by inhibition of vascular endothelial growth factor (VEGF) using soluble VEGF-receptor chimeric proteins. *Proc Natl Acad Sci U S A* 1995;92:10457-10461.

373. Robinson GS, Pierce EA, Rook SL, Foley E, Webb R, Smith LE. Oligodeoxynucleotides inhibit retinal neovascularization in a murine model of proliferative retinopathy. *Proc Natl Acad Sci U S A* 1996;93:4851-4856.

374. Shen WY, Garrett KL, Wang CG, et al. Preclinical evaluation of a phosphorothioate oligonucleotide in the retina of rhesus monkey. *Laboratory investigation; a journal of technical methods and pathology* 2002;82:167-182.

375. Preclinical and phase 1A clinical evaluation of an anti-VEGF pegylated aptamer (EYE001) for the treatment of exudative age-related macular degeneration. *Retina (Philadelphia, Pa* 2002;22:143-152.

376. Kong HL, Hecht D, Song W, et al. Regional suppression of tumor growth by in vivo transfer of a cDNA encoding a secreted form of the extracellular domain of the flt-1 vascular endothelial growth factor receptor. *Human gene therapy* 1998;9:823-833.

377. Shiose S, Sakamoto T, Yoshikawa H, et al. Gene transfer of a soluble receptor of VEGF inhibits the growth of experimental eyelid malignant melanoma. *Invest Ophthalmol Vis Sci* 2000;41:2395-2403.

378. Grant MB, Mames RN, Fitzgerald C, Ellis EA, Aboufriekha M, Guy J. Insulin-like growth factor I acts as an angiogenic agent in rabbit cornea and retina: comparative studies with basic fibroblast growth factor. *Diabetologia* 1993;36:282-291.

379. Smith LE, Kopchick JJ, Chen W, et al. Essential role of growth hormone in ischemia-induced retinal neovascularization. *Science (New York, NY* 1997;276:1706-1709.

380. Steele FR, Chader GJ, Johnson LV, Tombran-Tink J. Pigment epithelium-derived factor: neurotrophic activity and identification as a member of the serine protease inhibitor gene family. *Proc Natl Acad Sci U S A* 1993;90:1526-1530.

381. Tombran-Tink J, Chader GG, Johnson LV. PEDF: a pigment epithelium-derived factor with potent neuronal differentiative activity [letter]. *Exp Eye Res* 1991;53:411-414.

382. Cayouette M, Smith SB, Becerra SP, Gravel C. Pigment epithelium-derived factor delays the death of photoreceptors in mouse models of inherited retinal degenerations. *Neurobiol Dis* 1999;6:523-532.

383. Cao W, Tombran-Tink J, Elias R, Sezate S, Mrazek D, McGinnis JF. In vivo protection of photoreceptors from light damage by pigment epithelium-derived factor. *Invest Ophthalmol Vis Sci* 2001;42:1646-1652.

384. Ogata N, Wang L, Jo N, et al. Pigment epithelium derived factor as a neuroprotective agent against ischemic retinal injury. *Curr Eye Res* 2001;22:245-252.

385. Ogata N, Nishikawa M, Nishimura T, Mitsuma Y, Matsumura M. Unbalanced vitreous levels of pigment epithelium-derived factor and vascular endothelial growth factor in diabetic retinopathy. *Am J Ophthalmol* 2002;134:348-353.

386. Ogata N, Nishikawa M, Nishimura T, Mitsuma Y, Matsumura M. Inverse levels of pigment epithelium-derived factor and vascular endothelial growth factor in the vitreous of eyes with rhegmatogenous retinal detachment and proliferative vitreoretinopathy. *Am J Ophthalmol* 2002;133:851-852.

387. Yamagishi S, Inagaki Y, Amano S, Okamoto T, Takeuchi M. Up-regulation of vascular endothelial growth factor and down-regulation of pigment epithelium-derived factor messenger ribonucleic acid levels in leptin-exposed cultured retinal pericytes. *Int J Tissue React* 2002;24:137-142.

388. Gao G, Li Y, Zhang D, Gee S, Crosson C, Ma J. Unbalanced expression of VEGF and PEDF in ischemia-induced retinal neovascularization. *FEBS Lett* 2001;489:270-276.

389. Cao Y. Endogenous angiogenesis inhibitors and their therapeutic implications. *Int J Biochem Cell Biol* 2001;33:357-369.

390. Lai YK, Shen WY, Brankov M, Lai CM, Constable IJ, Rakoczy PE. Potential long-term inhibition of ocular neovascularisation by recombinant adeno-associated virus-mediated secretion gene therapy. *Gene therapy* 2002;9:804-813.

391. Takagi H, Koyama S, Seike H, et al. Potential role of the angiopoietin/tie2 system in ischemia-induced retinal neovascularization. *Invest Ophthalmol Vis Sci* 2003;44:393-402.

392. Hangai M, Moon YS, Kitaya N, et al. Systemically expressed soluble Tie2 inhibits intraocular neovascularization. *Human gene therapy* 2001;12:1311-1321.

393. Zhang S, Leske DA, Holmes JM. Neovascularization grading methods in a rat model of retinopathy of prematurity. *Invest Ophthalmol Vis Sci* 2000;41:887-891.

394. Smith LE, Wesolowski E, McLellan A, et al. Oxygen-induced retinopathy in the mouse. *Invest Ophthalmol Vis Sci* 1994;35:101-111.

395. Holmes JM, Zhang S, Leske DA, Lanier WL. The effect of carbon dioxide on oxygen-induced retinopathy in the neonatal rat. *Curr Eye Res* 1997;16:725-732.

396. Kitzmann A, Leske D, Chen Y, Kendall A, Lanier W, Holmes J. Incidence and severity of neovascularization in oxygen- and metabolic acidosis-induced retinopathy depend on rat source. *Curr Eye Res* 2002;25:215-220.

397. Shen WY, Lee SY, Yeo I, et al. Predilection of the macular region to high incidence of choroidal neovascularization after intense laser photocoagulation in the monkey. *Arch Ophthalmol* 2004;122:353-360.

398. Semkova I, Peters S, Welsandt G, Janicki H, Jordan J, Schraermeyer U. Investigation of laser-induced choroidal neovascularization in the rat. *Invest Ophthalmol Vis Sci* 2003;44:5349-5354.

399. Okamoto N, Tobe T, Hackett SF, et al. Transgenic mice with increased expression of vascular endothelial growth factor in the retina: a new model of intraretinal and subretinal neovascularization. *The American journal of pathology* 1997;151:281-291.

400. Schwesinger C, Yee C, Rohan RM, et al. Intrachoroidal neovascularization in transgenic mice overexpressing vascular endothelial growth factor in the retinal pigment epithelium. *The American journal of pathology* 2001;158:1161-1172.

401. Soubrane G, Cohen SY, Delayre T, et al. Basic fibroblast growth factor experimentally induced choroidal angiogenesis in the minipig. *Curr Eye Res* 1994;13:183-195.

402. Chen Y, Leske DA, Zhang S, Karger RA, Lanier WL, Holmes JM. Duration of acidosis and recovery determine preretinal neovascularization in the rat model of acidosis-induced retinopathy. *Curr Eye Res* 2002;24:281-288.

403. Rubinson DA, Dillon CP, Kwiatkowski AV, et al. A lentivirus-based system to functionally silence genes in primary mammalian cells, stem cells and transgenic mice by RNA interference. *Nat Genet* 2003;33:401-406.

404. Tiscornia G, Singer O, Ikawa M, Verma IM. A general method for gene knockdown in mice by using lentiviral vectors expressing small interfering RNA. *Proc Natl Acad Sci U S A* 2003;100:1844-1848.

405. Arts GJ, Langemeijer E, Tissingh R, et al. Adenoviral vectors expressing siRNAs for discovery and validation of gene function. *Genome Res* 2003;13:2325-2332.

406. Hofmann A, Kessler B, Ewerling S, et al. Efficient transgenesis in farm animals by lentiviral vectors. *EMBO Rep* 2003;4:1054-1060.

407. Arendt CW, Tang G, Zilberstein A. Vector Systems for the Delivery of Small Interfering RNAs: Managing the RISC. *Chembiochem* 2003;4:1129-1136.

408. Andang M, Hinkula J, Hotchkiss G, et al. Dose-response resistance to HIV-1/MuLV pseudotype virus ex vivo in a hairpin ribozyme transgenic mouse model. *Proc Natl Acad Sci U S A* 1999;96:12749-12753.

409. Lan N, Howrey RP, Lee SW, Smith CA, Sullenger BA. Ribozyme-mediated repair of sickle beta-globin mRNAs in erythrocyte precursors. *Science (New York, NY* 1998;280:1593-1596.

410. LaVail MM, Yasumura D, Matthes MT, et al. Ribozyme rescue of photoreceptor cells in P23H transgenic rats: long-term survival and late-stage therapy. *Proc Natl Acad Sci U S A* 2000;97:11488-11493.

411. Jen KY, Gewirtz AM. Suppression of gene expression by targeted disruption of messenger RNA: available options and current strategies. *Stem Cells* 2000;18:307-319.

412. Hauswirth WW, Lewin AS. Ribozyme uses in retinal gene therapy. *Prog Retin Eye Res* 2000;19:689-710.

413. Nirenberg MW. Will Society be Prepared? *Science (New York, NY* 1967;157:633.

414. Nirenberg MW. Unpublished draft of introduction to the Nobel speech. *Draft Speech* 1968.

415. Terheggen HG, Lowenthal A, Lavinha F, Colombo JP, Rogers S. Unsuccessful trial of gene replacement in arginase deficiency. *Z Kinderheilkd* 1975;119:1-3.

416. Wade N. UCLA gene therapy racked by friendly fire. *Science (New York, NY* 1980;210:509-511.

417. Wade N. Gene therapy pioneer draws Mikadoesque rap. *Science (New York, NY* 1981;212:1253.

418. Wade N. Gene therapy caught in more entanglements. *Science (New York, NY* 1981;212:24-25.

419. Fletcher J. Testimony at a Hearing before the Subcommittee on Investigations and Oversight of the Committee on Science and Technology, U.S. House of Representatives, Nov. 16-18, 1982. *Human Genetic Engineering* 1983;170:342-386.

420. Anderson WF. Testimony at a Hearing before the Subcommittee on Investigations and Oversight of the Committee on Science and Technology, U.S. House of Representatives, Nov. 16-18, 1982. *Human Genetic Engineering* 1983;285-292.

421. Talbot M. Testimony at a Hearing before the Subcommittee on Investigations and Oversight of the Committee on Science and Technology, U.S. House of Representatives, Nov. 16-18, 1982. *Human Genetic Engineering* 1983;170:540-545.

422. Sun M. Cline loses two NIH grants. *Science (New York, NY* 1981;214:1220.

423. Sun M. Martin Cline loses appeal on NIH grant. *Science (New York, NY* 1982;218:37.

424. Cline MJ. Genetic engineering of mammalian cells: its potential application to genetic diseases of man. *J Lab Clin Med* 1982;99:299-308.

425. Cline MJ. Testimony at a Hearing before the Subcommittee on Investigations and Oversight of the Committee on Science and Technology, U.S. House of Representatives, Nov. 16-18, 1982. *Human Genetic Engineering* 1983;170:442-461.

426. In: Register F (ed); 1984:17846.

427. Anderson WF. Human Gene Therapy. *Science (New York, NY* 1992;256:808-813.

428. Graham FL, Smiley J, Russell WC, Nairn R. Characteristics of a human cell line transformed by DNA from human adenovirus type 5. *Journal of General Virology* 1977;36:59-74.

429. Engelhardt JF, Litzky L, Wilson JM. Prolonged transgene expression in cotton rat lung with recombinant adenoviruses defective in E2a. *Human gene therapy* 1994;5:1217-1229.

430. Armentano D, Zabner J, Sacks C, et al. Effect of the E4 region on the persistence of transgene expression from adenovirus vectors. *Journal of virology* 1997;71:2408-2416.

431. Chen HH, Mack LM, Kelly R, Ontell M, Kochanek S, Clemens PR. Persistence in muscle of an adenoviral vector that lacks all viral genes. *Proc Natl Acad Sci U S A* 1997;94:1645-1650.

432. Worgall S, Wolff G, Falck-Pedersen E, Crystal RG. Innate immune mechanisms dominate elimination of adenoviral vectors following in vivo administration. *Human gene therapy* 1997;8:37-44.

433. Jooss K, Yang Y, Wilson JM. Cyclophosphamide diminishes inflammation and prolongs transgene expression following delivery of adenoviral vectors to mouse liver and lung. *Human gene therapy* 1996;7:1555-1566.

434. Kay MA, Meuse L, Gown AM, et al. Transient immunomodulation with anti-CD40 ligand antibody and CTLA4Ig enhances persistence and secondary adenovirus-mediated gene transfer into mouse liver. *Proc Natl Acad Sci U S A* 1997;94:4686-4691.

435. Kagami H, Atkinson JC, Michalek SM, et al. Repetitive adenovirus administration to the parotid gland: role of immunological barriers and induction of oral tolerance. *Human gene therapy* 1998;9:305-313.

436. Kay MA, Holterman AX, Meuse L, et al. Long-term hepatic adenovirus-mediated gene expression in mice following CTLA4Ig administration. *Nat Genet* 1995;11:191-197.

437. Raper SE, Chirmule N, Lee FS, et al. Fatal systemic inflammatory response syndrome in a ornithine transcarbamylase deficient patient following adenoviral gene transfer. *Molecular genetics and metabolism* 2003;80:148-158.

438. Stone D, Liu Y, Li ZY, Tuve S, Strauss R, Lieber A. Comparison of adenoviruses from species B, C, E, and F after intravenous delivery. *Mol Ther* 2007;15:2146-2153.

439. Schiedner G, Morral N, Parks RJ, et al. Genomic DNA transfer with a high-capacity adenovirus vector results in improved in vivo gene expression and decreased toxicity. *Nat Genet* 1998;18:180-183.

440. Gahery-Segard H, Molinier-Frenkel V, Le Boulaire C, et al. Phase I trial of recombinant adenovirus gene transfer in lung cancer. Longitudinal study of the immune responses to transgene and viral products. *J Clin Invest* 1997;100:2218-2226.

441. Hong SS, Karayan L, Tournier J, Curiel DT, Boulanger PA. Adenovirus type 5 fiber knob binds to MHC class I alpha2 domain at the surface of human epithelial and B lymphoblastoid cells. *The EMBO journal* 1997;16:2294-2306.

442. Bergelson JM, Cunningham JA, Droguett G, et al. Isolation of a common receptor for Coxsackie B viruses and adenoviruses 2 and 5. *Science (New York, NY* 1997;275:1320-1323.

443. Wickham TJ, Filardo EJ, Cheresh DA, Nemerow GR. Integrin alpha v beta 5 selectively promotes adenovirus mediated cell membrane permeabilization. *J Cell Biol* 1994;127:257-264.

444. Harris JD, Lemoine NR. Strategies for targeted gene therapy. *Trends Genet* 1996;12:400-405.

445. Davison E, Diaz RM, Hart IR, Santis G, Marshall JF. Integrin alpha5beta1-mediated adenovirus infection is enhanced by the integrin-activating antibody TS2/16. *Journal of virology* 1997;71:6204-6207.

446. Wickham TJ, Lee GM, Titus JA, et al. Targeted adenovirus-mediated gene delivery to T cells via CD3. *Journal of virology* 1997;71:7663-7669.

447. Goldman CK, Rogers BE, Douglas JT, et al. Targeted gene delivery to Kaposi's sarcoma cells via the fibroblast growth factor receptor. *Cancer Res* 1997;57:1447-1451.

448. Wickham TJ, Tzeng E, Shears LL, 2nd, et al. Increased in vitro and in vivo gene transfer by adenovirus vectors containing chimeric fiber proteins. *Journal of virology* 1997;71:8221-8229.

449. Rosenfeld MA, Siegfried W, Yoshimura K, et al. Adenovirus-mediated transfer of a recombinant alpha 1-antitrypsin gene to the lung epithelium in vivo. *Science (New York, NY* 1991;252:431-434.

450. Akli S, Caillaud C, Vigne E, et al. Transfer of a foreign gene into the brain using adenovirus vectors. *Nat Genet* 1993;3:224-228.

451. Le Gal La Salle G, Robert JJ, Berrard S, et al. An adenovirus vector for gene transfer into neurons and glia in the brain. *Science (New York, NY* 1993;259:988-990.

452. Zhao H, Ivic L, Otaki JM, Hashimoto M, Mikoshiba K, Firestein S. Functional expression of a mammalian odorant receptor. *Science (New York, NY* 1998;279:237-242.

453. Roberts DM, Nanda A, Havenga MJ, et al. Hexon-chimaeric adenovirus serotype 5 vectors circumvent pre-existing anti-vector immunity. *Nature* 2006;441:239-243.

454. Shiver JW, Fu TM, Chen L, et al. Replication-incompetent adenoviral vaccine vector elicits effective anti-immunodeficiency-virus immunity. *Nature* 2002;415:331-335.

455. Letvin NL, Mascola JR, Sun Y, et al. Preserved CD4+ central memory T cells and survival in vaccinated SIV-challenged monkeys. *Science (New York, NY* 2006;312:1530-1533.

456. Cepko C. Preparation of a specific retrovirus producer cell line. *Current protocols in molecular biology / edited by Frederick M Ausubel [et al* 2001;Chapter 9:Unit9 10.

457. Kordower JH, Emborg ME, Bloch J, et al. Neurodegeneration prevented by lentiviral vector delivery of GDNF in primate models of Parkinson's disease. *Science (New York, NY* 2000;290:767-773.

458. Manno CS, Pierce GF, Arruda VR, et al. Successful transduction of liver in hemophilia by AAV-Factor IX and limitations imposed by the host immune response. *Nat Med* 2006;12:342-347.

459. Wu X, Li Y, Crise B, Burgess SM. Transcription start regions in the human genome are favored targets for MLV integration. *Science (New York, NY* 2003;300:1749-1751.

460. Saleh M. A retroviral vector that allows efficient co-expression of two genes and the versatility of alternate selection markers. *Human gene therapy* 1997;8:979-983.

461. Haynes C, Erlwein O, Schnierle BS. Modified envelope glycoproteins to retarget retroviral vectors. *Current gene therapy* 2003;3:405-410.

462. Burns JC, Friedmann T, Driever W, Burrascano M, Yee JK. Vesicular stomatitis virus G glycoprotein pseudotyped retroviral vectors: concentration to very high titer and efficient gene transfer into mammalian and nonmammalian cells. *Proceedings of the National Academy of Sciences of the United States of America* 1993;90:8033-8037.

463. Mazarakis ND, Azzouz M, Rohll JB, et al. Rabies virus glycoprotein pseudotyping of lentiviral vectors enables retrograde axonal transport and access to the nervous system after peripheral delivery. *Human molecular genetics* 2001;10:2109-2121.

464. Liu SL, Halbert CL, Miller AD. Jaagsiekte sheep retrovirus envelope efficiently pseudotypes human immunodeficiency virus type 1-based lentiviral vectors. *Journal of virology* 2004;78:2642-2647.

465. Zeilfelder U, Bosch V. Properties of wild-type, C-terminally truncated, and chimeric maedi-visna virus glycoprotein and putative pseudotyping of retroviral vector particles. *Journal of virology* 2001;75:548-555.

466. Stitz J, Buchholz CJ, Engelstadter M, et al. Lentiviral vectors pseudotyped with envelope glycoproteins derived from gibbon ape leukemia virus and murine leukemia virus 10A1. *Virology* 2000;273:16-20.

467. VandenDriessche T, Naldini L, Collen D, Chuah MK. Oncoretroviral and lentiviral vector-mediated gene therapy. *Methods Enzymol* 2002;346:573-589.

468. Lewis BC, Chinnasamy N, Morgan RA, Varmus HE. Development of an avian leukosis-sarcoma virus subgroup A pseudotyped lentiviral vector. *Journal of virology* 2001;75:9339-9344.

469. Kumar M, Bradow BP, Zimmerberg J. Large-scale production of pseudotyped lentiviral vectors using baculovirus GP64. *Human gene therapy* 2003;14:67-77.

470. Rambukkana A, Kunz S, Min J, Campbell KP, Oldstone MB. Targeting Schwann cells by nonlytic arenaviral infection selectively inhibits myelination. *Proc Natl Acad Sci U S A* 2003;100:16071-16076.

471. Mochizuki H, Schwartz JP, Tanaka K, Brady RO, Reiser J. High-titer human immunodeficiency virus type 1-based vector systems for gene delivery into nondividing cells. *Journal of virology* 1998;72:8873-8883.

472. Medina MF, Kobinger GP, Rux J, et al. Lentiviral vectors pseudotyped with minimal filovirus envelopes increased gene transfer in murine lung. *Mol Ther* 2003;8:777-789.

473. Sinn PL, Hickey MA, Staber PD, et al. Lentivirus vectors pseudotyped with filoviral envelope glycoproteins transduce airway epithelia from the apical surface independently of folate receptor alpha. *Journal of virology* 2003;77:5902-5910.

474. Kobinger GP, Weiner DJ, Yu QC, Wilson JM. Filovirus-pseudotyped lentiviral vector can efficiently and stably transduce airway epithelia in vivo. *Nature biotechnology* 2001;19:225-230.

475. Kang Y, Stein CS, Heth JA, et al. In vivo gene transfer using a nonprimate lentiviral vector pseudotyped with Ross River Virus glycoproteins. *Journal of virology* 2002;76:9378-9388.

476. Glimm H, Kiem HP, Darovsky B, et al. Efficient gene transfer in primitive CD34+/CD38lo human bone marrow cells reselected after long-term exposure to GALV-pseudotyped retroviral vector. *Human gene therapy* 1997;8:2079-2086.

477. Ghazizadeh S, Carroll JM, Taichman LB. Repression of retrovirus-mediated transgene expression by interferons: implications for gene therapy. *Journal of virology* 1997;71:9163-9169.

478. Cherry SR, Biniszkiewicz D, van Parijs L, Baltimore D, Jaenisch R. Retroviral expression in embryonic stem cells and hematopoietic stem cells. *Mol Cell Biol* 2000;20:7419-7426.

479. Hacein-Bey-Abina S, Le Deist F, Carlier F, et al. Sustained correction of X-linked severe combined immunodeficiency by ex vivo gene therapy. *The New England journal of medicine* 2002;346:1185-1193.

480. Hacein-Bey-Abina S, Von Kalle C, Schmidt M, et al. LMO2-associated clonal T cell proliferation in two patients after gene therapy for SCID-X1. *Science (New York, NY* 2003;302:415-419.

481. Aiuti A, Slavin S, Aker M, et al. Correction of ADA-SCID by stem cell gene therapy combined with nonmyeloablative conditioning. *Science (New York, NY* 2002;296:2410-2413.

482. Morgan RA, Dudley ME, Wunderlich JR, et al. Cancer regression in patients after transfer of genetically engineered lymphocytes. *Science (New York, NY* 2006;314:126-129.

483. Ott MG, Schmidt M, Schwarzwaelder K, et al. Correction of X-linked chronic granulomatous disease by gene therapy, augmented by insertional activation of MDS1-EVI1, PRDM16 or SETBP1. *Nat Med* 2006;12:401-409.

484. Tuszynski MH, Thal L, Pay M, et al. A phase 1 clinical trial of nerve growth factor gene therapy for Alzheimer disease. *Nat Med* 2005;11:551-555.

485. Mavilio F, Pellegrini G, Ferrari S, et al. Correction of junctional epidermolysis bullosa by transplantation of genetically modified epidermal stem cells. *Nat Med* 2006;12:1397-1402.

486. Kafri T, Blomer U, Peterson DA, Gage FH, Verma IM. Sustained expression of genes delivered directly into liver and muscle by lentiviral vectors. *Nature Genetics* 1997;17:314-317.

487. Xu K, Ma H, McCown TJ, Verma IM, Kafri T. Generation of a stable cell line producing high-titer self-inactivating lentiviral vectors. *Mol Ther* 2001;3:97-104.

488. Yanez-Munoz RJ, Balaggan KS, MacNeil A, et al. Effective gene therapy with nonintegrating lentiviral vectors. *Nat Med* 2006;12:348-353.

489. Parolin C, Sodroski J. A defective HIV-1 vector for gene transfer to human lymphocytes. *Journal of Molecular Medicine* 1995;73:279-288.

490. Poznansky M, Lever A, Bergeron L, Haseltine W, Sodroski J. Gene transfer into human lymphocytes by a defective human immunodeficiency virus type 1 vector. *Journal of virology* 1991;65:532-536.

491. Reiser J, Harmison G, Kluepfel-Stahl S, Brady RO, Karlsson S, Schubert M. Transduction of nondividing cells using pseudotyped defective high-titer HIV type 1 particles. *Proceedings of the National Academy of Sciences of the United States of America* 1996;93:15266-15271.

492. Whitwam T, Peretz M, Poeschla EM. Identification of a central DNA flap in feline immunodeficiency virus. *Journal of virology* 2001;75:9407-9414.

493. Kemler I, Barraza R, Poeschla EM. Mapping of the encapsidation determinants of feline immunodeficiency virus. *Journal of virology* 2002;76:11889-11903.

494. Bonini C, Ferrari G, Verzeletti S, et al. HSV-TK gene transfer into donor lymphocytes for control of allogeneic graft-versus-leukemia [see comments]. *Science (New York, NY* 1997;276:1719-1724.

495. Montini E, Cesana D, Schmidt M, et al. Hematopoietic stem cell gene transfer in a tumor-prone mouse model uncovers low genotoxicity of lentiviral vector integration. *Nature biotechnology* 2006;24:687-696.

496. Hacker CV, Vink CA, Wardell TW, et al. The integration profile of EIAV-based vectors. *Mol Ther* 2006;14:536-545.

497. Lodish H, Berk A, Zipursky SL, Matsudaira P, Baltimore D, Darnell JE. *Molecular Cell Biology*. 4th ed. New York: W. H. Freeman & Co.; 1999.

498. Saenz DT, Poeschla EM. FIV: from lentivirus to lentivector. *The journal of gene medicine* 2004;6 Suppl 1:S95-104.

499. Talbott RL, Sparger EE, Lovelace KM, et al. Nucleotide sequence and genomic organization of feline immunodeficiency virus. *Proceedings of the National Academy of Sciences of the United States of America* 1989;86:5743-5747.

500. Pedersen NC. The feline immunodeficiency virus. In: Levy JA (ed), *The Retroviridae.* New York: Plenum Press; 1993:181-228.

501. Elder JH, Phillips TR. Molecular properties of feline immunodeficiency virus (FIV). *Infectious Agents and Disease* 1993;2:361-374.

502. Lerner DL, Wagaman PC, Phillips TR, et al. Increased mutation frequency of feline immunodeficiency virus lacking functional deoxyuridine-triphosphatase. *Proceedings of the National Academy of Sciences of the United States of America* 1995;92:7480-7484.

503. Olmsted RA, Hirsch VM, Purcell RH, Johnson PR. Nucleotide sequence analysis of feline immunodeficiency virus: genome organization and relationship to other lentiviruses. *Proceedings of the National Academy of Sciences of the United States of America* 1989;86:8088-8092.

504. Loewen N, Fautsch M, Peretz M, et al. Genetic modification of human trabecular meshwork with lentiviral vectors. *Human gene therapy* 2001;12:2109-2119.

505. Tomonaga K, Miyazawa T, Kawaguchi Y, Kohmoto M, Inoshima Y, Mikami T. Comparison of the Rev transactivation of feline immunodeficiency virus in feline and non-feline cell lines. *Journal of Veterinary Medical Science* 1994;56:199-201.

506. McAllister RM, Nicolson M, Gardner MB, et al. RD-114 virus compared with feline and murine type-C viruses released from RD cells. *Nature New Biol* 1973;242:75-78.

507. McAllister RM, Nicolson M, Gardner MB, et al. C-type virus released from cultured human rhabdomyosarcoma cells. *Nature New Biol* 1972;235:3-6.

508. Takeuchi Y, Cosset FL, Lachmann PJ, Okada H, Weiss RA, Collins MK. Type C retrovirus inactivation by human complement is determined by both the viral genome and the producer cell. *Journal of virology* 1994;68:8001-8007.

509. Neiman PE. Measurement of RD114 virus nucleotide sequences in feline cellular DNA. *Nat New Biol* 1973;244:62-64.

510. Chang LJ, Urlacher V, Iwakuma T, Cui Y, Zucali J. Efficacy and safety analyses of a recombinant human immunodeficiency virus type 1 derived vector system. *Gene therapy* 1999;6:715-728.

511. Berkowitz R, Ilves H, Lin WY, et al. Construction and molecular analysis of gene transfer systems derived from bovine immunodeficiency virus. *Journal of virology* 2001;75:3371-3382.

512. Pawliuk R, Westerman KA, Fabry ME, et al. Correction of sickle cell disease in transgenic mouse models by gene therapy. *Science (New York, NY* 2001;294:2368-2371.

513. Ralph GS, Radcliffe PA, Day DM, et al. Silencing mutant SOD1 using RNAi protects against neurodegeneration and extends survival in an ALS model. *Nat Med* 2005;11:429-433.

514. Consiglio A, Quattrini A, Martino S, et al. In vivo gene therapy of metachromatic leukodystrophy by lentiviral vectors: correction of neuropathology and protection against learning impairments in affected mice. *Nat Med* 2001;7:310-316.

515. Dupre L, Trifari S, Follenzi A, et al. Lentiviral vector-mediated gene transfer in T cells from Wiskott-Aldrich syndrome patients leads to functional correction. *Mol Ther* 2004;10:903-915.

516. Kazuki Y, Hoshiya H, Kai Y, et al. Correction of a genetic defect in multipotent germline stem cells using a human artificial chromosome. *Gene therapy* 2008.

517. Wolff JA, Malone RW, Williams P, et al. Direct gene transfer into mouse muscle in vivo. *Science (New York, NY* 1990;247:1465-1468.

518. Zhu N, Liggitt D, Liu Y, Debs R. Systemic gene expression after intravenous DNA delivery into adult mice. *Science (New York, NY* 1993;261:209-211.

519. Cheng L, Ziegelhoffer PR, Yang NS. In vivo promoter activity and transgene expression in mammalian somatic tissues evaluated by using particle bombardment. *Proc Natl Acad Sci U S A* 1993;90:4455-4459.

520. Xiang Z, Ertl HC. Manipulation of the immune response to a plasmid-encoded viral antigen by coinoculation with plasmids expressing cytokines. *Immunity* 1995;2:129-135.

521. Felgner JH, Kumar R, Sridhar CN, et al. Enhanced gene delivery and mechanism studies with a novel series of cationic lipid formulations. *J Biol Chem* 1994;269:2550-2561.

522. Wang CY, Huang L. pH-sensitive immunoliposomes mediate target-cell-specific delivery and controlled expression of a foreign gene in mouse. *Proc Natl Acad Sci U S A* 1987;84:7851-7855.

523. Dzau VJ, Mann MJ, Morishita R, Kaneda Y. Fusigenic viral liposome for gene therapy in cardiovascular diseases. *Proc Natl Acad Sci U S A* 1996;93:11421-11425.

524. Stavridis JC, Deliconstantinos G, Psallidopoulos MC, Armenakas NA, Hadjiminas DJ, Hadjiminas J. Construction of transferrin-coated liposomes for in vivo transport of exogenous DNA to bone marrow erythroblasts in rabbits. *Experimental cell research* 1986;164:568-572.

525. Wagner E, Cotten M, Foisner R, Birnstiel ML. Transferrin-polycation-DNA complexes: the effect of polycations on the structure of the complex and DNA delivery to cells. *Proc Natl Acad Sci U S A* 1991;88:4255-4259.

526. Ferkol T, Kaetzel CS, Davis PB. Gene transfer into respiratory epithelial cells by targeting the polymeric immunoglobulin receptor. *J Clin Invest* 1993;92:2394-2400.

527. Madon J, Blum HE. Receptor-mediated delivery of hepatitis B virus DNA and antisense oligodeoxynucleotides to avian liver cells. *Hepatology (Baltimore, Md* 1996;24:474-481.

528. Kusano KF, Pola R, Murayama T, et al. Sonic hedgehog myocardial gene therapy: tissue repair through transient reconstitution of embryonic signaling. *Nat Med* 2005;11:1197-1204.

529. Hood JD, Bednarski M, Frausto R, et al. Tumor regression by targeted gene delivery to the neovasculature. *Science (New York, NY* 2002;296:2404-2407.

530. Ortiz-Urda S, Thyagarajan B, Keene DR, et al. Stable nonviral genetic correction of inherited human skin disease. *Nat Med* 2002;8:1166-1170.

531. Murphy M, Gomos-Klein J, Stankic M, Falck-Pedersen E. Adeno-associated virus type 2 p5 promoter: a rep-regulated DNA switch element functioning in transcription, replication, and site-specific integration. *Journal of virology* 2007;81:3721-3730.

532. Nakai H, Montini E, Fuess S, Storm TA, Grompe M, Kay MA. AAV serotype 2 vectors preferentially integrate into active genes in mice. *Nat Genet* 2003;34:297-302.

533. Blacklow NR, Hoggan MD, Rowe WP. Serologic evidence for human infection with adenovirus-associated viruses. *Journal of the National Cancer Institute* 1968;40:319-327.

534. Berns KI, Giraud C. Biology of adeno-associated virus. *Current topics in microbiology and immunology* 1996;218:1-23.

535. Berns KI. Parvovirus replication. *Microbiological reviews* 1990;54:316-329.

536. Yan Z, Zak R, Zhang Y, Engelhardt JF. Inverted terminal repeat sequences are important for intermolecular recombination and circularization of adeno-associated virus genomes. *Journal of virology* 2005;79:364-379.

537. Yan Z, Lei-Butters DC, Zhang Y, Zak R, Engelhardt JF. Hybrid adeno-associated virus bearing nonhomologous inverted terminal repeats enhances dual-vector reconstruction of minigenes in vivo. *Human gene therapy* 2007;18:81-87.

538. Laughlin CA, Tratschin JD, Coon H, Carter BJ. Cloning of infectious adeno-associated virus genomes in bacterial plasmids. *Gene* 1983;23:65-73.

539. Hermonat PL, Muzyczka N. Use of adeno-associated virus as a mammalian DNA cloning vector: transduction of neomycin resistance into mammalian tissue culture cells. *Proc Natl Acad Sci U S A* 1984;81:6466-6470.

540. Wright JF, Qu G, Tang C, Sommer JM. Recombinant adeno-associated virus: formulation challenges and strategies for a gene therapy vector. *Current opinion in drug discovery & development* 2003;6:174-178.

541. Donsante A, Vogler C, Muzyczka N, et al. Observed incidence of tumorigenesis in long-term rodent studies of rAAV vectors. *Gene therapy* 2001;8:1343-1346.

542. Medicine JoG. Gene Therapy Clinical Trials Worldwide. Wiley Co.

543. Wagner JA, Messner AH, Moran ML, et al. Safety and biological efficacy of an adeno-associated virus vector-cystic fibrosis transmembrane regulator (AAV-CFTR) in the cystic fibrosis maxillary sinus. *The Laryngoscope* 1999;109:266-274.

544. Crystal RG, Sondhi D, Hackett NR, et al. Clinical protocol. Administration of a replication-deficient adeno-associated virus gene transfer vector expressing the human CLN2 cDNA to the brain of children with late infantile neuronal ceroid lipofuscinosis. *Human gene therapy* 2004;15:1131-1154.

545. McPhee SW, Janson CG, Li C, et al. Immune responses to AAV in a phase I study for Canavan disease. *The journal of gene medicine* 2006;8:577-588.

546. Flotte TR, Brantly ML, Spencer LT, et al. Phase I trial of intramuscular injection of a recombinant adeno-associated virus alpha 1-antitrypsin (rAAV2-CB-hAAT) gene vector to AAT-deficient adults. *Human gene therapy* 2004;15:93-128.

547. During MJ, Kaplitt MG, Stern MB, Eidelberg D. Subthalamic GAD gene transfer in Parkinson disease patients who are candidates for deep brain stimulation. *Human gene therapy* 2001;12:1589-1591.

548. Wagner JA, Nepomuceno IB, Shah N, et al. Maxillary sinusitis as a surrogate model for CF gene therapy clinical trials in patients with antrostomies. *The journal of gene medicine* 1999;1:13-21.

549. Croteau GA, Martin DB, Camp J, et al. Evaluation of exposure and health care worker response to nebulized administration of tgAAVCF to patients with cystic fibrosis. *The Annals of occupational hygiene* 2004;48:673-681.

550. Muzyczka N, Warrington KH, Jr. Custom adeno-associated virus capsids: the next generation of recombinant vectors with novel tropism. *Human gene therapy* 2005;16:408-416.

551. McCarty DM, Fu H, Monahan PE, Toulson CE, Naik P, Samulski RJ. Adeno-associated virus terminal repeat (TR) mutant generates self-complementary vectors to overcome the rate-limiting step to transduction in vivo. *Gene therapy* 2003;10:2112-2118.

552. Choi VW, McCarty DM, Samulski RJ. AAV hybrid serotypes: improved vectors for gene delivery. *Current gene therapy* 2005;5:299-310.

553. Mount JD, Herzog RW, Tillson DM, et al. Sustained phenotypic correction of hemophilia B dogs with a factor IX null mutation by liver-directed gene therapy. *Blood* 2002;99:2670-2676.

554. Snyder RO, Miao CH, Patijn GA, et al. Persistent and therapeutic concentrations of human factor IX in mice after hepatic gene transfer of recombinant AAV vectors. *Nat Genet* 1997;16:270-276.

555. Chamberlain JR, Schwarze U, Wang PR, et al. Gene targeting in stem cells from individuals with osteogenesis imperfecta. *Science (New York, NY* 2004;303:1198-1201.

556. Luo J, Kaplitt MG, Fitzsimons HL, et al. Subthalamic GAD gene therapy in a Parkinson's disease rat model. *Science (New York, NY* 2002;298:425-429.

557. Marconi P, Krisky D, Oligino T, et al. Replication-defective herpes simplex virus vectors for gene transfer in vivo. *Proceedings of the National Academy of Sciences of the United States of America* 1996;93:11319-11320.

558. Thompson RL, Sawtell NM. The herpes simplex virus type 1 latency-associated transcript gene regulates the establishment of latency. *Journal of virology* 1997;71:5432-5440.

559. Federoff HJ, Geschwind MD, Geller AI, Kessler JA. Expression of nerve growth factor in vivo from a defective herpes simplex virus 1 vector prevents effects of axotomy on sympathetic ganglia. *Proc Natl Acad Sci U S A* 1992;89:1636-1640.

560. Wang S, Vos JM. A hybrid herpesvirus infectious vector based on Epstein-Barr virus and herpes simplex virus type 1 for gene transfer into human cells in vitro and in vivo. *Journal of virology* 1996;70:8422-8430.

561. Kesari S, Randazzo BP, Valyi-Nagy T, et al. Therapy of experimental human brain tumors using a neuroattenuated herpes simplex virus mutant. *Laboratory investigation; a journal of technical methods and pathology* 1995;73:636-648.

562. Kramm CM, Chase M, Herrlinger U, et al. Therapeutic efficiency and safety of a second-generation replication-conditional HSV1 vector for brain tumor gene therapy. *Human gene therapy* 1997;8:2057-2068.

563. During MJ, Naegele JR, O'Malley KL, Geller AI. Long-term behavioral recovery in parkinsonian rats by an HSV vector expressing tyrosine hydroxylase. *Science (New York, NY* 1994;266:1399-1403.

564. Wood MJ, Byrnes AP, Pfaff DW, Rabkin SD, Charlton HM. Inflammatory effects of gene transfer into the CNS with defective HSV-1 vectors. *Gene therapy* 1994;1:283-291.

565. Kucharczuk JC, Randazzo B, Chang MY, et al. Use of a "replication-restricted" herpes virus to treat experimental human malignant mesothelioma. *Cancer Res* 1997;57:466-471.

566. Dewey RA, Morrissey G, Cowsill CM, et al. Chronic brain inflammation and persistent herpes simplex virus 1 thymidine kinase expression in survivors of syngeneic glioma treated by adenovirus-mediated gene therapy: implications for clinical trials. *Nat Med* 1999;5:1256-1263.

567. Lu Y, McNearney TA, Lin W, Wilson SP, Yeomans DC, Westlund KN. Treatment of inflamed pancreas with enkephalin encoding HSV-1 recombinant vector reduces inflammatory damage and behavioral sequelae. *Mol Ther* 2007;15:1812-1819.

568. Chattopadhyay M, Wolfe D, Mata M, Huang S, Glorioso JC, Fink DJ. Long-term neuroprotection achieved with latency-associated promoter-driven herpes simplex virus gene transfer to the peripheral nervous system. *Mol Ther* 2005;12:307-313.

569. Puskovic V, Wolfe D, Wechuck J, et al. HSV-mediated delivery of erythropoietin restores dopaminergic function in MPTP-treated mice. *Mol Ther* 2006;14:710-715.

570. Laing JM, Gober MD, Golembewski EK, et al. Intranasal administration of the growth-compromised HSV-2 vector DeltaRR prevents kainate-induced seizures and neuronal loss in rats and mice. *Mol Ther* 2006;13:870-881.

571. Hacein-Bey-Abina S, von Kalle C, Schmidt M, et al. A serious adverse event after successful gene therapy for X-linked severe combined immunodeficiency. *The New England journal of medicine* 2003;348:255-256.

572. Stocking C, Bergholz U, Friel J, et al. Distinct classes of factor-independent mutants can be isolated after retroviral mutagenesis of a human myeloid stem cell line. *Growth Factors* 1993;8:197-209.

573. Bordignon C, Notarangelo LD, Nobili N, et al. Gene therapy in peripheral blood lymphocytes and bone marrow for ADA- immunodeficient patients. *Science (New York, NY* 1995;270:470-475.

574. Blaese RM, Culver KW, Miller AD, et al. T lymphocyte-directed gene therapy for ADA-SCID: initial trial results after 4 years. *Science (New York, NY* 1995;270:475-480.

575. Kohn DB, Weinberg KI, Nolta JA, et al. Engraftment of gene-modified umbilical cord blood cells in neonates with adenosine deaminase deficiency. *Nat Med* 1995;1:1017-1023.

576. Hoogerbrugge PM, van Beusechem VW, Fischer A, et al. Bone marrow gene transfer in three patients with adenosine deaminase deficiency. *Gene therapy* 1996;3:179-183.

577. Kohn DB, Hershfield MS, Carbonaro D, et al. T lymphocytes with a normal ADA gene accumulate after transplantation of transduced autologous umbilical cord blood CD34+ cells in ADA-deficient SCID neonates. *Nat Med* 1998;4:775-780.

578. Manno CS, Chew AJ, Hutchison S, et al. AAV-mediated factor IX gene transfer to skeletal muscle in patients with severe hemophilia B. *Blood* 2003;101:2963-2972.

579. Nakai H, Thomas CE, Storm TA, et al. A limited number of transducible hepatocytes restricts a wide-range linear vector dose response in recombinant adeno-associated virus-mediated liver transduction. *Journal of virology* 2002;76:11343-11349.

580. Nakai H, Yant SR, Storm TA, Fuess S, Meuse L, Kay MA. Extrachromosomal recombinant adeno-associated virus vector genomes are primarily responsible for stable liver transduction in vivo. *Journal of virology* 2001;75:6969-6976.

581. Nakai H, Storm TA, Kay MA. Recruitment of single-stranded recombinant adeno-associated virus vector genomes and intermolecular recombination are responsible for stable transduction of liver in vivo. *Journal of virology* 2000;74:9451-9463.

582. Muruve DA, Barnes MJ, Stillman IE, Libermann TA. Adenoviral gene therapy leads to rapid induction of multiple chemokines and acute neutrophil-dependent hepatic injury in vivo. *Human gene therapy* 1999;10:965-976.

583. Lieber A, He CY, Meuse L, et al. The role of Kupffer cell activation and viral gene expression in early liver toxicity after infusion of recombinant adenovirus vectors. *Journal of virology* 1997;71:8798-8807.

584. Marshall E. Gene therapy death prompts review of adenovirus vector. *Science (New York, NY* 1999;286:2244-2245.

585. Chiang YP, Bassi LJ, Javitt JC. Federal budgetary costs of blindness. *Milbank Q* 1992;70:319-340.

586. Loewen N, Fautsch MP, Teo WL, Bahler CK, Johnson DH, Poeschla EM. Long-term, targeted genetic modification of the aqueous humor outflow tract coupled with noninvasive imaging of gene expression in vivo. *Invest Ophthalmol Vis Sci* 2004;45:3091-3098.

587. Wenkel H, Streilein JW. Analysis of immune deviation elicited by antigens injected into the subretinal space. *Invest Ophthalmol Vis Sci* 1998;39:1823-1834.

588. Streilein JW. Unraveling immune privilege. *Science (New York, NY* 1995;270:1158-1159.

589. Wilson SE, Schultz GS, Chegini N, Weng J, He YG. Epidermal growth factor, transforming growth factor alpha, transforming growth factor beta, acidic fibroblast growth factor, basic fibroblast growth factor, and interleukin-1 proteins in the cornea. *Exp Eye Res* 1994;59:63-71.

590. Wilbanks GA, Streilein JW. Studies on the induction of anterior chamber-associated immune deviation (ACAID). 1. Evidence that an antigen-specific, ACAID-inducing, cell-associated signal exists in the peripheral blood. *J Immunol* 1991;146:2610-2617.

591. Griffith TS, Brunner T, Fletcher SM, Green DR, Ferguson TA. Fas ligand-induced apoptosis as a mechanism of immune privilege. *Science (New York, NY* 1995;270:1189-1192.

592. Borras T, Tamm ER, Zigler JS, Jr. Ocular adenovirus gene transfer varies in efficiency and inflammatory response. *Invest Ophthalmol Vis Sci* 1996;37:1282-1293.

593. Tsubota K, Inoue H, Ando K, Ono M, Yoshino K, Saito I. Adenovirus-mediated gene transfer to the ocular surface epithelium. *Exp Eye Res* 1998;67:531-538.

594. Spencer B, Agarwala S, Miskulin M, Smith M, Brandt CR. Herpes simplex virus-mediated gene delivery to the rodent visual system. *Invest Ophthalmol Vis Sci* 2000;41:1392-1401.

595. Tsai EY, Falvo JV, Tsytsykova AV, et al. A lipopolysaccharide-specific enhancer complex involving Ets, Elk-1, Sp1, and CREB binding protein and p300 is recruited to the tumor necrosis factor alpha promoter in vivo. *Mol Cell Biol* 2000;20:6084-6094.

596. Larkin DF, Oral HB, Ring CJ, Lemoine NR, George AJ. Adenovirus-mediated gene delivery to the corneal endothelium. *Transplantation* 1996;61:363-370.

597. Fehervari Z, Rayner SA, Oral HB, George AJ, Larkin DF. Gene transfer to ex vivo stored corneas. *Cornea* 1997;16:459-464.

598. Oral HB, Larkin DF, Fehervari Z, et al. Ex vivo adenovirus-mediated gene transfer and immunomodulatory protein production in human cornea. *Gene therapy* 1997;4:639-647.

599. Hudde T, Rayner SA, De Alwis M, et al. Adeno-associated and herpes simplex viruses as vectors for gene transfer to the corneal endothelium. *Cornea* 2000;19:369-373.

600. Mashhour B, Couton D, Perricaudet M, Briand P. In vivo adenovirus-mediated gene transfer into ocular tissues. *Gene therapy* 1994;1:122-126.

601. Daheshia M, Kuklin N, Kanangat S, Manickan E, Rouse BT. Suppression of ongoing ocular inflammatory disease by topical administration of plasmid DNA encoding IL-10. *J Immunol* 1997;159:1945-1952.

602. Lai CM, Brankov M, Zaknich T, et al. Inhibition of angiogenesis by adenovirus-mediated sFlt-1 expression in a rat model of corneal neovascularization. *Human gene therapy* 2001;12:1299-1310.

603. Coster DJ, Williams KA. The impact of corneal allograft rejection on the long-term outcome of corneal transplantation. *Am J Ophthalmol* 2005;140:1112-1122.

604. Klebe S, Coster DJ, Sykes PJ, et al. Prolongation of sheep corneal allograft survival by transfer of the gene encoding ovine IL-12-p40 but not IL-4 to donor corneal endothelium. *J Immunol* 2005;175:2219-2226.

605. Klebe S, Sykes PJ, Coster DJ, Krishnan R, Williams KA. Prolongation of sheep corneal allograft survival by ex vivo transfer of the gene encoding interleukin-10. *Transplantation* 2001;71:1214-1220.

606. Gong N, Pleyer U, Yang J, et al. Influence of local and systemic CTLA4Ig gene transfer on corneal allograft survival. *The journal of gene medicine* 2006;8:459-467.

607. Gong N, Pleyer U, Volk HD, Ritter T. Effects of local and systemic viral interleukin-10 gene transfer on corneal allograft survival. *Gene therapy* 2007;14:484-490.

608. Beutelspacher SC, Pillai R, Watson MP, et al. Function of indoleamine 2,3-dioxygenase in corneal allograft rejection and prolongation of allograft survival by over-expression. *European journal of immunology* 2006;36:690-700.

609. Murthy RC, McFarland TJ, Yoken J, et al. Corneal transduction to inhibit angiogenesis and graft failure. *Invest Ophthalmol Vis Sci* 2003;44:1837-1842.

610. Nesburn AB, Ghiasi H, Wechsler SL. Ocular safety and efficacy of an HSV-1 gD vaccine during primary and latent infection. *Invest Ophthalmol Vis Sci* 1990;31:1497-1502.

611. Osorio Y, Ghiasi H. Comparison of adjuvant efficacy of herpes simplex virus type 1 recombinant viruses expressing TH1 and TH2 cytokine genes. *Journal of virology* 2003;77:5774-5783.

612. Osorio Y, Ghiasi H. Recombinant herpes simplex virus type 1 (HSV-1) codelivering interleukin-12p35 as a molecular adjuvant enhances the protective immune response against ocular HSV-1 challenge. *Journal of virology* 2005;79:3297-3308.

613. Daheshia M, Kuklin N, Manickan E, Chun S, Rouse BT. Immune induction and modulation by topical ocular administration of plasmid DNA encoding antigens and cytokines. *Vaccine* 1998;16:1103-1110.

614. Wasmuth S, Bauer D, Yang Y, Steuhl KP, Heiligenhaus A. Topical treatment with antisense oligonucleotides targeting tumor necrosis factor-alpha in herpetic stromal keratitis. *Invest Ophthalmol Vis Sci* 2003;44:5228-5234.

615. Kim B, Lee S, Suvas S, Rouse BT. Application of plasmid DNA encoding IL-18 diminishes development of herpetic stromal keratitis by antiangiogenic effects. *J Immunol* 2005;175:509-516.

616. Kim B, Tang Q, Biswas PS, et al. Inhibition of ocular angiogenesis by siRNA targeting vascular endothelial growth factor pathway genes: therapeutic strategy for herpetic stromal keratitis. *The American journal of pathology* 2004;165:2177-2185.

617. Azkur AK, Kim B, Suvas S, Lee Y, Kumaraguru U, Rouse BT. Blocking mouse MMP-9 production in tumor cells and mouse cornea by short hairpin (sh) RNA encoding plasmids. *Oligonucleotides* 2005;15:72-84.

618. Stechschulte SU, Joussen AM, von Recum HA, et al. Rapid ocular angiogenic control via naked DNA delivery to cornea. *Invest Ophthalmol Vis Sci* 2001;42:1975-1979.

619. Singh N, Amin S, Richter E, et al. Flt-1 intraceptors inhibit hypoxia-induced VEGF expression in vitro and corneal neovascularization in vivo. *Invest Ophthalmol Vis Sci* 2005;46:1647-1652.

620. Jani PD, Singh N, Jenkins C, et al. Nanoparticles sustain expression of Flt intraceptors in the cornea and inhibit injury-induced corneal angiogenesis. *Invest Ophthalmol Vis Sci* 2007;48:2030-2036.

621. Lai CM, Spilsbury K, Brankov M, Zaknich T, Rakoczy PE. Inhibition of corneal neovascularization by recombinant adenovirus mediated antisense VEGF RNA. *Exp Eye Res* 2002;75:625-634.

622. Moore JE, McMullen TC, Campbell IL, et al. The inflammatory milieu associated with conjunctivalized cornea and its alteration with IL-1 RA gene therapy. *Invest Ophthalmol Vis Sci* 2002;43:2905-2915.

623. Cheng HC, Yeh SI, Tsao YP, Kuo PC. Subconjunctival injection of recombinant AAV-angiostatin ameliorates alkali burn induced corneal angiogenesis. *Molecular vision* 2007;13:2344-2352.

624. Behrens A, Gordon EM, Li L, et al. Retroviral gene therapy vectors for prevention of excimer laser-induced corneal haze. *Invest Ophthalmol Vis Sci* 2002;43:968-977.

625. Seitz B, Moreira L, Baktanian E, et al. Retroviral vector-mediated gene transfer into keratocytes in vitro and in vivo. *Am J Ophthalmol* 1998;126:630-639.

626. Kamata Y, Okuyama T, Kosuga M, et al. Adenovirus-mediated gene therapy for corneal clouding in mice with mucopolysaccharidosis type VII. *Mol Ther* 2001;4:307-312.

627. Budenz DL, Bennett J, Alonso L, Maguire A. In vivo gene transfer into murine corneal endothelial and trabecular meshwork cells. *Invest Ophthalmol Vis Sci* 1995;36:2211-2215.

628. Borras T, Rowlette LL, Erzurum SC, Epstein DL. Adenoviral reporter gene transfer to the human trabecular meshwork does not alter aqueous humor outflow. Relevance for potential gene therapy of glaucoma. *Gene therapy* 1999;6:515-524.

629. Kee C, Sohn S, Hwang JM. Stromelysin gene transfer into cultured human trabecular cells and rat trabecular meshwork in vivo. *Invest Ophthalmol Vis Sci* 2001;42:2856-2860.

630. Comes N, Borras T. Functional delivery of synthetic naked siRNA to the human trabecular meshwork in perfused organ cultures. *Molecular vision* 2007;13:1363-1374.

631. Bennett J, Wilson J, Sun D, Forbes B, Maguire A. Adenovirus vector-mediated in vivo gene transfer into adult murine retina. *Invest Ophthalmol Vis Sci* 1994;35:2535-2542.

632. Chan AW, Chong KY, Martinovich C, Simerly C, Schatten G. Transgenic monkeys produced by retroviral gene transfer into mature oocytes. *Science (New York, NY* 2001;291:309-312.

633. Bradley JM, Vranka J, Colvis CM, et al. Effect of matrix metalloproteinases activity on outflow in perfused human organ culture. *Invest Ophthalmol Vis Sci* 1998;39:2649-2658.

634. Vittitow JL, Garg R, Rowlette LL, Epstein DL, O'Brien ET, Borras T. Gene transfer of dominant-negative RhoA increases outflow facility in perfused human anterior segment cultures. *Molecular vision* 2002;8:32-44.

635. Stamer WD, Peppel K, O'Donnell ME, Roberts BC, Wu F, Epstein DL. Expression of aquaporin-1 in human trabecular meshwork cells: role in resting cell volume. *Investigative Ophthalmology & Visual Science* 2001;42:1803-1811.

636. Zhao X, Pearson KE, Stephan DA, Russell P. Effects of prostaglandin analogues on human ciliary muscle and trabecular meshwork cells. *Invest Ophthalmol Vis Sci* 2003;44:1945-1952.

637. Stamer WD, Snyder RW, Smith BL, Agre P, Regan JW. Localization of aquaporin CHIP in the human eye: implications in the pathogenesis of glaucoma and other disorders of ocular fluid balance. *Invest Ophthalmol Vis Sci* 1994;35:3867-3872.

638. Gabelt BT, Hu Y, Vittitow JL, et al. Caldesmon transgene expression disrupts focal adhesions in HTM cells and increases outflow facility in organ-cultured human and monkey anterior segments. *Exp Eye Res* 2006;82:935-944.

639. Liu X, Hu Y, Filla MS, et al. The effect of C3 transgene expression on actin and cellular adhesions in cultured human trabecular meshwork cells and on outflow facility in organ cultured monkey eyes. *Molecular vision* 2005;11:1112-1121.

640. Challa P, Luna C, Liton PB, et al. Lentiviral mediated gene delivery to the anterior chamber of rodent eyes. *Molecular vision* 2005;11:425-430.

641. Khare PD, Loewen N, Teo W, et al. Durable, Safe, Multi-gene Lentiviral Vector Expression in Feline Trabecular Meshwork. *Mol Ther* 2008;16:97-106.

642. Balaggan KS, Binley K, Esapa M, et al. Stable and efficient intraocular gene transfer using pseudotyped EIAV lentiviral vectors. *The journal of gene medicine* 2006;8:275-285.

643. Wong LF, Azzouz M, Walmsley LE, et al. Transduction patterns of pseudotyped lentiviral vectors in the nervous system. *Mol Ther* 2004;9:101-111.

644. Hudde T, Apitz J, Bordes-Alonso R, et al. Gene transfer to trabecular meshwork endothelium via direct injection into the Schlemm canal and in vivo toxicity study. *Curr Eye Res* 2005;30:1051-1059.

645. Liton PB, Liu X, Stamer WD, Challa P, Epstein DL, Gonzalez P. Specific targeting of gene expression to a subset of human trabecular meshwork cells using the chitinase 3-like 1 promoter. *Invest Ophthalmol Vis Sci* 2005;46:183-190.

646. Gonzalez P, Caballero M, Liton PB, Stamer WD, Epstein DL. Expression analysis of the matrix GLA protein and VE-cadherin gene promoters in the outflow pathway. *Invest Ophthalmol Vis Sci* 2004;45:1389-1395.

647. Borras T, Xue W, Choi VW, et al. Mechanisms of AAV transduction in glaucoma-associated human trabecular meshwork cells. *The journal of gene medicine* 2006;8:589-602.

648. Perkins TW, Faha B, Ni M, et al. Adenovirus-mediated gene therapy using human p21WAF-1/Cip-1 to prevent wound healing in a rabbit model of glaucoma filtration surgery. *Arch Ophthalmol* 2002;120:941-949.

649. Atencio IA, Chen Z, Nguyen QH, Faha B, Maneval DC. p21WAF-1/Cip-1 gene therapy as an adjunct to glaucoma filtration surgery. *Current opinion in molecular therapeutics* 2004;6:624-628.

650. Yoon KC, Yang KJ, Seo JS, et al. Effect of human RAD50 gene therapy on glaucoma filtering surgery in rabbit eye. *Curr Eye Res* 2004;28:181-187.

651. Klocker N, Kermer P, Gleichmann M, Weller M, Bahr M. Both the neuronal and inducible isoforms contribute to upregulation of retinal nitric oxide synthase activity by brain-derived neurotrophic factor. *J Neurosci* 1999;19:8517-8527.

652. Krueger-Naug AM, Emsley JG, Myers TL, Currie RW, Clarke DB. Administration of brain-derived neurotrophic factor suppresses the expression of heat shock protein 27 in rat retinal ganglion cells following axotomy. *Neuroscience* 2003;116:49-58.

653. Henderson JT, Seniuk NA, Richardson PM, Gauldie J, Roder JC. Systemic administration of ciliary neurotrophic factor induces cachexia in rodents. *J Clin Invest* 1994;93:2632-2638.

654. Mansour-Robaey S, Clarke DB, Wang YC, Bray GM, Aguayo AJ. Effects of ocular injury and administration of brain-derived neurotrophic factor on survival and regrowth of axotomized retinal ganglion cells. *Proc Natl Acad Sci U S A* 1994;91:1632-1636.

655. Perez MT, Caminos E. Expression of brain-derived neurotrophic factor and of its functional receptor in neonatal and adult rat retina. *Neuroscience letters* 1995;183:96-99.

656. Kaplan DR, Miller FD. Neurotrophin signal transduction in the nervous system. *Current opinion in neurobiology* 2000;10:381-391.

657. Cheng L, Sapieha P, Kittlerova P, Hauswirth WW, Di Polo A. TrkB gene transfer protects retinal ganglion cells from axotomy-induced death in vivo. *J Neurosci* 2002;22:3977-3986.

658. Harwerth RS, Carter-Dawson L, Shen F, Smith EL, 3rd, Crawford ML. Ganglion cell losses underlying visual field defects from experimental glaucoma. *Invest Ophthalmol Vis Sci* 1999;40:2242-2250.

659. Martin KR, Quigley HA, Zack DJ, et al. Gene therapy with brain-derived neurotrophic factor as a protection: retinal ganglion cells in a rat glaucoma model. *Investigative Ophthalmology & Visual Science* 2003;44:4357-4365.

660. Davidson FF, Steller H. Blocking apoptosis prevents blindness in Drosophila retinal degeneration mutants. *Nature* 1998;391:587-591.

661. Takahashi R, Deveraux Q, Tamm I, et al. A single BIR domain of XIAP sufficient for inhibiting caspases. *J Biol Chem* 1998;273:7787-7790.

662. Schuettauf F, Vorwerk C, Naskar R, et al. Adeno-associated viruses containing bFGF or BDNF are neuroprotective against excitotoxicity. *Curr Eye Res* 2004;29:379-386.

663. Akimoto M, Miyatake S, Kogishi J, et al. Adenovirally expressed basic fibroblast growth factor rescues photoreceptor cells in RCS rats. *Invest Ophthalmol Vis Sci* 1999;40:273-279.

664. Leaver SG, Cui Q, Bernard O, Harvey AR. Cooperative effects of bcl-2 and AAV-mediated expression of CNTF on retinal ganglion cell survival and axonal regeneration in adult transgenic mice. *The European journal of neuroscience* 2006;24:3323-3332.

665. Leaver SG, Cui Q, Plant GW, et al. AAV-mediated expression of CNTF promotes long-term survival and regeneration of adult rat retinal ganglion cells. *Gene therapy* 2006;13:1328-1341.

666. Di Polo A, Aigner LJ, Dunn RJ, Bray GM, Aguayo AJ. Prolonged delivery of brain-derived neurotrophic factor by adenovirus-infected Muller cells temporarily rescues injured retinal ganglion cells. *Proceedings of the National Academy of Sciences of the United States of America* 1998;95:3978-3983.

667. Wu WC, Lai CC, Chen SL, et al. Long-term safety of GDNF gene delivery in the retina. *Curr Eye Res* 2005;30:715-722.

668. Ishikawa H, Takano M, Matsumoto N, et al. Effect of GDNF gene transfer into axotomized retinal ganglion cells using in vivo electroporation with a contact lens-type electrode. *Gene therapy* 2005;12:289-298.

669. Malik JM, Shevtsova Z, Bahr M, Kugler S. Long-term in vivo inhibition of CNS neurodegeneration by Bcl-XL gene transfer. *Mol Ther* 2005;11:373-381.

670. Qi X, Sun L, Lewin AS, Hauswirth WW, Guy J. Long-term suppression of neurodegeneration in chronic experimental optic neuritis: antioxidant gene therapy. *Invest Ophthalmol Vis Sci* 2007;48:5360-5370.

671. Kaplan J, Bonneau D, Frezal J, Munnich A, Dufier JL. Clinical and genetic heterogeneity in retinitis pigmentosa. *Hum Genet* 1990;85:635-642.

672. Bennett J, Tanabe T, Sun D, et al. Photoreceptor cell rescue in retinal degeneration (rd) mice by in vivo gene therapy. *Nat Med* 1996;2:649-654.

673. Jomary C, Vincent KA, Grist J, Neal MJ, Jones SE. Rescue of photoreceptor function by AAV-mediated gene transfer in a mouse model of inherited retinal degeneration. *Gene therapy* 1997;4:683-690.

674. Kumar-Singh R, Farber DB. Encapsidated adenovirus mini-chromosome-mediated delivery of genes to the retina: application to the rescue of photoreceptor degeneration. *Human molecular genetics* 1998;7:1893-1900.

675. Sung CH, Schneider BG, Agarwal N, Papermaster DS, Nathans J. Functional heterogeneity of mutant rhodopsins responsible for autosomal dominant retinitis pigmentosa. *Proc Natl Acad Sci U S A* 1991;88:8840-8844.

676. Kaushal S, Khorana HG. Structure and function in rhodopsin. 7. Point mutations associated with autosomal dominant retinitis pigmentosa. *Biochemistry* 1994;33:6121-6128.

677. Lewin AS, Drenser KA, Hauswirth WW, et al. Ribozyme rescue of photoreceptor cells in a transgenic rat model of autosomal dominant retinitis pigmentosa. *Nat Med* 1998;4:967-971.

678. Chen J, Flannery JG, LaVail MM, Steinberg RH, Xu J, Simon MI. bcl-2 overexpression reduces apoptotic photoreceptor cell death in three different retinal degenerations. *Proc Natl Acad Sci U S A* 1996;93:7042-7047.

679. Bennett J, Zeng Y, Bajwa R, Klatt L, Li Y, Maguire AM. Adenovirus-mediated delivery of rhodopsin-promoted bcl-2 results in a delay in photoreceptor cell death in the rd/rd mouse. *Gene therapy* 1998;5:1156-1164.

680. Uteza Y, Rouillot JS, Kobetz A, et al. Intravitreous transplantation of encapsulated fibroblasts secreting the human fibroblast growth factor 2 delays photoreceptor cell degeneration in Royal College of Surgeons rats. *Proceedings of the National Academy of Sciences of the United States of America* 1999;96:3126-3131.

681. McGee Sanftner LH, Abel H, Hauswirth WW, Flannery JG. Glial cell line derived neurotrophic factor delays photoreceptor degeneration in a transgenic rat model of retinitis pigmentosa. *Molecular Therapy: the Journal of the American Society of Gene Therapy* 2001;4:622-629.

682. Matsuda T, Cepko CL. Electroporation and RNA interference in the rodent retina in vivo and in vitro. *Proc Natl Acad Sci U S A* 2004;101:16-22.

683. Chalberg TW, Genise HL, Vollrath D, Calos MP. phiC31 integrase confers genomic integration and long-term transgene expression in rat retina. *Invest Ophthalmol Vis Sci* 2005;46:2140-2146.

684. Bemelmans AP, Bonnel S, Houhou L, et al. Retinal cell type expression specificity of HIV-1-derived gene transfer vectors upon subretinal injection in the adult rat: influence of pseudotyping and promoter. *The journal of gene medicine* 2005;7:1367-1374.

685. Kostic C, Chiodini F, Salmon P, et al. Activity analysis of housekeeping promoters using self-inactivating lentiviral vector delivery into the mouse retina. *Gene therapy* 2003;10:818-821.

686. Gruter O, Kostic C, Crippa SV, et al. Lentiviral vector-mediated gene transfer in adult mouse photoreceptors is impaired by the presence of a physical barrier. *Gene therapy* 2005;12:942-947.

687. Cheng L, Toyoguchi M, Looney DJ, Lee J, Davidson MC, Freeman WR. Efficient gene transfer to retinal pigment epithelium cells with long-term expression. *Retina (Philadelphia, Pa* 2005;25:193-201.

688. Tschernutter M, Schlichtenbrede FC, Howe S, et al. Long-term preservation of retinal function in the RCS rat model of retinitis pigmentosa following lentivirus-mediated gene therapy. *Gene therapy* 2005;12:694-701.

689. Bainbridge JW, Mistry A, Schlichtenbrede FC, et al. Stable rAAV-mediated transduction of rod and cone photoreceptors in the canine retina. *Gene therapy* 2003;10:1336-1344.

690. Lotery AJ, Yang GS, Mullins RF, et al. Adeno-associated virus type 5: transduction efficiency and cell-type specificity in the primate retina. *Human gene therapy* 2003;14:1663-1671.

691. Weber M, Rabinowitz J, Provost N, et al. Recombinant adeno-associated virus serotype 4 mediates unique and exclusive long-term transduction of retinal pigmented epithelium in rat, dog, and nonhuman primate after subretinal delivery. *Mol Ther* 2003;7:774-781.

692. Acland GM, Aguirre GD, Bennett J, et al. Long-term restoration of rod and cone vision by single dose rAAV-mediated gene transfer to the retina in a canine model of childhood blindness. *Mol Ther* 2005;12:1072-1082.

693. Natkunarajah M, Trittibach P, McIntosh J, et al. Assessment of ocular transduction using single-stranded and self-complementary recombinant adeno-associated virus serotype 2/8. *Gene therapy* 2008;15:463-467.

694. Folliot S, Briot D, Conrath H, et al. Sustained tetracycline-regulated transgene expression in vivo in rat retinal ganglion cells using a single type 2 adeno-associated viral vector. *The journal of gene medicine* 2003;5:493-501.

695. Lebherz C, Auricchio A, Maguire AM, et al. Long-term inducible gene expression in the eye via adeno-associated virus gene transfer in nonhuman primates. *Human gene therapy* 2005;16:178-186.

696. Smith JR, Verwaerde C, Rolling F, et al. Tetracycline-inducible viral interleukin-10 intraocular gene transfer, using adeno-associated virus in experimental autoimmune uveoretinitis. *Human gene therapy* 2005;16:1037-1046.

697. Bainbridge JW, Mistry A, Binley K, et al. Hypoxia-regulated transgene expression in experimental retinal and choroidal neovascularization. *Gene therapy* 2003;10:1049-1054.

698. Le Guiner C, Stieger K, Snyder RO, Rolling F, Moullier P. Immune responses to gene product of inducible promoters. *Current gene therapy* 2007;7:334-346.

699. Schlichtenbrede FC, da Cruz L, Stephens C, et al. Long-term evaluation of retinal function in Prph2Rd2/Rd2 mice following AAV-mediated gene replacement therapy. *The journal of gene medicine* 2003;5:757-764.

700. Pawlyk BS, Smith AJ, Buch PK, et al. Gene replacement therapy rescues photoreceptor degeneration in a murine model of Leber congenital amaurosis lacking RPGRIP. *Invest Ophthalmol Vis Sci* 2005;46:3039-3045.

701. Zeng Y, Takada Y, Kjellstrom S, et al. RS-1 Gene Delivery to an Adult Rs1h Knockout Mouse Model Restores ERG b-Wave with Reversal of the Electronegative Waveform of X-Linked Retinoschisis. *Invest Ophthalmol Vis Sci* 2004;45:3279-3285.

702. Min SH, Molday LL, Seeliger MW, et al. Prolonged recovery of retinal structure/function after gene therapy in an Rs1h-deficient mouse model of x-linked juvenile retinoschisis. *Mol Ther* 2005;12:644-651.

703. Smith AJ, Schlichtenbrede FC, Tschernutter M, Bainbridge JW, Thrasher AJ, Ali RR. AAV-Mediated gene transfer slows photoreceptor loss in the RCS rat model of retinitis pigmentosa. *Mol Ther* 2003;8:188-195.

704. Surace EM, Domenici L, Cortese K, et al. Amelioration of both functional and morphological abnormalities in the retina of a mouse model of ocular albinism following AAV-mediated gene transfer. *Mol Ther* 2005;12:652-658.

705. Dejneka NS, Surace EM, Aleman TS, et al. In utero gene therapy rescues vision in a murine model of congenital blindness. *Mol Ther* 2004;9:182-188.

706. Narfstrom K, Vaegan, Katz M, Bragadottir R, Rakoczy EP, Seeliger M. Assessment of structure and function over a 3-year period after gene transfer in RPE65-/- dogs. *Documenta ophthalmologica* 2005;111:39-48.

707. Narfstrom K, Katz ML, Ford M, Redmond TM, Rakoczy E, Bragadottir R. In vivo gene therapy in young and adult RPE65-/- dogs produces long-term visual improvement. *The Journal of heredity* 2003;94:31-37.

708. Narfstrom K, Katz ML, Bragadottir R, et al. Functional and structural recovery of the retina after gene therapy in the RPE65 null mutation dog. *Invest Ophthalmol Vis Sci* 2003;44:1663-1672.

709. Alexander JJ, Umino Y, Everhart D, et al. Restoration of cone vision in a mouse model of achromatopsia. *Nat Med* 2007;13:685-687.

710. Chang B, Dacey MS, Hawes NL, et al. Cone photoreceptor function loss-3, a novel mouse model of achromatopsia due to a mutation in Gnat2. *Invest Ophthalmol Vis Sci* 2006;47:5017-5021.

711. Hennig AK, Ogilvie JM, Ohlemiller KK, Timmers AM, Hauswirth WW, Sands MS. AAV-mediated intravitreal gene therapy reduces lysosomal storage in the retinal pigmented epithelium and improves retinal function in adult MPS VII mice. *Mol Ther* 2004;10:106-116.

712. Gorbatyuk MS, Pang JJ, Thomas J, Jr., Hauswirth WW, Lewin AS. Knockdown of wild-type mouse rhodopsin using an AAV vectored ribozyme as part of an RNA replacement approach. *Molecular vision* 2005;11:648-656.

713. Paskowitz DM, Greenberg KP, Yasumura D, et al. Rapid and stable knockdown of an endogenous gene in retinal pigment epithelium. *Human gene therapy* 2007;18:871-880.

714. Gorbatyuk M, Justilien V, Liu J, Hauswirth WW, Lewin AS. Suppression of mouse rhodopsin expression in vivo by AAV mediated siRNA delivery. *Vision research* 2007;47:1202-1208.

715. Tessitore A, Parisi F, Denti MA, et al. Preferential silencing of a common dominant rhodopsin mutation does not inhibit retinal degeneration in a transgenic model. *Mol Ther* 2006;14:692-699.

716. Moisseiev J, Alhalel A, Masuri R, Treister G. The impact of the macular photocoagulation study results on the treatment of exudative age-related macular degeneration. *Archives of ophthalmology* 1995;113:185-189.

717. Algvere PV, Seregard S. Age-related maculopathy: pathogenetic features and new treatment modalities. *Acta Ophthalmol Scand* 2002;80:136-143.

718. Bainbridge JW, Mistry A, De Alwis M, et al. Inhibition of retinal neovascularisation by gene transfer of soluble VEGF receptor sFlt-1. *Gene therapy* 2002;9:320-326.

719. Lamartina S, Cimino M, Roscilli G, et al. Helper-dependent adenovirus for the gene therapy of proliferative retinopathies: stable gene transfer, regulated gene expression and therapeutic efficacy. *The journal of gene medicine* 2007;9:862-874.

720. Balaggan KS, Binley K, Esapa M, et al. EIAV vector-mediated delivery of endostatin or angiostatin inhibits angiogenesis and vascular hyperpermeability in experimental CNV. *Gene therapy* 2006;13:1153-1165.

721. Kimura H, Sakamoto T, Cardillo JA, et al. Retrovirus-mediated suicide gene transduction in the vitreous cavity of the eye: feasibility in prevention of proliferative vitreoretinopathy. *Human gene therapy* 1996;7:799-808.

722. Hurwitz MY, Marcus KT, Chevez-Barrios P, Louie K, Aguilar-Cordova E, Hurwitz RL. Suicide gene therapy for treatment of retinoblastoma in a murine model. *Human gene therapy* 1999;10:441-448.

723. Hurwitz RL, Brenner MK, Poplack DG, Horowitz MC. Retinoblastoma treatment. *Science (New York, NY* 1999;285:663-664.

724. Chevez-Barrios P, Chintagumpala M, Mieler W, et al. Response of retinoblastoma with vitreous tumor seeding to adenovirus-mediated delivery of thymidine kinase followed by ganciclovir. *J Clin Oncol* 2005;23:7927-7935.

725. Ma D, Gerard RD, Li XY, Alizadeh H, Niederkorn JY. Inhibition of metastasis of intraocular melanomas by adenovirus-mediated gene transfer of plasminogen activator inhibitor type 1 (PAI-1) in an athymic mouse model. *Blood* 1997;90:2738-2746.

726. Xu L, Yee JK, Wolff JA, Friedmann T. Factors affecting long-term stability of Moloney murine leukemia virus-based vectors. *Virology* 1989;171:331-341.

727. Engelhardt JF, Yang Y, Stratford-Perricaudet LD, et al. Direct gene transfer of human CFTR into human bronchial epithelia of xenografts with E1-deleted adenoviruses. *Nat Genet* 1993;4:27-34.

728. Yang Y, Raper SE, Cohn JA, Engelhardt JF, Wilson JM. An approach for treating the hepatobiliary disease of cystic fibrosis by somatic gene transfer. *Proc Natl Acad Sci U S A* 1993;90:4601-4605.

729. Khurana VG, Weiler DA, Witt TA, et al. A direct mechanical method for accurate and efficient adenoviral vector delivery to tissues. *Gene therapy* 2003;10:443-452.

730. Chen AF, O'Brien T, Tsutsui M, et al. Expression and function of recombinant endothelial nitric oxide synthase gene in canine basilar artery. *Circ Res* 1997;80:327-335.

731. Johnson DH, Tschumper RC. Human trabecular meshwork organ culture. A new method. *Invest Ophthalmol Vis Sci* 1987;28:945-953.

732. Leavitt AD, Robles G, Alesandro N, Varmus HE. Human immunodeficiency virus type 1 integrase mutants retain in vitro integrase activity yet fail to integrate viral DNA efficiently during infection. *Journal of virology* 1996;70:721-728.

733. Donello JE, Loeb JE, Hope TJ. Woodchuck hepatitis virus contains a tripartite posttranscriptional regulatory element. *Journal of virology* 1998;72:5085-5092.

734. Zufferey R, Donello JE, Trono D, Hope TJ. Woodchuck hepatitis virus posttranscriptional regulatory element enhances expression of transgenes delivered by retroviral vectors. *Journal of virology* 1999;73:2886-2892.

735. Naviaux RK, Costanzi E, Haas M, Verma IM. The pCL vector system: rapid production of helper-free, high-titer, recombinant retroviruses. *Journal of virology* 1996;70:5701-5705.

736. Qiao J, Roy V, Girard MH, Caruso M. High translation efficiency is mediated by the encephalomyocarditis virus internal ribosomal entry sites if the natural sequence surrounding the eleventh AUG is retained. *Human gene therapy* 2002;13:881-887.

737. Zufferey R, Dull T, Mandel RJ, et al. Self-inactivating lentivirus vector for safe and efficient in vivo gene delivery. *Journal of virology* 1998;72:9873-9880.

738. Miyoshi H, Blomer U, Takahashi M, Gage FH, Verma IM. Development of a self-inactivating lentivirus vector. *Journal of virology* 1998;72:8150-8157.

739. Iwakuma T, Cui Y, Chang LJ. Self-inactivating lentiviral vectors with U3 and U5 modifications. *Virology* 1999;261:120-132.

740. Deglon N, Tseng JL, Bensadoun JC, et al. Self-inactivating lentiviral vectors with enhanced transgene expression as potential gene transfer system in Parkinson's disease. *Human gene therapy* 2000;11:179-190.

741. Cable DG, Caccitolo JA, Caplice N, et al. The role of gene therapy for intimal hyperplasia of bypass grafts. *Circulation* 1999;100:II392-396.

742. Boshart M, Weber F, Jahn G, Dorsch-Hasler K, Fleckenstein B, Schaffner W. A very strong enhancer is located upstream of an immediate early gene of human cytomegalovirus. *Cell* 1985;41:521-530.

743. Foecking MK, Hofstetter H. Powerful and versatile enhancer-promoter unit for mammalian expression vectors. *Gene* 1986;45:101-105.

744. Louis N, Evelegh C, Graham FL. Cloning and sequencing of the cellular-viral junctions from the human adenovirus type 5 transformed 293 cell line. *Virology* 1997;233:423-429.

745. Shaw G, Morse S, Ararat M, Graham FL. Preferential transformation of human neuronal cells by human adenoviruses and the origin of HEK 293 cells. *Faseb J* 2002;16:869-871.

746. Crandell RA, Fabricant CG, Nelson-Rees WA. Development, characterization, and viral susceptibility of a feline (Felis catus) renal cell line (CRFK). *In vitro* 1973;9:176-185.

747. Tschumper RC, Johnson DH. Trabecular meshwork cellularity. Differences between fellow eyes. *Invest Ophthalmol Vis Sci* 1990;31:1327-1331.

748. Johnson DH, Richardson TM, Epstein DL. Trabecular meshwork recovery after phagocytic challenge. *Curr Eye Res* 1989;8:1121-1130.

749. Ohno T, Gordon D, San H, et al. Gene therapy for vascular smooth muscle cell proliferation after arterial injury. *Science (New York, NY* 1994;265:781-784.

750. Simari RD, San H, Rekhter M, et al. Regulation of cellular proliferation and intimal formation following balloon injury in atherosclerotic rabbit arteries. *J Clin Invest* 1996;98:225-235.

751. Johnson DH, Tschumper RC. The effect of organ culture on human trabecular meshwork. *Exp Eye Res* 1989;49:113-127.

752. Karger RA, Chen Y, Leske DA, Holmes JM. Time course of neovascularization in a neonatal rat model of retinopathy of prematurity. Invest Ophthalmol Vis Sci; 2001:S241.

753. Kipar A, Kohler K, Leukert W, Reinacher M. A comparison of lymphatic tissues from cats with spontaneous feline infectious peritonitis (FIP), cats with FIP virus infection but no FIP, and cats with no infection. *Journal of Comparative Pathology* 2001;125:182-191.

754. Kipar A, Bellmann S, Kremendahl J, Kohler K, Reinacher M. Cellular composition, coronavirus antigen expression and production of specific antibodies in lesions in feline infectious peritonitis. *Veterinary Immunology & Immunopathology* 1998;65:243-257.

755. Bragg DC, Hudson LC, Liang YH, Tompkins MB, Fernandes A, Meeker RB. Choroid plexus macrophages proliferate and release toxic factors in response to feline immunodeficiency virus.[comment]. *Journal of Neurovirology* 2002;8:225-239.

756. Brandtzaeg P, Dale I, Gabrielsen TO. The leucocyte protein L1 (calprotectin): usefulness as an immunohistochemical marker antigen and putative biological function. *Histopathology* 1992;21:191-196.

757. Fagerhol MK. Nomenclature for proteins: is calprotectin a proper name for the elusive myelomonocytic protein? *Clinical molecular pathology* 1996;49:M74-M79.

758. Schafer BW, Heizmann CW. The S100 family of EF-hand calcium-binding proteins: functions and pathology. *Trends in biochemical sciences* 1996;21:134-140.

759. Beebe AM, Gluckstern TG, George J, Pedersen NC, Dandekar S. Detection of feline immunodeficiency virus infection in bone marrow of cats. *Veterinary Immunology and Immunopathology* 1992;35:37-49.

760. Chalfie M. Green fluorescent protein. *Photochem Photobiol* 1995;62:651-656.

761. Kirsch P, Hafner M, Zentgraf H, Schilling L. Time course of fluorescence intensity and protein expression in HeLa cells stably transfected with hrGFP. *Mol Cells* 2003;15:341-348.

762. Tsien RY. The green fluorescent protein. *Annu Rev Biochem* 1998;67:509-544.

763. Liu ML, Winther BL, Kay MA. Pseudotransduction of hepatocytes by using concentrated pseudotyped vesicular stomatitis virus G glycoprotein (VSV-G)-Moloney murine leukemia virus-derived retrovirus vectors: comparison of VSV-G and amphotropic vectors for hepatic gene transfer. *Journal of virology* 1996;70:2497-2502.

764. Liu HS, Jan MS, Chou CK, Chen PH, Ke NJ. Is green fluorescent protein toxic to living cells? *Biochem Biophys Res Commun* 1999;260:712-717.

765. Hanazono Y, Yu JM, Dunbar CE, Emmons RV. Green fluorescent protein retroviral vectors: low titer and high recombination frequency suggest a selective disadvantage. *Human gene therapy* 1997;8:1313-1319.

766. Vasquez EC, Beltz TG, Meyrelles SS, Johnson AK. Adenovirus-mediated gene delivery to hypothalamic magnocellular neurons in mice. *Hypertension* 1999;34:756-761.

767. Wahlfors J, Loimas S, Pasanen T, Hakkarainen T. Green fluorescent protein (GFP) fusion constructs in gene therapy research. *Histochem Cell Biol* 2001;115:59-65.

768. Huang WY, Aramburu J, Douglas PS, Izumo S. Transgenic expression of green fluorescence protein can cause dilated cardiomyopathy. *Nature Medicine* 2000;6:482-483.

769. Martinez-Serrano A, Villa A, Navarro B, Rubio FJ, Bueno C. Human neural progenitor cells: better blue than green?[comment]. *Nature Medicine* 2000;6:483-484.

770. Detrait ER, Bowers WJ, Halterman MW, et al. Reporter gene transfer induces apoptosis in primary cortical neurons. *Molecular Therapy: the Journal of the American Society of Gene Therapy* 2002;5:723-730.

771. Zhan GL, Miranda OC, Bito LZ. Steroid glaucoma: corticosteroid-induced ocular hypertension in cats. *Experimental Eye Research* 1992;54:211-218.

772. Akingbehin AO. Corticosteroid-induced ocular hypertension. II. An acquired form. *British Journal of Ophthalmology* 1982;66:541-545.

773. Chuck AS, Palsson BO. Consistent and high rates of gene transfer can be obtained using flow-through transduction over a wide range of retroviral titers. *Human gene therapy* 1996;7:743-750.

774. Tripathi RC. The functional morphology of the outflow systems of ocular and cerebrospinal fluids. *Exp Eye Res* 1977;25:65-116.

775. Chuck AS, Clarke MF, Palsson BO. Retroviral infection is limited by Brownian motion. *Human gene therapy* 1996;7:1527-1534.

776. Saenz DT, Teo W, Olsen JC, Poeschla EM. Restriction of feline immunodeficiency virus by Refl, Lvl, and primate TRIM5alpha proteins. *Journal of virology* 2005;79:15175-15188.

777. Park F, Ohashi K, Chiu W, Naldini L, Kay MA. Efficient lentiviral transduction of liver requires cell cycling in vivo. *Nat Genet* 2000;24:49-52.

778. Polansky JR. Current perspectives on the TIGR/MYOC gene (Myocilin) and glaucoma. *Ophthalmology clinics of North America* 2003;16:515-527, v-vi.

779. Morissette J, Clepet C, Moisan S, et al. Homozygotes carrying an autosomal dominant TIGR mutation do not manifest glaucoma. *Nat Genet* 1998;19:319-321.

780. Gould DB, Reedy M, Wilson LA, Smith RS, Johnson RL, John SW. Mutant myocilin nonsecretion in vivo is not sufficient to cause glaucoma. *Mol Cell Biol* 2006;26:8427-8436.

781. Wang RF, Schumer RA, Serle JB, Podos SM. A comparison of argon laser and diode laser photocoagulation of the trabecular meshwork to produce the glaucoma monkey model. *Journal of glaucoma* 1998;7:45-49.

782. Stjernschantz JW. From PGF(2alpha)-isopropyl ester to latanoprost: a review of the development of xalatan: the Proctor Lecture. *Invest Ophthalmol Vis Sci* 2001;42:1134-1145.

783. Rao PV, Deng PF, Kumar J, Epstein DL. Modulation of aqueous humor outflow facility by the Rho kinase-specific inhibitor Y-27632. *Invest Ophthalmol Vis Sci* 2001;42:1029-1037.

784. Rubin EJ, Gill DM, Boquet P, Popoff MR. Functional modification of a 21-kilodalton G protein when ADP-ribosylated by exoenzyme C3 of Clostridium botulinum. *Mol Cell Biol* 1988;8:418-426.

785. Aktories K, Weller U, Chhatwal GS. Clostridium botulinum type C produces a novel ADP-ribosyltransferase distinct from botulinum C2 toxin. *FEBS Lett* 1987;212:109-113.

786. Humphrey MB, Herrera-Sosa H, Gonzalez G, Lee R, Bryan J. Cloning of cDNAs encoding human caldesmons. *Gene* 1992;112:197-204.

787. Alm A, Villumsen J. PhXA34, a new potent ocular hypotensive drug. A study on dose-response relationship and on aqueous humor dynamics in healthy volunteers. *Arch Ophthalmol* 1991;109:1564-1568.

788. Yang J, Liu TJ, Lu Y. Effects of bicistronic lentiviral vector-mediated herpes simplex virus thymidine kinase/ganciclovir system on human lens epithelial cells. *Curr Eye Res* 2007;32:33-42.

789. van Dillen IJ, Mulder NH, Vaalburg W, de Vries EF, Hospers GA. Influence of the bystander effect on HSV-tk/GCV gene therapy. A review. *Current gene therapy* 2002;2:307-322.

790. Freeman SM, Whartenby KA, Freeman JL, Abboud CN, Marrogi AJ. In situ use of suicide genes for cancer therapy. *Seminars in oncology* 1996;23:31-45.

791. Fillat C, Carrio M, Cascante A, Sangro B. Suicide gene therapy mediated by the Herpes Simplex virus thymidine kinase gene/Ganciclovir system: fifteen years of application. *Current gene therapy* 2003;3:13-26.

792. Conti C, Mastromarino P, Orsi N. Role of membrane phospholipids and glycolipids in cell-to-cell fusion by VSV. *Comp Immunol Microbiol Infect Dis* 1991;14:303-313.

793. da Cruz L, Robertson T, Hall MO, Constable IJ, Rakoczy PE. Cell polarity, phagocytosis and viral gene transfer in cultured human retinal pigment epithelial cells. *Curr Eye Res* 1998;17:668-672.

794. Saenz D, Loewen N, Leske DA, Good M, Holmes JH, Poeschla EM. Class I lentiviral integrase mutants reveal cell-cycle dependent expression from persistent unintegrated proviral DNA: implications for HIV-1 persistence in vivo., *International Workshop on HIV Persistence during Therapy.* Saint Martin, French West Indies, Le Meridien Hotel; 2003.

795. Engelman A. In vivo analysis of retroviral integrase structure and function. *Adv Virus Res* 1999;52:411-426.

796. Rice P, Mizuuchi K. Structure of the bacteriophage Mu transposase core: a common structural motif for DNA transposition and retroviral integration. *Cell* 1995;82:209-220.

797. Doak TG, Doerder FP, Jahn CL, Herrick G. A proposed superfamily of transposase genes: transposon-like elements in ciliated protozoa and a common "D35E" motif. *Proc Natl Acad Sci U S A* 1994;91:942-946.

798. Kulkosky J, Jones KS, Katz RA, Mack JP, Skalka AM. Residues critical for retroviral integrative recombination in a region that is highly conserved among retroviral/retrotransposon integrases and bacterial insertion sequence transposases. *Mol Cell Biol* 1992;12:2331-2338.

799. Bloemer U, Naldini L, Kafri T, Trono D, Verma IM, Gage FH. Highly efficient and sustained gene transfer in adult neurons with a lentivirus vector. *Journal of virology* 1997;71:6641-6649.

800. Bushman FD, Engelman A, Palmer I, Wingfield P, Craigie R. Domains of the integrase protein of human immunodeficiency virus type 1 responsible for polynucleotidyl transfer and zinc binding. *Proc Natl Acad Sci U S A* 1993;90:3428-3432.

801. Bushman FD, Wang B. Rous sarcoma virus integrase protein: mapping functions for catalysis and substrate binding. *Journal of virology* 1994;68:2215-2223.

802. Englund G, Theodore TS, Freed EO, Engleman A, Martin MA. Integration is required for productive infection of monocyte-derived macrophages by human immunodeficiency virus type 1. *Journal of virology* 1995;69:3216-3219.

803. Engelman A, Englund G, Orenstein JM, Martin MA, Craigie R. Multiple effects of mutations in human immunodeficiency virus type 1 integrase on viral replication. *Journal of virology* 1995;69:2729-2736.

804. Park F, Ohashi K, Kay MA. Therapeutic levels of human factor VIII and IX using HIV-1-based lentiviral vectors in mouse liver. *Blood* 2000;96:1173-1176.

805. Lai CM, Shen WY, Constable I, Rakoczy PE. The use of adenovirus-mediated gene transfer to develop a rat model for photoreceptor degeneration. *Invest Ophthalmol Vis Sci* 2000;41:580-584.

806. Reichel MB, Ali RR, Thrasher AJ, Hunt DM, Bhattacharya SS, Baker D. Immune responses limit adenovirally mediated gene expression in the adult mouse eye. *Gene therapy* 1998;5:1038-1046.

807. Anglade E, Csaky KG. Recombinant adenovirus-mediated gene transfer into the adult rat retina. *Curr Eye Res* 1998;17:316-321.

808. Mitani K, Kubo S. Adenovirus as an integrating vector. *Current gene therapy* 2002;2:135-144.

809. Harui A, Suzuki S, Kochanek S, Mitani K. Frequency and stability of chromosomal integration of adenovirus vectors. *Journal of virology* 1999;73:6141-6146.

810. Reichel MB, Bainbridge J, Baker D, Thrasher AJ, Bhattacharya SS, Ali RR. An immune response after intraocular administration of an adenoviral vector containing a beta galactosidase reporter gene slows retinal degeneration in the rd mouse. *Br J Ophthalmol* 2001;85:341-344.

811. Kafri T, Morgan D, Krahl T, Sarvetnick N, Sherman L, Verma I. Cellular immune response to adenoviral vector infected cells does not require de novo viral gene expression: implications for gene therapy. *Proc Natl Acad Sci U S A* 1998;95:11377-11382.

812. Farson D, Witt R, McGuinness R, et al. A new-generation stable inducible packaging cell line for lentiviral vectors. *Human gene therapy* 2001;12:981-997.

813. Pacchia AL, Adelson ME, Kaul M, Ron Y, Dougherty JP. An inducible packaging cell system for safe, efficient lentiviral vector production in the absence of HIV-1 accessory proteins. *Virology* 2001;282:77-86.

814. Broussau S, Jabbour N, Lachapelle G, et al. Inducible packaging cells for large-scale production of lentiviral vectors in serum-free suspension culture. *Mol Ther* 2008;16:500-507.

12. Curriculum Vitae

Name: Nils Axel Loewen

Current Position: Resident in Ophthalmology

Education and Training

Albert-Ludwigs-University, Faculty of Medicine, Freiburg, Germany, 1992-1998: MD

Albert-Ludwigs-University, Electrophysiology, Freiburg, Germany, 1992-1998: Dr. Med.Sci.

Mayo Graduate School, Rochester, MN and The Open University, Milton Keynes, UK. 2000-2004: Ph.D. studies.

Positions and Employment

1998 – 2000 Transitional Year Intern, Ophthalmology, Karl-Eberhardt-University Tuebingen, Tuebingen, Germany

2000 – 2004 Postdoctoral Fellow, Molecular Medicine Program, Mayo Clinic, Rochester, MN

2004 – 2005 Intern in Internal Medicine, Medical College Wisconsin, Milwaukee, WI

2005 – present Resident in Ophthalmology, Feinberg School of Medicine, Northwestern University, Chicago, IL

Professional memberships

Association for Research in Vision and Ophthalmology

American Academy of Ophthalmology

American Society of Cataract and Refractive Surgery

American Society of Gene Therapy

Career Development Awards

Long-term in vivo Modification of Trabecular Meshwork with Regulated Feline Immunodeficiency Virus (FIV)-based Lentiviral Vectors. Fight For Sight Research Division of Prevent Blindness America: $14,000. 6/2001 - 6/2002.

Ocular anti-neovascular gene therapy with an FIV vector transducing pigment epithelium-derived factor in a model of OIR. Knights Templar Eye Foundation: $30,000. 6/2002 - 6/2003.

Honors and Awards

1998 German Society of Neuro-Ophthalmology, Research Recognition Award

2001 Glaucoma Research Foundation, ARVO Travel Grant

2004 Biannual Alcon Glaucoma Research Recognition Award

2006 Heed-Foundation Retreat

2006 Midwest Eye-Banks Award

2006 Beem-Fisher Research Recognition Award